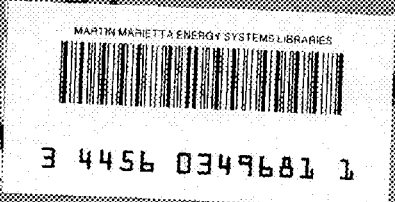


CENTRAL RESEARCH LIBRARY  
DOCUMENT COLLECTION



ORNL-17750  
Progress  
79

~~CONFIDENTIAL~~

BY ADVISOR 7/15/54

See Declassification Request Card for complete instructions on each copy.

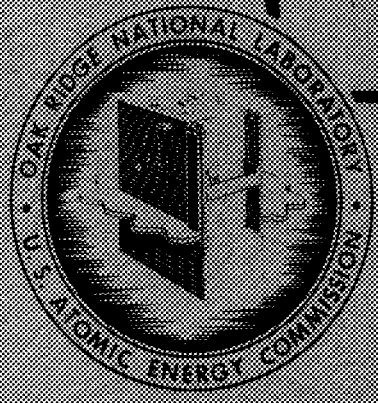
**ADVANCED RESEARCH AND DEVELOPMENT REPORT**  
**HOMOGENEOUS REACTOR PROJECT**  
**QUARTERLY PROGRESS REPORT**  
**FOR PERIOD ENDING JULY 31, 1954**

DECLASSIFIED

REPRODUCTION CHARGES: To: \_\_\_\_\_

PROPERTY OF ORNL

REMOVE FROM LIBRARY



CENTRAL RESEARCH LIBRARY  
DOCUMENT COLLECTION

**LIBRARY LOAN COPY**

DO NOT TRANSFER TO ANOTHER PERSON

If you wish someone else to see this document,  
send in name with document and the library will  
arrange a loan.

OAK RIDGE NATIONAL LABORATORY  
OPERATED BY  
CARBIDE AND CARBON CHEMICALS COMPANY  
A DIVISION OF UNION CARBIDE AND CARBON CORPORATION



POST OFFICE BOX P  
OAK RIDGE TENNESSEE

ORNL-1772

Contract No. W-7405-eng-26

**HOMOGENEOUS REACTOR PROJECT**

**QUARTERLY PROGRESS REPORT**

**For Period Ending July 31, 1954**

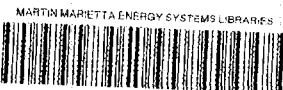
Project Director - J. A. Swartout  
Associate Director - C. E. Winters  
Project Engineer, Experimental Reactors - S. E. Beall  
Project Engineer, Large Reactors - W. C. Moore  
Corrosion - E. G. Bohlman  
Engineering Development - J. A. Lane  
Chemical Engineering - F. R. Bruce  
Supporting Chemistry - E. H. Taylor

Compiled by H. F. McDuffie

DATE ISSUED

OCT 11 1954

OAK RIDGE NATIONAL LABORATORY  
Operated by  
CARBIDE AND CARBON CHEMICALS COMPANY  
A Division of Union Carbide and Carbon Corporation  
Post Office Box P  
Oak Ridge, Tennessee



3 4456 0349681 1



EXTERNAL DISTRIBUTION

104. AF Plant Representative, Burbank
105. AF Plant Representative, Seattle
106. AF Plant Representative, Wood-Ridge
107. American Machine and Foundry Company
108. ANP Project Office, Fort Worth
- 109-119. Argonne National Laboratory
120. Armed Forces Special Weapons Project (Sandia)
121. Armed Forces Special Weapons Project, Washington
122. Atlantic Refining Co.
- 123-127. Atomic Energy Commission, Washington
128. Babcock and Wilcox
129. Battelle Memorial Institute
130. Bendix Aviation Corporation
- 131-133. Brookhaven National Laboratory
134. Bureau of Ships
135. Chicago Patent Group
136. Chief of Naval Research
137. Commonwealth Edison Company
138. Department of the Navy -- Op-362
139. Detroit Edison Company
140. Division of Research and Medicine, AEC, ORO
- 141-145. duPont Company, Augusta
146. duPont Company, Wilmington
147. Duquesne Light Company
148. Foster Wheeler Corporation
- 149-151. General Electric Company (ANPD)
152. General Electric Company (APS)
- 153-160. General Electric Company, Richland
161. Hanford Operations Office
162. Iowa State College
- 163-166. Knolls Atomic Power Laboratory
- 167-168. Los Alamos Scientific Laboratory
169. Nuclear Metals, Inc.
170. Monsanto Chemical Company
171. Mound Laboratory
172. National Advisory Committee for Aeronautics, Cleveland
173. National Advisory Committee for Aeronautics, Washington
- 174-175. Naval Research Laboratory
176. Newport News Shipbuilding and Dry Dock Company
177. New York Operations Office
- 178-179. North American Aviation, Inc.
180. Nuclear Development Associates, Inc.
181. Pacific-Northwest Power Group
182. Patent Branch, Washington
- 183-189. Phillips Petroleum Company (NRTS)
190. Powerplant Laboratory (WADC)
191. Pratt and Whitney Aircraft Division (Fox Project)
192. Rand Corporation
193. San Francisco Field Office

- 
- 194. Sylvania Electric Products, Inc.
  - 195. Tennessee Valley Authority (Dean)
  - 196. USAF Headquarters
  - 197. U. S. Naval Radiological Defense Laboratory
  - 198-199. University of California Radiation Laboratory, Berkeley
  - 200-201. University of California Radiation Laboratory, Livermore
  - 202. Walter Kidde Nuclear Laboratories, Inc.
  - 203-208. Westinghouse Electric Corporation
  - 209-223. Technical Information Service, Oak Ridge
  - 224. Materials Laboratory (WADC)
  - 225. ORNL Document Reference Library, Y-12 Branch
  - 226. Vitro Corporation of America
- 



Reports previously issued in this series are as follows:

ORNL-527	Date issued, December 28, 1949
ORNL-630	Period Ending February 28, 1950
ORNL-730	Feasibility Report – Date Issued, July 6, 1950
ORNL-826	Period Ending August 31, 1950
ORNL-925	Period Ending November 30, 1950
ORNL-990	Period Ending February 28, 1951
ORNL-1057	Period Ending May 15, 1951
ORNL-1121	Period Ending August 15, 1951
ORNL-1221	Period Ending November 15, 1951
ORNL-1280	Period Ending March 15, 1952
ORNL-1318	Period Ending July 1, 1952
ORNL-1424	Period Ending October 1, 1952
ORNL-1478	Period Ending January 1, 1953
ORNL-1554	Period Ending March 31, 1953
ORNL-1605	Period Ending July 31, 1953
ORNL-1658	Period Ending October 31, 1953
ORNL-1678	Period Ending January 31, 1954
ORNL-1753	Period Ending April 30, 1954





## CONTENTS

SUMMARY .....	1
PART I. EXPERIMENTAL REACTORS	
HOMOGENEOUS REACTOR EXPERIMENT .....	11
Disassembly of HRE .....	11
Inspection of Reactor Parts .....	11
HOMOGENEOUS REACTOR TESTS .....	13
Operational Planning .....	13
HRT Design .....	14
Flowsheet and general design considerations .....	14
Reactor area, building, and cells .....	15
Reactor equipment and equipment arrangements .....	22
Reactor vessel and core tank .....	23
Pressurizer .....	23
Gas separator .....	23
Main heat exchangers .....	25
Dump tanks, evaporators, and vapor separators .....	25
Catalytic recombiner-condenser .....	25
Equipment layouts .....	25
Steam system .....	25
HRT Nuclear Calculations .....	30
HRT breeding possibilities .....	30
Heat generation in the HRT blanket .....	30
Thermal stresses in HRT pressure vessel during shutdown .....	32
Criticality of $U^{235}$ - $H_2O$ - $D_2O$ systems in cylindrical geometry .....	32
HRT blanket dump tanks .....	33
HRT-Component Development .....	34
HRT-core hydraulic studies .....	34
HRT heat exchangers and circulating pumps .....	35
HRT fuel feed pumps .....	37
Small-component development .....	38
Simulated HRT explosion test .....	40
HRT mock-up .....	42
Controls and Instrumentation .....	43
Homogeneous reactor test instrumentation .....	43
PART II. REACTOR ANALYSIS	
REACTOR ANALYSIS .....	51
Homogeneous Reactor Kinetics .....	51
Relation between reactivity ramp rate and instantaneous reactivity addition .....	51
Calculation of maximum reactor power .....	51
Two-Region High-Purity Plutonium Producers .....	54
PART III. CORROSION	
PUMP-LOOP CORROSION TESTS .....	59
Pump-Loop Operation and Maintenance .....	59
Loop status .....	59



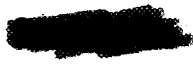
Westinghouse 100A pumps . . . . .	60
Results of Loop Tests . . . . .	60
General corrosion rates . . . . .	61
Corrosion testing in 1.34 <i>m</i> uranyl sulfate . . . . .	61
Effect of uranium concentration on the film-free corrosion rate of stainless steel at 250°C . . . . .	75
Corrosion rate of stainless steel at 250°C in 0.06 <i>m</i> uranyl sulfate containing 0.006 <i>m</i> sulfuric acid . . . . .	76
Corrosion of stainless steel in 0.17 <i>m</i> uranyl sulfate at 200 and 250°C . . . . .	77
Titanium-loop operations . . . . .	78
Galvanic corrosion . . . . .	79
RADIATION CORROSION . . . . .	82
Loop Package Testing and HB-4 Mock-up . . . . .	82
In-pile development loops . . . . .	82
In-pile HB-4 mock-up . . . . .	83
In-pile pumps . . . . .	87
LITR Installation . . . . .	88
Status . . . . .	88
Modification to permit cooling of hole liner . . . . .	88
Radioactive-Specimen Evaluation . . . . .	89
Loop-dismantling facility . . . . .	89
Corrosion examination facility . . . . .	89
HRE inspection . . . . .	89
LABORATORY CORROSION STUDIES . . . . .	91
Corrosion of Zircaloy-2 Weldments in Uranyl Sulfate Solutions at 250 and 300°C . . . . .	91
Stress-Corrosion Cracking . . . . .	94
Hydrogen in Metals . . . . .	95
Tests with High-Concentration Uranyl Sulfate Solutions . . . . .	97
Corrosion of type 347 stainless steel, Titanium 75A, and Zircaloy-2 at 300°C in oxygenated 5 <i>m</i> uranyl sulfate solution . . . . .	97
Blowdown experiments . . . . .	99
Corrosion of Micrometallic, Sintered, Type 304 Stainless Steel Filter Plate . . . . .	101
Corrosion of Pump-Bearing Materials . . . . .	102
Corrosion of Type 347 Stainless Steel and Titanium 75A in Thorium Nitrate Solution . . . . .	103
Small-Scale Dynamic-Corrosion Program . . . . .	104
McWherter-DeRieux toroid rotator I . . . . .	104
Toroid rotator II . . . . .	104

PART IV. ENGINEERING DEVELOPMENT

DEVELOPMENT OF FUEL-SYSTEM COMPONENTS . . . . .	109
Recombiner Development . . . . .	109
Small Reactor Components . . . . .	109
Allis-Chalmers 500-gpm pump and 20-cfm gas circulator . . . . .	109
ORNL gas circulator . . . . .	109
ORNL 5-gpm pump . . . . .	109
Large Reactor Components . . . . .	110
50-Mw main fuel heat exchanger . . . . .	110
Large heat exchanger . . . . .	110
Main gas condenser . . . . .	112
4000-gpm Loop . . . . .	112



DEVELOPMENT OF BLANKET-SYSTEM COMPONENTS .....	114
Circulating-Loop Tests .....	114
Effect of oxygen on erosion-corrosion attack by ThO <sub>2</sub> slurries .....	114
Slurry attack on Carboloy and Stellite 98M2 .....	120
5-gpm-loop construction .....	121
200-gpm-loop construction .....	122
HRT Gas-Separator Slurry Test .....	122
High-Pressure Abrasion Tester .....	123
Small-Scale Slurry Blanket Mock-up .....	123
Full-Scale HRT Slurry Blanket Mock-up .....	124
Caking, Plugging, and Sedimentation Properties of Slurries .....	125
Plugging of pipes by sedimentation .....	125
Plugging of pipes by pumped solids .....	125
Caking phenomena in loops .....	125
Sedimentation properties .....	126
Centrifugal sedimentation .....	126
Adhesion to polished surfaces .....	127
Temperature rise of quiescent slurry layer .....	127
BOILING REACTOR STUDIES .....	128
Vapor Transport in the Liquid .....	128
Vapor Separation .....	128
Forced Circulation .....	129
Separator Pumps .....	130
General Studies .....	131
METALLURGY .....	132
Properties of Titanium and Zirconium Alloys .....	132
Iodide-titanium .....	132
Tensile properties of welded Zircaloy-2 .....	132
Corrosion of Welds .....	132
Miscellaneous Service Assistance .....	133
Tubing failures from Loop H pressurizer mixing line .....	133
Metallographic examination of dynamic-corrosion specimens .....	135
Titanium pressurizer failure .....	136
Stress-corrosion cracking .....	136
PART V. CHEMICAL ENGINEERING DEVELOPMENTS	
SLURRY FUEL AND BLANKET STUDIES .....	139
Thorium Oxide Slurry Irradiation Studies .....	139
In-pile studies .....	139
Out-of-pile studies .....	139
Chemistry of Thorium Oxide Slurries .....	140
Reactions with uranium oxide .....	140
Effect of electrolytes .....	140
Abrasive Properties of Thorium Oxide .....	141
Effect of method of preparation of thorium oxalate .....	141
Mixed-oxide studies .....	142
Thorium Hydroxide Studies .....	142
Crystalline character .....	142
Thorium Oxide Slurry Preparation Equipment .....	142



PLUTONIUM-PRODUCER BLANKET PROCESSING ..... 143

    Solubility of Pu(IV) in Uranyl Sulfate Solutions ..... 143

    Adsorption of Plutonium on Stainless Steel and Titanium ..... 143

    Particle Size of PuO<sub>2</sub> ..... 144

    Rate of PuO<sub>2</sub> Precipitation from Pu(IV) Solution ..... 144

    Rate of Precipitation of PuO<sub>2</sub> from Pu(VI) Solutions ..... 145

    Neptunium Chemistry ..... 146

    Determination of Reactor Neutron-Capture Cross Section of Np<sup>239</sup> ..... 146

    Blanket-Processing Flow Sheet ..... 146

THERMAL-BREEDER FUEL AND BLANKET PROCESSING ..... 148

    Chemical Flow Sheet ..... 148

    Fuel Cost for Thermal Breeder Reactor ..... 148

    Calculation of Radiation Hazard of Reactor Fuel ..... 149

    Fission-Product and Corrosion-Product Chemistry ..... 150

        Rare earths ..... 150

        Iron ..... 152

        Iodine ..... 152

    Engineering Studies ..... 152

        Hydroclone separation equipment ..... 152

        Methods for sizing samples ..... 154

        High-pressure test loop ..... 154

        Process-design studies ..... 154

SUMMARY OF WORK BY VITRO LABORATORY ..... 157

    CaF<sub>2</sub> Process ..... 157

    Rare-Earth Sulfate Solubility ..... 157

    Iodine Removal ..... 158

PART VI. SUPPORTING CHEMICAL RESEARCH

RADIATION CORROSION STUDIES ..... 161

    In-Pile Experiments ..... 161

    Out-of-Pile Experiments ..... 161

THORIUM NITRATE RADIATION STUDIES ..... 165

ANALYTICAL CHEMISTRY RESEARCH ..... 167

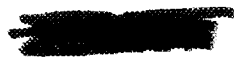
    Objectives ..... 167

    Statistical Evaluation of the Polarographic Determination of Nickel in Homogeneous  
    Reactor Fuel ..... 167

    Statistical Evaluation of the Polarographic Determination of Copper in Homogeneous  
    Reactor Fuel ..... 167

    Titration of Uranium in Homogeneous Reactor Fuel Solutions ..... 167

Np<sup>239</sup> CAPTURE CROSS SECTION ..... 168



# HRP QUARTERLY PROGRESS REPORT

## SUMMARY

### PART I EXPERIMENTAL REACTORS

#### Homogeneous Reactor Experiment

After decontaminating the HRE and reducing the radioactivity in the cells from 500 to 1000 r/hr to levels of 10 to 50 r/hr, it was possible to remove all reactor components within a 30-day period. By June 30, the concrete-block shield had been dismantled and excavation had begun for the HRT shielding pit. Contaminated components were stored in a water-filled pool where they are being cut open for detailed examination. The reactor core, the pressurizer, and the main heat exchanger have already been opened.

#### Homogeneous Reactor Test

The Homogeneous Reactor Test (HRT) is the 5- to 10-Mw experimental reactor facility which is being constructed at ORNL to test flow-sheet and equipment designs being considered for full-scale power stations. A schedule for three possible reactor-test demonstrations (heavy-water reflector, thorium oxide slurry blanket, and natural-uranium solution blanket) is presented.

The procurement for the first demonstration is reported as being 60% complete, and there is a commitment of \$617,690 in contracts. A condensed construction calendar is presented, and it shows the completion of pre-start-up testing in the fall of 1955.

The design of the HRT is entering the final stages. The HRT will be constructed as a two-region reactor with a dilute  $\text{UO}_2\text{SO}_4\text{-D}_2\text{O}$  solution in the core and a  $\text{D}_2\text{O}$  reflector. It is being designed to operate at 300°C and 2000 psia and to produce 5 Mw of heat in the core. Presented here are the flow-sheet and design basis, a description of the reactor cell (a steel tank designed to contain the reactor fluids in the event of a brittle failure of the reactor vessel), a discussion of the problems of maintaining a pressure balance between the core and blanket systems, and a report of the status of the reactor and major equipment design.

The HRT, operating with  $\text{U}^{233}$  fuel and a  $\text{ThO}_2$  blanket, will come close to breeding at 280°C.

An appreciable uncertainty in the anticipated breeding ratio exists because of a lack of information on alpha for the  $\text{U}^{233}$  resonances. Reduction of the HRT operating temperature to 200°C or less would reduce the uncertainty due to resonance captures and would increase the breeding ratio to 1.07 or greater. To demonstrate breeding at 280°C conclusively, the core diameter, as well as the diameter of the pressure vessel, would have to be increased by a few inches. For example, a 40-in. core and a 6-ft pressure vessel would result in a breeding ratio of 1.11 or greater.

The heating and consequent thermal stresses of the HRT pressure vessel during a shutdown have been estimated and found to be small. The maximum total tensile stress is less than 13,000 psi, of which 4,000 psi is due to thermal stress. The heating rate is less than 6°F per minute.

The critical concentrations of  $\text{U}^{235}$  were calculated for long storage cylinders reflected by light water and moderated with  $\text{H}_2\text{O}$ ,  $\text{D}_2\text{O}$ , or mixtures of the two. For each moderator, there is a diameter for which the linear concentration is a minimum; the minimum concentration decreases from 0.65 kg of  $\text{U}^{235}$  per foot for  $\text{H}_2\text{O}$  moderator at a diameter of 9.5 in. to 0.38 kg of  $\text{U}^{235}$  per foot for pure  $\text{D}_2\text{O}$  moderator at 24 in. The addition of cadmium coating to the pipes gives similar results, but the minima and the corresponding diameters are considerably larger; thus the minimum for  $\text{H}_2\text{O}$  is 0.82 kg of  $\text{U}^{235}$  per foot at 12 in. and for  $\text{D}_2\text{O}$  the minimum is somewhat less than 0.62 kg of  $\text{U}^{235}$  per foot at a diameter greater than 32 in.

Estimates were made of the criticality of the horizontal 24-in.-dia dump tanks for the HRT blanket for the situations where the fuel solution becomes mixed with the blanket materials - pure  $\text{D}_2\text{O}$ ,  $\text{UO}_2\text{SO}_4$  solution, or  $\text{ThO}_2$  slurry. The quantity of fuel in the reactor will depend on the blanket material, but the calculations indicate that the tanks will be safe, by a comfortable margin, for any loading under consideration.

A full-scale carbon-steel flow model of the straight-through 32-in.-dia HRT core was completed, and a number of tests were performed. No

## HRP QUARTERLY PROGRESS REPORT

satisfactory combination of screens has been found for the single-cone 90-deg diffuser, and it may be necessary to provide a double-cone diffuser instead.

A full-scale flow model of an alternate HRT core design, which utilizes concentric inlet and outlet pipes, was also tested during the past quarter. Pressure-drop and flow patterns were determined at flow rates of 40 to 400 gpm, and satisfactory performance was demonstrated.

The Foster Wheeler Corp. has begun the design of the HRT fuel and blanket heat exchangers. Delivery of the units is scheduled for February 1955.

Construction of the two Westinghouse Model 400A fuel circulating pumps is essentially complete. Design of the test loops for these pumps is complete, and material is on order or on hand.

The redesign of the Model 150C pump by Westinghouse to meet the requirements of various blanket tests is complete. Test loops will be constructed at ORNL and will be similar to the loops for the 400A pump.

A prototype of the HRT fuel feed pump has been operated at 2000 psi with good results. A Hydro-pulse pump, which may replace portions of the Pulsafeeder fuel-feed system, has been received.

The steam pressurizer designed for the HRT requires electric heaters which are easy to operate and service and are also safe in the event of reactor accidents. Experiments have demonstrated that the present design, which uses Calrods cast into an aluminum matrix, appears to be feasible for HRT use.

Vaned elbows would be desirable in HRT locations where flow patterns are important. In a series of performance tests, it was shown that stable flow was re-established between 5 and 10 diameters downstream of vaned single- and double-mitred elbows.

A full-scale dump-tank-evaporator mock-up similar to the dump-tank-evaporator designed for the HRT has been constructed and is ready to be tested. A low-pressure entrainment separator, such as might be attached to the evaporator, has been assembled to evaluate wire-mesh demisters. Entrainment is provided by mixing a compressed-air stream and a recirculating water stream.

The observed behavior of the HRE charcoal adsorbers conformed approximately to the design theory. The same charcoal beds can be used in

the HRT after some simple maintenance is carried out to ensure good operation.

Tests which simulate the rapid release of steam as a result of a brittle fracture of the HRT high-pressure system indicate that the final pressure of the expanded system can be calculated with sufficient accuracy for the design of the shielding tank.

Basic concepts of the HRT control panel have been formulated, and a panel arrangement has been mocked up in plywood. After practical testing, Chromel-Alumel has been selected as the most likely combination to minimize galvanic corrosion of thermocouple leads when the reactor cells are flooded for maintenance. An arrangement has been recommended for mounting ion and fission chambers about the reactor vessel. Prototype  $\frac{1}{2}$ -in. high-pressure shut-off valves are in fabrication. Collaboration has been maintained with the Design Section in designing other valves. Several instrument drawings have been prepared, and instrument procurement is under way.

### PART II REACTOR ANALYSIS

Simple formulas which give the maximum power resulting from addition of reactivity and which relate a reactivity ramp rate to an instantaneous addition of reactivity have been found to give excellent agreement with results obtained from integration of the nonlinear dynamic equations.

Additional calculations for two-region high-purity plutonium-production reactors show the optimum blanket-feed enrichment to be about 0.9%, corresponding to an operating enrichment of 0.55%. The lowest unit costs are obtained with about a 4-ft-dia core.

### PART III CORROSION

#### Pump-Loop Corrosion Tests

A series of dynamic loop runs in which 1.34 *m* uranyl sulfate was circulated at temperatures of 200 to 300°C has been completed. The results showed that at the 1.34 *m* level the extent of corrosion of type 347 stainless steel was high at all flow rates and that the corrosion rate of the film-free metal was approximately six times greater at 1.34 *m* than at 0.17 *m* for any given temperature. As at the 0.02 and 0.17 *m* level, oxide coatings

that formed on stainless steel at 200 and 225°C were not protective and allowed a relatively high corrosion rate. At higher temperatures the oxide coatings afforded protection to the underlying metal. The difference in the protectiveness was apparently related to the difference in chemical composition. At 250°C and higher, the bulk film was composed completely of alpha iron oxide (anhydrous), but at 200 and 225°C, 20 to 90% of the film was composed of a hydrated iron oxide.

In one run the titanium loop was operated with 1.34 *m* uranyl sulfate at 300°C, and under these conditions the solution existed as two immiscible liquids. A second run, identical to the first except that 0.3 *m* sulfuric acid was added to prevent the formation of a second liquid phase, has also been made. In neither case did the titanium or zirconium specimens show measurable corrosion damage. To date, both zirconium and titanium have shown a very high degree of corrosion resistance to all concentrations of uranyl sulfate at all temperatures in the absence of radiation.

The corrosion resistance of 300 series stainless steels to 0.06 *m* uranyl sulfate containing 0.006 *m* sulfuric acid at 250°C has been determined. In the above system the critical velocity was about 35 fps, and, at flow rates less than the critical velocity, a corrosion rate of 1 mpy was observed. Above the critical velocity the corrosion rate was approximately 120 mpy.

Whether iodine is added to a uranyl sulfate solution as iodide or iodate ions, very nearly all of the iodine collects in the gas phase as elemental iodine and causes severe pitting of stainless steel in the gas phase. Neither titanium nor zirconium, however, is corroded to any measurable extent by the iodine vapors.

#### Radiation Corrosion

The performance of the in-pile loop in out-of-pile testing continues to be satisfactory. The activity of the  $\text{Cu}^{++}$  ion as a hydrogen-oxygen recombiner was found to be about a factor of 2 lower than expected. A  $\text{Cu}^{++}$  ion concentration of 0.031 *m* instead of the calculated 0.013 *m* is required to maintain a suitably low equilibrium pressure of  $2\text{H}_2 + \text{O}_2$ . The stability of the  $\text{Cu}^{++}$  is satisfactory.

Metal bearings for replacement of the Graphitar in the in-pile circulating pump do not appear to be satisfactory as presently designed. The pump

bearings have been redesigned in an effort to improve the performance of all-metal (or equivalent) bearings.

A second in-pile loop package assembly (Serial No. CC) has been satisfactorily tested in the in-pile loop mock-up. In the course of this test the entire loop package and shield-plug assembly was taken to the LITR to check its fit in the HB-4 beam-hole liner. Insertion of the assembly went smoothly; during removal, however, a rubber seal gasket was torn and became wedged in the annulus between the loop package can and the beam-hole liner, which made removal of the assembly very difficult. The design of this feature of the installation has now been modified so that this rubber gasket is at the entry of the beam hole. The Loop CC package assembly is now being used to check the loop dismantling facility.

Installation of equipment at the LITR is complete and is now under test. A loop (Serial No. DD) and shield-plug assembly for installation in the LITR is ready for testing in the in-pile mock-up.

Preliminary evaluation of the data obtained from the sample coupons from the HRE indicates results not inconsistent with those obtained in the out-of-pile dynamic loop tests.

#### Laboratory Corrosion Studies

Tests with high-concentration uranyl sulfate solutions at temperatures above the two-phase separation temperature indicate that the heavy phase is quite corrosive to type 347 stainless steel although not to Titanium 75A or Zircaloy-2. Attempts to remove portions of the heavy phase at temperature and pressure through a dip tube failed because the tube uniformly plugged with a hard, difficultly soluble solid.

Tests with specimens machined from weldments in which Zircaloy-2 base plates were joined by Zircaloy-2 weld wire by the ORNL Heliarc weld method showed general, moderate, white deposits on weld-skin regions, showed no attack on machined or other regions, and generally appeared acceptable on the basis of three-week tests in simulated HRT solutions containing (1) 0.08 *m* uranyl sulfate, 0.0065 *m* cupric sulfate, and 0.008 *m* sulfuric acid, tested under 150 psi oxygen at 300°C; and (2) 1.56 *m* uranyl sulfate with 0.00035 *m* cupric sulfate under 150 psi oxygen at 250°C. Similar specimens prepared by the Newport News Shipbuilding & Dry Dock Co., contractor for HRT core-tank fabri-

## HRP QUARTERLY PROGRESS REPORT

cation, exhibited slight dark oxide spots but no significant other attack when exposed under the latter (2) conditions. However, an iodide-zirconium weld on Zircaloy-2 base and also an argon-faced Zircaloy-2 weld on a 2.9% titanium--Zircaloy-2 base metal, received from this contractor, showed substantial general pitting attack on the weld regions under the same conditions.

Type 347 stainless steel, in a three-week test at 250°C in a solution which, at 25°C, contained 1.31 M thorium nitrate and 2.26 M nitric acid, gave an average corrosion rate of 4.5 mpy. Titanium 75A underwent practically no attack under these conditions.

### PART IV ENGINEERING DEVELOPMENT

#### Development of Fuel-System Components

Assembly of the high-pressure recombiner loop was completed, and the electrical control and electrolytic cell power circuit should be completed soon.

The Allis-Chalmers Mfg. Co. has completed preliminary designs for a 500-gpm canned-rotor pump and a 20-cfm canned-rotor gas circulator.

The ORNL 5-gpm pump, with minor modifications, has been converted to a high-suction-pressure canned-rotor gas circulator. A reverse thrust bearing was installed so that the circulator will operate in a vertical position with the motor end placed down.

The operating endurance test of the ORNL pump to determine the life expectancy of the various parts has continued. One pump has run for a total of about 2700 hr while circulating water at a temperature of 250°C.

The design of the 50-Mw main fuel heat exchanger is nearing completion; tube-joint welding, with the use of the manually operated Heliarc torch mechanism, is progressing.

The Foster Wheeler Corp. is undertaking a study to determine the largest practicable heat exchanger which can be made with reasonable economy. The study to date has been limited to a single-pass, straight, fixed-tube-sheet heat exchanger.

No further work is being done on the main gas condenser at the present time.

The addition of an 8-in. oil diffusion pump to the vacuum system reduced the pressure in the large (4000-gpm) pump loop to 4 to 6  $\mu$  and in-

creased the sensitivity for detecting leaks. Actual operation has been delayed to perfect leak-hunting techniques and to train personnel in the use of the necessary equipment.

#### Development of Blanket-System Components

Thorium oxide made from the formate was circulated at a concentration of about 400 g of thorium per kilogram of H<sub>2</sub>O for 1455 hr at 250°C; the slurry contained about 500 ppm of oxygen. After a small initial attack of the stainless steel, the attack rate declined to almost zero. Lindsay oxide (from high-temperature calcination of thorium oxalate) showed some beneficial effect from oxygen, with a greater initial attack due, it is believed, to a higher initial pH and to a greater hardness which may be possessed by the Lindsay oxide.

Carballoy and Stellite 98M2 showed a moderate resistance to attack by circulating, non-oxygenated, Lindsay oxide slurry, as compared with the excellent resistance of titanium, zirconium, gold, and platinum.

In preliminary tests, an axial gas separator gave essentially the same performance with slurries up to 150 g of thorium per kilogram of water as with water. A moderate radial concentration gradient was indicated, but no thoria actually settled out.

Fresh oxide slurry which was allowed to compact under gravity for seven days flowed freely out of a small tube, but a sample of thoria slurry (750 g of thorium per kilogram of H<sub>2</sub>O) from a loop test required a shear stress of 0.03 psi after standing in a horizontal tube for 1 hr.

Hard cakes which have been observed in a few loop tests could not be reproduced by centrifugal action in either 60 or 250°C tests.

The sedimentation properties of thoria change drastically during the first few hours of circulation at 250°C. Fresh material which initially settled to a critical density of almost 2000 g of thorium per kilogram of H<sub>2</sub>O settled, after removal from the loop, to only about 210 g of thorium per kilogram of H<sub>2</sub>O after circulation at 250°C for 1½ hr. After 1000 hr of circulation at 250°C the settled density at room temperature was 142 g of thorium per kilogram of H<sub>2</sub>O.

#### Boiling Reactor Studies

Power densities as high as 5.8 kw/liter have been obtained in a 6 × 6 in. natural-circulation

atmospheric-pressure apparatus. Vapor fractions up to 0.65 were observed. The pressure drop permissible for a vapor separator has been computed.

Computations have been made of the net positive suction head available in a high-pressure-pumped boiling system with introduction of cooled condensate ahead of the pump.

Studies have continued on the separator pump. In one test with water, seven-tenths of the inlet velocity pressure was recovered.

### Metallurgy

No evidence of hydrogen embrittlement of iodide-titanium, as measured by changes in impact behavior, was produced by exposure to acidified uranyl sulfate solution in unirradiated dynamic-corrosion test loops. This tends to confirm the results of previous tests but cannot be considered conclusive for all possible environments.

Tensile tests at elevated temperature (600°F) have been run on welded Zircaloy-2 to obtain information required for the HRT core tank.

Welded specimens of type 347 stainless steel, with both high-ferrite and low-ferrite weld deposits, and welded specimens of titanium and of Zircaloy-2, which had been exposed in dynamic-corrosion test loops to high-concentration aqueous uranyl sulfate solutions, were examined to determine the relative behavior of the weld deposits and base metal. Weld deposits in stainless steels were less corrosion resistant than the base metal, but the low-ferrite welds appeared to be superior to the high-ferrite weld metal in this environment. The titanium and Zircaloy-2, both welds and base metal, were substantially unaffected in this exposure.

Metallographic examinations were made of both seamless and welded stainless steel tubing failures and of specially prepared test specimens exposed in dynamic-corrosion test loops to high-concentration aqueous uranyl sulfate solutions at high velocities and at 225°C. The materials exhibited intergranular corrosion attack and, in the case of the particular specimen of welded tubing used here, a preferential attack at the weld seam. The results indicate the necessity for further study of the problem and for the application of rigid procurement specifications to small-diameter stainless steel tubing to be used in critical conditions of corrosion environment.

Metallographic examination of a failure in a

tubular titanium pressurizer showed, in the area of failure, the structure which is characteristic of titanium that has been heated substantially higher than the contemplated operating temperature. Grain coarsening had occurred, and there was evidence that during heating the metal had first transformed to the high-temperature beta phase and subsequently transformed to the characteristic Widmanstätten alpha structure on cooling.

## PART V

### CHEMICAL ENGINEERING DEVELOPMENTS

#### Slurry Fuel and Blanket Studies

Emphasis in the thorium oxide slurry program has shifted to a study of the effect of neutron irradiation on slurry properties and a study of gas production and recombination in the slurry system. No gas production was observed during 30 days of irradiation of a pure thorium oxide slurry. During five days of irradiation of a thorium oxide slurry containing 4 mole % of enriched uranium, non-equilibrium gas pressures of 2500 psi at 205°C were observed, but, at temperatures above 270°C, an equilibrium gas pressure of less than 100 psi in excess of steam pressure was obtained, indicating that rapid catalytic recombination was taking place at 270°C. Initial out-of-pile studies on gas recombination showed, in a system containing mixed thorium-uranium oxide with a thorium concentration of 500 g/liter, with equal slurry and gas volumes, and with 1000 psi of oxygen plus hydrogen in excess of steam pressure, a hydrogen combination rate of approximately 0.15 mole/hr/liter of slurry at 290°C and 0.01 mole/hr/liter of slurry at 270°C.

Mixtures of  $\text{UO}_3 \cdot \text{H}_2\text{O}$  platelets and various thorium oxide preparations reacted at 250°C in water to give an orange-colored solid, presumably a solid solution of  $\text{UO}_3$  in  $\text{ThO}_2$ . Under hydrogen pressure at 250°C, uranium was reduced and crystal growth was promoted.

Sodium pyrophosphate was found to be a good deflocculent for oxide prepared by calcination of thorium oxalate. For a constant calcination temperature (650°C), the abrasiveness of the oxide from the calcination of thorium oxalate depended on the method of preparation of the oxalate and presumably on the particle size of the oxalate. The addition of  $\text{Al}_2\text{O}_3$  to  $\text{ThO}_2$  markedly inhibited thorium oxide crystallization; however, no decrease

## HRP QUARTERLY PROGRESS REPORT

in abrasiveness over that of the pure oxide was observed. Thorium hydroxide, as precipitated from formate solution and after being dried at 105°C, was amorphous to X rays. Autoclaving the moist hydroxide at 250°C in water or drying the hydroxide at 500°C converted it to crystalline ThO<sub>2</sub> but did not appreciably increase its abrasive properties.

### Plutonium-Producer Blanket Processing

The primary objective of processing the plutonium-producer blanket is to remove the plutonium, and possibly the neptunium, as rapidly as possible in order to minimize Pu<sup>240</sup> build-up. The chemistry of plutonium and neptunium under reactor conditions is being studied so that a satisfactory process may be specified.

The solubility of Pu(IV) in 1.0 to 1.6 *m* UO<sub>2</sub>SO<sub>4</sub> solution at 300°C has been redetermined as 3.0 ± 0.6 mg per kilogram of H<sub>2</sub>O, which agrees with the accepted value. As much plutonium as 0.1 mg/cm<sup>2</sup> was adsorbed on both titanium and type 347 stainless steel without equilibrium being attained. At 250°C, less than 1 min was required for half the plutonium to precipitate from a 1.35 *m* UO<sub>2</sub>SO<sub>4</sub> solution with a Pu(IV) content of 0.1 g per kilogram of H<sub>2</sub>O.

Although the solubility of neptunium in 1.2 *m* UO<sub>2</sub>SO<sub>4</sub> at 275°C under 120 psi of O<sub>2</sub> and 240 psi of H<sub>2</sub> is greater than 100 mg per kilogram of H<sub>2</sub>O, it is encouraging to note that a preliminary value of the Np<sup>239</sup> cross section of <100 barns has been reported. If the cross section is as low as 50 barns, it appears that it will not be necessary to remove the neptunium from the reactor along with the plutonium.

### Thermal-Breeder Fuel and Blanket Processing

An estimate of the cost of chemical processing for the aqueous homogeneous thermal breeder reactor indicated that for a three-reactor station, each reactor 450 Mw, the cost of chemical processing would be about 0.8 mill per kilowatt-hour of electricity produced. The D<sub>2</sub>O and U<sup>233</sup> inventory charges for both reactor and chemical plant will raise the total fuel cost to about 2 mills/kwhr. The scheme of processing found to be the most economical consisted of the removal of insoluble fission and corrosion products by a liquid-solid Hydroclone on a one-day cycle, a thorex plant being used both for blanket processing and con-

trolling the build-up of soluble fission products in the fuel solution.

A study of the radiation hazards of a reactor fuel leak points out the need for processing to control the I<sup>131</sup> concentration in the fuel, as well as concentrations of the rare earths, barium, and strontium.

Studies of the behavior of individual rare-earth fission products indicated that the equilibrium solubility of these elements in the fuel solution is markedly depressed, by the presence of other rare earths, below the previously reported solubility for these elements alone.

Preliminary results indicate that under optimum flow conditions the Dorr TM-3 hydroclone liquid-solid separators will remove 75% of nominal 8-μ thorium oxide from a dilute thorium oxide slurry and 50 to 60% of nominal 4.5-μ thorium oxide. In both cases the thorium oxide slurries used contained a higher percentage (up to 75%) of particles 2 μ or smaller, which probably accounts for the apparently low solid recoveries.

Preliminary equipment flow sheets have been worked out for the HRT chemical processing facility, and cell designs have been completed.

### Summary of Work by Vitro Laboratory

Removal of fluoride from the calcium fluoride column effluent, in the process for removing fission products from a uranyl sulfate core solution, in two steps gave a product with a fluoride content of 0.076 g per kilogram of H<sub>2</sub>O. The solubility of individual rare earths in simulated fuel solution was found to be depressed by the presence of other rare earths.

## PART VI

### SUPPORTING CHEMICAL RESEARCH

#### Radiation Corrosion Studies

A continuation of studies previously reported has produced data which extend the over-all picture of corrosion of type 347 stainless steel by aqueous solutions of uranyl sulfate under reactor irradiation. Both in-pile and out-of-pile experiments are characterized by a rapid initial rate of oxygen consumption followed by a much slower rate. On continued exposure to radiation a second rapid rate, substantially the same as the initial rate, is shown. The period of slow oxygen consumption has been lengthened by a pretreatment which consisted in heating the system for an extended

period outside the reactor before exposing it to the in-pile environment.

Variables which have been suggested as possibly affecting the observed corrosion results, including the presence and absence of chromate and iodine (iodide or iodate), are being studied systematically.

One out-of-pile experiment with a platinum-lined bomb indicated a rapid rate of corrosion for pin specimens, an effect which is believed to be largely electrochemical.

Out-of-pile experiments in all-titanium systems have been started.

#### Thorium Nitrate Radiation Studies

The hydrogen yield and the nitrogen yield from reactor irradiation of 5.8 *m* thorium nitrate solution containing one atom of U<sup>235</sup> for every 500 atoms of thorium have been measured to be 0.25 molecule of H<sub>2</sub> per 100 ev and 0.05 molecule of N<sub>2</sub> per 100 ev. In this case, 81% of the energy has been estimated to be fission energy. These numbers are to be compared with previously determined values of

$$G_{H_2} = 0.04 \text{ and } G_{N_2} = 2 \text{ to } 5 \times 10^{-3}$$

for 5.8 *m* thorium nitrate solution containing no

uranium. In this case, essentially none of the energy is fission energy. Any further increase in the uranium-thorium ratio should not greatly increase the gas yields since most of the energy is already fission energy.

#### Analytical Chemistry Research

A program of research directed toward improving the precision and accuracy of analytical procedures used for samples of highly radioactive homogeneous reactor fuel solutions has been initiated. The precision of presently used procedures for nickel, copper, and uranium, in the absence of radiation, has been evaluated. Relative standard deviations of 0.55, 0.95, and 0.6%, respectively, were measured. Extension to remote-control conditions in the presence of high levels of radioactivity is planned.

#### Np<sup>239</sup> Capture Cross Section

The potential importance of the Np<sup>239</sup> cross section in relation to the production of low g/T plutonium in a homogeneous reactor has prompted an experimental program for determining the value of this cross section. Based on very preliminary data, the capture cross section of Np<sup>239</sup> for LITR neutrons appears to be fairly definitely less than 100 barns.



Part I

EXPERIMENTAL REACTORS

.

.

.

.

.

.

# HOMOGENEOUS REACTOR EXPERIMENT

S. E. Beall, Section Chief  
J. J. Hairston

## DISASSEMBLY OF HRE

The final reactor component was removed from the HRE shield on May 21, approximately 30 calendar days after partial decontamination was completed. Among the tools employed successfully in the course of the disassembly operation were remotely operated socket and end wrenches, an air-powered hack saw, a cutting torch, and an Electro Arc metal disintegrator. A direct-wired television camera and receiving unit proved to be of little value in the confined space of the cells, where proper lighting was difficult.

The recorded data (Table 1) from the various reactor cells indicate the reduction in initial radioactivity resulting from decay and chemical decontamination at the time dismantling was begun on April 8.

All parts containing radioactivity in excess of a few roentgens per hour were stored in a 15-ft-deep water-filled pool; equipment with less radioactivity was either decontaminated for re-use or buried. Early in June, approximately 90 days after the reactor had last operated at 400 kw, the radioactivity levels of various components in the storage pool were measured with a standard Cutie Pie (Table 2). The entire source in these equipment pieces was fission-product radioactivity which had not been removed in the chemical decontamination treatment.<sup>1</sup> Neutron-absorbing shielding surrounding the reactor vessel prevented significant activation of materials in other cells.

After removing and storing the various vessels, valves, and piping, the concrete-block shield was torn down. Most of the 45,000 high-density (3.5) concrete blocks used to construct the 5- to 7-ft-

thick shield were salvaged. Where sections of the block stack had been constructed with mortared joints to support equipment, it was found that shocking the wall with one-quarter-stick charges of dynamite made removal very easy, although the percentage of broken blocks was increased.

By the end of June, no portion of the HRE shielded structure remained, and excavation for the Homogeneous Reactor Test was begun.

## INSPECTION OF REACTOR PARTS

The first component inspected was the 18-in.-dia stainless steel core, which had accumulated a neutron exposure of approximately  $10^{19}$  neutrons/cm<sup>2</sup>. It was possible to drill into the tank through 5 to 8 ft of water and then to cut out a segment roughly 6 in. in diameter by using an air-powered hack saw. This segment contained the core inlet line and was expected to be one of the weakest points with respect to corrosion. Details of the inspection are reported in Part III, Corrosion.

The top portion of the 4-in.-dia schedule-160 pressurizer pipe was removed by cutting with an electric grinder, the abrasive disk operating under water.

The heat exchanger was disassembled by first burning off the head-to-shell bolts and removing the tube bundle and head plate. The head plate was bolted and seal-welded to the tube sheet. After the inlet and exit nozzles were cut off and the bolts were removed, the seal weld was ground out with a grinding disk on a flexible shaft. All this work was done with the heat exchanger submerged in water at a depth of 3 to 5 ft. Discussions were held with Westinghouse and Naval Reactor Branch representatives to decide on a joint program for examining the crevices between the tubes and the carbon-steel tube sheet.

<sup>1</sup>S. E. Beall *et al.*, *HRP Quar. Prog. Rep. Apr. 30, 1954*, ORNL-1753, p 3-6.

TABLE 1. RADIOACTIVITY LEVELS OF CELLS IN THE HRE

Time	Low-Pressure Cell (r/hr)	Reactor Cell (r/hr)	Pump-Heat Exchanger Cell (r/hr)
March 4 (24 hr after shutdown)	1805	629	574
April 8 (after final decontamination)	55	11	22

**HRP QUARTERLY PROGRESS REPORT**

**TABLE 2. RADIATION SURVEY OF COMPONENTS IN STORAGE POOL AFTER PARTIAL CHEMICAL DECONTAMINATION AND 90-DAY DECAY**

Component	Positions	Reading (r/hr)	Shielding
Main circulating pump	Intake flange	2	4 $\frac{5}{8}$ in. of air
	Discharge flange	2	4 $\frac{5}{8}$ in. of air
	Impeller-housing flange	1	At contact
	Rear	1	4 $\frac{5}{8}$ in. of air
Fuel feed pump	Discharge flange	0.60	At contact
	Filter	4.5	4 $\frac{5}{8}$ in. of air
	Check housing	5	At contact
High-pressure gas bleed valve	Low-pressure flange	0.80	At contact
	High-pressure flange	0.72	At contact
	Top of operator	0.04	At contact
Steamer pot, fed by condensate from dump-tank steam	Top of pot	2	At contact
	Middle of pot	2.8	At contact
	Bottom of pot	0.80	At contact
Off-gas condenser, vapors from catalytic recombiner	Top of condenser	1	At contact
	Middle of condenser	0.60	At contact
	Bottom of condenser	0.70	At contact
Steamer pot, fed by condensate from flame recombiner	Top of pot	1	At contact
	Middle of pot	1	At contact
	Bottom of pot	1	At contact
Gas condenser, for steam from dump-tank evaporator	Top (near the leak)	5.2	At contact
	Middle of condenser	1.2	At contact
	Bottom of condenser	1.4	At contact
Fuel dump valve and attached lines	Rupture-disk flange	3	At contact
	Open lines on rupture disk	2.2	At contact
	Low-pressure flange	3	At contact
	Top of operator	1	At contact
	High-pressure flange	1	At contact
	Valve seat	4	At contact
Flame recombiner	At spark plugs	6	At contact
	Middle of recombiner	0.30	At contact
	Bottom of recombiner	1.5	At contact
Core-to-dump-tank let-down heat exchanger	Top line	3	Through 10 in. of water
Core-to-dump-tank throttling valve	Top of operator	0.30	At contact
	Middle of valve	0.90	At contact
	Valve seat	3	At contact
	Low-pressure flange	0.30	At contact
Main-heat-exchanger tube bundle	At U section of tubes	2.4	Through 13.5 in. of water

## HOMOGENEOUS REACTOR TEST

S. E. Beall, Project Engineer

S. I. Kaplan

### OPERATIONAL PLANNING

The Homogeneous Reactor Test (HRT) is the experimental reactor facility being designed and constructed at ORNL as the step in homogeneous reactor development between the 1-Mw HRE and a "full-scale" power station. The HRT will provide an integrated test at 5 to 10 Mw for the flow-sheet and equipment designs on which the full-scale effort will be based. Furthermore, its design is such that several homogeneous systems (e.g., slurries, thermal breeder, and plutonium producer) may be tested with comparatively minor modifications of the original reactor installation.

During the past quarter, the status of several desirable experiments has been evaluated to determine the most logical order of demonstration. Table 3 is the result of this deliberation. The first experiment is intended to prove the basic component design as well as over-all long-term operational reliability and ease of maintenance. Evaluation of the concept of continuous chemical processing will also be included.

This quarterly report is primarily concerned with the first experiment, the study of basic operational

problems of aqueous homogeneous systems. At the present time, the design and procurement of equipment and materials for the HRT installation are approximately 60% complete. Orders have been placed or contracts awarded for the following items:

Item	Approximate Cost
Installation of steel-lined reactor pit	\$238,388
Core and pressure vessel	90,000 (est)
Main heat exchangers (2)	58,302
Circulating pumps (4)	120,000 (est)
Seamless, type 347 stainless steel pipe, 1/4-in. IPS to 24-in.-OD IPS	72,000
Type 347 stainless steel flanges and butt-welding fittings, 1/4-in. IPS to 24-in.-OD IPS	35,000
Gaskets, bellows, bolting, etc., for above	4,000
<b>Total</b>	<b>\$ 617,690</b>

TABLE 3. EXPERIMENTS PLANNED FOR THE HRT FACILITY

Power levels, up to 10 Mw  
 Temperatures, up to 300°C  
 Pressures, up to 2000 psi

Experiment	Period	Purpose	Fuel	Blanket	Other
1	1955	1. Demonstrate operational reliability and ease of maintenance	U <sup>235</sup> as UO <sub>2</sub> SO <sub>4</sub>	D <sub>2</sub> O	Zr core tank; type 347 stainless steel circulating system
	1956	2. Demonstrate continuous removal of fission products from fuel	in D <sub>2</sub> O		
2	1956	1. Demonstrate concept of slurries for thermal breeders	U <sup>233</sup> as UO <sub>2</sub> SO <sub>4</sub>	Thoria slurry	Zr core tank; type 347 stainless steel circulating system
	1957	2. Demonstrate chemical process to remove U <sup>235</sup> from thorium	in D <sub>2</sub> O		
3	After 1957	1. Demonstrate production of weapons-grade plutonium	U <sup>235</sup> as UO <sub>2</sub> SO <sub>4</sub>	U <sup>238</sup> as UO <sub>2</sub> SO <sub>4</sub>	Zr core tank; stainless steel or titanium circulating system
		2. Demonstrate continuous separation of plutonium	in D <sub>2</sub> O	D <sub>2</sub> O	

**HRP QUARTERLY PROGRESS REPORT**

A detailed schedule listing the completion deadlines for major phases in the design and construction of all HRT components was published<sup>2</sup> on June 8, 1954. The reactor is to be completely assembled, tested, and ready for start-up by January 1, 1956; the intervening time has been proportioned so as to permit early starting of the initial construction phases while allowing the maximum development time for the more complex components such as letdown valves, pumps, and heat exchangers.

The construction calendar shown in Fig. 1 is based upon the use of stainless steel components for the fuel and blanket systems, with a zirconium-alloy core. Designs for most major reactor components were completed by July 31, 1954, as scheduled. After construction of the steel-lined reactor pit is completed in November 1954, installation of the reactor will commence with the placement of the low-pressure fuel system vessels and will continue with the mounting of low-pressure blanket vessels while the fuel vessels are being piped together. The installation of components

of the high-pressure fuel and blanket systems and the subsequent assembly of the circulating loops are expected by the fall of 1955, as shown in Fig. 1.

**HRT DESIGN**

R. B. Briggs, Section Chief

- |                   |                           |
|-------------------|---------------------------|
| R. E. Aven        | J. R. McWherter           |
| R. H. Chapman     | R. G. Pitkin <sup>3</sup> |
| R. D. Cheverton   | J. N. Robinson            |
| W. R. Gall        | C. L. Segaser             |
| P. N. Haubenreich | W. Terry                  |
| J. W. Hill, Jr.   | T. H. Thomas              |
| T. H. Mauney      | R. Van Winkle             |
| F. C. Zapp        |                           |

**FLOW SHEET AND GENERAL DESIGN CONSIDERATIONS**

During this quarter the problems of building the HRT to serve also as a pilot plant for the development of chemical processes for producing fissionable materials were studied in some detail.

<sup>2</sup>S. I. Kaplan, *HRT Schedule*, memorandum to distribution, June 8, 1954.

<sup>3</sup>On loan from Vitro Corporation.

OFFICIAL USE ONLY  
ORNL-LR-DWG 2780

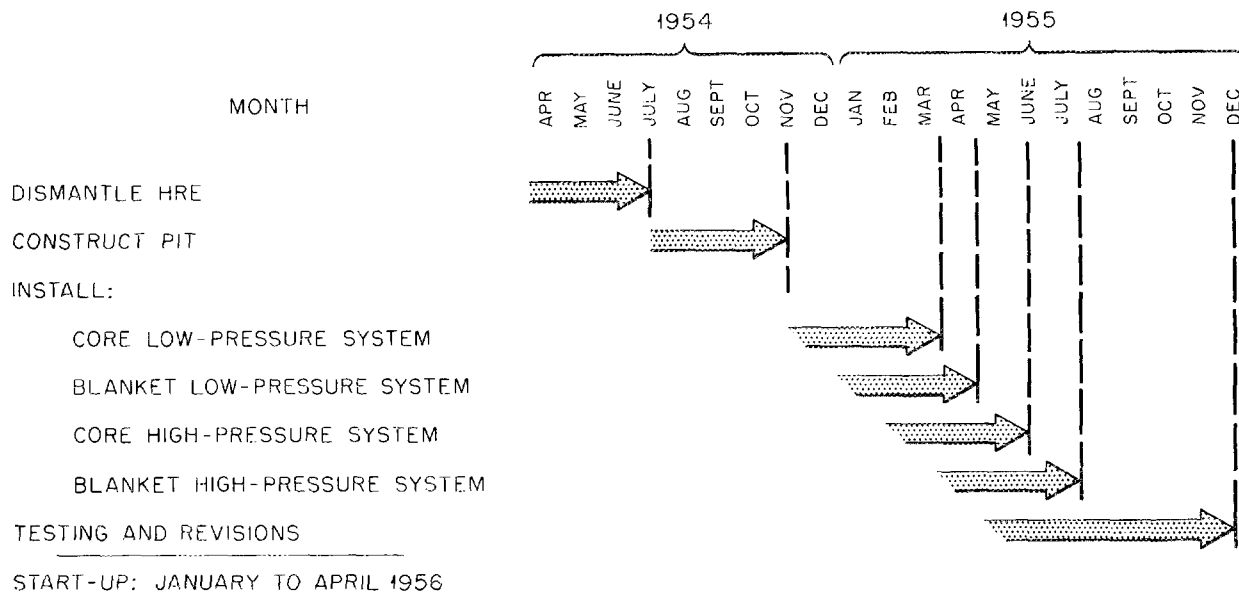


**Fig. 1. Calendar for Completion of Construction of HRT Components.**

It became evident that designing and procuring the titanium equipment necessary to handle the concentrated uranyl sulfate solutions required for plutonium production in the blanket would delay the construction of a reactor by many months. Development of methods and equipment for handling thorium oxide slurries for producing  $U^{233}$  would result in similar delays. Although the demonstrations of these two reactor concepts remain as important future goals, the general operational problems of aqueous homogeneous reactors were deemed sufficiently important to speed the design and construction of a system based on the original HRT concept, that is, a two-region reactor with a dilute  $D_2O$ -uranyl sulfate solution in the core and a  $D_2O$  blanket, with stainless steel being used as the material of construction in all but a few critical places.

The most recent flow sheet for the HRT is shown in Fig. 2, and a flow sheet for the steam system is shown in Fig. 3. Design data for the HRT are presented in Table 4.

The reactor is designed to operate at a maximum temperature of  $300^\circ C$  and pressure of 2000 psia to produce 5 Mw of heat in the core. Copper will be included in the fuel to catalyze the recombination of most of the  $D_2$  and  $O_2$ . Some gas will be discharged to the low-pressure system to remove  $Xe^{135}$  and the other gaseous fission products. Designs of the high-pressure circulating system and the low-pressure system for the core are duplicated for the blanket, with some changes in equipment size to accommodate the larger volumes of blanket fluid.

The steam system for the HRT is somewhat more complicated than that used for the HRE. An air-cooled condenser is specified that can condense all the steam generated in the reactor heat exchangers. All the steam will be delivered to this condenser during the low-power experiments and during experiments in which the power is varied rapidly over a wide range. During periods of continuous operation of the reactor at design power levels, part of the steam will be diverted to the turbogenerator used on the HRE to develop its full 350-kva capability. The turbogenerator can also be operated on plant process steam to provide emergency power for the reactor.

#### REACTOR AREA, BUILDING, AND CELLS

The concept of the reactor area has progressed to a point where final design drawings are being

prepared for modification of Building 7500 and for the reactor shield. A plot plan is shown in Fig. 4. Plan and elevation of Building 7500, including the reactor cell, control gallery, and a preliminary proposal for the chemical processing area, are presented in Figs. 5 and 6.

The requirements which govern the design of the HRT reactor shield, in the order of importance, are:

- (1) safety,
- (2) satisfactory installation, operation, and maintenance of the reactor,
- (3) minimum design time,
- (4) flexibility,
- (5) economy.

Not only must the radiation to which personnel are subjected during normal operation be kept within standard tolerances, but every probable contingency must be investigated and evaluated so that personnel will never be in danger.

The schedule for the HRT necessitates complete design of the reactor cell before the components of the reactor are completely designed. It is also proposed that this cell be capable of housing future experimental reactors. These requirements call for a versatile design which will permit installation, operation, maintenance, and alteration of the HRT as well as of a later reactor of similar size, without major changes being made in the cell structure.

It is desired that the methods for meeting the above requirements be consistent with maximum economy, since the ultimate goal of the Project is the production of economical power.

The reactor cell is to be set in a pit, the top of the reactor shield being flush with the building floor. This arrangement will result in maximum use of available space and facilities and in economy of shielding materials, for only the upper portion of the reactor must be shielded.

About 7 ft of barytes concrete or equivalent shielding must be provided between the reactor and personnel, and about 5 ft of shielding is needed between the reactor auxiliaries and personnel.

The structural design of the reactor cell was largely dictated by the necessity for containing the fuel and blanket in the most severe accident conceivable — a brittle failure of the reactor vessel — which is only a remote possibility. Release of the fuel and blanket in such a failure would cause a maximum pressure rise in the cell of about 22.5 psi, and it was found that an economical design would result if the cell normally

TABLE 4. HRT DESIGN BASIS

	Core	Blanket
Power, kw	5000	220
Pressure, psia	2000	2000
Vessel ID, in.	32	60
Vessel thickness, in.	$\frac{1}{4}$	4.4
Blanket thickness, in.		$13\frac{3}{4}$
Vessel material	Zircaloy-2	Stainless-steel-clad carbon steel
Vessel volume, liters	290	1550
Specific power, kw/liter	17.3	0.142
Solution circulating rate, gpm	400 at 256°C	230 at 278°C
Inlet temperature	256°C (494°F)	278°C (533°F)
Outlet temperature	300°C (572°F)	282°C (539°F)
Solution	UO <sub>2</sub> SO <sub>4</sub> -D <sub>2</sub> O + CuSO <sub>4</sub>	D <sub>2</sub> O + CuSO <sub>4</sub>
Uranium concentration, g/kg of D <sub>2</sub> O	10.4	
Uranium enrichment, % U <sup>235</sup>	93	
Heat capacity (2000 psi), Btu/lb·°F	1.24 (Av from 494 to 572°F)	1.24 at 539°F 1.23 at 533°F
Thermal conductivity, Btu/hr·ft <sup>2</sup> (°F/ft)	0.35 at 536°F	0.337 at 536°F
Viscosity, lb/hr·ft	0.24 at 300°C 0.29 at 256°C	0.260 at 282°C 0.263 at 278°C
Density, lb/ft <sup>3</sup>	50.60 at 300°C 55.90 at 256°C	52.2 at 282°C 52.6 at 278°C
G for D <sub>2</sub> O decomposition, molecules of D <sub>2</sub> per 100 ev	1.67	0.5
Rate of formation* of D <sub>2</sub> , lb moles/sec	0.00179	0.000024
Rate of formation* of O <sub>2</sub> , lb moles/sec	0.00089	0.000012
Vapor pressure of D <sub>2</sub> O over solution, psia	~1246 at 300°C	~924 at 280°C
Compressibility factor of D <sub>2</sub> O vapor	0.702 at 300°C	0.702 at 300°C
Heat of recombination of D <sub>2</sub> and O <sub>2</sub> , Btu/min	11,300 (199 kw)	297 (5.2 kw)
Heat of vaporization of D <sub>2</sub> O, Btu/lb	550 at 300°C (11,000 Btu/lb mole)	600 at 282°C (12,000 Btu/lb mole)
Gas dissolved in solution leaving at 2000 psia		
Gram moles of D <sub>2</sub> per liter	0.10 at 300°C	0.13 at 282°C
Gram moles of O <sub>2</sub> per liter	0.05 at 300°C	0.06 at 282°C
Volume of gas (D <sub>2</sub> and O <sub>2</sub> ) generated,* ft <sup>3</sup> /sec		
At 2000 psia	0.0148 at 300°C	0.00019 at 282°C
At STP	0.963	0.0128
CuSO <sub>4</sub> (recombination agent) to recombine 100% of gas, gram mole/liter	0.005	0.00004

\*Without internal catalyst.

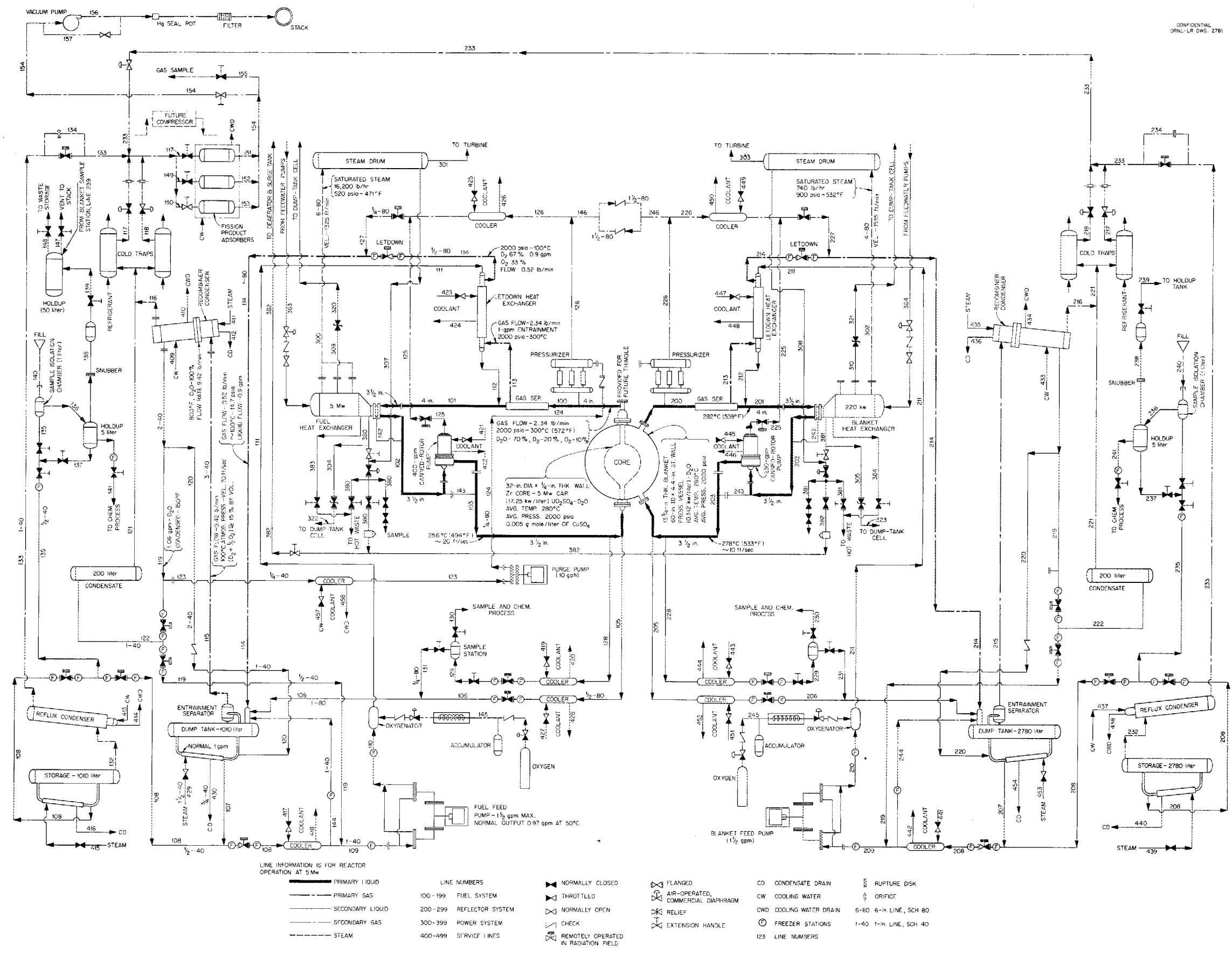


Fig. 2. HRT Reactor Flow Sheet.

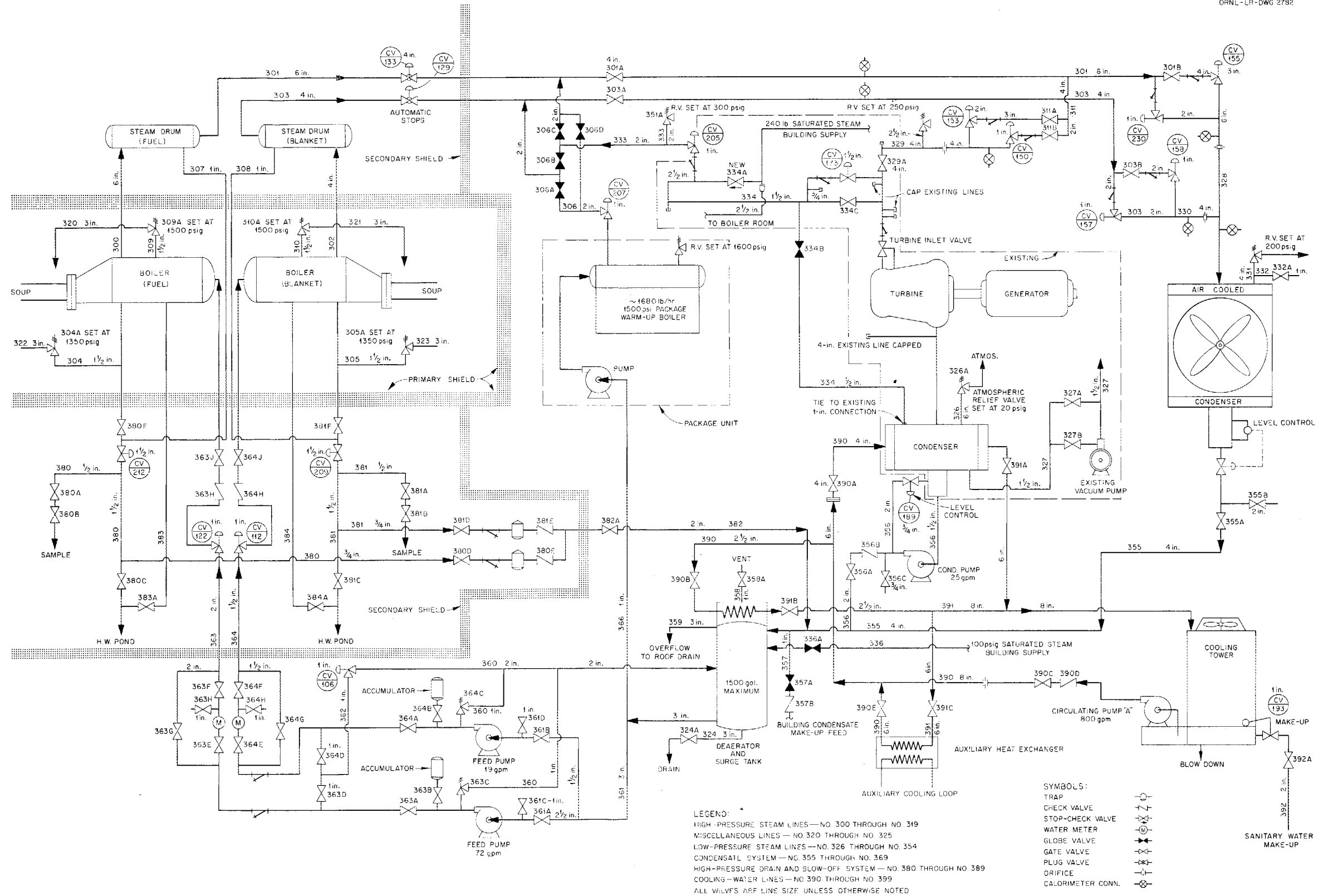


Fig. 3. HRT Steam-System Flow Sheet.

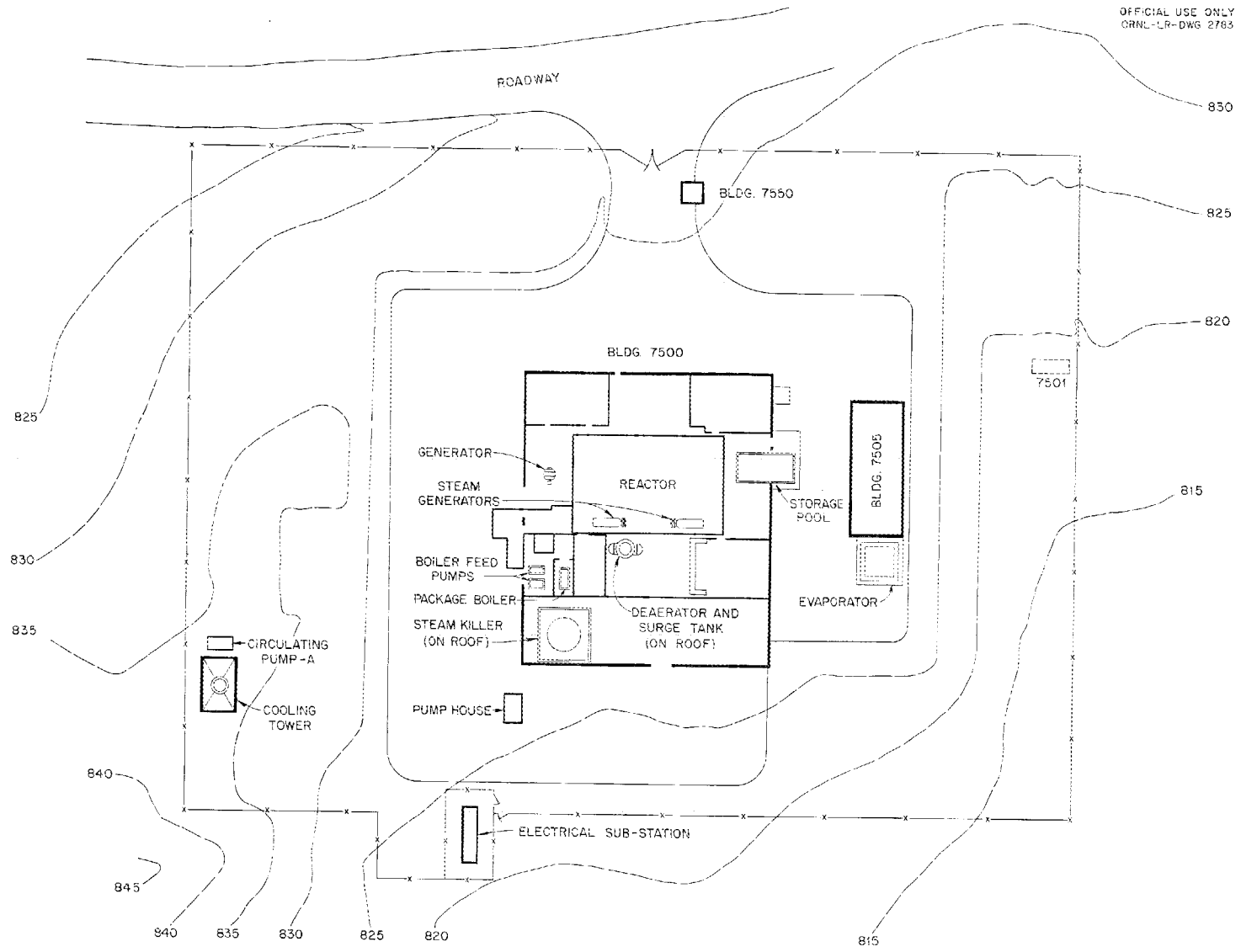


Fig. 4. Plot Plan of Reactor Area.

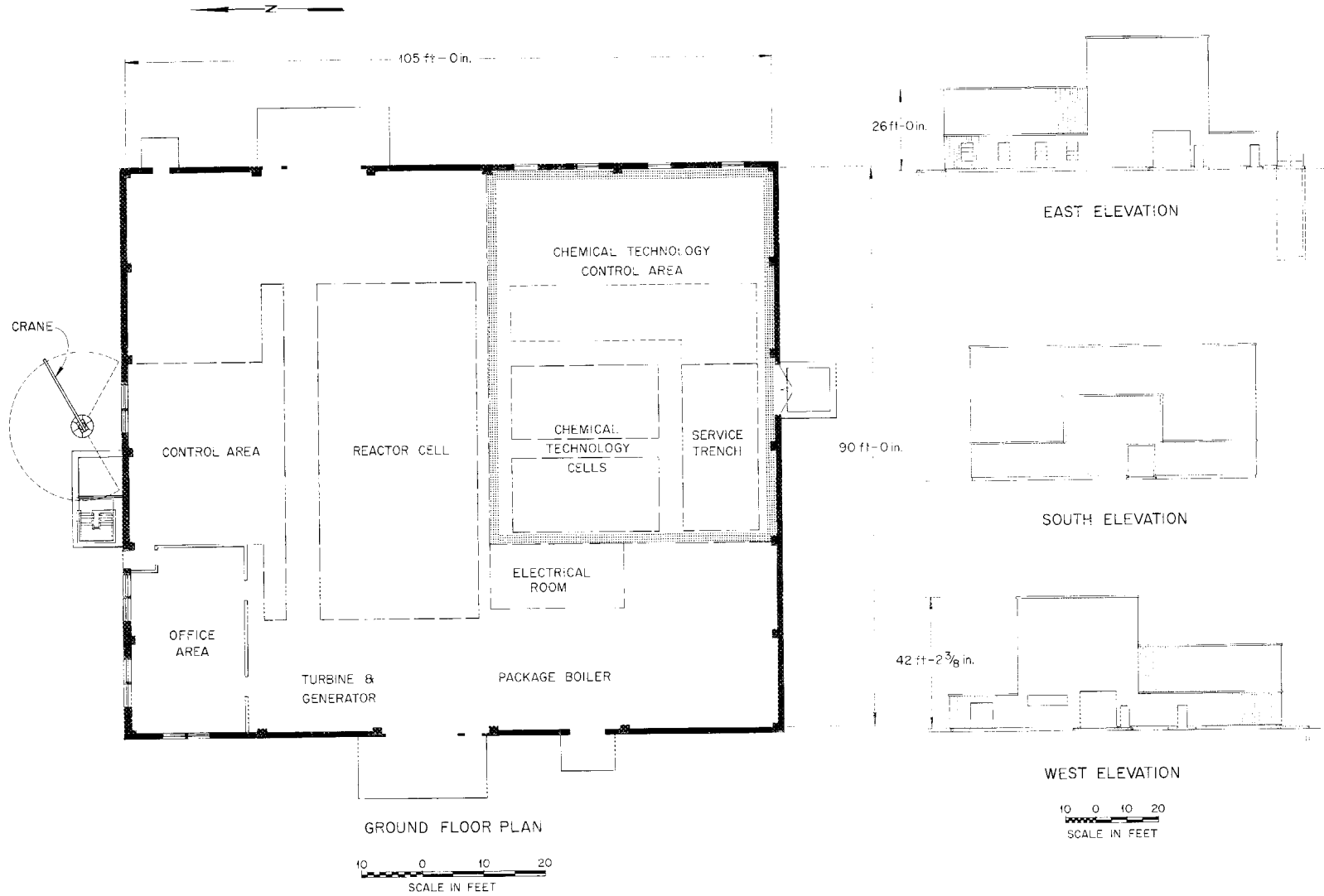


Fig. 5. Plan and Elevations of Building 7500.

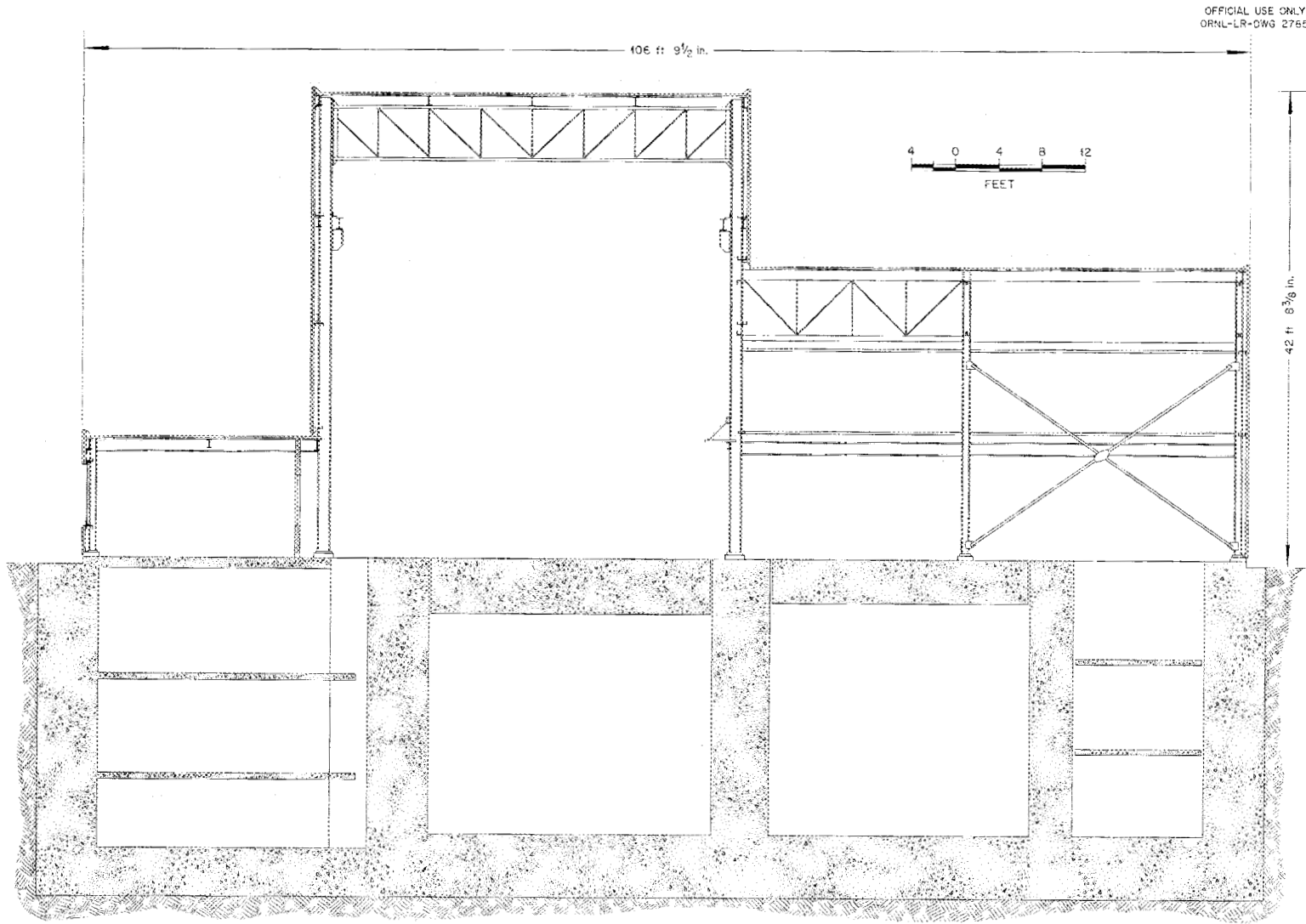


Fig. 6. Structural Details for Building 7500.

## HRP QUARTERLY PROGRESS REPORT

operated at 7 psia, which would permit a rise to 30 psia or about 15 psig. A pressure of over 7.5 psig would lift the 5-ft-thick roof plugs; therefore it is necessary to anchor the plugs to resist the higher pressure.

The cell is being designed as a structural-steel tank, with stainless steel cladding on the floor and the lower 4 ft of the wall. A steel tank was selected instead of the concrete tank proposed originally because it was competitive costwise and had other inherent advantages. Steel is a more reliable structural material and is more elastic than concrete. It was believed that a contraction during setting of the concrete, earth settlements, porosity in the concrete, earth tremors, or the blast resulting from a reactor failure might permit leakage into or out of the cell, whereas steel could, through its elasticity, absorb these effects without harm. Cladding of light-gage metal on concrete is a difficult and expensive job, and the absence of leaks is never certain, whereas steel plate can be furnished with a cladding and can be welded with assurance of leaktightness.

In order to facilitate the installation of pipes and conduits passing through the control-room side of the reactor cell, it was decided that the wall should be a 5½-ft-thick tank, filled with a mixture of barytes aggregate and water. A pipe can be run through the wall at any location by burning a hole in the wall, putting the pipe in place, and seal-welding the pipe to the wall.

The reactor cell is being separated into two equal compartments by a watertight partition to permit flooding either half with water for underwater maintenance. This partition will be provided with a sliding door to permit flow of air or gases in normal operation or in an emergency. Each half of the cell will be provided with two space coolers to remove heat which results from attenuation of radiation or from leakage through insulation. Strips of space are being left open along the cell column lines to permit addition of shielding partitions if these are necessary later to permit personnel access for maintenance.

Two feet of shielding will be provided immediately around the reactor in the form of a spherical shell filled with borated water or with barytes, sand, and water. Cooling water will be circulated in the tank to remove the heat generated by the attenuation of radiation. A perforated steel shell will be included around the reactor to retain frag-

ments which would otherwise be dangerous as missiles. The proximity of the shield to the reactor reduces the problem of activation of argon in the air and effects an economy of shielding material.

If it is assumed that the radioactive material is uniformly dispersed throughout the shield after a release of fuel, the rate of outleakage under the pressure differential must be such that contamination in the building is within an acceptable personnel tolerance. The total outleakage is influenced by two factors — the tightness of the sealing system and the length of time that the cell remains at a positive pressure. Two methods of sealing the cell are presently under consideration: (1) sealing all joints with Neoprene gaskets and (2) providing a layer of steel plates between the two layers of roof plugs and seal-welding the joints in the plates. The welded-steel-plate scheme shows the greatest promise of limiting the leak rate to a satisfactory value. To limit the time at which the cell remains at a positive pressure, it is proposed to provide a system of spray nozzles. Actuated by the pressure rise, the nozzles would spray a fog of cooling water into the cell from above, which would reduce the temperature and pressure and settle the radioactive materials.

The present Building 7500 will be extended southward 25 ft to include space for chemical processing facilities. These facilities will consist of cells similar to the reactor cell, serviced by an overhead crane, and of an operating area. Details of this facility have not been developed sufficiently for inclusion in this report.

### REACTOR EQUIPMENT AND EQUIPMENT ARRANGEMENTS

Designs proposed for major equipment items and layouts of equipment in the reactor cells have been presented in previous quarterly reports.<sup>4,5</sup> Beginning with this report the status of the design of major components and systems will be presented, but drawings of the equipment will be included only after review and at least tentative acceptance by the HRT Design Review Committee. In this way it is hoped to minimize the confusion which results from the successive reporting of many different designs for a particular piece of equipment.

<sup>4</sup>R. B. Briggs *et al.*, *HRP Quar. Prog. Rep. Jan. 31, 1954*, ORNL-1678, p 21.

<sup>5</sup>R. B. Briggs *et al.*, *HRP Quar. Prog. Rep. Apr. 30, 1954*, ORNL-1753, p 22.

### REACTOR VESSEL AND CORE TANK

The design of the reactor vessel and core tank remains essentially the same as reported previously.<sup>5</sup> A mock-up of the reactor is being fabricated by the Newport News Shipbuilding & Dry Dock Co. for use in relating the stresses and stress distribution in the core tank to differences in pressure between the liquid in the core tank and that in the blanket surrounding the core. The tests are scheduled for August.

Fabrication details are being developed for both the core tank and the pressure vessel. Detailed analyses are being made of proposals for the flanged connection between the zirconium core tank and the stainless steel connecting piping. The firm proposal for the reactor will be discussed in the next quarterly report.

### PRESSURIZER

Drawings of designs for the pressurizer, heaters, and level indicator were included in the previous quarterly report<sup>5</sup> with a discussion of the problems of balancing the pressure between the core and blanket of a two-region reactor. The present concepts are the same, except that the vapor volume of 30 liters has been increased to 60 liters in both the blanket and the core pressurizers. Preliminary kinetics calculations indicate that a combined volume of 120 liters will be sufficient to limit the pressure rise there to 100 psi when 53 liters of liquid is expelled from the core during the most severe probable power surge. More detailed calculations will be done on the ORACLE to confirm the preliminary results.

A part of the pressurizer problem is that of regulating the pressure in the core and the blanket systems while the fluids are being dumped to the low-pressure storage tanks. Although the vapor spaces of the core and the blanket pressurizers will be joined with a pipe to equalize the pressures, it is desired that the dumping of fluid be controlled so that there will be little or no transfer of vapor (and entrained liquid) between systems.

Studies have been made under the assumption that there is no open connection between pressurizers. Figure 7 shows the calculated pressure vs time relationships that would exist if no attempt were made to control the flow from either system during a dump through the lines as presently sized. Pressure differences greater than allowable between core and blanket would exist in a "free

dump," but calculations indicate that a reasonably good pressure balance can be obtained by appropriate throttling of dump valves with a differential-pressure instrument slaved to a rate-of-pressure-change instrument.

Data from two HRE dump tests have been used to check the accuracy of the method of predicting pressure as a function of the fraction of the initial contents dumped from the system. It has been found that the calculated pressures are lower than the observed values during the initial stages and that good agreement is obtained for the last half of the dump. Because of the lack of conclusive experimental and theoretical work in the realm of discharging saturated or nearly saturated water through a dumping line and valve and because of the non-steady-state conditions that obtain during dumping, it is necessary to construct an apparatus to simulate the problem. A model which will have similar proportions of liquid and vapor, dimensionally similar dump lines, valves, and pressure-relief system, and similar controls throughout is being designed and will be constructed by October. An existing autoclave whose volume is approximately 6% of the HRT volume is being modified to serve as the outer pressure vessel for the dump test apparatus. This equipment will be used to

- (1) obtain pressure data for a variety of dumping tests,
- (2) determine the feasibility of controlling pressures and pressure differences under all conceivable dumping conditions,
- (3) obtain fundamental data on flow of flashing mixtures,
- (4) demonstrate operation of the proposed pressure-relief system that connects the vapor spaces of the core and blanket pressurizers and determine the entrainment or liquid carry-over that might result when this pressure-relief system has to function,
- (5) provide the opportunity to test sensitivity and reliability of pressure-control instruments during normal operation of the pressurizers.

### GAS SEPARATOR

The final design of the gas separator, pending results of tests at high temperature and pressure, is shown in Fig. 8. It must separate 1 vol % of  $D_2$ ,  $O_2$ , and  $D_2O$  vapor from 400 gpm of  $D_2O$ , and it is designed for an efficiency greater than 95%. The separator is similar to the one discussed in

HRP QUARTERLY PROGRESS REPORT

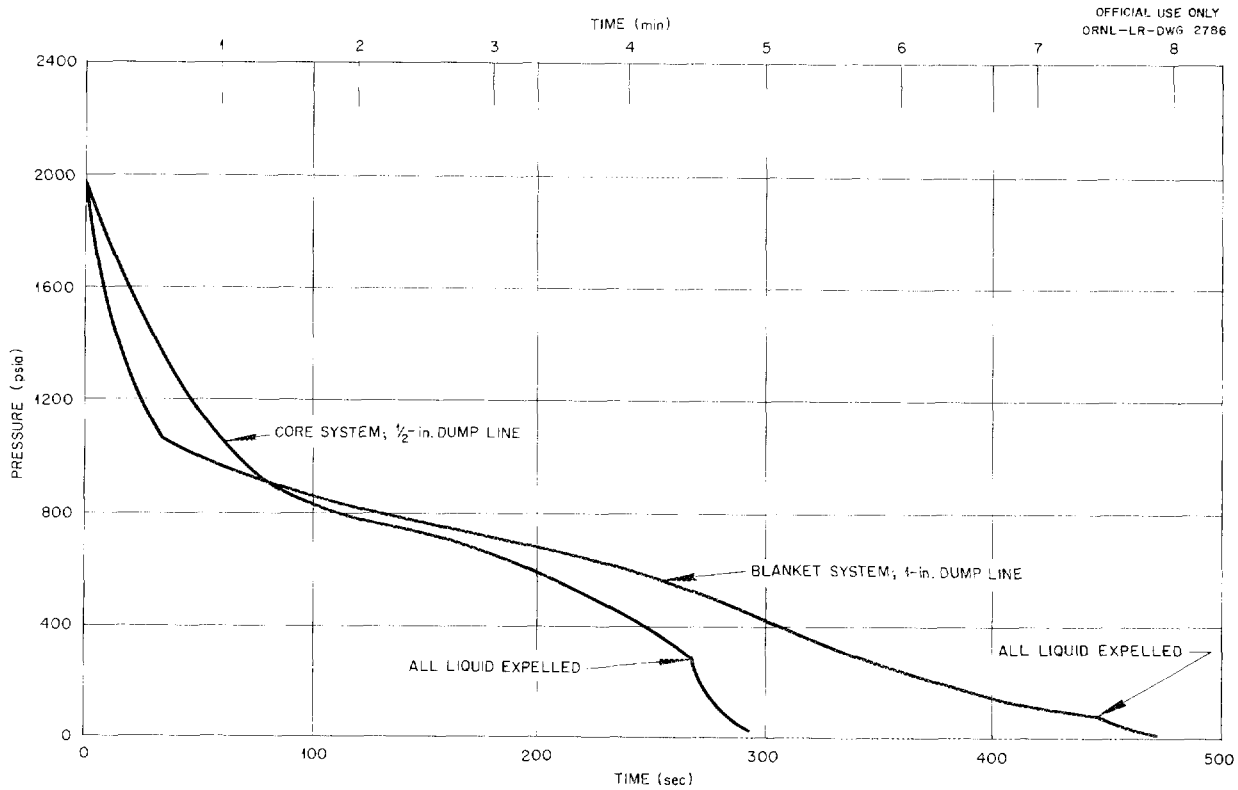


Fig. 7. Calculated Pressures During an Uncontrolled Dump of the HRT Core and Blanket Systems.

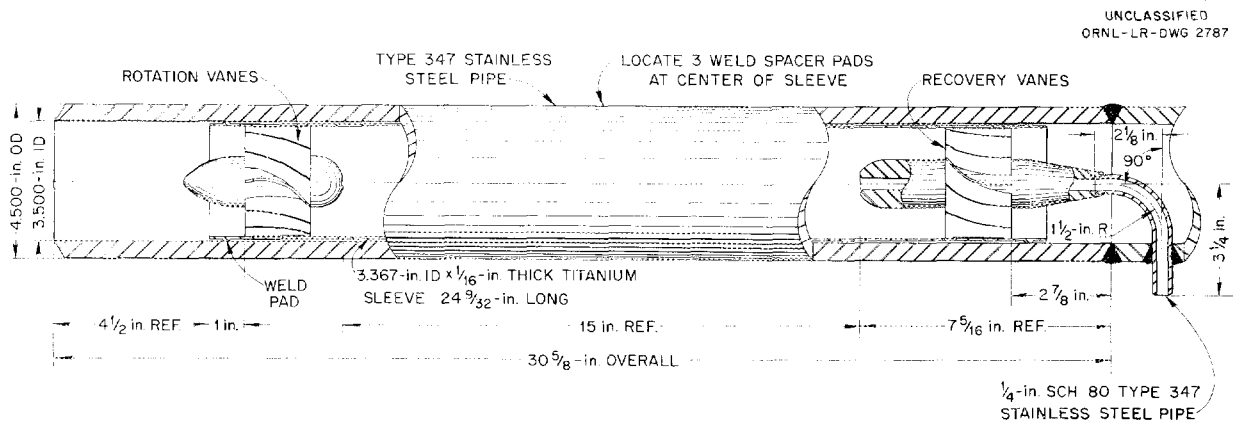


Fig. 8. HRT Gas Separator.

previous reports except that the vanes, nozzles, and a sleeve which are in contact with high-velocity fluid are made of titanium to minimize corrosion.

#### MAIN HEAT EXCHANGERS

A contract is being negotiated with the Foster Wheeler Corp. for the fabrication of the heat exchangers for the core and blanket systems at a cost of \$29,300 each. Foster Wheeler design engineers are preparing shop drawings for the exchangers with some modification of the design reported in ORNL-1678. Details of the final design will appear in the next quarterly report.

#### DUMP TANKS, EVAPORATORS, AND VAPOR SEPARATORS

The final design, pending results of tests, of the fuel dump tanks, evaporator, and vapor separator is shown in Fig. 9. The tanks are schedule-30 stainless steel pipe, 16 ft 10 in. long, including end caps, and 14 in. in diameter. They are connected, as shown, by 4-in. schedule-40 stainless steel pipes which are jacketed over 12 ft of the inclined lengths. The jacketed pipes are the evaporators which are used to supply steam to dilute the decomposition gases below the explosive limit before they enter the recombiner, to change the fuel concentration in the reactor, and to keep the materials in the tanks thoroughly mixed. Each pipe is designed to evaporate  $\frac{1}{2}$  gpm of  $D_2O$  with 75-psig steam in the jacket and is estimated to circulate 45 gpm of liquid. The total volume of the tanks is 900 liters, and the piping and evaporators contain an additional 100 liters of "ever-safe" storage capacity. Seven hundred liters of fuel solution will be stored in the tanks.

Identical tanks, with slight modification of the 4-in. piping, will be used for the fuel outer dump tanks. The inner and outer blanket dump tanks will be similar to the fuel tanks except that they will be fabricated of 24-in. schedule-30 stainless steel pipe and will have a volume of 2800 liters, including evaporators and piping. There will be 2000 liters of  $D_2O$  stored in the blanket tanks.

A separator has been included to reduce the entrainment of liquid in the steam passing to the

recombiner to 1 ppm. This is done to minimize the collection of uranium in the catalyst bed. The separator is a 12-in. schedule-40 stainless steel pipe containing baffles and wire mesh. Vapor and entrained liquid enter the separators through tangential inlets to remove large particles. Most of the remaining entrainment is separated by means of corrugated plates and successive 6-in. thicknesses of coarse and fine wire mesh, which are washed by a small amount of  $D_2O$  condensed on a coil in the top of the separator. More complete details of the dump tanks, evaporators, and separator have been reported.<sup>6,7</sup>

#### CATALYTIC RECOMBINER-CONDENSER

A design for the catalytic recombiner-condenser was reported in ORNL-1753. Some changes are being made in the design; these involve increasing the length and decreasing the diameter and number of tubes in order to obtain better desuperheating of the steam from the recombiner. The final design will be discussed in the next quarterly report.

#### EQUIPMENT LAYOUTS

The most recent arrangement of equipment in the reactor cell to conform to changes made in construction of the cell is shown in Figs. 10, 11, and 12. Only those components associated with the fuel system are shown, but a similar arrangement is proposed for the blanket. A part of each cell will be left vacant for later installation of equipment for recombining decomposition gases and for removing gaseous fission products at high pressure. The layout has been approved for detailing.

#### STEAM SYSTEM

The detailed design of the steam system is proceeding on the basis of the flow sheet shown in Fig. 3. It is expected that the details will be completed before September 1.

<sup>6</sup>C. L. Segaser, *Continuation of HRT Fuel Solution Evaporator Study*, ORNL CF-54-6-31 (June 4, 1954).

<sup>7</sup>C. L. Segaser, *HRT Entrainment Separator Design Study*, ORNL CF-54-7-122 (July 23, 1954).

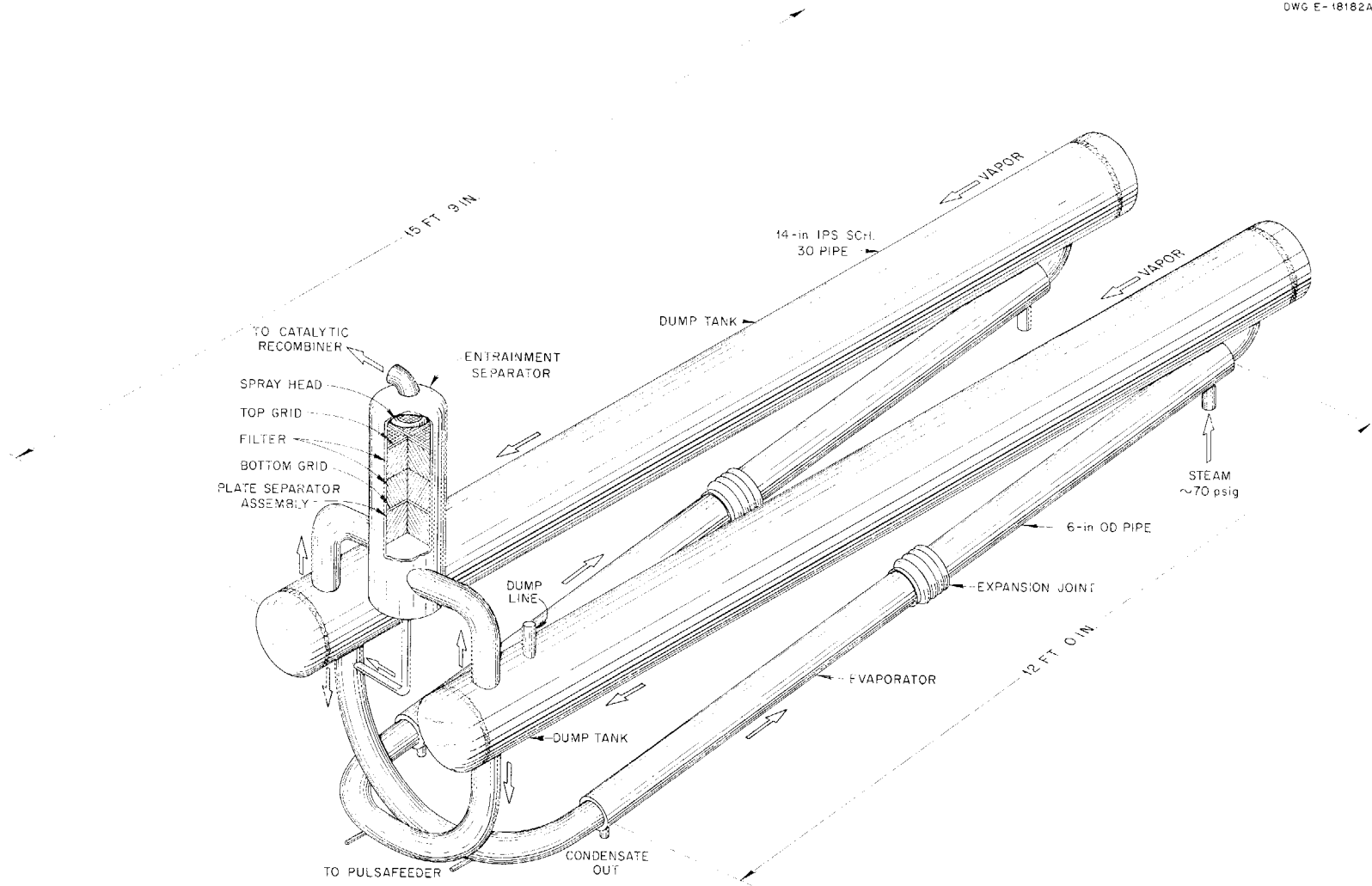


Fig. 9. Arrangement of Dump Tanks, Evaporator, and Entrainment Separator for HRT.

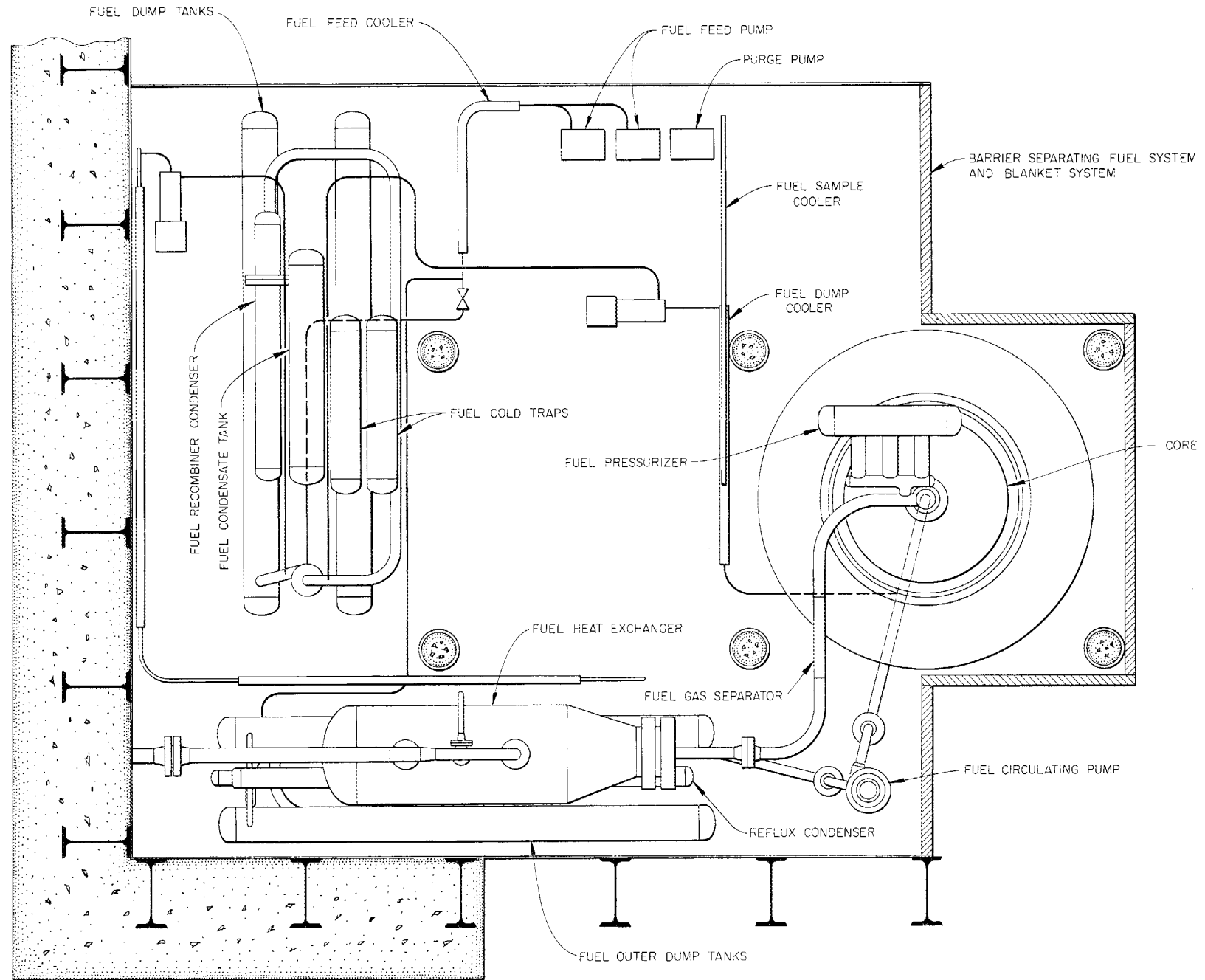


Fig. 10. Plan of HRT Equipment Layout.

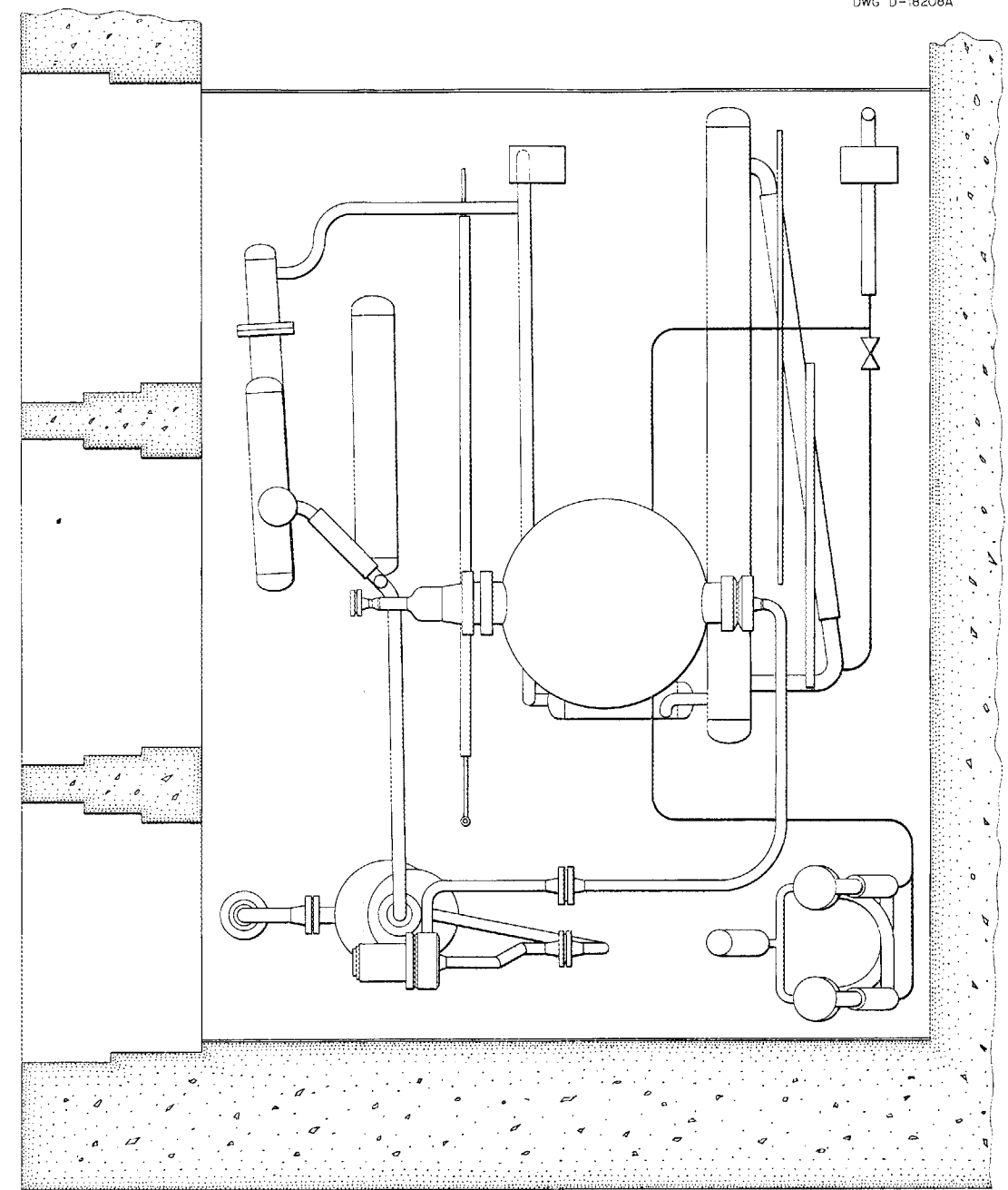


Fig. 11. Elevation of HRT Equipment Layout.



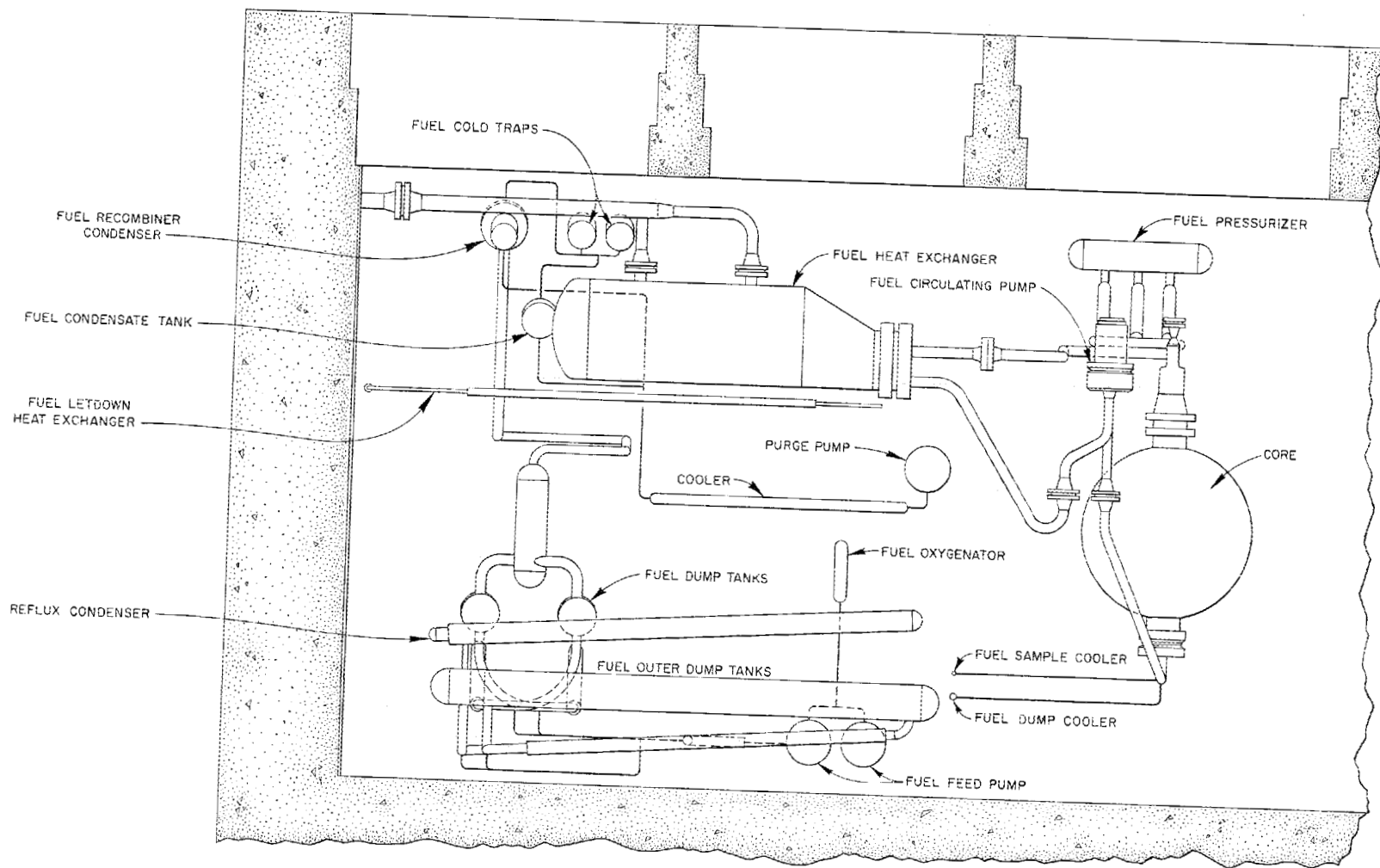


Fig. 12. South Elevation of HRT Equipment Layout.

# HRP QUARTERLY PROGRESS REPORT

## HRT NUCLEAR CALCULATIONS

M. C. Edlund, Section Chief

T. B. Fowler            P. M. Wood  
L. C. Noderer           S. Visner<sup>8</sup>

## HRT BREEDING POSSIBILITIES

Due to its rather small diameter (32-in. core, 60-in. pressure vessel), the HRT operating with  $U^{233}$  fuel at 280°C and containing 1349 g of thorium per kilogram of  $D_2O$  in the blanket will be a mixed thermal-resonance reactor in which about one-third of the fission captures occur in the resonances of  $U^{233}$ . Hence, there exists a considerable uncertainty in the theoretical breeding ratio because of a lack of precise information on the capture-to-fission ratio,  $\alpha$ , for the resonances and the details of the resonance structure.

Estimates of the initial breeding ratio of the HRT at 280°C, based on several assumed average values of  $\eta$  for resonance captures, in which a total resonance integral of 400b and  $\eta$  (thermal) = 2.32 was assumed, are as follows:

$\eta$ (resonance)	Breeding Ratio
2.32	1.02
2.10	0.96
1.90	0.92
1.70	0.87

Although the critical fuel concentration and hence the uncertainty in the breeding ratio can be decreased by lowering the thorium concentration in the blanket, the breeding ratio falls below unity because of increased neutron leakage.

The uncertainty in the breeding ratio can be reduced by either (1) lowering the operating temperature of the reactor to 200°C or less or (2) increasing the core diameter to above 32 in.

The critical concentration of the HRT is markedly dependent on temperature because of its small size and the density effect on the migration length of neutrons in  $D_2O$ . A decrease in the temperature from 280 to 200°C reduces the critical concentration and the uncertainty in the breeding ratio by a factor of about 2. Estimates of the breeding ratio for the HRT, if  $\alpha$  is assumed to be independent of neutron energy, corresponding to  $\eta = 2.32$ , are given as a function of reactor temperature in

<sup>8</sup>HRT Section.

Fig. 13. At 200°C, the breeding ratio is estimated to be 1.12 for  $\eta$  (resonance) = 2.32 and 1.07 for  $\eta$  (resonance) = 1.70.

Breeding at an operating temperature of 280°C probably can only be demonstrated in reactors somewhat larger than the proposed HRT. A relatively small increase in the core diameter, from 32 to 40 in., decreases the critical concentration (Fig. 14) and gives a breeding ratio of 1.16 for  $\eta$  (resonance) = 2.32 and 1.12 for  $\eta$  (resonance) = 1.70 (Fig. 13).

## HEAT GENERATION IN THE HRT BLANKET D<sub>2</sub>O Blanket

The heat generation in the  $D_2O$  of the blanket region will be due to the absorption of gamma rays generated in the core region and in the pressure vessel as well as the gamma and beta energy released following neutron absorption in the  $D_2O$  itself. In addition to the energy absorbed in the

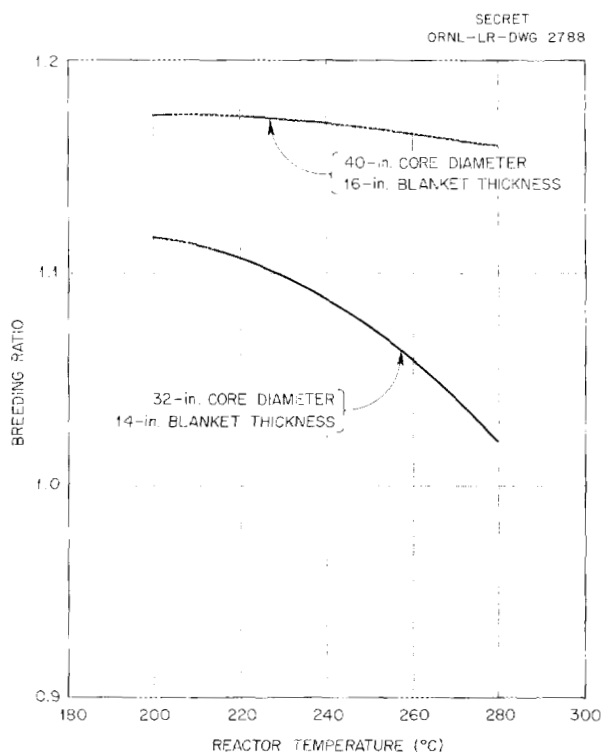


Fig. 13. Breeding Ratio in Spherical Two-Region Reactors. Blanket composition, 1349 g of Th per kg of  $D_2O$  ( $ThO_2$ - $D_2O$  slurry); core solution,  $U^{233}$  as  $UO_2SO_4$  in  $D_2O$ ; core tank, Zircaloy-2.

blanket region, the blanket fluid will be required to carry away the heat generated in the pressure vessel.

Estimates of the heat production from each of these sources<sup>9</sup> give the result that the heat that must be carried away by the blanket fluid is as follows:

Heat Generation	Mev/sec × 10 <sup>17</sup>
Core gammas	4.01
Blanket gammas	0.16
Pressure-vessel heat	7.91
Pressure-vessel gammas absorbed in D <sub>2</sub> O	1.55
<b>Total</b>	<b>13.63 (218 kw)</b>

**Thorium Blanket**

The gamma-heat generation in the ThO<sub>2</sub>-D<sub>2</sub>O

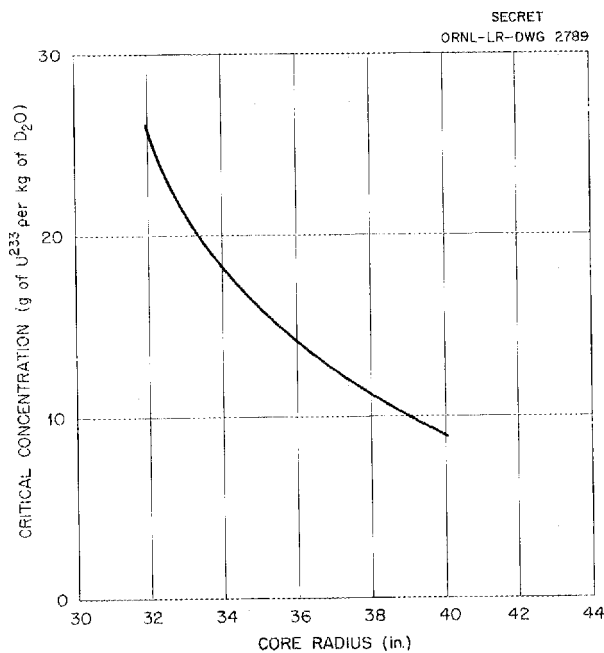


Fig. 14. Critical Concentration of U<sup>233</sup> in Core of Spherical Two-Region Reactors with ThO<sub>2</sub>-D<sub>2</sub>O Slurry Blanket. Blanket concentration, 1349 g of Th per kg of D<sub>2</sub>O; core tank, 1/4-in. Zircaloy-2; core solution, U<sup>233</sup> as UO<sub>2</sub>SO<sub>4</sub> in D<sub>2</sub>O; reactor temperature, 280°C; pressure vessel 6 ft inside diameter.

slurry blanket, containing 633 g of thorium per kilogram of D<sub>2</sub>O, obtained by the method used for the D<sub>2</sub>O blanket is as follows:

Heat Generation	Mev/sec × 10 <sup>17</sup>
Core gammas	5.6
Blanket gammas	11.5
Pressure-vessel heat plus pressure-vessel gammas absorbed in blanket	2.5
<b>Total</b>	<b>19.6 (314 kw)</b>

In addition to the heat production from gammas, there will be heat produced by fissions in the U<sup>233</sup> which is produced in the blanket. The build-up of U<sup>233</sup> as a function of operating time is given in Fig. 15 for the ThO<sub>2</sub>-D<sub>2</sub>O slurry blankets containing 633 and 1349 g of thorium per kilogram of D<sub>2</sub>O. The fission power and total heat generation

<sup>9</sup>P. M. Wood, *Heat Generation in the Blanket Region of the HRT with D<sub>2</sub>O Reflector and ThO<sub>2</sub> Slurry Blanket, and Buildup of U-233 in the ThO<sub>2</sub> Blanket*, ORNL CF-54-6-184 (June 15, 1954).

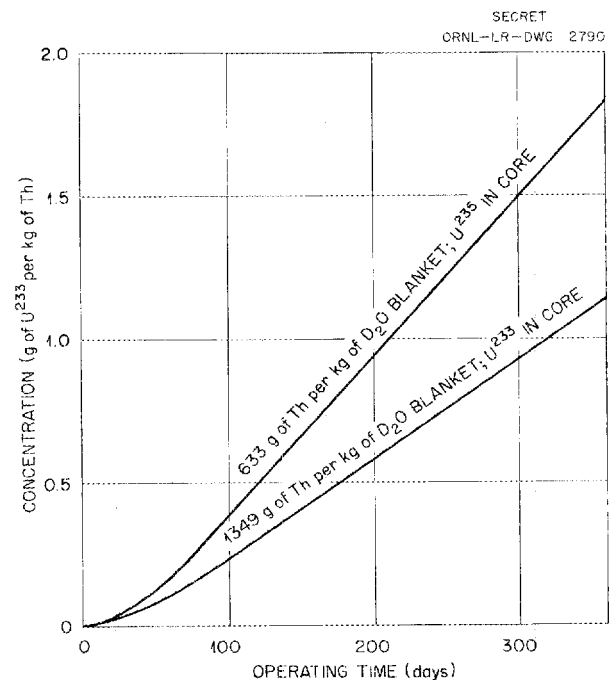


Fig. 15. Build-up of U<sup>233</sup> in Blanket of HRT Operating at a Core Power of 5 Mw (280°C).

## HRP QUARTERLY PROGRESS REPORT

for the blanket containing 633 g of thorium per kilogram of  $D_2O$  are presented in Fig. 16. After operation for a year at a 5-Mw core power, the total heat production in the blanket containing 633 g of thorium per kilogram of  $D_2O$  will be approximately 700 kw.

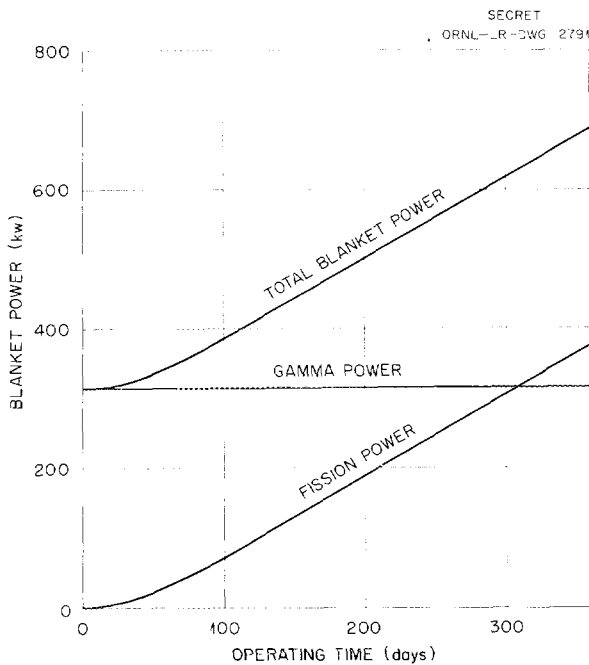


Fig. 16. Power in Blanket of HRT Operating at a Core Power of 5 Mw with  $ThO_2-D_2O$  Slurry Blanket of 633 g of Th per kg of  $D_2O$ .

### THERMAL STRESSES IN HRT PRESSURE VESSEL DURING SHUTDOWN

During the few minutes required to empty the core and blanket high-pressure systems, there is a question as to whether the part of the pressure vessel which is exposed to direct radiation from the core may be inadequately cooled. In answer to this question, calculations of the temperature rise and thermal stress in the pressure vessel when the reactor is "dumped" were made.<sup>10</sup> They show that there is no possibility of damage due to this cause.

As the decay of the reactor power depends on

<sup>10</sup>P. M. Wood, *Heating and Thermal Stress in HRT Pressure Vessel During a Shutdown*, ORNL CF-54-7-158 (July 27, 1954).

many factors, two limiting situations were considered:

*Case 1.* - The reactor continues to operate at a 5-Mw core power as the blanket level is lowered. The maximum resulting tensile stress is 13,000 psi, of which 4000 psi is the thermal stress. Under this condition, the temperature of the pressure vessel is estimated to rise  $6^\circ F$  per minute.

*Case 2.* - The chain reaction immediately decays to a low level, leaving only the fission-product decay gammas as a radiation source. The maximum tensile thermal stress resulting from this situation is 325 psi. The average temperature rise in the vessel is estimated to be  $0.6^\circ F$  per minute.

It is evident from these results that there is no possibility of damage to the pressure vessel due to the stresses resulting from shutdown. The temperature rise resulting from a "dump," which will last no longer than 10 min, will be considerably less than  $60^\circ F$ .

### CRITICALITY OF $U^{235}-H_2O-D_2O$ SYSTEMS IN CYLINDRICAL GEOMETRY

In order to specify the safe storage of large quantities of enriched fuel solution in the HRT dump tanks, criticality calculations were performed for long right-circular cylinders at  $20^\circ C$ , the moderator being  $H_2O$ ,  $D_2O$ , or mixtures of the two.<sup>11</sup> Since the tanks may be covered with water during maintenance of the reactor, the pipes were considered as having an infinite  $H_2O$  reflector. Also, the effect of coating the pipes with a poison (e.g., cadmium) for thermal neutrons was also considered. To minimize computational labor, the Feynman-Welton approximation to the two-group diffusion theory was used. The second moments of the synthetic Yukawa slowing-down kernel for the  $H_2O-D_2O$  mixtures were derived from multigroup calculations of the critical buckling of bare spheres.<sup>12</sup>

The results of the calculations are plotted in Fig. 17 for the infinite  $H_2O$  reflector with no cadmium and in Fig. 18 for the cadmium-coated

<sup>11</sup>S. Visner and L. C. Noderer, *Criticality of  $U^{235}-H_2O-D_2O$  Systems in Cylindrical Geometry*, ORNL CF-54-5-170 (May 20, 1954).

<sup>12</sup>G. M. Safanov, *A Study of Homogeneous  $H_2O$ ,  $D_2O$ ,  $U^{235}$  Reactors with a Note on Optimum Moderating Mixtures for a Minimum  $U^{235}$  Requirement*, RM-842 (Rand) (May 1, 1952).

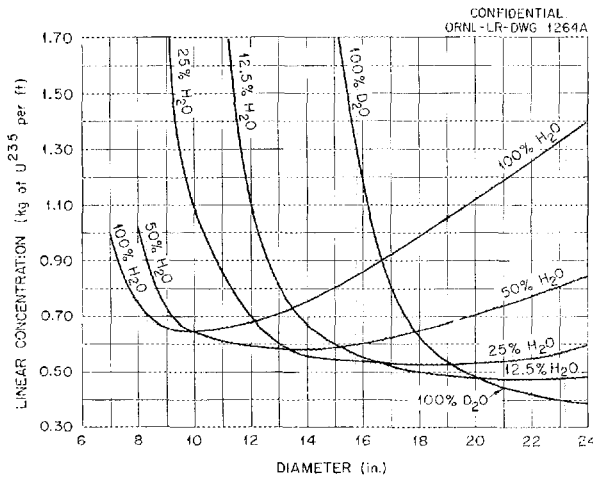


Fig. 17. Criticality of Circular Cylinders of Infinite Length (H<sub>2</sub>O Reflected, 20°C).

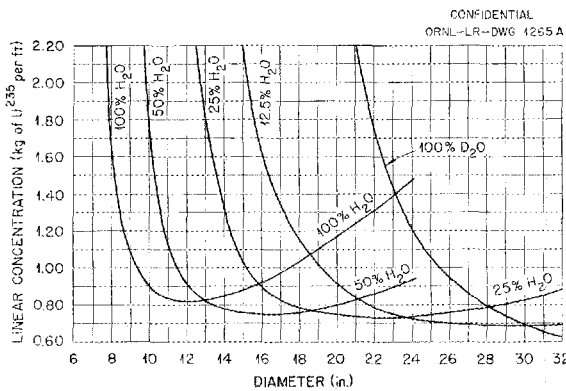


Fig. 18. Criticality of Cadmium-Coated Circular Cylinders of Infinite Length (H<sub>2</sub>O Reflected, 20°C).

cylinders. The envelopes to these curves would define the minimum linear concentration for criticality in any size of pipe, and if the presence of H<sub>2</sub>O and D<sub>2</sub>O in any ratio is possible, the envelopes determine the upper limit to the safe fuel concentration. Furthermore, since the minimum represented by the envelope increases as the pipe diameter decreases, a horizontal pipe will not become critical if the moderator alone is removed (e.g., by evaporation), if the remaining solution is conservatively considered as constrained in a full circular cylinder of decreasing diameter. The conservatism arises obviously because the partially

filled horizontal cylinder has a greater neutron-leakage probability than an upright cylinder of the same cross-sectional area.

Since criticality experiments with pure H<sub>2</sub>O moderator and no cadmium have indicated a minimum in linear concentration 10% lower than the calculations plotted in Fig. 17, the results obtained here by means of the two-group diffusion model are apparently not conservative. The reliability of the calculations for the pipes with cadmium coating is probably better, since there was no need to evaluate the return of neutrons thermalized in the reflector; furthermore, criticality is attained in larger diameter pipes, which minimizes the error introduced by the assumed neutron-slown-down model.

#### HRT BLANKET DUMP TANKS

The capacity of the HRT dump tanks for the blanket was considered in terms of the operational requirements of the reactor, and the configuration was considered in terms of criticality in the event that the blanket material becomes mixed with fuel solution if the core tank ruptures.<sup>13</sup> Similar considerations for the core dump tanks were given previously.<sup>14</sup> A solution volume of 2000 liters should prove to be adequate for normal operation but will not allow the system to be filled with D<sub>2</sub>O for rinsing, which might be desirable when uranyl sulfate solution or thorium oxide slurry is used. In this case, rinsing will be accomplished primarily by steaming the system with the use of the low-pressure evaporator. For operation at 280°C with a concentration in the blanket of 633 g of thorium per kilogram of D<sub>2</sub>O, there will be in the reactor approximately 14 kg of U<sup>235</sup>. A 24-in.-dia pipe 33 ft long would have a volume of approximately 3000 liters and would permit the distribution of the fuel at 0.47 kg per linear foot if an accident should make this necessary. If the poisoning provided by the uranium or thorium is taken into account, this arrangement should be safe for any conceivable contingency, including the admixture of light water to the contents of the dump tanks. This can be seen in Table 5, where the critical concentrations are listed for several situations.

<sup>13</sup>S. Visner, *Dump Tanks for HRT Blanket*, ORNL CF-54-6-16 (June 3, 1954).

<sup>14</sup>S. E. Beall *et al.*, *HRP Quar. Prog. Rep. Apr. 30, 1954*, ORNL-1753, p 19-21.

**HRP QUARTERLY PROGRESS REPORT**

**TABLE 5. CRITICALITY OF HORIZONTAL DUMP TANKS FOR HRT BLANKET, 24-in. DIAMETER, 20°C**

	Blanket					
	D <sub>2</sub> O		UO <sub>2</sub> SO <sub>4</sub> * (355 g of U per kg of D <sub>2</sub> O)		ThO <sub>2</sub> ** (633 g of Th per kg of D <sub>2</sub> O)	
	No cadmium	Cadmium coated	No cadmium	Cadmium coated	No cadmium	Cadmium coated
	Critical Concentration (kg of U <sup>235</sup> per foot)					
Mole fraction of H <sub>2</sub> O in solvent						
0	0.38	1.21	14.4	∞	∞	∞
1/8	0.48	0.73	0.86	1.52	∞	∞
1/4	0.60	0.73	0.80	1.04	∞	∞
1/2	0.85	0.93	0.95	1.06	4.44	6.59
1	1.40	1.47				
Actual design loading	0.15		0.23		0.47	

\*Ratio of U to U<sup>235</sup>, 0.24.

\*\*Ratio of Th to U<sup>235</sup>, 0.54.

**HRT-COMPONENT DEVELOPMENT**

C. B. Graham, Section Chief

**HRT-CORE HYDRAULIC STUDIES**

I. Spiewak

W. C. Cosby            J. A. Hafford

R. Goodman            P. H. Harley

L. B. Lesem

**Straight-Through HRT Core**

During the past quarter a full-scale carbon-steel flow model (Fig. 19) of the straight-through HRT core was completed, and a number of preliminary tests were run. The diffuser-screen combination first specified (six screens of 0.51 solidity ratio) proved to be unsatisfactory, and modifications are now being made. All screen combinations tried so far in the 90-deg diffuser have exhibited some separated or unstable flow; in some cases, there was strong backflow around the periphery, and, in others, there was extensive stagnation in the center. Some tests indicated an amount of separation which may be tolerable, but reproducibility was poor.

<sup>15</sup>P. H. Harley, L. B. Lesem, and I. Spiewak, *Flow Tests of Full Scale Alternate HRT Core Model*, confidential memorandum to C. B. Graham, June 28, 1954.

Flow tests of the 90-deg diffuser are continuing. However, it appears that it may be necessary to use a double cone (Fig. 20) with nine screens, which is a more conservative design. Final specifications should be available by August 9.

**Concentric HRT Core**

A full-scale flow model of the alternate HRT core, in which concentric inlet and outlet pipes were utilized, was also tested during the past quarter.<sup>15</sup> Pressure-drop and flow patterns were determined at flow rates of 40 to 400 gpm. The pressure drop was 1.1 inlet velocity heads, or 5.2 ft of fluid at the rated 400 gpm. The flow pattern (Fig. 21) indicated the presence of a central jet which diverged at about a 9-deg angle and was surrounded by a well-mixed region filling the remainder of the sphere. The temperature distribution in an HRT of this configuration would consist in a cold inlet jet surrounded by a region at close to outlet temperature.

Tests were also conducted to determine the effect of density differences on the flow pattern, and they indicated that the flow pattern was unchanged by density effects. Density differences were shown to promote natural-convection cooling of the core during pump shutdown.

UNCLASSIFIED  
ORNL-LR-DWG 2792

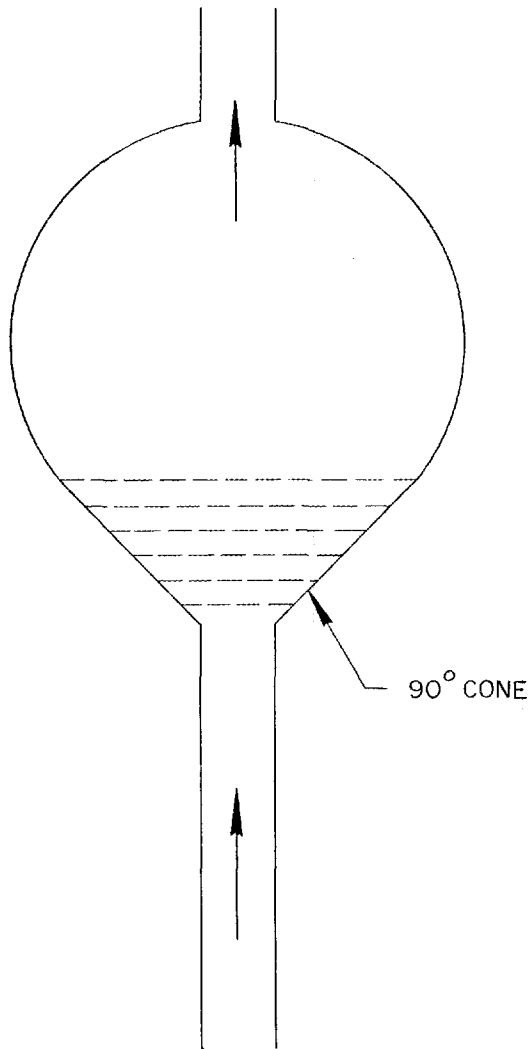


Fig. 19. HRT Flow Model with Single-Cone Diffuser.

**Scale-up of Concentric Core**

A 48-in. carbon-steel flow model geometrically similar to a 6-ft-dia core operating at 300 to 400 Mw was also tested to determine the factors involved in scaling-up concentric cores.<sup>16</sup> The results were very similar to those described above for the HRT-scale model. It was necessary to insert the 12-in. inlet pipe about 6 in. into the sphere to avoid bypassing to the outlet.

<sup>16</sup>L. B. Lesem and P. H. Harley, *Scale-Up of Alternate HRT Core*, ORNL CF-54-5-47 (May 7, 1954).

UNCLASSIFIED  
ORNL-LR-DWG 2793

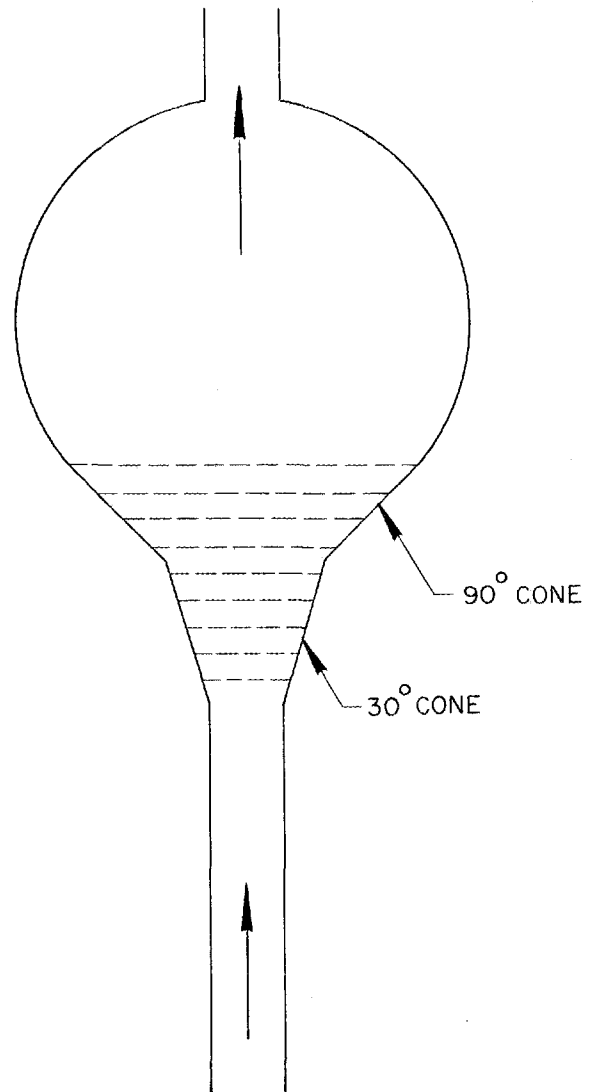


Fig. 20. HRT Flow Model with Double-Cone Diffuser.

**HRT HEAT EXCHANGERS AND  
CIRCULATING PUMPS**

W. L. Ross  
L. F. Goode      R. E. Wascher

**HRT Heat Exchangers**

The Foster Wheeler Corp. has been selected to perform the design and fabrication of the HRT fuel and blanket heat exchangers. Design has begun. It is intended that the two exchangers be identical

**HRP QUARTERLY PROGRESS REPORT**

SECRET  
ORNL-LR-DWG 2794

except for possible minor design deviations in the blanket heat exchanger, which will permit slurry operation.

The basic unit, as presently conceived, is shown in Fig. 22. Purchase of material is expected to begin in August 1954, and delivery of the units is scheduled for February 1955.

**HRT Fuel Pumps**

The construction of the two Westinghouse 400A pumps presently on order<sup>17</sup> is essentially complete. A delay in the construction of the test facility for the Westinghouse pump has caused the delivery dates of these pumps to be moved back to August. The pumps will receive approximately 200 hr of factory tests before shipment. The tests will include (1) 48 hr of bearing run in operation at temperature and pressure, (2) measurement of axial thrust over the normal load range, (3) plotting of head-capacity and other performance-characteristic curves, and (4) 100 hr of operation at rated-system conditions with a motor load of 15 hp.

Because of time considerations, it was decided that test loops for the above pumps would be built here rather than at Westinghouse. The design of these loops is complete, and all material has been ordered or is on hand. Figure 23 is a layout drawing of the loop.

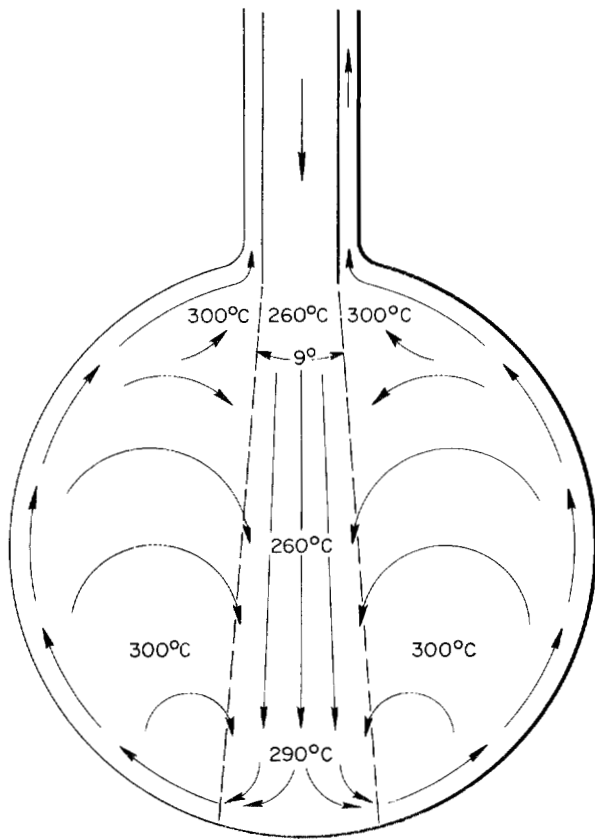


**Fig. 21. Flow Pattern and Temperature Distribution in Alternate HRT Core.**

<sup>17</sup>C. B. Graham *et al.*, *HRP Quar. Prog. Rep. Apr. 30, 1954*, ORNL-1753, p 44-48.

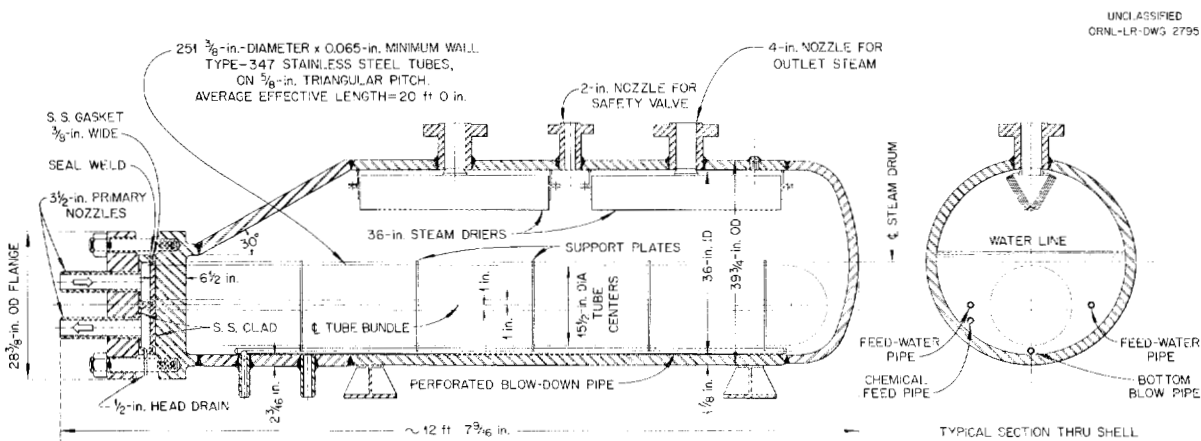
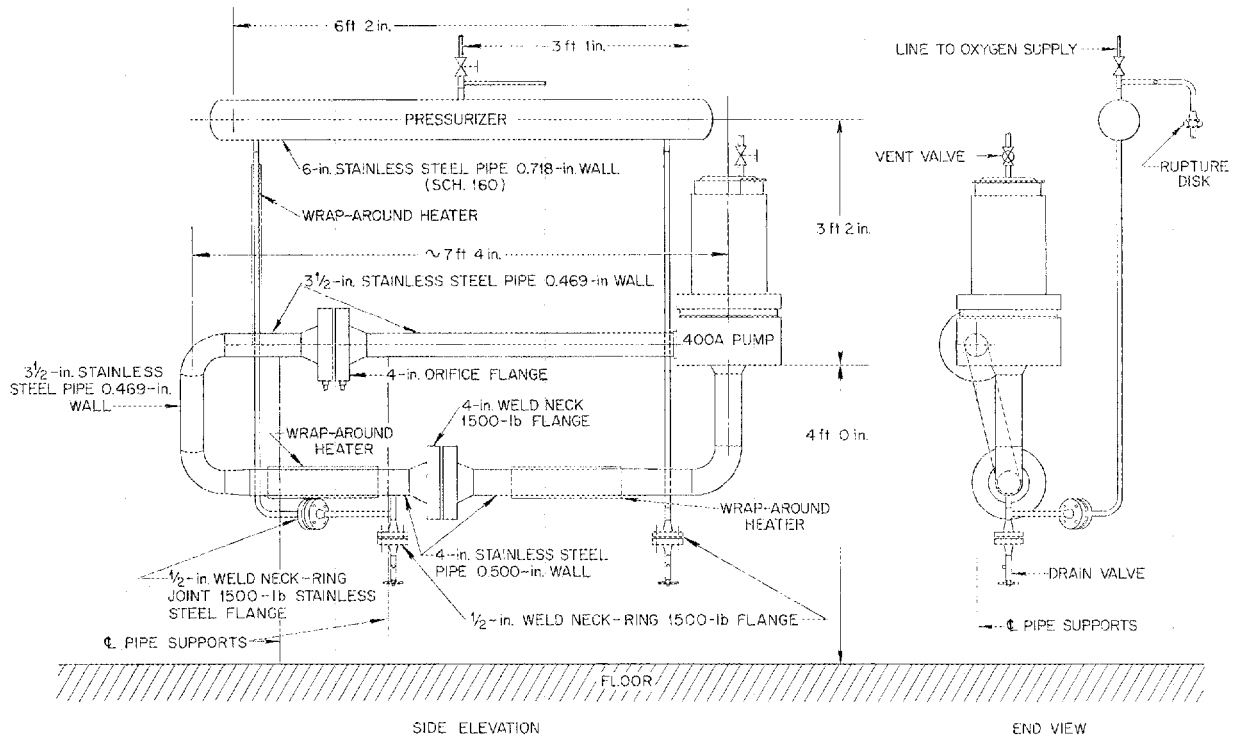


**Fig. 22. Proposed HRT 5-Mw Heat-Exchanger Design.**

UNCLASSIFIED  
ORNL-LR-DWG 2796



GENERAL NOTES:

1. A SUITABLE STRUCTURE (SIMILAR TO THOSE IN OTHER LOOP AREAS) SHALL BE BUILT AROUND LOOP. PROVIDE ADEQUATE MEANS FOR VENTILATION AND ACCESS AS REQUIRED.
2. DESIGN PRESSURE 2000 psi; DESIGN TEMPERATURE 600°F.
3. LOOP SHALL BE HYDROSTATICALLY TESTED TO 3000 psi.

MATERIAL--PIPE AND FITTINGS:

PIPING--SEAMLESS ASTM A-312-51T TYPE 347 STAINLESS STEEL.  
FITTINGS--ASTM A-182 52aT TYPE 347 STAINLESS STEEL.

Fig. 23. Experimental Test Loop for 400A Pump.

**HRT Blanket Pumps**

The redesign of the 150C pump by Westinghouse to meet the requirements of various blanket tests is complete. One design is for a pump which will deliver 300 gpm with a head of 65 ft. By modifying the impeller of this pump, it will deliver 230 gpm with a head of 50 ft. The other design is for a slurry pump which will deliver 200 gpm with a head of 100 ft. The design of both of the above pumps is such that metal pump parts in all regions of high velocity and/or turbulence can be fabricated from or lined with titanium. The estimated characteristic curve for the 300-gpm pump is shown in Fig. 24.

One each of the 300-, 230-, and 200-gpm pumps should be delivered about November 1, 1954.

Test loops for the 300- and 230-gpm pumps will be constructed here and will be similar in design to the loops for the 400A pump. The loop for the 200-gpm slurry pump is discussed in Part V, Chemical Engineering Developments.

**HRT FUEL FEED PUMPS**

J. S. Culver                      J. M. Baker

**Reactor Feed Pumps**

A prototype of the HRT pump has been operated at 2000 psi with the use of salvaged Pulsafeeder parts from HRE equipment. Modified check valves have been installed on the pumping heads and have operated successfully up to 89 strokes/min.

A Hydropulse pump has been ordered and should arrive in a few days. This unit will possibly

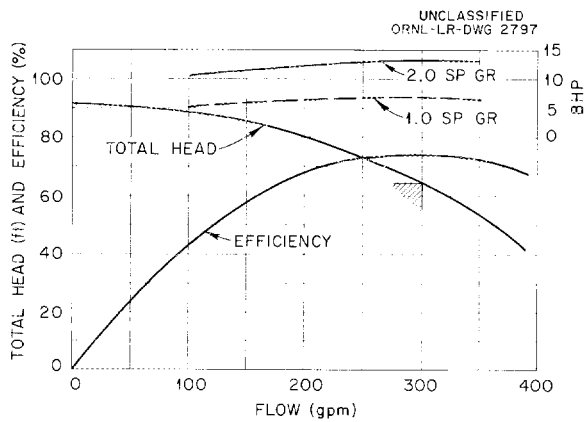


Fig. 24. Curve for 300-gpm Pump.

supply a packaged drive unit and the isolation system and will be used to drive the two Pulsafeeder heads on hand to be tested. Other equipment that has been ordered will allow continued testing of a reciprocating pump drive similar to that on the HRE.

Strain-gage tests up to 3500 psi showed the HRE head design, with some minor changes, to be adequate with respect to stress. Work is progressing on a new diaphragm contour which will lower diaphragm stress at some sacrifice in head capacity; however, since the HRT pump will be a duplex unit, this poses no serious problem.

The response from vendors on the HRT pumps has required that the pumping heads be built at the Laboratory and that the drive units be purchased outside if the HRT schedule is to be met.

Materials for these pumps will be procured immediately, and fabrication of the heads will be started as soon as the material is received.

SMALL-COMPONENT DEVELOPMENT

I. Spiewak

- |                  |               |
|------------------|---------------|
| D. M. Eissenberg | P. H. Harley  |
| R. Goodman       | A. L. Johnson |
| J. A. Hafford    | L. B. Lesem   |

Pressurizer Electric Heaters

The steam pressurizer used on the HRT requires heaters that are easy to operate and service and that are also safe in the event of reactor accidents. Electric heaters, in general, are very easy to use; however, it is necessary to develop a design which is foolproof from the safety standpoint.

The design shown in Fig. 25 appears to be feasible for HRT use. Calrods are cast into an aluminum matrix, the inside of which is machined to fit snugly over the pipe to be heated. A close fit is assured by clamping the clamshell heater against the pipe wall. The total rated power of the heater is 7 kw.

This type of heater has been tested on a bomb made of 2-in. heavy-walled pipe such as is used in the HRT pressurizer. The heat-transfer coefficients between heater and pipe, with good clamping, varied from 140 to 220 Btu/hr-ft<sup>2</sup>·°F. This meant that the bomb could be maintained at a 2000-psi pressure with the heater less than 50°F hotter than the bomb. With a loose fit to provide heater-pipe contact, the heat-transfer coefficient was 20 to 45 Btu/hr-ft<sup>2</sup>·°F, which was not considered adequate because a high ΔT was required to maintain bomb pressure.

A fusible zinc plug which melts at 787°F and breaks the Calrod electric circuits is used as a foolproof safety device on the heater (Fig. 26). After the zinc melts, the copper connector is forced into the ceramic cup by the spring. In tests, the fusible plug was found to prevent the pipe-wall temperature from exceeding 700°F when the liquid level fell in the test bomb. The maximum heater

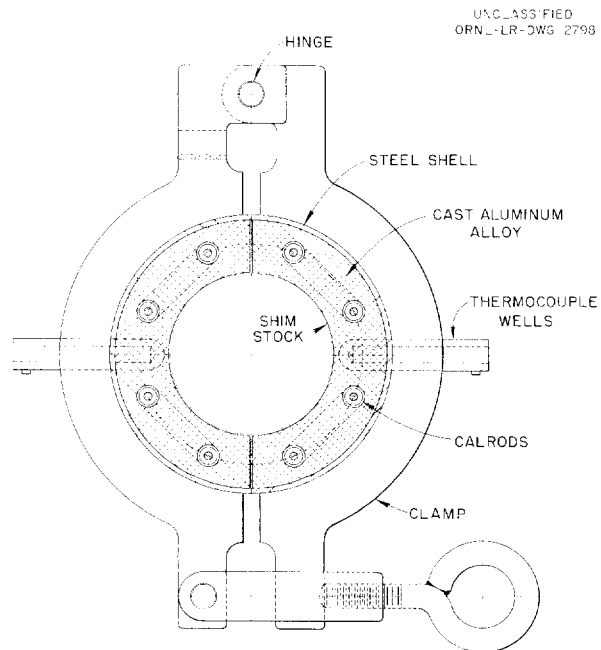


Fig. 25. Pressurizer Heater (End View).

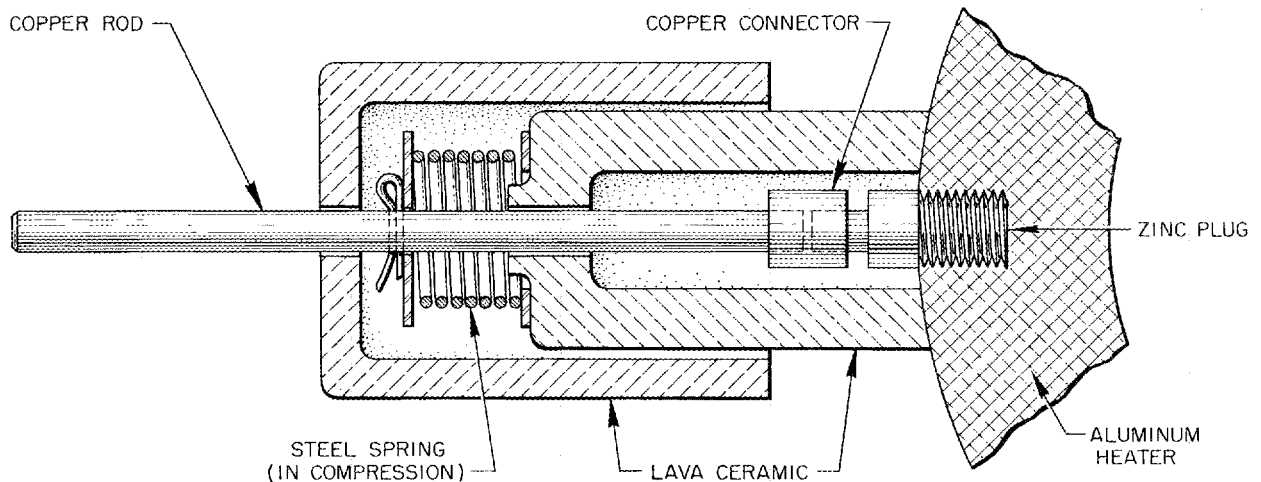


Fig. 26. Fusible Connector for Clamshell Heater.

temperature at shutoff was about 860°F. These tests used a gravity-loaded (rather than a spring-loaded) system. The spring design, which will be tested shortly, is preferred because the gravity load sometimes contacted metal when it fell and re-established the heater circuit.

The following independent safety devices are in the HRT pressurizer heater circuit: (1) low-liquid-level alarm, (2) high-heater-temperature thermocouple alarm, and (3) fusible plug.

If all of these safeguards were to fail, it has been demonstrated that the stainless steel pipe would maintain its strength sufficiently to the temperature where the heater fails. In high-pressure runs, the bomb has withstood 5 hr of operation above 500°C, 1.5 hr above 600°C, and 0.7 hr above 700°C. In one test, with the heaters at rated current, the aluminum melted out and the Calrods finally failed when the pipe temperature was about 775°C (1427°F) with 2450-psi internal pressure. There was no damage to the bomb.

#### Vaned Elbows

The velocity distributions following various types of 3-in. 90-deg elbows were measured.<sup>18</sup> It was found that for short radius, long radius, and mitred elbows more than 20 pipe diameters are

<sup>18</sup>P. H. Harley, *Velocity Distribution of Flow Through 90° Elbows*, ORNL CF-54-6-210 (June 29, 1954).

required for the flow to restabilize. On the other hand, for vaned single- and double-mitred elbows, stable flow was re-established between 5 and 10 diameters. This indicates that vaned elbows would be desirable in HRT locations where flow patterns are important, for example, preceding the core and the pump.

#### Dump Tank

A full-scale dump-tank-evaporator mock-up (see p 25) similar to that designed for the HRT has been constructed and is ready for testing. The important points which are to be checked are the heat-transfer coefficients in the evaporator section, the liquid recirculation rate, and the quantity of entrainment which is generated.

#### Entrainment Separator

Between the dump tank and the recombiner of the HRT, it is necessary to remove almost all the entrained uranyl sulfate. This prevents loss of uranium and plugging of the recombiner catalyst.

A low-pressure entrainment-separator test has been assembled to evaluate wire-mesh demisters (Fig. 27). Two sizes of knitted wire have been tried, 280 and 110  $\mu$  OD. Entrainment was provided by mixing a compressed-air stream and a recirculating water stream. The mixture is admitted tangentially into the lower portion of a

## HRP QUARTERLY PROGRESS REPORT

6-in. glass column. A section of centrifugal separator is followed by any desired amount of wire mesh. Above the mesh there is a steam-heated bed of 1/4-in. Berl Saddles, simulating recombiner packing. Determination of entrainment separation

is made by analyzing the liquid (~40 g of NiSO<sub>4</sub> per liter) for nickel over a period of time.

The results to date are summarized in Table 6. The amount of NiSO<sub>4</sub> collected on the Berl Saddles was between 1 and 2% of the entrainment lost in each run.

Further testing will be directed at optimizing a combination for HRT use, since the preliminary results are quite promising.

### Charcoal Adsorbers

The performance of the HRE charcoal adsorbers has been evaluated.<sup>19</sup> The observed behavior conformed approximately to the design theory. Because of heavy overloads caused by leaks, occasional activity was discharged to the stack. It was concluded that the same charcoal beds could be used in the HRT after some simple maintenance was carried out to ensure good operation.

### SIMULATED HRT-EXPLOSION TEST

J. S. Culver

C. H. Gabbard

P. Pasqua

S. R. West

In the event of a brittle-fracture type of failure in the blanket vessel of the HRT, the total contents of the core and blanket at 2000 psi and 300°C would be discharged into the shield (see p 15). To contain the radioactive solution and gases, the shield is provided with a steel liner and tight-fitting top plugs which must be designed to withstand the maximum pressure to be expected.

Calculations were made in order to determine the maximum theoretical pressure which might occur; however, it was desired to check experimentally this value and determine the effect of

UNCLASSIFIED  
ORNL-LR-DWG 2800

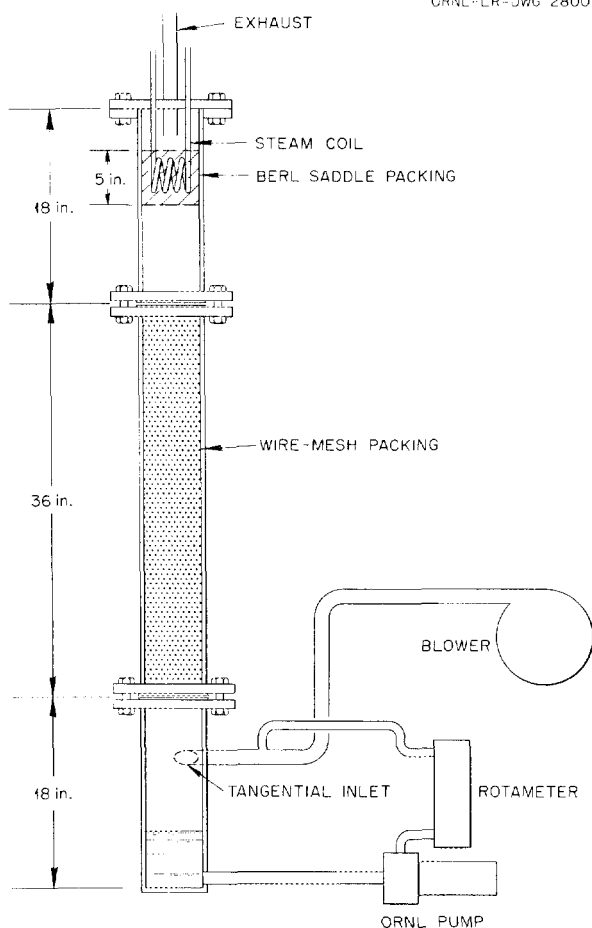


Fig. 27. Low-Pressure Entrainment Test Loop.

<sup>19</sup>J. Spiewak, *Use of HRE Charcoal Adsorbers in the HRT*, ORNL CF-54-7-26 (July 8, 1954).

TABLE 6. RESULTS OF LOW-PRESSURE TEST OF ENTRAINMENT-SEPARATOR

Run	Mesh	Air (scfm)	Liquid (gpm)	Liquid Fraction Lost	NiSO <sub>4</sub> in Gas by Weight (ppm)
1	None	15	12.3	$1.0 \times 10^{-4}$	300
2	6-in. fine	16	10	$1.8 \times 10^{-6}$	4
3	12-in. coarse	16	10	$1.2 \times 10^{-5}$	32

condensation, cooling sprays, and other factors which are difficult to predict.

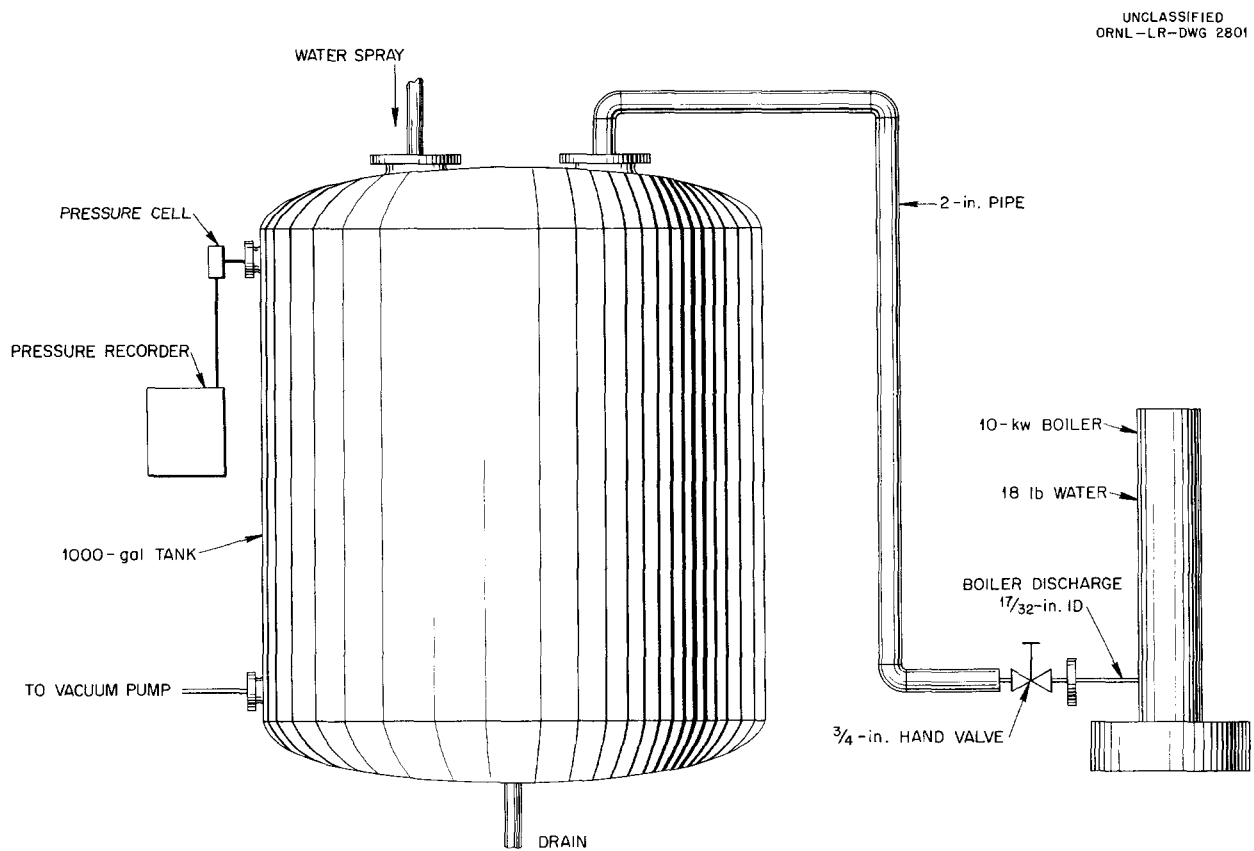
The apparatus, shown in Fig. 28, was composed of existing equipment and was so arranged that initial tank conditions could be varied as desired. a vacuum pump was used to exhaust the tank to the desired pressure, and a water spray could be operated to hasten cooling during the time the boiler blew down.

Eighteen pounds of water was charged into the boiler for each run; this gave the same ratio of liquid to tank volume as would occur in the reactor if the total contents of the core and blanket were discharged into the shield.

The test consists in pumping the tank down to the desired pressure (presumably  $\frac{1}{2}$  atm in the reactor) and heating the boiler until a pressure of 1250 psig is attained. The hand valve is then opened as rapidly as possible, and the tank-pressure rise is measured on a Brush recorder.

Runs were made with initial tank pressures at atmospheric pressure and at 15 and 28.5 in. Hg (vacuum); one run was also made at 15 in. Hg (vacuum) with a water spray of 10 gal/min. The pressure-time curves of these runs as taken from the Brush recorder are shown in Fig. 29. The maximum pressure was found to vary directly with the initial tank pressure, and the only effect of the water spray was to bring the pressure down to atmospheric 6 sec sooner. Figure 30 shows the maximum tank pressure vs the initial tank pressure. Temperature-time curves taken on the inside and outside walls of the tank showed that the actual average temperature rise was 11.5°F. Theoretical curves corrected for this heat loss correspond very closely with the experimental values.

The apparatus is being rebuilt to use a 2-in. rupture disk in place of the hand valve, and the diameter of the boiler discharge is also being increased from  $\frac{17}{32}$  to  $1\frac{1}{2}$  in. in diameter. This



UNCLASSIFIED  
ORNL-LR-DWG 2801

Fig. 28. HRT-Explosion Test Apparatus.

**HRP QUARTERLY PROGRESS REPORT**

UNCLASSIFIED  
ORNL-LR-DWG 2802

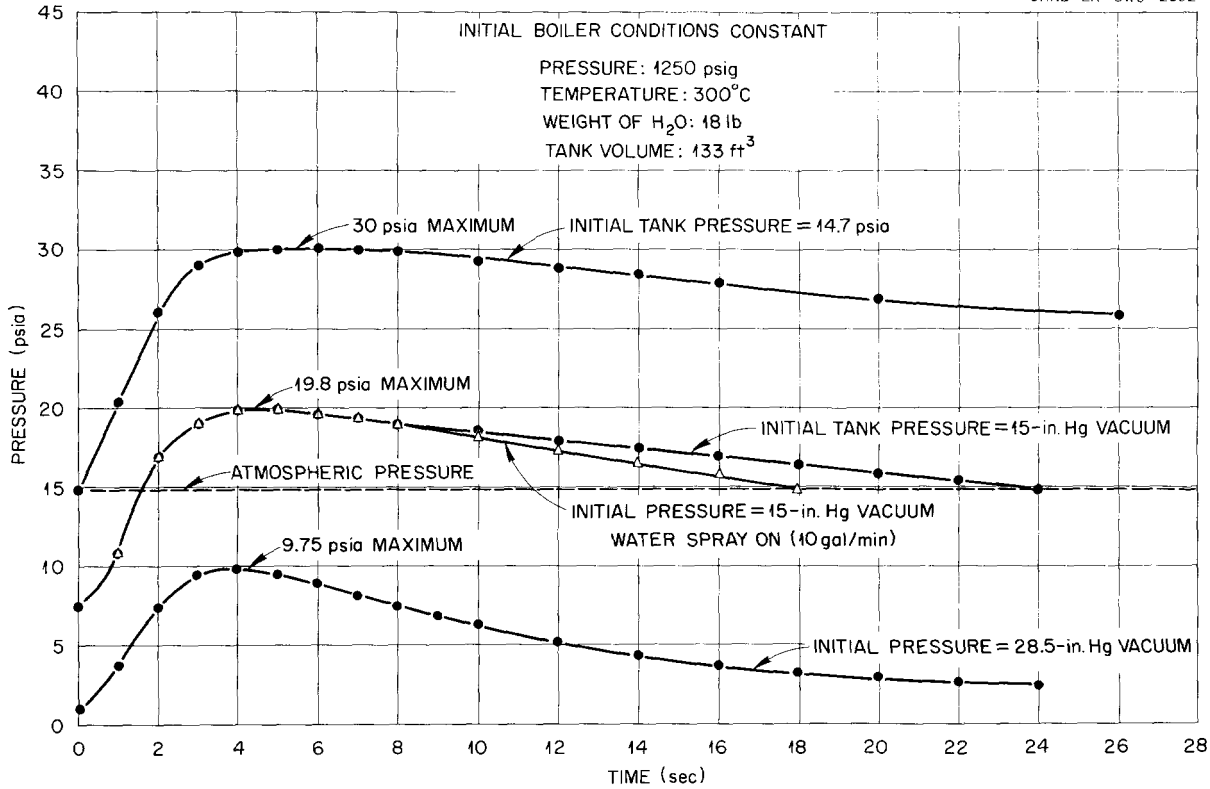


**Fig. 29 . Simulated HRT Explosion – Tank Pressure vs Time.** Initial boiler conditions constant; pressure, 1250 psig; temperature, 300°C; weight of water, 18 lb; tank volume, 133 ft<sup>3</sup>.

should give a much shorter discharge time than that which was required to open the valve. Results obtained with this setup should more closely simulate a sudden rupture of the pressure vessel in the shield.

**HRT MOCK-UP**

W. L. Ross  
L. F. Goode

A mock-up of critical HRT components was described in the previous quarterly report.<sup>17</sup> This system will test the engineering operation of the high-pressure loop and the letdown system. The following is the status of the various loop components:

**HRT-Type Components**

400A pump                      August delivery  
Gas separator                On hand

Pressurizer                    Designed  
Letdown heat exchanger    Designed  
Letdown valve                September delivery  
Pulsafeeder                   HRE type on hand; HRT type ordered  
Pipe and fittings             August delivery

**Auxiliaries**

Heat exchanger                August delivery  
80-kw boiler                  September delivery  
Air compressor                September delivery  
Dump tank                      Installed  
Reflux condenser              Being installed  
Valves and instruments       On hand or on order

An 80-kw test-model steam-condensing heat exchanger (Fig. 31) is being provided for the HRT mock-up loop. This model, jointly designed and fabricated by ORNL and the Foster Wheeler Corp., will serve as the loop heater and is expected to

provide tube-joint design, fabrication, testing, inspection, and corrosion data which are directly applicable to both the HRT and the large heat exchangers.

**CONTROLS AND INSTRUMENTATION**

**HOMOGENEOUS REACTOR TEST INSTRUMENTATION**

J. N. Baird, Jr.

- |                |              |
|----------------|--------------|
| M. C. Becker   | R. L. Moore  |
| A. M. Billings | R. E. Toucey |
| J. R. Brown    | E. Vincens   |
| J. C. Gundlach | W. P. Walker |
| P. F. Huray    | K. W. West   |

**Control Panel**

Agreement has been reached with the Operations Group that the HRT panel will combine graphic and nongraphic sections with a console.

A panel arrangement proposed for the HRT has been mocked up by using plywood, instrument photographs, cardboard symbols, and colored Scotch tape (Fig. 32). In this mock-up, the central section contains strip-chart instruments which record fuel and blanket temperatures, fuel and blanket heat-exchanger differential temperatures, neutron counting rates, Monitron outputs,  $\ln N$ , and 12 important temperatures. To the left and right of the strip-chart instruments are, respectively, graphic layouts of the core and blanket systems. At the extreme left is a graphic jumper diagram with sockets so that unnecessary or undesirable interlock contacts may be conveniently identified and jumpered out. Turbogenerator instruments and controls are shown at the extreme right of the mock-up.

A 108-point automatic temperature scanner has

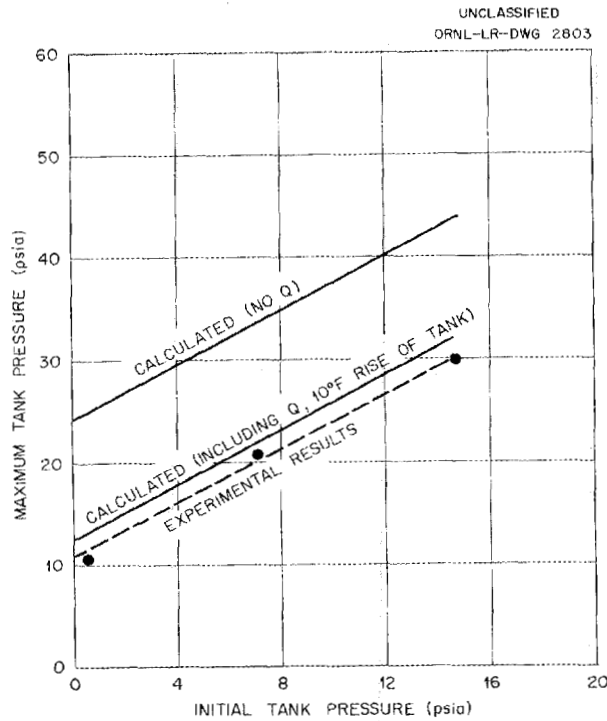


**Fig. 30. Simulated HRT Explosion - Maximum Tank Pressure vs Initial Tank Pressure.**

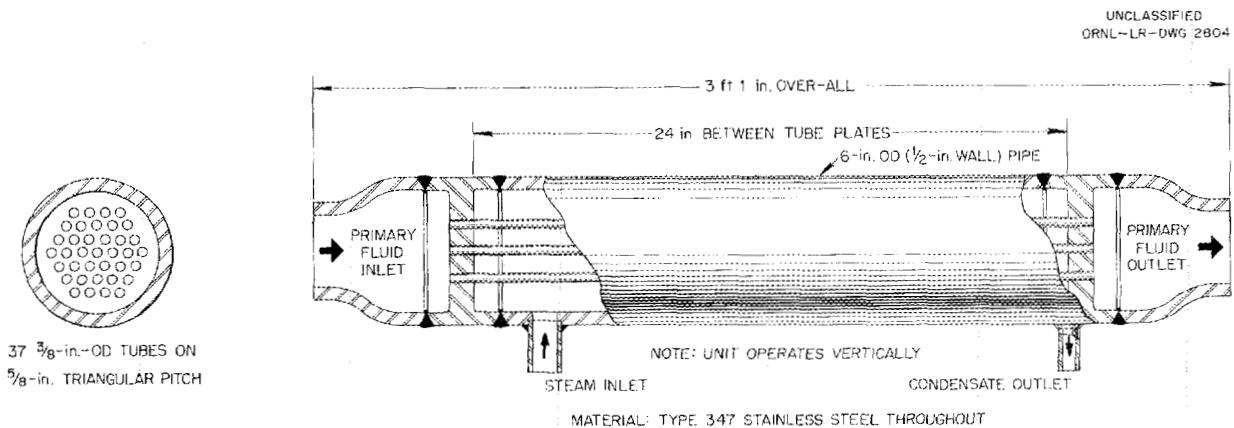


**Fig. 31. HRT Mock-up of 80-kw Test Model Heat Exchanger.**

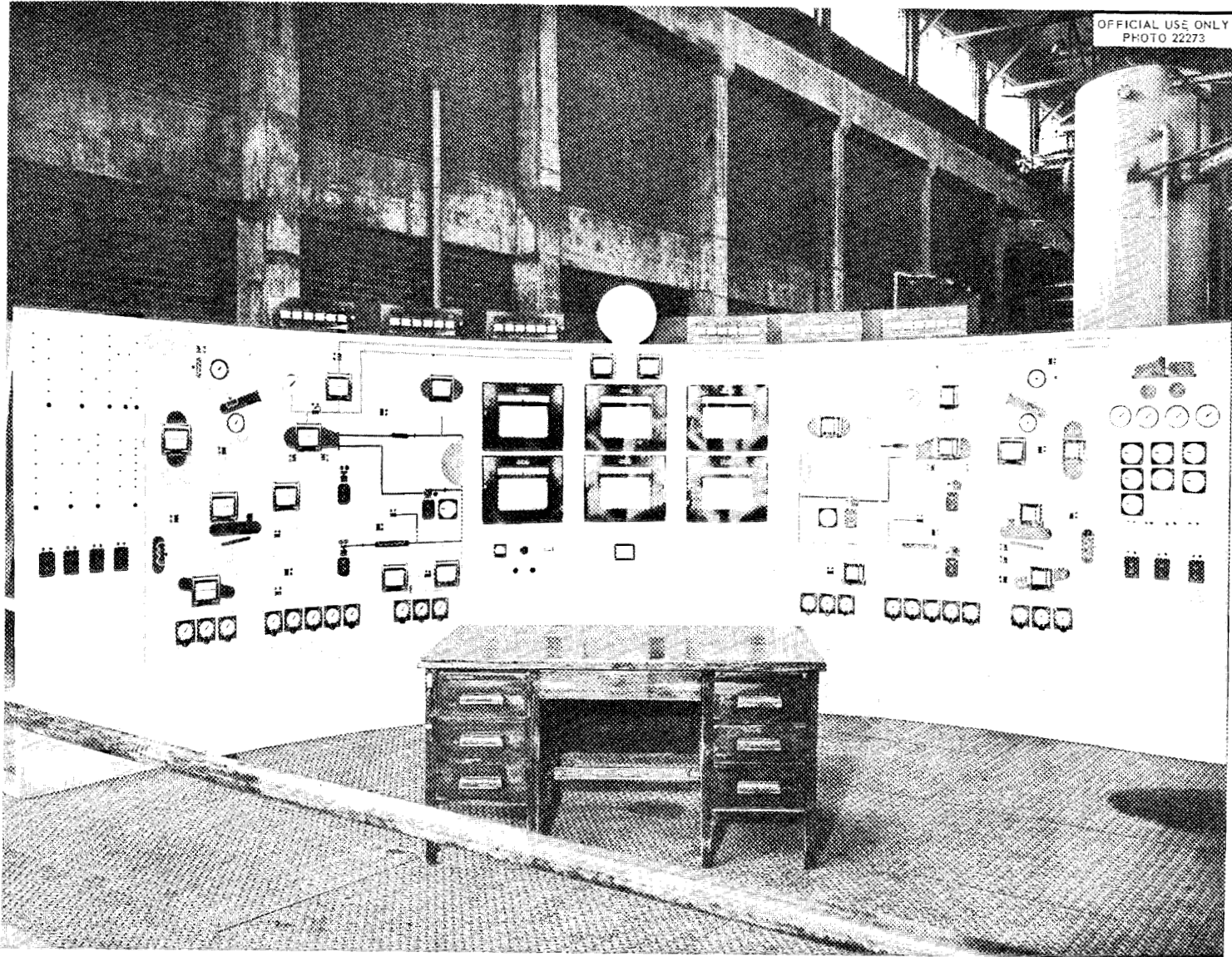


Fig. 32. Mock-up of HRT Control Panel.

been ordered. Its location has not yet been decided.

**Waterproofing of instrumentation**

When the reactor cell is filled with process water for maintenance purposes, galvanic corrosion of the thermocouple wires may occur.<sup>20</sup> Two factors would aggravate this situation: the strongly anodic behavior of iron, which is normally used with constantan within the 0 to 400°C temperature range, and the large mass of the type 347 stainless steel reactor system compared to that of the iron thermocouple wire coupled to it.

A test was made in order to determine thermocouple combinations which would be least subject to galvanic action in process water. Six-inch pieces of bare thermocouple wire were equally spaced about a bar of type 347 stainless steel  $\frac{1}{2} \times \frac{3}{4} \times 6$  in. long and supported from an insulating block. The wires and bar were submerged in 5 in. of tap water. A microammeter, calibrated in voltage, and a decade resistance box were placed consecutively in series with each pair of materials, and the generated voltages were measured as follows:

Materials	Voltage Measured (v)
Type 347 stainless steel vs	
Fe	-0.20
Constantan (of Cu-constantan)	0.06
Constantan (of Fe-constantan)	0.04
Alumel	0.02
Cu	0.03
Chromel	0.00
Constantan (of Cu-constantan) vs	
Fe	-0.26
Constantan (of Fe-constantan)	0.04
Alumel	-0.04
Cu	-0.06
Chromel	0.00
Cu vs	
Fe	0.26
Constantan (of Cu-constantan)	-0.02
Constantan (of Fe-constantan)	-0.05
Alumel	-0.02
Chromel	0.00

<sup>20</sup>E. G. Bohlman, memorandum, June 28, 1954.

Chromel vs

Fe	0.02
Constantan (of Cu-constantan)	+0.00
Constantan (of Fe-constantan)	+0.00
Alumel	+0.00
Cu	+0.00

Of the standard thermocouple combinations, Chromel and Alumel produced the least voltage when coupled together or when either was coupled to type 347 stainless steel.

In a second practical test, a thermocouple with 75-ft No. 16 fibre-glass-insulated duplex iron-constantan leads was immersed in tap water. After approximately 12 hr of immersion, the measured emf was 1.65 mv in error, equivalent to about 31°C. A comparable Chromel-Alumel thermocouple similarly immersed showed an error of 0.16 mv, equivalent to 4°C. These voltage errors are attributed to galvanic action.

On the bases of these tests, Chromel-Alumel thermocouples have been specified for HRT use. Further tests of these thermocouples will be performed by the Corrosion Section.

**Nuclear Instrumentation**

The method chosen for the mounting of nuclear-control ionization chambers is shown in Fig. 33. The chambers are positioned in slanting tubes filled with water and surrounded by shielding material such as concrete or barytes-and-water.

The sloped arrangement permits the use of water as the shielding material in the beam holes and eliminates the expense of the concrete plugs normally used, with a saving of several thousand dollars.

Nuclear instrumentation in the HRT will be limited to two fission chambers with counting-rate circuits and recorders and one differential ion chamber with a logarithmic amplifier and recorder.

**Control-Valve Program**

Contracts have been awarded to The Annin Company, Associated Valve & Engineering Co., Kieley & Mueller, Inc., and Atwood & Morrill Co. for the fabrication of  $\frac{1}{2}$ -in. shut-off valves for operation at 2000 psi and 300°C. Another similar test valve is being fabricated in the ORNL shops. These valves will be sealed against 2000-psi pressure by bellows manufactured by Breeze Corporations, Inc.

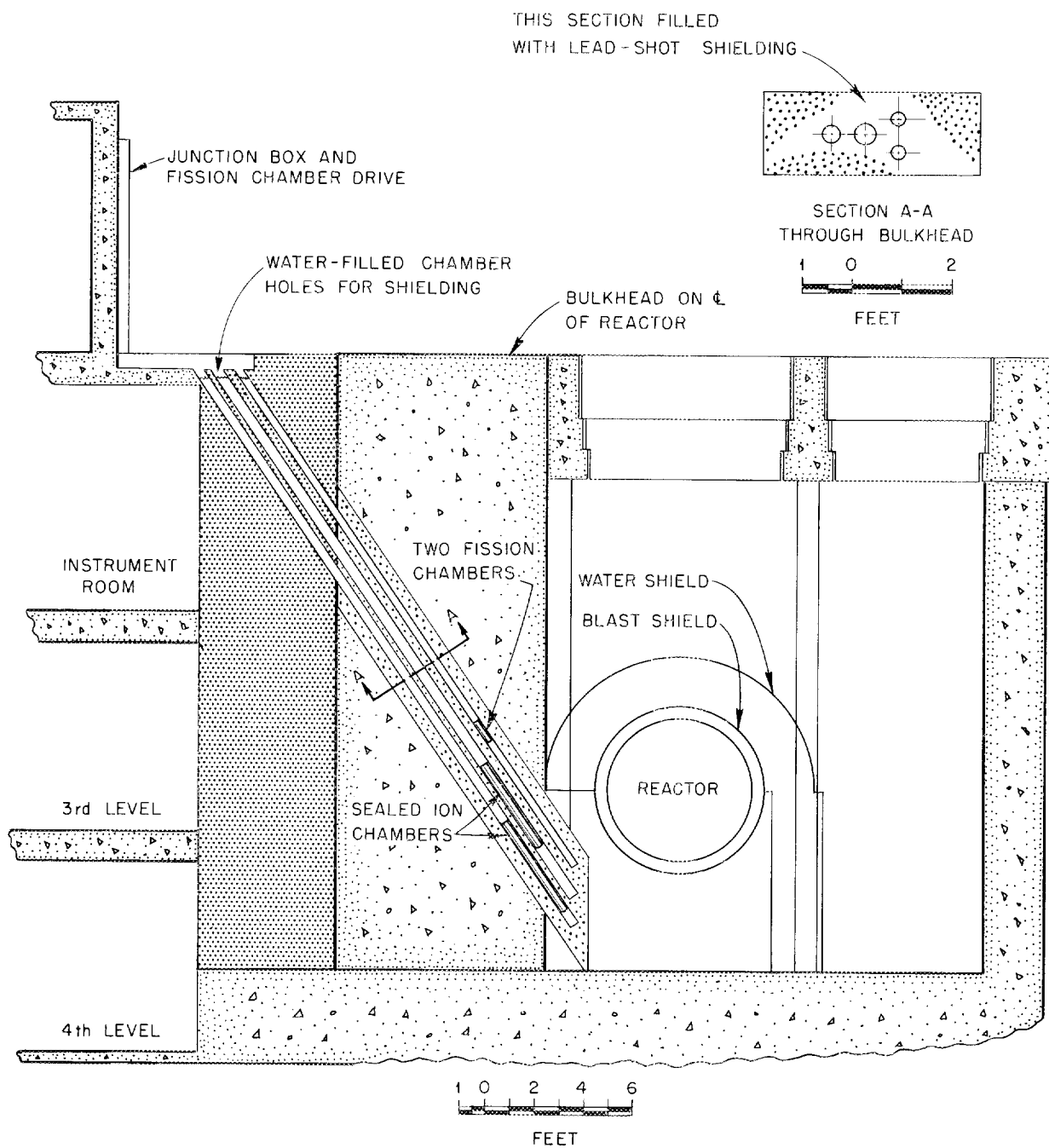


Fig. 33. Nuclear-Instrument Installation for HRT.

Core and blanket flow systems have been arranged so that the bellows of all bellows-sealed valves are on the low-pressure side. Consequently, valves similar to those used in the HRE are applicable, and, for the purposes of the HRT as presently considered, can be substituted for the high-pressure prototype valves described above.

Collaboration has been maintained with the Design Section in the following matters:

1. redesign of a metallic operator for HRE type valves,
2. design of a  $\frac{1}{8}$ -in. 2000-psi hand valve,
3. adaptation of a Minneapolis-Honeywell 4-H pneumatic operator for automatic control of the  $\frac{1}{8}$ -in. valve,
4. preparation of specifications for a  $\frac{1}{2}$ -in. bellows-sealed valve for use at pressures below 500 psi.

A  $\frac{1}{2}$ -in. Clifford bellows made of type 321 stainless steel and rated at 3600 psi was cycled at 1000 psi and room temperature for 337,000 cycles before failure. An identical bellows, made of type 347 stainless steel, will probably be used in the  $\frac{1}{8}$ -in. valves. Life tests will be repeated on the type 347 stainless steel bellows.

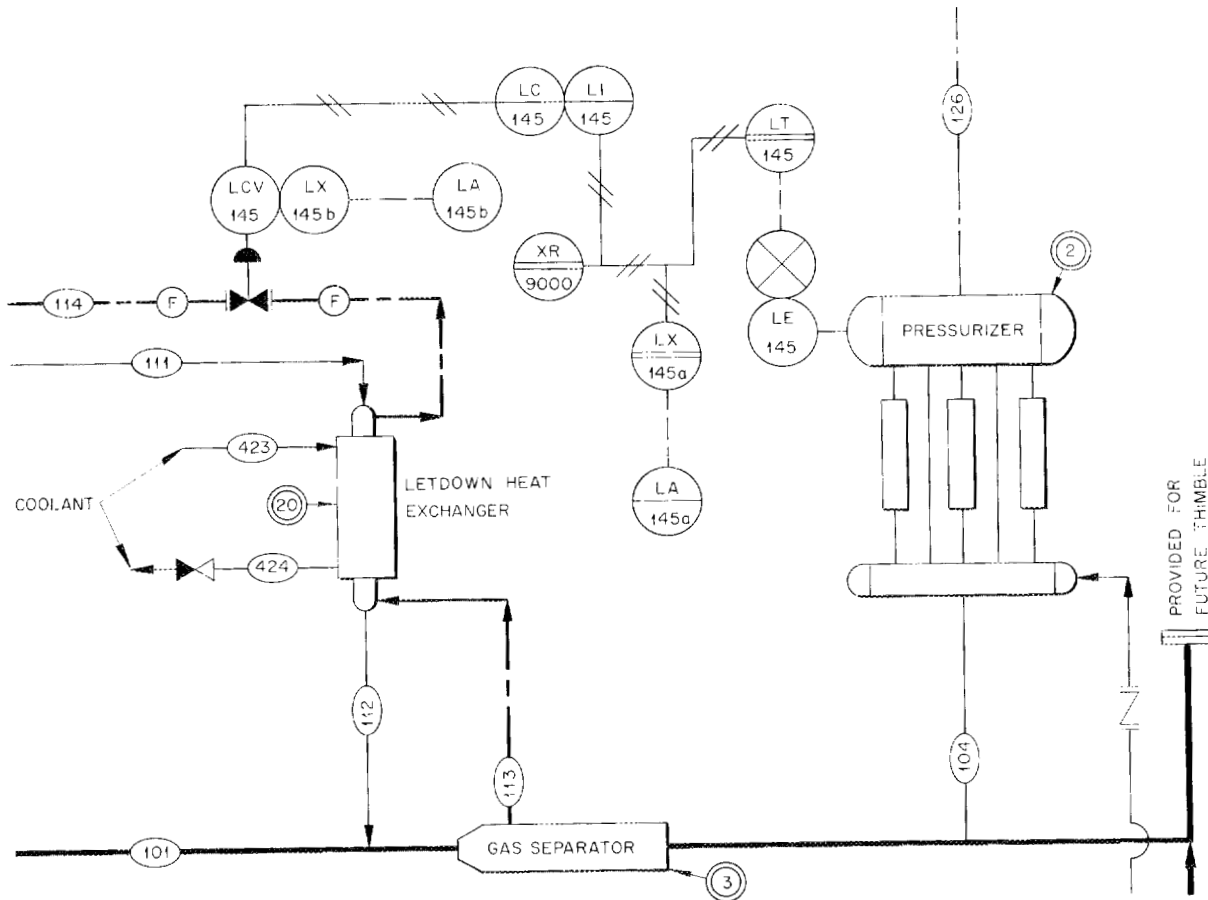
### General

The following instrument drawings have been prepared:

	Drawing No.
Engineering Flow Sheet - Blanket	E-18377
Engineering Flow Sheet - Core	E-18376
Nuclear Instrumentation - Block Diagram	E-18378
Health Physics Instrumentation - Block Diagram	D-18379

The engineering flow sheets have been divided into groups of related equipment for the purpose of preparing instrumentation application diagrams, such as the one shown in Fig. 34. Approximately 50 similar sheets have been prepared in order to describe the instrumentation of the entire HRT reactor system.

The procurement of these instruments has begun, and specifications have been approved for 15 components.



LE	DISPLACEMENT TYPE, INDUCTANCE PICKUP; 2000 psi, 300°C, 0-5 in. H <sub>2</sub> O; 1mv/v; ACCURACY ± 5%
LT	FOXBORO DYNALOG OR MINNEAPOLIS-HONEYWELL TO PNEUMATIC TRANSDUCER 3-15 psi.
XR	3-15 psi; 0-100%; POINT 1 OF 4 pt CC RECORDER
LI	3-15 psi; INDICATE 0-100; WITH SET POINT; TRANSFER SWITCH; VALUE POSITION INDICATOR.
LC	3-15 psi; PROPORTIONAL PLUS DERIVATIVE
LX(a)	3-15 psi; PRESSURE SWITCH
LA(c)	ANNUNCIATOR
LX(b)	VALVE SWITCH
LA(b)	VALVE POSITION LIGHT
LCV	1/2 in., 2000 psi; 300°C INLET, 500 psi 250°C BELLOWS, AIR TO OPEN; 20-30 psi LOADING.

**Fig. 34. Instrument Application Diagram.**

Part II

REACTOR ANALYSIS



## REACTOR ANALYSIS

M. C. Edlund, Section Chief

H. C. Claiborne	P. R. Kasten
J. DiLorenzo	L. C. Noderer
T. B. Fowler	M. Tobias
P. M. Wood	

### HOMOGENEOUS REACTOR KINETICS

#### Relation Between Reactivity Ramp Rate and Instantaneous Reactivity Addition

In evaluating the safety of a reactor it is necessary to know the amount of reactivity which can be added to the reactor core. All reactivity additions have a time element, but the effects of reactivity additions can be most easily studied if instantaneous reactivity additions are considered; hence, a relation between reactivity ramp rate and instantaneous reactivity addition would facilitate safety calculations.

For plausible ramp rates (about 1%/sec) in the HRT and other homogeneous, aqueous reactors, large power surges can occur only if the initial power is low. At low initial power, the rise in power accompanying reactivity addition is not significant until the reactor is near prompt critical. It is, therefore, a good approximation to assume that the reactor power does not rise until the reactivity exceeds prompt critical. If no reactivity compensation takes place, the reactor power is given by

$$(1) \quad x = e^{bt^2/2\tau}$$

The nomenclature for the above and following equations is given at the end of this section.

If the power is assumed to follow Eq. 1 and if an incompressible fluid model is chosen, the maximum reactivity added to the core can be estimated. Under the above conditions, the time,  $t_c$ , during which prompt reactivity is added is given by

$$(2) \quad b \approx \left| \frac{\partial k}{\partial T} \right| S P_0 e^{bt_c^2/2\tau}$$

If it is assumed that the power necessary to compensate reactivity addition is small compared with the peak power during the initial power surge, the equivalent prompt reactivity addition,  $\Delta k_{eqp}$ , is given by

$$(3) \quad \Delta k_{eqp} = bt_c$$

Combining Eqs. 2 and 3 gives

$$(4) \quad \Delta k_{eqp} = \left( 2 b \tau \ln \frac{b}{\omega_n^2 \tau} \right)^{1/2}$$

In order to test the validity of Eq. 4 over certain parameter values, a number of specific cases were run on the ORACLE. (In all ORACLE calculations, the mathematical model consisted of Eqs. 6-9 in ORNL-1205.) The cases considered both reactivity ramp rates and instantaneous reactivity additions, and equivalence was assumed when a given ramp rate and a given instantaneous addition caused an equal pressure rise in the reactor core (equal power maxima were also considered). The results are given in Table 7. Over the parameter ranges studied, the agreement is within 3%, the calculated values being consistently low. However, in Table 7, parameter  $C_2$  was not varied. The influence of  $C_2$  upon the validity of Eq. 4 was investigated by comparing only one particular ramp rate with the equivalent instantaneous reactivity addition for various values of  $C_2$ . Although not given here, the  $p_{max}$  obtained for the cases of Table 7 with  $b = 0.015$  was always very close to that obtained with  $\Delta k_e = 0.015$ . This is indicated in Table 7 by  $\Delta k_{eqp}(\text{ORACLE})_{p_{max}} + \beta$  being compared with  $b$ . In all calculations  $\beta$  was 0.005. As predicted by Eq. 4, the results given in Table 8 show that various combinations of  $L$ ,  $v_s$ , and  $C_2$  did not change the equivalence between ramp rate and instantaneous reactivity addition.

#### Calculation of Maximum Reactor Power

The core pressure rise is dependent upon the maximum reactor power, and if the reactor power curve can be calculated, the core pressure can be obtained also. In this section, an approximation to the maximum core power will be obtained.

If no delayed neutrons are considered and if the fluid is assumed to be incompressible, the

**HRP QUARTERLY PROGRESS REPORT**

**TABLE 7. COMPARISON OF THE  $\Delta k_{eqp}$  OBTAINED BY ORACLE CALCULATIONS WITH THE  $\Delta k_{eqp}$  OBTAINED BY EQ. 4**

Based on equality of peak core pressures and on equality of peak core powers\*

Parameter Values**				Equivalent Prompt Reactivity		
L (ft)	$v_s$ (fps)	$b$ (sec <sup>-1</sup> )	$P_0$ (kw)	$\Delta k_{eqp}$ (ORACLE) <sub>p<sub>max</sub></sub>	$\Delta k_{eqp}$ (ORACLE) <sub>x<sub>max</sub></sub>	$\Delta k_{eqp}$ (Eq. 4)
5	2380	0.012	10 <sup>-3</sup>	0.0087	0.0088	0.0086
	2380	0.013	10 <sup>-3</sup>	0.0091	0.00925	0.0090
	2380	0.014	10 <sup>-3</sup>	0.0095	0.0096	0.00935
	2380	0.015	10 <sup>-3</sup>	0.00985	0.00995	0.0097
	2380	0.012	10 <sup>-4</sup>	0.0093	0.00945	0.0092
	2380	0.013	10 <sup>-4</sup>	0.00975	0.00985	0.0096
	2380	0.014	10 <sup>-4</sup>	0.0103	0.01025	0.0100
	2380	0.015	10 <sup>-4</sup>	0.0107	0.0106	0.0104
	1400	0.012	10 <sup>-3</sup>	0.0087	0.0088	0.0086
	1400	0.013	10 <sup>-3</sup>	0.00915	0.00925	0.0090
	1400	0.014	10 <sup>-3</sup>	0.0095	0.0096	0.00935
	1400	0.015	10 <sup>-3</sup>	0.0099	0.00995	0.0097
	1400	0.012	10 <sup>-4</sup>	0.0094	0.00945	0.0092
	1400	0.013	10 <sup>-4</sup>	0.0098	0.00985	0.0096
	1400	0.014	10 <sup>-4</sup>	0.0103	0.01025	0.0100
	1400	0.015	10 <sup>-4</sup>	0.0107	0.01065	0.0104
10	2380	0.012	10 <sup>-3</sup>	0.0087	0.00875	0.0086
	2380	0.013	10 <sup>-3</sup>	0.0091	0.00915	0.0090
	2380	0.014	10 <sup>-3</sup>	0.0095	0.00955	0.00935
	2380	0.015	10 <sup>-3</sup>	0.0099	0.0099	0.0097
	2380	0.012	10 <sup>-4</sup>	0.0094	0.0094	0.0092
	2380	0.013	10 <sup>-4</sup>	0.0098	0.0098	0.0096
20	2380	0.012	10 <sup>-3</sup>	0.0087	0.0088	0.0086
	2380	0.013	10 <sup>-3</sup>	0.0092	0.00915	0.0090

\*Equality between a given reactivity ramp rate and an instantaneous reactivity increase is assumed whenever the maximum core pressures (or core powers) in the two cases are the same. To make the comparison, corresponding cases, with instantaneous reactivity additions assumed, were run on the ORACLE.

\*\*The  $C_2$  parameter, which was dimensionless, was not varied from zero.

maximum power is given by<sup>1</sup>

$$(5) \quad x_{max} = \frac{m^2}{2\omega_n^2}$$

If, on the other hand, the power is allowed to rise exponentially in an incompressible fluid for a given time  $t_c$ , where  $t_c$  is the time required for the temperature rise to compensate exactly for the

<sup>1</sup>W. C. Sangren, *Kinetic Calculations for Homogeneous Reactors*, ORNL-1205 (April 15, 1952) p 22.

initial  $\Delta k_{eqp}$ , the maximum power is given by<sup>2</sup>

$$(6) \quad x_{max} = \frac{m^2}{\omega_n^2}$$

The latter model thus gives a maximum power twice as great as that calculated from the former exact model. By analogy, the latter method can be used for mathematical models where an exact solution is not known, if the  $x_{max}$  obtained is

<sup>2</sup>*Ibid.*, p 24.

TABLE 8. COMPARISON OF PEAK CORE PRESSURES AND PEAK CORE POWERS BETWEEN AN INSTANTANEOUS REACTIVITY INCREASE,  $a$ , OF  $0.015 \Delta k_e$  AND A REACTIVITY RAMP RATE,  $b$ , OF  $0.015 \Delta k_e / \text{sec}$  FOR VARIOUS PARAMETER VALUES\*

Parameter Values				$\Delta p_{\text{max}}$ (psi)		$x_{\text{max}}, P_{\text{max}}/P_0 \times 10^{-8}$	
$L$ (ft)	$v_s$ (fps)	$C_2$ (dimensionless)	$P_0$ (kw)	$a = 0.015$	$b = 0.015$	$a = 0.015$	$b = 0.015$
10	2380	0.2	$10^{-3}$	335	332	1.70	1.68
	1400	0.2	$10^{-3}$	368	370	2.85	2.88
	1400	0.4	$10^{-3}$	415	425	3.05	3.10
	2380	0.4	$10^{-3}$	465	475	1.87	1.87
20	2380	0.2	$10^{-3}$	610	600	2.20	2.16
	1400	0.2	$10^{-3}$	730	730	4.37	4.50
	2380	0.4	$10^{-3}$	730	730	2.35	2.40
	1400	0.4	$10^{-3}$	760	790	4.51	4.72

\*Peak pressures and powers obtained by ORACLE calculations.

divided by 2. Such a method applied to the HRT mathematical system<sup>3</sup> gives

$$(7) \quad x_{\text{max}} = \frac{m^2}{2\omega_n^2} F,$$

where  $F$  is a function of the particular physical reactor system.

In the derivation of Eq. 7 the assumption is made that the power always rises exponentially during the time of interest. This is not actually true, and so the inertia of the fluid may act to reduce  $x_{\text{max}}$  at times near the peak power. Equation 7 is therefore written as

$$(8) \quad x_{\text{max}} = \frac{m^2}{C_3 \omega_n^2} F.$$

To evaluate  $C_3$ , a number of specific cases were run on the ORACLE. These values are summarized in Table 9 where it is illustrated that while  $C_3$  did vary it was reasonably constant about 2.3. Thus, while  $F$  is a very important correction in Eq. 7, it overcorrects to a small extent. For values of  $F > 2$ , it appears that the maximum power following a reactivity increase is given adequately by

$$(9) \quad x_{\text{max}} = \frac{m^2}{2.2\omega_n^2} F.$$

<sup>3</sup>Ibid., Eqs. 6, 7, 8, and 9.

<sup>4</sup>P. R. Kasten, *Design Basis for Volume of Pressurizer in HRT*, ORNL CF-54-5-188 (May 24, 1954).

### Nomenclature

- $a$  = instantaneous reactivity addition at time zero,  $\Delta k_e(0)$ ,
- $b$  = reactivity ramp rate,  $\Delta k_e / \text{sec}$ ,
- $C_2$  = factor to account for finite volume of pressurizer fluid,<sup>4</sup>
  - $C_2 = 0$  is equivalent to an infinite pressurizer volume,
  - $C_2 = 0.2$  is equivalent to a 60-liter pressurizer volume,
  - $C_2 = 0.4$  is equivalent to a 120-liter pressurizer volume,

## HRP QUARTERLY PROGRESS REPORT

$C_3$  = "constant" appearing in Eq. 8, to relate  $x_{\max}$  of the mathematical model chosen, to the correct  $x_{\max}$  as obtained on ORACLE,

$$F = \frac{\omega_b^2(1 + C_2) + Jm + m^2}{\omega_b^2}, \text{ a function of the specific physical reactor system, }^{4,5}$$

$k_e$  = effective multiplication constant of reactor system,

$\Delta k_e$  = reactivity =  $k_e - 1$  = instantaneous reactivity addition,

$\Delta k_{eqp}$  = equivalent prompt reactivity, associated with a given ramp rate,

$\Delta k_{eqp}$  (Eq. 4) =  $\Delta k_{eqp}$  as calculated from Eq. 4,

$\Delta k_{eqp}$  (ORACLE) $_{p_{\max}}$  =  $\Delta k_{eqp}$  as obtained from ORACLE calculations, based on equal core-pressure rise,

$\Delta k_{eqp}$  (ORACLE) $_{x_{\max}}$  =  $\Delta k_{eqp}$  as obtained from ORACLE calculations, based on equal core-power rise,

$\partial k_e / \partial T$  = temperature coefficient of reactivity,  $\Delta k_e / ^\circ C$ ,

$L$  = length of  $3\frac{1}{2}$ -in. piping between reactor core and surface of pressurizer liquid, ft,

$m$  =  $\Delta k_{eqp} / \tau$ ,  $\Delta k_e(0) / \tau$ ,

$p_{\max}$  = maximum rise in reactor core pressure, psi,

$P$  = reactor power, kw,

$P_0$  = initial reactor power, kw,

$S$  = reciprocal volume heat capacity of core liquid,  $^\circ C / kw \cdot sec$ ,

$t$  = time (time during which prompt reactivity is added), sec,

$t_c$  = time during which reactivity is added, time required for core temperature rise to compensate  $\Delta k_e(0)$ , sec,

$v_s$  = velocity of sound in core fluid, ft/sec,

$x$  =  $P / P_0$ ,

$x_{\max}$  = maximum value of  $x$  during power surge,

$\beta$  = fraction of fission neutrons which are delayed,

$\tau$  = average lifetime of prompt neutrons, sec,

$$\omega_b^2 = \frac{1}{\tau} \left| \frac{\partial k_e}{\partial T} \right| S P_0, \text{ sec}^{-2}.$$

### TWO-REGION HIGH-PURITY PLUTONIUM PRODUCERS

In connection with the K-49 reactor program as outlined in KA-328,<sup>6</sup> calculations have been made to determine the nuclear characteristics of a two-region converter that will produce power and low  $g/T$  (<1% Pu<sup>240</sup>/Pu<sup>239</sup>) plutonium at the smallest unit cost.

The last quarterly report<sup>7</sup> contained a description of the method of calculation and the characteristics

<sup>5</sup>P. R. Kasten and V. K. Paré, *Safety of HRT*, ORNL CF-54-3-164 (March 25, 1954).

<sup>6</sup>C. E. Center, *Proposal for the Production of Very Low  $g/T$  Plutonium*, KA-328 (Jan. 25, 1954).

<sup>7</sup>M. C. Edlund et al., *HRP Quar. Prog. Rep. Apr. 30, 1954*, ORNL-1753, p 9-18.

TABLE 9. VALUES OF  $C_3$  WHICH WILL GIVE CORRESPONDENCE BETWEEN THE PEAK POWERS OBTAINED BY EQ. 8 AND THOSE OBTAINED BY ORACLE CALCULATIONS

$L$ (ft)	$v_s$ (fps)	$C_2$ (dimensionless)	$P_0$ (kw)	$\alpha [\Delta k_e (0)]$	$F$ (dimensionless)	$C_3$ (dimensionless)
5	2380	0	$10^{-3}$	0.015	1.4	2.15
	1400	0	$10^{-3}$	0.015	2.16	2.19
10	2380	0	$10^{-3}$	0.015	1.74	2.38
	2380	0.2	$10^{-3}$	0.015	1.94	2.26
	2380	0.4	$10^{-3}$	0.015	2.14	2.23
	1400	0.2	$10^{-3}$	0.015	3.36	2.32
	1400	0.4	$10^{-3}$	0.015	3.56	2.32
	2380	0	$10^{-3}$	0.015	2.43	2.38
20	2380	0.2	$10^{-3}$	0.015	2.63	2.37
	2380	0.4	$10^{-3}$	0.015	2.83	2.37
	1400	0.2	$10^{-3}$	0.015	5.35	2.43
	1400	0.4	$10^{-3}$	0.015	5.55	2.44

of 20 two-region converters. These results were obtained with standard desk-type calculating machines and required considerable labor. Since then, many of the calculations involving nuclear characteristics, product quality, and economics have been performed with the assistance of the ORACLE.<sup>8</sup>

An additional 30 reactors have been investigated with the aid of the ORACLE. The primary purpose of the additional calculations was to investigate the effect of using slightly enriched (0.85 to 1.0%) blanket feed.

The results, shown in Table 10, indicate that reductions up to 14% in the unit cost of plutonium were obtained when compared with the previously reported unit costs of plutonium from reactors using normal or depleted uranium feed to the blanket. The optimum feed enrichment is apparently about 0.9% for both the 12- and 14-ft reactors for an operating enrichment of 0.55% in

the blanket. An additional 4% decrease in unit cost resulted from increasing the pressure vessel from 12 to 14 ft in diameter.

The optimum operating enrichment of the blanket is apparently about 0.5% when a feed of 0.85% enrichment is used, which agrees well with the optimum previously reported for operation with normal uranium feed.

These additional calculations, in all cases, show that operating with a 4-ft-dia core gives the lowest unit cost. It is debatable, however, whether real advantage is gained by reducing the core diameter below 5 or 6 ft. The power density in a 4-ft core is over three times that in a 6-ft core (100 kw/liter for a 6-ft core; 340 kw/liter for a 4-ft core). Also, the effects of inlet and exit piping, which are more important with decreased core size, have thus far been neglected.

It is emphasized that these calculations were performed for a constant core power of 320 Mw; consequently, the total power of the systems studied varied considerably. If comparison were made at equal total power, the differences would not be so pronounced.

<sup>8</sup>T. B. Fowler and R. A. Willoughby, *ORACLE Code for the Two-Group, Two-Region Homogeneous Reactor Calculation*, ORNL CF-54-7-38 (July 7, 1954).

TABLE 10. CHARACTERISTICS OF THREE PLUTONIUM PRODUCERS\*

Reactor No.	Core Diameter (ft)	Pressure Vessel Diameter (ft)	Blanket Feed Enrichment (wt %)	Blanket Enrichment (wt %)	Blanket Power (Mw)	Core Concentration (g of U per liter)	Blanket Poisons (%)	Product Quality $N_{40}/N_{49}$ (%)	Net Pu Produced (kg/yr)	Relative Unit Cost (\$)
3	4	12	0.7115	0.247	139	6.62	8.0	0.440	172	1.000
2	5	12	0.7115	0.247	141	2.53	8.0	0.440	167	1.021
21	4	12	1.00	0.553	446	5.26	5.0	0.268	304	0.709
22	5	12	1.00	0.553	450	3.07	5.0	0.270	296	0.726
23	6	12	1.00	0.553	437	2.07	5.0	0.272	280	0.760
24	4	12	0.85	0.553	449	3.52	5.0	0.372	305	0.703
25	5	12	0.85	0.553	452	3.06	5.0	0.373	297	0.723
26	6	12	0.85	0.553	439	2.06	5.0	0.374	280	0.757
27	4	12	0.85	0.661	605	4.95	4.5	1.28	362	0.846
28	5	12	0.85	0.661	606	2.90	4.5	1.28	352	0.868
29	6	12	0.85	0.661	583	1.95	4.5	1.28	330	0.907
30	4	12	0.85	0.395	276	5.67	5.0	0.239	237	0.814
31	5	12	0.85	0.395	279	3.29	5.0	0.241	231	0.832
32	6	12	0.85	0.395	152	2.21	5.0	0.243	220	0.868
33	4	14	0.7115	0.247	152	6.09	8.0	0.495	187	0.941
34	6	14	0.7115	0.247	157	2.36	8.0	0.494	180	0.979
35	4	14	0.7115	0.474	371	5.50	8.0	0.432	280	0.744
36	5	14	0.7115	0.474	380	3.21	5.0	0.433	277	0.751
37	6	14	0.7115	0.474	380	2.15	5.0	0.433	270	0.767
38	4	14	0.7115	0.553	476	5.29	5.0	1.32	319	0.706
39	5	14	0.7115	0.553	486	3.12	4.5	1.32	316	0.713
40	6	14	0.7115	0.553	485	2.07	4.5	1.32	308	0.729
41	4	14	1.00	0.553	470	5.31	4.5	0.282	321	0.693
42	5	14	1.00	0.553	480	3.13	5.0	0.283	318	0.700
43	6	14	1.00	0.553	479	2.08	5.0	0.284	310	0.716
44	4	14	0.85	0.553	473	5.30	5.0	0.392	322	0.690
45	5	14	0.85	0.553	483	3.13	5.0	0.393	319	0.696
46	6	14	0.85	0.553	481	2.08	5.0	0.393	311	0.712
47	4	14	0.85	0.661	648	4.99	4.5	1.33	389	0.823
48	6	14	0.85	0.661	655	1.97	4.5	1.32	375	0.854
49	5	14	0.85	0.395	292	3.32	5.0	0.255	242	0.816
50	6	14	0.85	0.395	292	2.22	5.0	0.256	236	0.834

\*Core power, 320 Mw; core and blanket operating temperatures, 270 and 250°C, respectively; core enrichment, 50.9%; core poisons, 7%.

Part III

CORROSION



## PUMP-LOOP CORROSION TESTS

J. C. Griess

H. C. Savage

### PUMP-LOOP OPERATION AND MAINTENANCE

H. C. Savage

F. J. Walter

#### Loop Status

Fourteen dynamic test loops are now available for corrosion testing. In general, each loop contains standard pin and coupon corrosion specimens. All fourteen loops are shielded for protection to personnel from high-pressure leaks or ruptures.

A brief summary of the status of each corrosion test loop is given below. Corrosion data and test results are given in the section "Loop Test Results."

Loop A is being used for corrosion studies with 0.06 *m* uranyl sulfate containing 0.006 *m* sulfuric acid and oxygen at 320°C. To date, this loop has been operated for nearly 4500 hr at approximately 320°C and approximately 2000 psi. During this period, both the pump and the loop have performed satisfactorily. Corrosive attack on the pump and on observable parts of the loop has been slight.

Loop B is being used for a series of short-term tests in a study of the corrosive effect of dilute nitric acid on stainless steel. During this quarter, several tests to determine the effect of small quantities of various compounds (chromium sulfate, manganous sulfate, and sodium tungstate) on corrosion of stainless steel by uranyl sulfate have been completed.

In Loop C, a series of short-term tests, designed to evaluate gas-phase corrosion when the uranyl sulfate solution contained halogen compounds, was completed during this quarter.

At the end of the present test (0.11 *m* uranyl sulfate with 0.015 *m* sulfuric acid and oxygen at 250°C for 1000 hr), Loop C will be replaced with a new multipass loop similar to the one presented in another report.<sup>1</sup>

In Loop D, a series of short-term tests, designed to evaluate the effect of compounds such as sodium tungstate and potassium dichromate on corrosion of stainless steel by uranyl sulfate, was completed during this quarter. Two short-term tests with 1.34 *m* uranyl sulfate and oxygen have also been completed.

At the present time, Loop D is being equipped with a Lapp CPS-1 Pulsafeeder which will make both Loops C and D available for continuous, controlled-rate addition studies.

Loop E is being used for corrosion studies with 0.06 *m* uranyl sulfate containing 0.006 *m* sulfuric acid and oxygen at 200°C.

In Loop F, a series of short-term tests with 1.34 *m* uranyl sulfate and oxygen in the temperature range 250 to 300°C has been completed. During a test at 300°C with 1.34 *m* uranyl sulfate, liquid samples indicated that the solution was definitely in the two-liquid-phase region.

In Loop G (All-Titanium Loop), the titanium pressurizer which failed because of overheating<sup>2</sup> has been replaced with a new titanium pressurizer equipped with a 1750-w calrod heater cast in 2S aluminum. The loop main line has also been equipped with a 1750-w calrod heater cast in 2S aluminum. Loop G has also been provided with a new control system which incorporates high-temperature cutouts for both heaters.

This loop was operated for 327 hr with 1.34 *m* uranyl sulfate and oxygen at 300°C. Liquid samples indicate that the solution was definitely in the two-liquid-phase region during this test. No noticeable corrosion was observed on either the loop or the pump as a result of operation in the two-liquid-phase region.

Loop G is now operating at 300°C with 1.34 *m* uranyl sulfate containing 0.3 *m* sulfuric acid (enough acid to prevent formation of two liquid phases) and oxygen.

During this quarter, Loop H has been used for the study of corrosion of stainless steel by 1.34 *m* uranyl sulfate and oxygen at 225 and 250°C. One short-term test with 0.43 *m* uranyl sulfate and oxygen at 250°C has also been completed.

During operation with 1.34 *m* uranyl sulfate and oxygen, three 1/4-in. mixing tubes failed because of excessive or selective corrosion. A complete analysis of these failures is presented in the metallurgy section of this report. In an effort to eliminate this type of failure, Loop H has been

<sup>1</sup>J. R. McWherter and R. L. Cauble, *HRP Quar. Prog. Rep.* Mar. 31, 1953, ORNL-1554, Fig. 17, p 28.

<sup>2</sup>H. C. Savage and F. J. Walter, *HRP Quar. Prog. Rep.* Apr. 30, 1954, ORNL-1753, p 59-61.

## HRP QUARTERLY PROGRESS REPORT

equipped with a  $\frac{3}{8}$ -in. pipe mixing line containing a titanium flow restrictor and a titanium liner downstream from the restrictor.

The Westinghouse 100A thermal spacer (42S1AP20) with a titanium face plate was removed from Loop H after 1259 hr in 1.34 *m* uranyl sulfate and 200 hr in 0.43 *m* uranyl sulfate. The crevice corrosion pits mentioned in an earlier report<sup>2</sup> did not appear to have grown significantly deeper.

Loop I is being used for the study of corrosion by 0.06 *m* uranyl sulfate containing 0.006 *m* sulfuric acid and oxygen at 225 and 250°C.

A series of short-term tests with 1.34 *m* uranyl sulfate and oxygen at 200°C has been completed in Loop J. One 1000-hr test with 0.11 *m* uranyl sulfate containing 0.015 *m* sulfuric acid and oxygen at 300°C has also been completed.

Loop K has not been operated this quarter.

A series of short-term tests with 1.34 *m* uranyl sulfate and oxygen at 275°C has been completed in Loop L. A Westinghouse 100A thermal spacer (No. XX) with a new titanium face plate was removed from this loop after 380 hr. The type 347 stainless steel side of the stainless steel-titanium interface was rather badly corroded, particularly around the outer periphery (Fig. 35).

Loop M is still being used for corrosion tests on special samples exposed to uranyl sulfate solutions.

Loop N has not been operated this quarter.

The HRE Mock-up (Building 9204-1, Y-12 Area) has been completely dismantled for inspection. When all the components have been inspected, a complete report on the operating history and the extent of corrosive attack will be written.

### Westinghouse 100A Pumps

The Westinghouse 100A pumps continue to give good service. No pumps failed and none were rebuilt during this quarter. During the past year, two rotor stub shafts broke near the impeller keyway. Since this is an unusual type of failure, these stub shafts have been turned over to the Metallurgy Group for examination.

### RESULTS OF LOOP TESTS

J. C. Griess

The corrosion resistance of a number of metals and alloys to uranyl sulfate solutions has been investigated during the past quarter. The largest effort has been expended at the 1.34 *m* uranyl

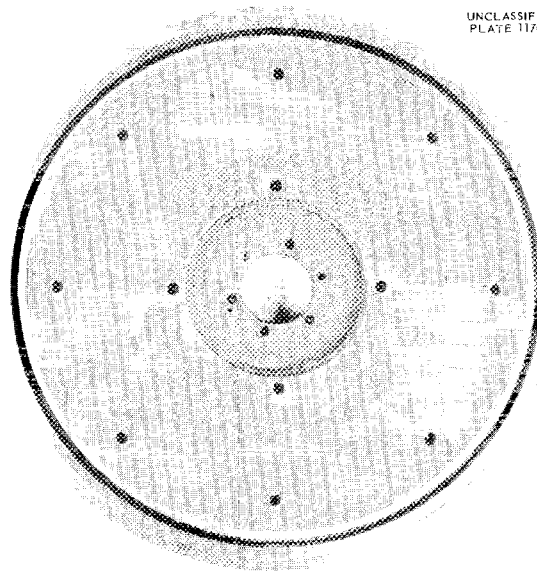


Fig. 35. Modified Westinghouse 100A Thermal Spacer No. XX Showing Stainless Steel Side of Titanium-Type 347 Stainless Steel Interface, Not Defilmed.

sulfate level where data have been obtained at 200 to 300°C. At this concentration the rate and/or the extent of attack of stainless steel were high at all temperatures but the general nature of attack was the same as at the 0.17 and 0.02 *m* levels. For example, at temperatures less than 250°C attack was continuous even at low flow rates, but at 250 and 275°C the oxide film that formed at low flow rates during the initial period appeared to minimize subsequent attack.

A review of the corrosion results obtained in 0.17 *m* uranyl sulfate at 200 and 225°C has been made, and it shows that at low flow rates (~15 fps) type 347 stainless steel corroded at a lower rate than type 304L at both temperatures but that at high flow rates both alloys were attacked at the same rate. At low flow both steels corroded faster at 225°C than at 250°C. This latter fact appears to be related to the chemical composition of the oxide film deposited on the surface of the stainless steel during the corrosion process.

A series of runs has been made with 0.06 *m* uranyl sulfate containing 0.006 *m* sulfuric acid at 250°C. Under the conditions of the test the corrosion rate after the initial period of rapid attack was 1 mpy at flow rates as low as 15 fps. At flow rates in excess of the critical velocity the rate of attack was quite severe, amounting to 120 mpy.

The titanium loop has been operated successfully at 300°C with 1.34 *m* uranyl sulfate. Throughout this run the uranyl sulfate solution existed as two immiscible liquid phases well dispersed in one another. The corrosion damage to the loop as well as to the titanium and zirconium corrosion specimens was practically nil, as has been the case at all other temperatures and concentrations investigated to date.

In the sections which follow, all the data obtained during the past quarter are presented and the more pertinent data are discussed.

#### General Corrosion Rates

The average corrosion rates of pin-type corrosion specimens exposed in the loops during the past quarter are presented in Table 11. The presentation is the same as it has been in a number of previous reports,<sup>3-8</sup> and the same precautions given before should be exercised in using the data. All corrosion rates reported in Table 11 are average rates for the given exposure period. At flow rates less than the critical velocity, corrosion is not a constant rate process; the rate is usually high at the beginning of the exposure and decreases to a steady, usually low, rate after 50 to 200 hr. Thus the average rates given in Table 11 are greatly dependent on the duration of the test. The data at low flow rates, then, are of only limited value in an absolute sense but are of value for comparison of one alloy with another. At high flow rates the corrosion process usually occurs at

a constant rate, and the data in Table 11 have a quantitative significance in those cases.

In addition to the data presented in Table 11 a number of specimens of different types have been tested in uranyl sulfate solutions as a service for other groups. The results of these tests are described in the appropriate sections.

#### Corrosion Testing in 1.34 *m* Uranyl Sulfate

Because of a change in the relative emphasis on the objectives of the HRP program in which the plutonium producer was placed secondary to a breeder, only preliminary testing with 1.34 *m* uranyl sulfate was completed. However, the temperature range of 200 to 300°C was explored.

**200°C.** Three runs, J-35, -36, and -37, were made at 200°C, and, unfortunately, the velocity of the solution past the pins at low flow rates was different in all cases. In these runs the indicated corrosion rates were very high, suggesting a high continuing rate even at low flow rates. However, the previously reported data for 0.17 *m* solutions run at 200°C indicated that long-term tests are required to determine whether the heavy oxide coating deposited at this temperature will give some measure of protection. It should be noted in Table 11 that in all runs at the low flow rate the type 347 stainless steel specimens were more heavily attacked than the type 304L stainless steel specimens. This fact is contrary to the observations made under the same conditions at the 0.17 *m* uranyl sulfate level. At the high flow rate runs J-36 and J-37 agreed, and there was no difference in the corrosion rate of types 304L and 347 stainless steel pins. The average corrosion rate was 260 mpy.

At low flow the corrosion specimens, when removed from the loop, were covered with a thin, reddish-brown film, under which there was a much heavier, black film or scale. The red covering was nonadherent and was easily removed with a soft brush. The black film, however, was more tightly adherent but the oxide coating did not appear to be so hard as the oxide coatings formed at higher temperatures. At high flow rates all specimens had a rather thin film, which was obviously porous and of no value in preventing corrosion, as was shown by the constant, high corrosion rate at high velocity.

**225°C.** A total of six runs, H-28 through H-33, has been made with 1.34 *m* uranyl sulfate at 225°C;

<sup>3</sup>J. C. Griess, J. M. Ruth, and R. E. Wacker, *HRP Quar. Prog. Rep. Jan. 1, 1953*, ORNL-1478, p 63.

<sup>4</sup>J. C. Griess and R. E. Wacker, *HRP Quar. Prog. Rep. Mar. 31, 1953*, ORNL-1554, p 49.

<sup>5</sup>J. C. Griess and R. E. Wacker, *HRP Quar. Prog. Rep. July 31, 1953*, ORNL-1605, p 74.

<sup>6</sup>J. C. Griess and R. E. Wacker, *HRP Quar. Prog. Rep. Oct. 31, 1953*, ORNL-1658, p 45.

<sup>7</sup>J. C. Griess and R. E. Wacker, *HRP Quar. Prog. Rep. Jan. 31, 1954*, ORNL-1678, p 50.

<sup>8</sup>J. C. Griess and R. E. Wacker, *HRP Quar. Prog. Rep. Apr. 30, 1954*, ORNL-1753, p 61-81.

TABLE 11. CORROSION RESULTS OF PIN-TYPE SPECIMENS EXPOSED TO CIRCULATING URANYL SULFATE SOLUTIONS

Run No.	Test Conditions						Corrosion Rate (mpy)			
	Uranium Concentration (molality)	Temperature (°C)	Time (hr)	Additions	Flow Rate (fps ± 10%)	Pin Material	Number of Pins	Minimum	Average	Maximum
B-39	0.17	250	27	1000–2000 ppm O <sub>2</sub> , MnSO <sub>4</sub> <sup>a</sup>	17	Type 304L stainless steel	5	150	160	160
						Type 347 stainless steel	5	150	160	160
						Type 309SCb stainless steel	2	150	150	150
						Platinum	1 <sup>b</sup>			
						Type 304L stainless steel	5	190	250	360
						Type 347 stainless steel	5	200	230	300
						Type 309SCb stainless steel	2	210	250	280
B-40	0.17	250	200	1000–2000 ppm O <sub>2</sub> , MnSO <sub>4</sub> <sup>c</sup>	17	Type 304L stainless steel	3	72	83	93
						Type 347 stainless steel	5	27	34	43
						Type 309SCb stainless steel	2	41	51	60
						Platinum	1 <sup>b</sup>			
						Type 304L stainless steel	5	240	280	360
						Type 347 stainless steel	5	240	260	310
						Type 309SCb stainless steel	2	270	270	270
B-41	0.17	250	200	2000–4400 ppm O <sub>2</sub> , 100 ppm W as Na <sub>2</sub> WO <sub>4</sub>	17	Type 304L stainless steel	4	26	32	37
						Type 347 stainless steel	4	24	25	26
						Type 309SCb stainless steel	2	19	20	20
						Platinum	1 <sup>b</sup>			
						Type 304L stainless steel	5	270	330	480
						Type 347 stainless steel	5	250	280	340
						Type 309SCb stainless steel	2	280	300	320
						Platinum	1 <sup>b</sup>			
C-38 <sup>d</sup>	0.17	250	194 <sup>e</sup>	1000–1500 ppm O <sub>2</sub> , 50 ppm I as KI	10	Type 304L stainless steel	5	3.0	17	30
						Type 347 stainless steel	5	9.6	23	28
						Type 309SCb stainless steel	2	28	29	29
						Zircaloy-2	1 <sup>b</sup>			
						Gold	1			

TABLE 11. (continued)

Run No.	Test Conditions						Corrosion Rate (mpy)			
	Uranium Concentration (molality)	Temperature (°C)	Time (hr)	Additions	Flow Rate (fps ± 10%)	Pin Material	Number of Pins	Minimum	Average	Maximum
C-40	0.08	250	18	1000-2000 ppm O <sub>2</sub> , 0.016 M H <sub>2</sub> SO <sub>4</sub>	12-19	Type 304L stainless steel	6	63	73	79
						Type 347 stainless steel	23	33	67	76
						Type 309SCb stainless steel	6	33	47	90
						Type 347 stainless steel	4 <sup>f</sup>	72	80	100
						Carpenter 20	3	46	52	60
D-26	0.17	250	200	1000-2000 ppm O <sub>2</sub> , 100 ppm W as Na <sub>2</sub> WO <sub>4</sub>	18	Type 304L stainless steel	4	2.2	3.4	5.0
						Type 347 stainless steel	6	4.2	18	31
						Type 309SCb stainless steel	2	16	22	28
						Titanium 75A	1 <sup>b</sup>			
					69	Type 304L stainless steel	5	72	140	190
						Type 347 stainless steel	5	150	180	200
						Type 309SCb stainless steel	2	200	210	220
						Titanium 75A	1 <sup>b</sup>			
D-27 <sup>g</sup>	1.34	250	200	1000-2000 ppm O <sub>2</sub>	18	Type 304L stainless steel	6	210	310	400
						Type 304L stainless steel	3 <sup>b</sup>	13	70	110
						Type 304L stainless steel	1 <sup>i</sup>		430	
						Type 304L stainless steel	1 <sup>j</sup>		60	
						Type A212B steel	3 <sup>k</sup>	63	73	83
					69	Type 304L stainless steel	7	800	870	980
						Type 304L stainless steel	3 <sup>b</sup>	420	490	550
						Type 304L stainless steel	1 <sup>j</sup>		110	
						Type A212B steel	3 <sup>k</sup>			
D-30	0.17	250	200	1000-2000 ppm O <sub>2</sub> , 200 ppm Cr as K <sub>2</sub> Cr <sub>2</sub> O <sub>7</sub>	16	Type 304L stainless steel	5	1.0	1.0	1.0
						Type 347 stainless steel	5	1.1	1.3	1.4
						Type 309SCb stainless steel	2	1.7	1.8	1.8
						Type 304L stainless steel	1 <sup>l</sup>		35	
						Platinum	1	0.17		

PERIOD ENDING JULY 31, 1954

TABLE 11. (continued)

Run No.	Test Conditions						Corrosion Rate (mpy)			
	Uranium Concentration (molality)	Temperature (°C)	Time (hr)	Additions	Flow Rate (fps ± 10%)	Pin Material	Number of Pins	Minimum	Average	Maximum
D-30	0.17	250	200	1000-2000 ppm O <sub>2</sub> , 200 ppm Cr as K <sub>2</sub> Cr <sub>2</sub> O <sub>7</sub>	69	Type 304L stainless steel	5	100	140	200
						Type 347 stainless steel	5	100	160	230
						Type 309SCb stainless steel	2	160	170	170
						Type 304L stainless steel	1 <sup>l</sup>		230	
						Platinum	1		0.26	
D-31	0.17	250	402	1000-2000 ppm O <sub>2</sub> , 200 ppm Cr as K <sub>2</sub> Cr <sub>2</sub> O <sub>7</sub>	16	Type 304L stainless steel	4	0.25	0.54	0.85
						Type 347 stainless steel	5	0.55	0.73	0.89
						Type 309SCb stainless steel	2	0.59	0.70	0.80
						Type 321 stainless steel	2	0.63	0.66	0.68
						Platinum	1 <sup>b</sup>			
					69	Type 304L stainless steel	4	150	170	220
						Type 347 stainless steel	5	200	240	270
						Type 309SCb stainless steel	2	220	240	250
						Type 321 stainless steel	2	240	290	330
						Platinum	1 <sup>b</sup>			
E-28	0.17	225	1000	1000-2000 ppm O <sub>2</sub>	14	Type 304L stainless steel	5	13	38	55
						Type 347 stainless steel	5	7.2	7.7	8.7
						Type 309SCb stainless steel	2	8.0	10	12
					17	Type 304L stainless steel	5	74	86	100
						Type 347 stainless steel	5	10	11	13
						Type 309SCb stainless steel	2	68	84	100
					73	Type 304L stainless steel	5	130	140	170
						Type 347 stainless steel	5	120	140	180
						Type 309SCb stainless steel	2	160	200	230
F-34	1.34	250	117	1000-2000 ppm O <sub>2</sub>	12	Type 304L stainless steel	4	170	190	250
						Type 347 stainless steel	4	100	120	130
						Type 309SCb stainless steel	2	270	330	380
						Zircaloy-2	1 <sup>b</sup>			

TABLE 11. (continued)

Run No.	Test Conditions						Corrosion Rate (mpy)			
	Uranium Concentration (molality)	Temperature (°C)	Time (hr)	Additions	Flow Rate (fps ± 10%)	Pin Material	Number of Pins	Minimum	Average	Maximum
F-34	1.34	250	117	1000-2000 ppm O <sub>2</sub>	12	Titanium 75A Gold	1 <sup>b</sup> 1 <sup>b</sup>			
F-35	1.34	300	60	500-1500 ppm O <sub>2</sub> , 0.1 m H <sub>2</sub> SO <sub>4</sub>	11	Type 304L stainless steel Type 347 stainless steel Type 309SCb stainless steel Type 304L stainless steel Zirconium-2½% tin Titanium 75A Titanium 150A	3 4 2 1 <sup>l</sup> 1 <sup>b</sup> 1 1	230 260 240	240 280 240 370	250 290 240
F-36	1.34	300	25	500-1500 ppm O <sub>2</sub> , 0.3 m H <sub>2</sub> SO <sub>4</sub>	11	Type 304L stainless steel Type 347 stainless steel Type 309SCb stainless steel Type 347 stainless steel	5 5 2 1 <sup>l</sup>	920 1500 710	2100 2000 780 1600	2600 2400 850
F-37	1.34	275	4	500-1000 ppm O <sub>2</sub>	17	Type 304L stainless steel Type 347 stainless steel Type 309SCb stainless steel Type 321 stainless steel	5 5 2 2	390 340 250 310	480 400 260 330	670 430 270 350
					60-80	Type 304L stainless steel Type 347 stainless steel Type 309SCb stainless steel Type 321 stainless steel	5 5 2 2	490 500 440 470	610 650 530 690	710 810 610 900
F-38	1.34	275	123	1000-2000 ppm O <sub>2</sub>	15	Type 304L stainless steel Type 347 stainless steel Type 309SCb stainless steel Type 321 stainless steel	5 5 2 2	500 200 420 190	550 200 480 270	630 210 520 350
					74	Type 304L stainless steel Type 347 stainless steel	5 5	1100 970	1300 1300	1500 1500

PERIOD ENDING JULY 31, 1954

TABLE 11. (continued)

Run No.	Test Conditions						Corrosion Rate (mpy)			
	Uranium Concentration (molality)	Temperature (°C)	Time (hr)	Additions	Flow Rate (fps ± 10%)	Pin Material	Number of Pins	Minimum	Average	Maximum
F-38	1.34	275	123	1000–2000 ppm O <sub>2</sub>	74	Type 309SCb stainless steel	2	1400	1500	1700
						Type 321 stainless steel	2	1100	1100	1100
G-9	1.34	300	327	1000–2000 ppm O <sub>2</sub>	75	Titanium RC-70	1		0	
						Titanium 75A	2		0	
						Titanium 100A	1		0	
						Titanium 150A	1		0	
						Zirconium, crystal-bar	2		0	
						Zirconium–2.5% tin	2		0	
						Zircaloy-2	3		0	
G-11	1.34	300	150	1000–2000 ppm O <sub>2</sub> , 0.3 m sulfuric acid	75	Titanium RC-70	1		0	
						Titanium RC-55	2	0	0.1	0.2
						Titanium 75A	2	0	0	0
						Titanium 100A	1		0.1	
						Titanium 150A	1		0.1	
						Titanium, 3% Al, 2.5% tin	1		0.1	
						Titanium, 3% Al, 5% Cr	1		0.2	
						Zirconium, crystal-bar	1		0	
						Zirconium–2.5% tin	1		0	
Zircaloy-2	2		0							
H-31	1.34	225	70	1000–2000 ppm O <sub>2</sub>	19	Type 304L stainless steel	4	180	210	270
						Type 347 stainless steel	5	130	150	180
						Type 309SCb stainless steel	2	170	180	190
						Type 316 stainless steel	2	190	200	200
					64	Type 304L stainless steel	4	450	500	520
						Type 347 stainless steel	5	420	560	620
						Type 309SCb stainless steel	2	480	490	500
						Type 316 stainless steel	2	330	330	330

TABLE 11. (continued)

Run No.	Test Conditions						Corrosion Rate (mpy)			
	Uranium Concentration (molality)	Temperature (°C)	Time (hr)	Additions	Flow Rate (fps ± 10%)	Pin Material	Number of Pins	Minimum	Average	Maximum
H-32	1.34	225	151	1000-2000 ppm O <sub>2</sub>	18	Type 304L stainless steel	4	130	150	150
						Type 347 stainless steel	4	84	93	110
						Type 309SCb stainless steel	2	360	360	360
						Type 316 stainless steel	2	250	260	270
						Gold	1		13	
					64	Type 304L stainless steel	4	560	580	610
						Type 347 stainless steel	4	630	690	740
						Type 309SCb stainless steel	2	580	600	620
						Type 316 stainless steel	2	520	560	600
						Zircaloy-2	1 <sup>b</sup>			
H-33	1.34	225	188	1000-2000 ppm O <sub>2</sub>	18	Type 304L stainless steel	4	91	110	140
						Type 347 stainless steel	5	67	76	88
						Type 309SCb stainless steel	3	150	220	270
						Type 430 stainless steel	1		120	
					64	Type 304L stainless steel	4	580	630	720
						Type 347 stainless steel	4	500	600	660
						Type 309SCb stainless steel	3	690	710	720
						Type 430 stainless steel	1		650	
						Type 304 stainless steel	1 <sup>m</sup>		570	
H-34	1.34	250	200	1000-2000 ppm O <sub>2</sub>	18	Type 304L stainless steel	3	610	710	860
						Type 347 stainless steel	3	100	140	190
						Type 309SCb stainless steel	2	760	880	1000
						Type 304 stainless steel	2	300	340	370

PERIOD ENDING JULY 31, 1954

TABLE 11. (continued)

Run No.	Test Conditions						Corrosion Rate (mpy)			
	Uranium Concentration (molality)	Temperature (°C)	Time (hr)	Additions	Flow Rate (fps ± 10%)	Pin Material	Number of Pins	Minimum	Average	Maximum
H-34	1.34	250	200	1000-2000 ppm O <sub>2</sub>	18	Type 318 stainless steel	1		71	
						Misco C <sup>n</sup>	1		120	
						Misco 4 <sup>n</sup>	1		890	
						Titanium RC-70	1 <sup>b</sup>			
					64	Type 304L stainless steel	3	1200	1300	1400
						Type 347 stainless steel	3	1200	1500	1800
						Type 309SCb stainless steel	2	1500	1600	1700
						Type 304 stainless steel	2	1900	2200	2400
						Type 318 stainless steel	1		1200	
						Misco 4	1		2900	
Titanium 75A	1 <sup>b</sup>									
H-35	1.34	250	98	1000-2000 ppm O <sub>2</sub>	16 <sup>o</sup>	Type 304L stainless steel	4	380	470	540
						Type 347 stainless steel	4	460	480	510
						Type 309SCb stainless steel	2	550	560	570
						Type 304 stainless steel	2	550	580	610
						Type 318 stainless steel	2	540	590	630
					64	Type 304L stainless steel	4	860	890	940
						Type 347 stainless steel	5	1100	1200	1300
						Type 309SCb stainless steel	2	850	880	900
						Type 304 stainless steel	2	1000	1200	1300
						Type 318 stainless steel	1		1300	
H-36	1.34	250	123	1000-2000 ppm O <sub>2</sub>	18	Type 304L stainless steel	4	600	660	720
						Type 347 stainless steel	4	620	650	680
						Type 309SCb stainless steel	2	800	820	840
						Type 304 stainless steel	1		710	
						Type 318 stainless steel	2	700	730	750
						Type 304L stainless steel	1 <sup>i</sup>		700	

TABLE 11. (continued)

Run No.	Test Conditions						Corrosion Rate (mpy)			
	Uranium Concentration (molality)	Temperature (°C)	Time (hr)	Additions	Flow Rate (fps ± 10%)	Pin Material	Number of Pins	Minimum	Average	Maximum
H-36	1.34	250	123	1000-2000 ppm O <sub>2</sub>	64	Type 304L stainless steel	4	910	980	1100
						Type 347 stainless steel	5	1100	1200	1300
						Type 309SCb stainless steel	2	1000	1200	1400
						Type 304 stainless steel	2	1200	1300	1400
						Type 318 stainless steel	1		1400	
H-37	0.43	250	200	1000-2000 ppm O <sub>2</sub>	17	Type 304L stainless steel	5	230	240	250
						Type 347 stainless steel	5	190	200	220
						Type 309SCb stainless steel	2	260	270	270
						Type 321 stainless steel	2	190	200	210
					64	Type 304L stainless steel	5	350	390	430
						Type 347 stainless steel	5	400	420	440
						Type 309SCb stainless steel	2	480	500	510
						Type 321 stainless steel	2	400	410	410
I-10	0.06	250	906	1000-2000 ppm O <sub>2</sub> , 0.006 m H <sub>2</sub> SO <sub>4</sub>	15-19	Type 304L stainless steel	20	0.94	2.9	4.9
						Type 347 stainless steel	21	2.9	3.9	11
						Titanium RC-70	1 <sup>b</sup>			
					31	Type 304L stainless steel	14	5.4	21	57
						Type 347 stainless steel	14	5.2	28	78
					41	Type 304L stainless steel	14	36	72	94
						Type 347 stainless steel	14	6.8	70	88
					I-11	0.06	250	500	1000-2000 ppm O <sub>2</sub> , 0.006 m H <sub>2</sub> SO <sub>4</sub>	15-19
Type 347 stainless steel	20	1.9	5.5	8.2						
Titanium RC-70	1 <sup>b</sup>									
31	Type 304L stainless steel	13	10	39						77
	Type 347 stainless steel	13	11	36						67
41	Type 304L stainless steel	13	32	66						90
	Type 347 stainless steel	13	18	60						76

PERIOD ENDING JULY 31, 1954

TABLE 11. (continued)

Run No.	Test Conditions						Corrosion Rate (mpy)				
	Uranium Concentration (molality)	Temperature (°C)	Time (hr)	Additions	Flow Rate (fps ± 10%)	Pin Material	Number of Pins	Minimum	Average	Maximum	
I-12	0.06	250	250	1000–2000 ppm O <sub>2</sub> , 0.006 m H <sub>2</sub> SO <sub>4</sub>	15–19	Type 304L stainless steel	19	3.2	7.4	11	
						Type 347 stainless steel	20	5.6	9.8	12	
						Titanium RC-70	1 <sup>b</sup>				
						Type 304L stainless steel	13	8.0	37	83	
						Type 347 stainless steel	13	11	41	78	
						Type 304L stainless steel	13	11	72	89	
J-35	1.34	200	200	600–800 ppm O <sub>2</sub>	5	Type 304L stainless steel	3	94	110	120	
						Type 347 stainless steel	3	210	220	230	
						Type 309SCb stainless steel	2	110	130	140	
						Type 316 stainless steel	1		75		
						Type 430 stainless steel	1		130		
						Carpenter 20	1		100		
						Platinum	1 <sup>b</sup>				
						Stellite 98M2	1		3500		
J-36	1.34	200	400	900–1300 ppm O <sub>2</sub>	<17	Type 304L stainless steel	5	36	43	50	
						Type 347 stainless steel	4	54	65	88	
						Type 309SCb stainless steel	2	100	110	120	
						Platinum	1 <sup>b</sup>				
						Type 304L stainless steel	4	210	250	280	
						Type 347 stainless steel	4	210	260	290	
J-37	1.34	200	200	900–1300 ppm O <sub>2</sub>	19	Type 304L stainless steel	6	110	130	140	
						Type 347 stainless steel	6	210	220	230	
						Type 309SCb stainless steel	2	91	96	100	
						75	Type 304L stainless steel	6	220	240	300
							Type 347 stainless steel	6	240	300	410

TABLE 11. (continued)

Run No.	Test Conditions						Corrosion Rate (mpy)			
	Uranium Concentration (molality)	Temperature (°C)	Time (hr)	Additions	Flow Rate (fps ± 10%)	Pin Material	Number of Pins	Minimum	Average	Maximum
J-37	1.34	200	200	900-1300 ppm O <sub>2</sub>	75	Type 309SCb stainless steel	2	130	140	140
L-26	1.34	275	116	1000-2000 ppm O <sub>2</sub>	8-11	Type 304L stainless steel	12	150	310	680
						Type 347 stainless steel	12	120	120	130
						Type 309SCb stainless steel	4	200	480	730
						Type 430 stainless steel	2	140	200	260
						Titanium RC-70	2 <sup>b</sup>			
						Zircaloy-2	2 <sup>b</sup>			
						Zirconium-2½% tin	2 <sup>b</sup>			
						Zirconium, crystal-bar	1 <sup>b</sup>			
Platinum	1 <sup>b</sup>									
L-27	1.34	275	350	1000-2000 ppm O <sub>2</sub>	9-12	Type 304L stainless steel	13	48	79	160
						Type 347 stainless steel	13	28	36	43
						Type 309SCb stainless steel	5	53	190	340
						Type 430 stainless steel	3	87	100	120
						Titanium RC-70	2 <sup>b</sup>			
						Zircaloy-2	2 <sup>b</sup>			
						Zirconium-2½% tin	2 <sup>b</sup>			
L-28	1.34	275	59	1000-2000 ppm O <sub>2</sub>	8-11	Type 304L stainless steel	13	17	29	73
						Type 347 stainless steel	13	14	19	27
						Type 309SCb stainless steel	5	17	42	79
						Type 430 stainless steel	3	15	30	43
						Titanium RC-70	2 <sup>b</sup>			
						Zircaloy-2	1 <sup>b</sup>			
						Zirconium-2½% tin	2 <sup>b</sup>			
L-29	1.34	275	68	1000-2000 ppm O <sub>2</sub>	15	Type 304L stainless steel	4	730	780	830
						Type 347 stainless steel	5	430	490	530
						Type 309SCb stainless steel	2	850	860	870
						Type 318 stainless steel	1		540	

PERIOD ENDING JULY 31, 1954

TABLE 11. (continued)

Run No.	Test Conditions						Corrosion Rate (mpy)								
	Uranium Concentration (molarity)	Temperature (°C)	Time (hr)	Additions	Flow Rate (fps ± 10%)	Pin Material	Number of Pins	Minimum	Average	Maximum					
L-29	1.34	275	68	1000-2000 ppm O <sub>2</sub>	15	Type 316 stainless steel	1 <sup>f</sup>	1300							
						Type 304L stainless steel	1 <sup>l</sup>	750							
						Type 304L stainless steel	5	1200	1300	1400					
						Type 347 stainless steel	6	1300	1400	1500					
						Type 309SCb stainless steel	2	1400	1500	1500					
						Type 304L stainless steel	1 <sup>l</sup>	1300							
L-30	0.87	250	150	1000-2000 ppm O <sub>2</sub>	15	Type 304L stainless steel	5	360	400	440					
						Type 347 stainless steel	5	260	300	330					
						Type 309SCb stainless steel	2	400	410	410					
						Type 318 stainless steel	1		330						
						Type 316 stainless steel	1 <sup>f</sup>		440						
										75	Type 304L stainless steel	6	570	700	1100
											Type 347 stainless steel	6	600	700	820
											Type 309SCb stainless steel	2	670	700	740
M-16	0.06	250	200	700-1700 ppm O <sub>2</sub> , 0.016 m H <sub>2</sub> SC <sub>4</sub>	14	Type 304L stainless steel	4	5.1	5.4	6.0					
						Type 347 stainless steel	4	6.3	7.0	7.7					
						Type 304L stainless steel	3 <sup>p</sup>	4.4	4.7	4.9					
						Type 347 stainless steel	3 <sup>p</sup>	5.2	5.7	6.4					
										68	Type 304L stainless steel	3	110	110	110
											Type 347 stainless steel	3	100	110	110
											Type 309SCb stainless steel	2	120	120	120
											Type 347 stainless steel	1 <sup>p</sup>		130	
											Type 304L stainless steel	3 <sup>q</sup>	94	120	170
											Type 304L stainless steel	2 <sup>r</sup>	0.59	0.90	1.2
Mock-up Run 16	0.42	250 <sup>s</sup>	985	100-500 ppm O <sub>2</sub>	4 <sup>t</sup>	Type 304L stainless steel	5	14	15	16					
						Type 347 stainless steel	5	12	13	13					
						Type 309SCb stainless steel	2	15	16	16					
						Titanium 75A	1 <sup>b</sup>								
						Zircaloy-2	1 <sup>b</sup>								

Footnotes for Table 11

<sup>a</sup>During this run about 1 liter of a uranyl sulfate solution (40 g of uranium per liter) containing 0.5 g of manganese as manganous sulfate was pumped into the loop. The run was terminated by a power failure.

<sup>b</sup>These pins were not defilmed; all showed weight gains due to a deposition of iron and chromium oxides.

<sup>c</sup>During the first 125 hr of this run about 5.5 liters of a uranyl sulfate solution (40 g of uranium per liter) containing 2.5 g of manganese as manganous sulfate was pumped into the loop.

<sup>d</sup>There were no specimens in run C-39.

<sup>e</sup>During the first two days of this run the iodine concentration decreased from 50 ppm to <1 ppm. After 154 hr of operation the loop temperature was lowered to 150°C, and the run continued at this temperature for 40 hr, at which time it appeared that all the iodine was in solution.

<sup>f</sup>Cast.

<sup>g</sup>There were no specimens in runs D-28 and D-29.

<sup>h, i, j, k</sup> - These specimens were treated by the following Chromalloy process: *h*, CR95-12 (XP-443); *i*, CR80-12 (XP-145); *j*, CR95-12 (XP-142); and *k*, CR90-10 (XP-448) and CR75-10 (XP-470). The specimens given treatment *k* and tested at 69 fps dissolved completely. This gives a corrosion rate of >9.7 mpy. These specimens will be

discussed in the metallurgy section.

<sup>l</sup>Gold-plated specimens.

<sup>m</sup>Sensitized.

<sup>n</sup>Cast alloys obtained from the Michigan Steel Casting Co. and had the following composition (the balance being iron):

Alloy	Composition (wt %)			
	Ni	Cr	C	Si
Misco C	10.0	28.7	0.22	1.73
Misco 4	0.15	13.1	0.07	1.41

<sup>o</sup>The flow was actually lower than 16 fps because there was a partial plugging of the coupon holder in series with this holder.

<sup>p</sup>Electropolished.

<sup>q</sup>Specimens treated at 1900°F for ½ hr in moist H<sub>2</sub>, 1% H<sub>2</sub>O.

<sup>r</sup>Specimens were given a Chromalloy treatment followed by ½ hr at 1900°F in moist H<sub>2</sub>, 1% H<sub>2</sub>O. Specimens were not defilmed; hence the actual corrosion rate would be somewhat higher.

<sup>s</sup>Pressurizer temperature was 265°C.

<sup>t</sup>The velocity was increased 100% for the last 170 hr of this run.

## HRP QUARTERLY PROGRESS REPORT

runs H-28 through H-30 were reported previously.<sup>8</sup> During this series three runs were terminated because of loop failures and this fact accounts for the similarity of times in several runs. In all three cases the mixing line failed due to corrosion (see p 133) for description of failures).

During runs H-28 through H-30 the pump had a stainless steel impeller and thermal spacer, both of which showed very heavy corrosion damage. In runs H-31 through H-33 both the impeller and the thermal spacer were of titanium and showed no corrosion damage. This fact may have accounted for the general lack of agreement between the two sets of runs. During the first three runs there was no consistency of data, either within one run or between runs. However, the last three runs gave fairly consistent data and only these three runs are considered here. At low flow rates after about 50 hr types 347, 304L, and 309SCb stainless steel showed a corrosion rate of 39, 72, and 250 mpy, respectively. At high flow rates all three alloys had the same corrosion rate, 600 mpy. Visual examination of the pins showed that at 18 to 19 fps all type 347 stainless steel pins had continuous films on their surfaces but that both types 309SCb and 304L pins were partially free of film. This fact probably accounts for the high rate of corrosion of the latter two alloys. Thus at low flow, types 304L and 347 stainless steel behaved the same at the 1.34 *m* level as at the 0.17 *m* level (see later section, this report).

The coupon data did not show a critical velocity so clearly defined as usual, but generally the weight loss increased linearly with velocity up to 25 to 35 fps, at which point the weight loss increased more rapidly, and in a sense this could be called the critical-velocity region. The results obtained with coupons generally agreed with those obtained with pins exposed at the same velocity.

At 225°C the specimens at low flow rates were covered with a heavy black scale which was identical in appearance to that formed at higher temperatures. At high flow rates there was a thin black deposit on the specimens which may have formed on them after the pump was stopped and while the loop was cooling. This latter statement was suggested by the weight of the film on the specimens exposed at 64 fps being about the same in all six runs, regardless of exposure time.

**250°C.** A series of three runs was made at 250°C with 1.34 *m* uranyl sulfate in Loop H. It

can be seen in Table 11, runs H-34 through H-36, that the agreement from run to run at low flow was poor. All pins were partially free of film at all exposure times, and this fact accounts for the high and irregular corrosion rates. The very low rates shown by the type 347 pins in run H-34, lower by a factor of 5 than those of type 304L pins exposed under the same condition, are unexplained. The coupon data indicated a critical velocity of about 10 fps, and, since the pins were exposed at 18 to 19 fps, it is not surprising that they were partially free of film. At high flow rates all specimens were free of film and showed corrosion rates of about 1400 mpy.

**275°C.** At 275°C a total of five runs was made. In runs L-26 through L-28 pins were exposed at very low flow rates, 8 to 10 fps. In runs L-29 and F-38 pins were exposed at 15 and 75 fps. In all runs coupon-type specimens were exposed, and the coupons indicated a critical velocity range of 15 to 25 fps. At 8 to 10 fps all pin-type specimens had complete and heavy black films. In all runs the data for all type 347 stainless steel pins were in good agreement, and after the specimens had lost about 30 to 35 mg/cm<sup>2</sup>, corrosion practically stopped. The type 304L pins, on the other hand, did not show good agreement in any given run but, generally, the data suggested that there was a tendency for the pins to stop corroding after an average weight loss of 70 to 90 mg/cm<sup>2</sup>. Type 309SCb stainless steel showed a constant corrosion rate of 150 mpy after the initial rapid attack, even though a film was present on its surface.

At flow rates of about 15 fps all pins were covered with films when they were removed from the loop, although there were indications that the pins had been partially free of film during part of the run. In runs L-29 and F-38 the agreement between weight losses of type 347 pins was good; the loss in each case was about 70 mg/cm<sup>2</sup>. The type 304L pins also showed fair agreement and lost between 120 and 170 mg/cm<sup>2</sup>. In both runs, pins exposed at 75 fps remained film free and corroded at a rate of about 1450 mpy. The observed rate was definitely lower than was expected, and this fact may have been related to the shortness of the runs or to inaccuracies in the temperature control.

**300°C.** Two runs were attempted with 1.34 *m* uranyl sulfate at 300°C with stainless steel pin specimens. In run F-35 only 0.1 *m* sulfuric acid

was added to the system, and throughout the run the solution existed as two liquid phases. The duration of the run was only 60 hr, and it can be seen from Table 11 that the extent of attack was high. The coupons, although completely covered with a heavy film at all flow rates, showed an apparent critical velocity of about 20 to 30 fps. In run F-36 0.3 *m* sulfuric acid was incorporated in the 1.34 *m* uranyl sulfate, and in this case the uranyl sulfate solution remained in a single phase. The duration of the test was only 25 hr, and the extent of corrosion was high.

In summary, then, it can be stated that, qualitatively, the effect of temperature on the extent and/or rate of corrosion of stainless steel by 1.34 *m* uranyl sulfate was very similar to that with 0.17 *m*, and even 0.02 *m*, uranyl sulfate. Thus at temperatures of 200 and 225°C the film formed did not appear to be so protective as films formed at higher temperatures (as was the case at all concentrations investigated). That the effect of temperature on the film-free corrosion rate was the same at the 1.34 *m* level as at the 0.17 *m* level can be seen in Fig. 36, where the logarithm of the corrosion rate is plotted against the reciprocal of the absolute temperature. The point at  $1/T = 0.00183$  (275°C) in the 1.34 *m* solution does not fit the curve, but, as mentioned previously, this point may be in error. At 300°C no point was obtained because in the two short runs that were made all specimens developed heavy films.

#### Effect of Uranium Concentration on the Film-Free Corrosion Rate of Stainless Steel at 250°C

In a previous quarterly progress report<sup>6</sup> it was shown that the corrosion rate of stainless steel at high flow rates in uranyl sulfate solutions containing about 1000 ppm of oxygen at 250°C was a linear function of the log of the uranium concentration over the range of 0.04 to 1.34 *m*. Since that time additional data have been obtained which show that a straight line exists over only the range of 0.04 to 0.25 *m* and that at uranyl sulfate concentrations greater than 0.43 *m* the corrosion rate increases very rapidly as the concentration increases. Figure 37 shows the corrected curve for the corrosion rate of stainless steel in the absence of a protective scale as a function of uranyl sulfate concentration at 250°C. In all cases the solution contained about 1000 ppm oxygen. The points on the curve at 1.34 *m* came from runs H-31 through

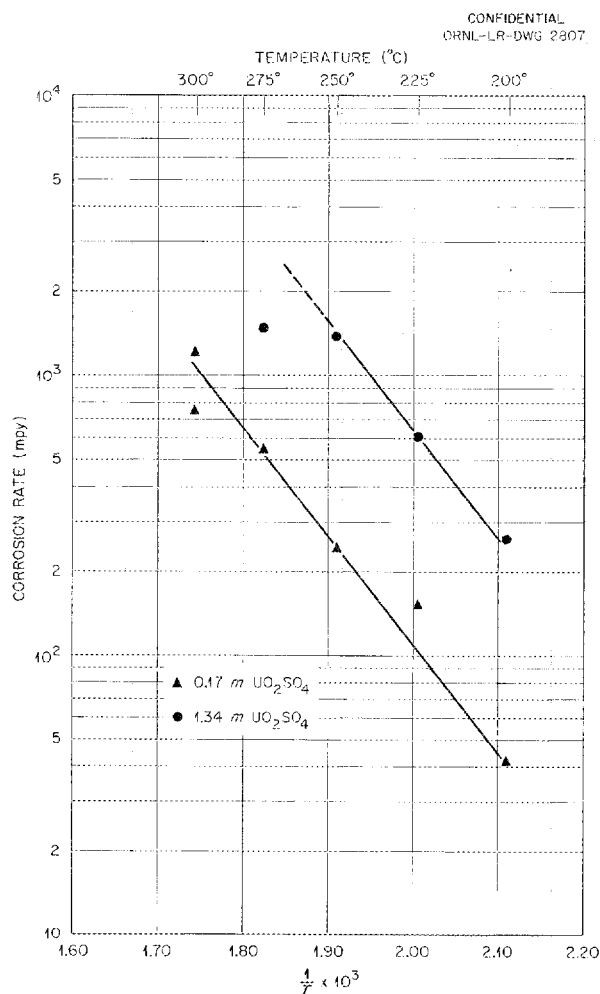


Fig. 36. The Effect of Temperature on the Corrosion Rate of Film-Free Stainless Steel in Uranyl Sulfate Solutions with Approximately 1000 ppm of Oxygen.

H-33; the one at 0.87 *m* from run L-30; and that at 0.43 *m* from run H-37. The points on the curve at the four lowest concentrations are the same as those previously reported,<sup>6</sup> and it has been shown in these cases that the addition of sulfuric acid up to 25 mole % of the uranium had no effect on the corrosion rate of the film-free metal. Qualitatively it is known that increasing the amount of dissolved oxygen in the system increases the corrosion rate, as does the presence of copper in the solution. Within rather narrow limits all austenitic stainless steels have shown identical corrosion rates under the above conditions.

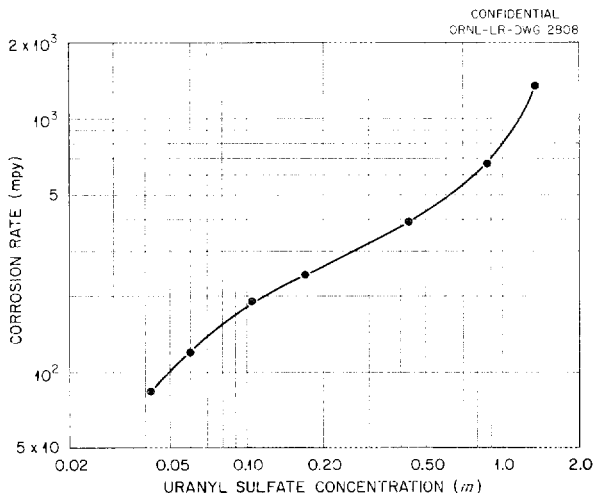


Fig. 37. The Corrosion Rate of Film-Free Austenitic Stainless Steels by Uranyl Sulfate Solutions Containing Approximately 1000 ppm of Oxygen at 250°C.

**Corrosion Rate of Stainless Steel at 250°C in 0.06 m Uranyl Sulfate Containing 0.006 m Sulfuric Acid**

Several previous runs<sup>3-5</sup> have been made in 0.06 m uranyl sulfate at 250°C but in one case no acid was added and some of the uranium hydrolytically precipitated from the solution. In another case 0.015 m sulfuric acid was used, which stabilized the solution but was considerably more than was necessary. Further experimentation indicated that 0.006 m sulfuric acid was sufficient to stabilize the uranyl sulfate even at 320°C and for that reason a series of runs covering the temperature range of 200 to 320°C is in progress with 0.06 m uranyl sulfate containing 0.006 m sulfuric acid. The data obtained at 250°C have been completed and are reported below. The results obtained at the other temperatures will be given in a future report. All of the pin data are presented in Table 11 (runs I-10 through I-12) and in Fig. 38 where the average weight loss of the pins has been plotted against the time of the test.

At all flow rates types 347 and 304L stainless steel behaved in a similar fashion, and for that reason only the average of all pins has been used in Fig. 38. At flow rates of 15 to 19 fps all pins had continuous, black films on their surfaces, and

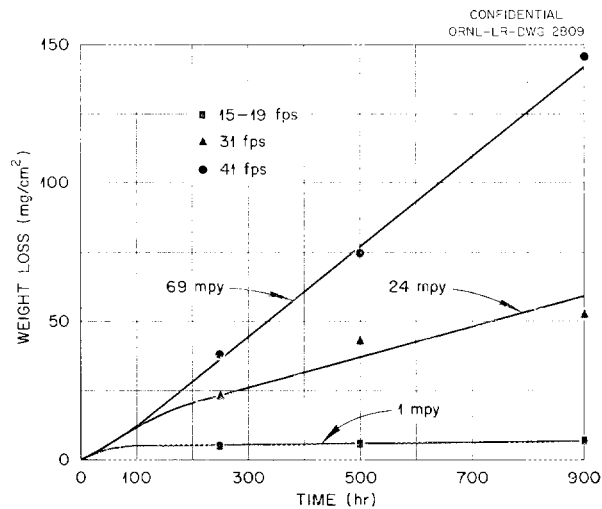


Fig. 38. Corrosion of Stainless Steel in 0.06 m Uranyl Sulfate Solution Containing 0.006 m Sulfuric Acid and Approximately 1000 ppm of Oxygen at 250°C.

it can be seen that after the initial period of rapid attack the corrosion rate was 1 mpy.

At a flow rate of 31 fps very nearly all pins had only partial films. Generally the pins were film-free in two or three places but the surface area which remained free of film varied from pin to pin, and this fact explains the large spread in weight loss observed at this flow rate (Table 11). The slope of the line as drawn in Fig. 38 corresponds to a uniform, over-all corrosion rate of 24 mpy; in actuality, the rate approximates the very high bare-metal rates in the film-free areas.

All pins were free of film on about half their surfaces at 41 fps. While there was a large spread in the extent of corrosion from pin to pin, a straight line could be drawn through the points representing the average of the large number of pins. The corrosion rate of 69 mpy obtained from the slope of the line is in good agreement with the film-free rate of 120 mpy previously reported, if it is remembered that the average pin was heavily corroded on only about half its surface (see runs A-41 through A-45<sup>5</sup> and Fig. 37 in this report).

The weight losses of the coupons as a function of velocity are shown in Fig. 39, from which it can be seen that the critical velocity was about 35 fps. The corrosion rates of the coupon exposed to the highest flow in each run were 99, 94, and

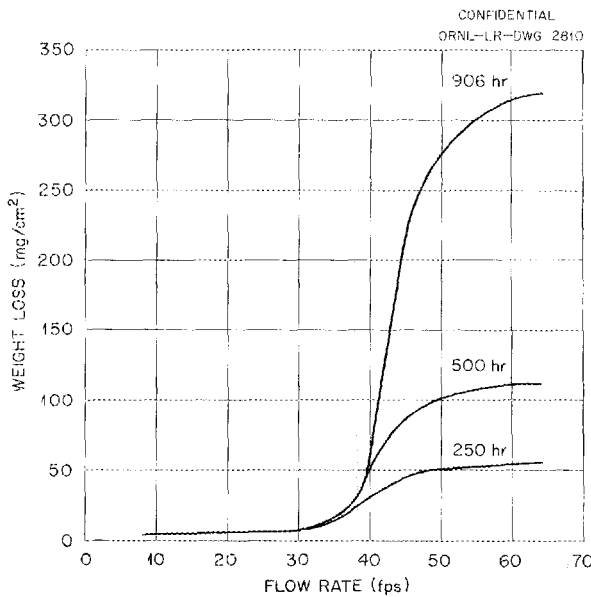


Fig. 39. Corrosion of Type 347 Stainless Steel Coupons in 0.06 *m* Uranyl Sulfate Containing 0.006 *m* Sulfuric Acid and Approximately 1000 ppm of Oxygen at 250°C.

150 mpy. While the agreement between runs was poor, the average rate is close to the value of 120 mpy previously reported.

**Corrosion of Stainless Steel in 0.17 *m* Uranyl Sulfate at 200 and 225°C**

225°C. One run, E-28, in which 0.17 *m* uranyl sulfate was circulated at 225°C was completed during the past month. The results of this run, coupled with those previously reported,<sup>6</sup> clearly show the behavior of types 347 and 304L stainless steel under these conditions. Figure 40 shows the results obtained from pin-type specimens at both high and low flow rates. Only the points at 1000 hr are new; all other points have been reported previously.<sup>6</sup> Each point on the graph represents the average of a large number of pins, and from the slopes of the lines as drawn it is obvious that there was a large difference in the corrosion rate of types 304L and 347 stainless steel at low flow. At high flow both types of steel corroded at the same rate, 150 mpy. When the pins were examined as they were removed from the loop, the reason for the difference in corrosion rates was obvious. At 15 fps type 347 stainless steel pins were

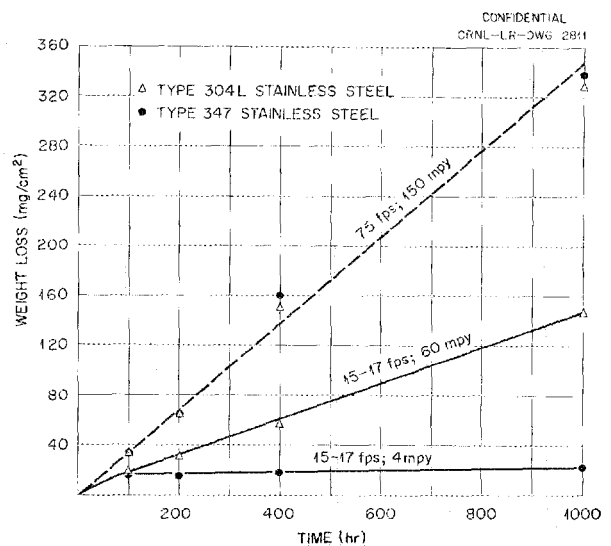


Fig. 40. Corrosion of Stainless Steel in 0.17 *m* Uranyl Sulfate at 225°C.

covered with a uniform black film, whereas the type 304L pins exposed under the same conditions had heavy films on only about half of their surfaces. At 75 fps all pins were free of film. The coupon results have been given previously<sup>6</sup> except for the 1000-hr curve, which was in agreement with the others.

From the pin data it would seem that in 0.17 *m* uranyl sulfate at 225°C the critical velocity was lower for type 304L stainless steel than for type 347. If this is true, the flow rate of 15 to 17 fps was either in the critical velocity range or slightly in excess of it for type 304L stainless steel and less than the critical velocity for type 347. One other possibly important difference between types 304L and 347 stainless steel was the grain size of the alloys. The type 304L stainless steel pins had an ASTM No. 4 grain size and the type 347 had a No. 8 grain size. A study of the effect of grain size of the alloy on the stability of the oxide film has been initiated in cooperation with the HRP Metallurgy Group.

200°C. The results of corrosion tests in 0.17 *m* uranyl sulfate at 200°C have been reported previously,<sup>6</sup> but in that report the types 304L and 347 stainless steel specimens were treated together. Figure 41 presents the data obtained for the two stainless steels, and it can be seen that there is a large difference between them at the

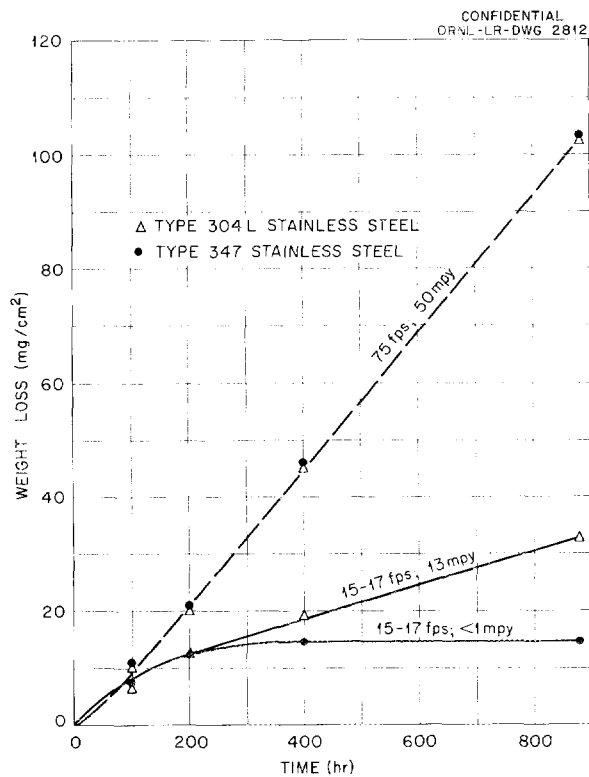


Fig. 41. Corrosion of Stainless Steel in 0.17 m Uranyl Sulfate at 200°C.

low flow rate but that there is no difference at 75 fps. The average corrosion rates for the pins at the lower flow rate were less than 1 mpy for the type 347 stainless steel pins and 13 mpy for the type 304L pins; at 75 fps both alloys corroded at the rate of 50 mpy. At 15 to 17 fps both types had identical film weights, about 7 mg/cm<sup>2</sup> after 880 hr of test; at 75 fps both had relatively heavy film weights, about 4 mg/cm<sup>2</sup> after 880 hr. Hence at 200°C, even though the metal was covered with a heavy film, the steel continued to corrode at a rate dependent on the velocity with which the solution flowed past the specimens. In view of the film on the specimens at all flow rates, it is difficult to rationalize the fact that types 304L and 347 stainless steels behaved differently at 15 fps but showed the same rate of attack at 75 fps. Further study will be necessary to explain this observation.

### Titanium-Loop Operations

During the last quarter the titanium loop, Loop G, was reassembled and more complete instrumentation was included (see section on "Pump-Loop Operation and Maintenance"). Two runs, G-9 and G-11, were made during the past quarter. (Run G-10 was of very short duration.) In run G-9, 1.34 m uranyl sulfate was circulated at 300°C for 327 hr, and throughout this run the uranyl sulfate was present in two liquid phases. This fact was demonstrated by the solution samples being removed from the loop with the pump both off and on. The sample valve was located near the top of the loop, and samples taken with the pump off showed uranium concentrations ranging between 90 and 115 g of uranium per liter (at 25°C) and uranium-sulfur ratios of about 0.85. With the pump on, the uranium concentration varied between 300 and 350 g of uranium per liter and showed that the two phases were well dispersed in each other. Run G-11 was identical to run G-9 except that 0.3 m sulfuric acid was added to the uranyl sulfate solution to prevent the formation of two liquid phases. The duration of this run was only 150 hr, and samples removed from the loop with the pump off and on showed that the solution remained in a single phase.

The corrosion damage to the loop and to the titanium and zirconium corrosion specimens was nil during both runs. The appearance of the loop, which was blue to pink before the runs, did not change. The titanium corrosion specimens developed blue films and showed no weight change within the limits of detection. The zirconium specimens (including Zircaloy-1, Zircaloy-2, and crystal-bar zirconium) developed thin, black, lustrous films and showed very slight weight gains (<0.2 mg/cm<sup>2</sup>). One zirconium and two titanium pins, however, became loose in the holder during run G-9 and the ends of these pins, as well as the titanium holder, showed heavy corrosion damage. This same phenomenon has occurred at all concentrations and temperatures and again demonstrates that in the absence of a surface film both titanium and zirconium corrode rapidly. However, the stability of the films formed on titanium and zirconium in strongly acid solutions is, as demonstrated above, truly remarkable.

### Galvanic Corrosion

A series of experiments has been completed in which various couples of dissimilar metals were exposed to uranyl sulfate solutions. The five couples that have been investigated were: titanium with type 347 stainless steel, Zircaloy-2, and gold, and stainless steel with Zircaloy-2 and gold. Since it was not certain in all cases which metal would be anodic to the other, two coupons of each couple were exposed to the uranyl sulfate solution. In one of the two coupons the first metal served as the coupon ( $\sim 12 \text{ cm}^2$  surface area) and the second metal was a screw or inset ( $\sim 0.12 \text{ cm}^2$ ) located in the center of the coupon. In the second coupon the metals were reversed. If a galvanic effect existed, the active metal would have the smaller surface area in one case and this fact would make the detection of a galvanic effect easier.

Coupons of the above types were tested in the following solutions: 0.17 *m* uranyl sulfate at 250°C for 100 hr, 1.34 *m* uranyl sulfate at 250°C for 108 hr, and 1.34 *m* uranyl sulfate at 200°C for 200 hr. Enlarged photographs were taken before and after each run to determine the extent of localized attack.

Within the limits of detection no evidence of accelerated attack on any metal was obtained. It must be remembered, however, that only three conditions were examined for short times and that under other conditions a galvanic effect may have been apparent. It is also possible that at lower temperatures galvanic effects may be more serious than at high temperatures.

Further evidence that there is no galvanic action between titanium and stainless steel in uranyl sulfate solutions at temperatures of 200°C or higher is supplied from two sources. First, most of the stainless steel impellers in use in the 100A pumps have titanium rings fitted over the stainless steel hub. Neither the titanium nor the stainless steel adjoining it has shown selective attack. Secondly, all the pin and coupon holders now in use are made of titanium. While the ends of all specimens (stainless steel and other alloys) in contact with the holders are wrapped with Teflon tape, electrical insulation between the specimen and the holder frequently does not exist, and in these cases the stainless steel specimens have not corroded to any greater or lesser degree than when the metals were electrically insulated.

Several runs were made during the past quarter in which inorganic compounds were added to uranyl sulfate solutions to test their inhibitory action. Of the three tested, manganous sulfate, sodium tungstate, and potassium dichromate, only the last compound was effective, and its beneficial effect was very marked. The possibility that dichromate ions might demonstrate inhibitory action was suggested by G. H. Jenks, and as a result runs D-30 and D-31 were made. It can be seen from Table 11 that the pins exposed at 16 fps suffered very little corrosion damage. In fact, the average weight loss of the pin specimen was only  $0.6 \text{ mg/cm}^2$  in both the 200- and 400-hr runs, indicating no additional corrosion during the last 200 hr. Under the same conditions but in the absence of the 200 ppm of chromium the average weight loss would have been  $12 \text{ mg/cm}^2$  at both exposure times. The coupons showed a critical velocity of 50 to 60 fps, whereas in the absence of the dichromate ions the critical velocity would have been 15 to 25 fps. Other experiments are planned to determine the effectiveness of dichromate additions at other uranyl sulfate concentrations and other temperatures.

From the experimental results it has been observed that at flow rates where a stable film forms, type 309SCb stainless steel corrodes faster than does either type 304L or type 347 at high temperatures. The temperature needed to observe this effect is dependent on the uranyl sulfate concentration and is as high as 300°C in the case of 0.02 *m* uranyl sulfate and as low as 225°C at the 1.34 *m* level. At the 1.34 *m* concentration level type 309SCb stainless steel corrodes at approximately the same rate as types 304L and 347 at 200°C. However, it is superior in its corrosion resistance to the latter two alloys at temperatures below 200°C and is inferior at higher temperatures. At high flow rates where a stable film does not form, all three alloys corrode at the same rate at any given uranium concentration and temperature. Type 309SCb stainless steel contains nominally 25% chromium, whereas types 304L and 347 contain 18%. The fact that type 309SCb stainless steel corrodes faster than types 347 and 304L appears to be related to the oxidation of chromium or chromic oxide to the soluble hexavalent state by the combination of uranyl sulfate, oxygen, and high temperature. It has been pointed out before that an increase in either the uranium or oxygen concen-

## HRP QUARTERLY PROGRESS REPORT

trations and/or an increase in the temperature causes an increase in the rate and extent of formation of hexavalent chromium. Since type 309SCb stainless steel contains more chromium than either type 304L or type 347, it seems reasonable to conclude that the oxide formed on its surface contains a higher concentration of chromium than that formed on the other two types. Under conditions where chromic oxide is soluble, the chromium would be partially leached from the oxide films protecting the steel, thereby making the oxide films porous. Thus, films formed on type 309SCb stainless steel would be more porous and less protective than those formed on type 347 or 304L because of the greater porosity of the film due to the leaching of the chromium from the oxide film.

From chemical analyses of the 1.34 *m* uranyl sulfate solutions it was observed that at any temperature the iron concentration in solution attained an equilibrium value after two or three days of operation. There were small fluctuations of the concentration of iron, but they were probably related to sampling and analytical errors. The average equilibrium values of ferric iron in 1.34 *m* uranyl sulfate were 45 ppm at 200°C, 35 ppm at 225°C, 25 ppm at 250°C, and 20 ppm at 275°C.

The total chromium concentrations of the systems were followed in all runs but only occasionally was the valence state of the chromium determined. Qualitatively, at least, the trivalent chromium paralleled the ferric ion concentration, but at any temperature it seemed to be somewhat higher than iron. The analytical method used for determining the valence state of chromium was not sufficiently precise to allow definite numerical values for the trivalent chromium concentration to be given.

In run C-38 the 0.17 *m* uranyl sulfate contained 50 ppm iodine as potassium iodate. After the solution had been circulated at 250°C for two days, the total iodine concentration of the solution was about 1 ppm, and the remainder had to be in the gas phase. Later, the loop temperature was reduced to 150°C and the circulation was continued. After one day the iodine was again present in the solution; however, the valence state was not determined.

At the conclusion of run C-38 the corrosion specimens exposed in the aqueous phase showed no abnormal corrosion; that is, there was no evidence of pitting. There were titanium, zirconium, and stainless steel specimens suspended in the gas

phase of the pressurizer, and neither the titanium nor the zirconium showed corrosion damage except for the development of very thin oxide films, probably no greater than 2000 Å thick. The stainless steel was very extensively pitted; some of the pits attained a depth of 20 mils during the 154 hr of operation. At 250°C the gas volume of the loop was 2.5 liters, and, since the solution volume was 12 liters containing 50 ppm iodine, nearly all of which evidently collected in the gas phase, the concentration of iodine in the gas phase was about 0.24 g of iodine per liter.

In the last quarterly report<sup>8</sup> it was shown that when potassium iodide was added to uranyl sulfate under the same conditions as above, iodine also collected in the gas phase. Hence, it appears that if iodine is added either as iodide or iodate to a uranyl sulfate solution and if the solution is circulated in the presence of oxygen at 250°C, iodine collects in the gas phase and presents a serious corrosion problem. However, since the iodine is volatile, it may be possible to remove it or to keep it at a low value by a suitable trapping technique.

In previous reports<sup>6-8</sup> some results were given concerning the chemical nature of the bulk oxide films deposited on the stainless steel specimens during the corrosion process. Additional information has been obtained during the past quarter, particularly by means of X-ray diffraction examinations performed by the Y-12 X-ray Laboratory. To date, 20 samples of the bulk oxide film formed on stainless steel specimens during the corrosion process have been examined, and 8 of these were formed at either 200 or 225°C during exposure to uranyl sulfate concentrations ranging from 0.06 to 1.34 *m*. On three occasions the film did not contain any detectable amount of a hydrated oxide of iron and chromium, but in the other five cases the film contained 20 to 90% of a hydrated oxide. Similarly, 12 scales, formed at temperatures of 250 to 320°C, have been examined and in not a single case has even a detectable trace of a hydrated iron oxide been found. Usually the oxide has consisted of the anhydrous  $\alpha$  iron oxide containing chromic oxide in solid solution. Occasionally there have been a few weak lines in the X-ray patterns which have not been identifiable, and it may be that they are attributable to basic iron sulfates. In this connection several scales have been recently analyzed chemically, and in nearly all cases a small amount of sulfur (as

sulfate) has been found. In one case as much as 0.8% sulfur was found, but usually only about 0.4% has been observed. Further work which is now in progress may more clearly define the composition of the oxides formed on stainless steel specimens. It should be noted that the above analyses are for the bulk oxide, and it may be that in most cases there is a thin oxide film which has a substantially different chemical analysis between the outer heavy film and the metal.

Several type 304L stainless steel pins listed in Table 11 were gold plated before exposure to uranyl sulfate solutions. The pins were plated at the Y-12 Plating Shop and were given a flash of copper before the gold was deposited on them. The gold plate was 0.001 in. thick and was expected to be nearly free of pores. The results showed that even under the mildest of conditions the gold did not remain on the specimens. In spite of the thickness of the deposit, the gold plate was probably rather porous and the solution attacked the thin copper coating and the steel at the pores and undercut the gold and allowed it to peel off. The results clearly demonstrated the impracticality of attempting to protect stainless steel in a high-temperature uranyl sulfate solution by means of a thin plated coating of a noble metal deposited over a flash coating of copper.

Several different alloys that have been subjected to uranyl sulfate solutions have been examined metallographically. The results of these examinations are discussed in the section on Metallurgy. It is, however, worth mentioning here that in almost all cases both types 316 and 316L stainless steel have shown an intergranular type of attack.

Titanium and zirconium (Zircaloy-1, Zircaloy-2, and crystal-bar zirconium) have shown excellent corrosion resistance to all concentrations of uranyl sulfate at all temperatures. Included under titanium are the following grades: Rem-Cru-70, Rem-Cru-55, Titanium 75A, Titanium 100A, and Titanium 150A. Also, a number of specimens of Rem-Cru-70 welded to Rem-Cru-70 with Titanium 75A welding rod have been exposed, and the resistance of the welded specimens has been as high as that of the unwelded specimens. In fact, after exposure it has not been possible to distinguish any difference in surface appearance between the weld itself and the rest of the pin. Two other titanium alloys are presently under investigation - the 5% aluminum-2.5% tin alloy and the 3% aluminum-5% chromium alloy. Preliminary experiments indicate that the corrosion resistance of these two alloys is nearly as high as that of the other titanium alloys.

RADIATION CORROSION

G. H. Jenks

H. C. Savage

LOOP PACKAGE TESTING AND HB-4 MOCK-UP

G. H. Jenks	N. C. Bradley
H. C. Savage	D. T. Jones
W. N. Bley	R. A. Lorenz

In-Pile Development Loops

Two additional test runs (HT-6 and HT-7) have been made in one of the two in-pile development loops (identified as Loop HT) during the past quarter. The purpose of these runs was twofold: to obtain corrosion data on the in-pile-type coupons and to test the performance of the all-metal (Stellite 98M2-Stellite 98M2) bearings in the 5-gpm circulating pump used in the in-pile loops.

Before run HT-6 was started, new, type 347 stainless steel coupons were installed in the core position in the loop. The coupons in the line position were not replaced and had been in the loop since the start of run HT-3.<sup>9</sup> The new coupons in the core position were pretreated by operating the loop for 24 hr with oxygenated water at 250°C. Test run HT-6 was then made with 0.17 *m* uranyl sulfate solution containing 0.013 *m* copper sulfate with 0.0085 *m* sulfuric acid. The maximum velocity past the test specimens in the tapered holder was increased to approximately 70 fps from the normal 40 fps by an increase in the pump speed. From previous test work in a 100A circulating test loop this velocity was considered to be sufficient to give a velocity corrosion effect after pretreatment. The complete operating history of run HT-6 is given in Table 12.

<sup>9</sup>G. H. Jenks, R. A. Lorenz, H. C. Savage, and D. T. Jones, *HRP Quar. Prog. Rep. Apr. 30, 1954*, ORNL-1753, p 81-94.

Run HT-6 was terminated after 133 hr because a lead wire to the line heater burned out. The sample units were removed from the core position, and corrosion rates as a function of velocity were determined, as shown in Table 13. It can be seen that a velocity corrosion effect was produced with a maximum rate of 140 mpy on the coupon with the highest average velocity. The average over-all corrosion rate of the system based on nickel analysis was 0.9 mpy. About two-thirds of the nickel in solution came from the new set of test coupons in the core position. If the corrosion of these coupons is disregarded, there was an approximate corrosion rate of only 0.3 mpy for the remainder of the system, including the test coupons in the line position.

The results of the chemical analyses of solution samples taken during the run are plotted in Fig. 42. Since the pump contained all-metal (Stellite 98M2) bearings, cobalt from these bearings is found in solution. The chloride analyses of the original and final solution were <1 ppm.

Immediately following run HT-6, run HT-7 was started. New, type 347 stainless steel coupons were installed in the core position. The loop was given a "standard" pretreatment followed by operation with uranyl sulfate solution containing copper sulfate and excess sulfuric acid. No significant corrosion data were obtained from run HT-7 because there were a loss of oxygen and a partial precipitation of the uranyl sulfate after approximately 75 hr. Both the core and line coupon specimens were removed at this point. Operating history of run HT-7 is given in Table 14.

No over-all corrosion rate, based on nickel solution, was calculated because of the loss of

TABLE 12. COMPLETE OPERATING HISTORY OF RUN HT-6

Solution	Time (hr)	Temperature (°C)	Pressure (psi)	Gas
Water	24	250	1000	Oxygen (~500 ppm)
0.17 <i>m</i> uranyl sulfate + 0.013 <i>m</i> copper sulfate + 0.0085 <i>m</i> H <sub>2</sub> SO <sub>4</sub>	133	250	1100	Oxygen (160-400 ppm)

oxygen. The core sample specimens exposed during run HT-7 showed virtually no velocity effect but had an abnormally high (20 to 40 mpy) corrosion rate. As a result of the partial precipitation of the uranyl sulfate solution, these results are probably not significant. The in-line corrosion specimens showed virtually no velocity effect with a relatively low (0.59 mpy) corrosion rate, even though they were exposed to circulating solution, runs HT-3-HT-7, inclusive. This low rate probably results from the protective film formed on these specimens during runs HT-3 through HT-5. A summary of all conditions of exposure and corrosion rates of the in-line coupons is given in Table 15.

TABLE 13. CORROSION OF IN-PILE LOOP, TYPE 347 STAINLESS STEEL COUPONS IN THE CORE POSITION, RUN HT-6

Velocity Range (fps)	Weight Loss (mg/cm <sup>2</sup> )	Average Corrosion Rate (mpy)
15.1-17.4	4.0	13
17.4-21.1	1.5	4.9
21.1-26.5	1.5	4.9
26.5-34.3	2.9	9.5
34.3-52.8	15	49
52.8-60.8	28	93
60.8-73.3	41	140
73.3-43.5	32	110
43.5-30.6	6.5	21
30.6-23.3	4.0	13
23.3-18.5	1.6	5.3
18.5-16.2	1.2	3.9

The results of run HT-6, along with in-pile loop runs previously reported, indicate that the out-of-pile corrosion behavior of the in-pile type coupons is similar to the out-of-pile corrosion data from the 100A circulating test loops. The protective film formed during pretreatment with oxygenated water and short-term operation with uranyl sulfate solution can be removed, with resultant bare-metal attack, by increasing the velocity past the coupons. Additional tests with these specimens in in-pile loops will be continued as the equipment is available. At present both in-pile development loops are being used in an effort to improve the performance and reliability of the ORNL 5-gpm canned-rotor pumps used in the in-pile loops. The 5-gpm pumps are discussed under a separate heading.

**In-Pile HB-4 Mock-up**

During the past quarter a second in-pile corrosion test loop, Serial No. CC, was installed in the mock-up in Building 9204-1, Y-12 Area. This test loop contained a pump with Stellite 98M2 journal bushings and Graphitar No. 14 bearings. Corrosion test specimens in the core and in-line positions were type 347 stainless steel mounted in titanium tapered holders. In addition, impact specimens of Zircaloy-2 were installed in the core position. A rubber seal gasket was incorporated in the loop assembly between the shield plug connector and loop container to allow cooling water circulation in the annulus between the loop container and the LITR hole liner to keep the hole liner as cool as possible.

In attempting to install the loop and plug assembly in the duplicate hole liner in the in-pile mock-up, it was found that the liner was too small. At this point it was decided to try installation of the loop assembly in the LITR. Therefore the loop was transported to the LITR and installed

TABLE 14. COMPLETE OPERATING HISTORY OF RUN HT-7

Solution	Time (hr)	Temperature (°C)	Pressure (psi)	Gas
5% (by wt) HNO <sub>3</sub>	24	90	150	Helium
Water	24	250	1000	Helium
0.17 m UO <sub>2</sub> SO <sub>4</sub> + 0.013 m CuSO <sub>4</sub> + 0.0085 m H <sub>2</sub> SO <sub>4</sub>	75	250	1000	Oxygen (0-450 ppm)

# HRP QUARTERLY PROGRESS REPORT

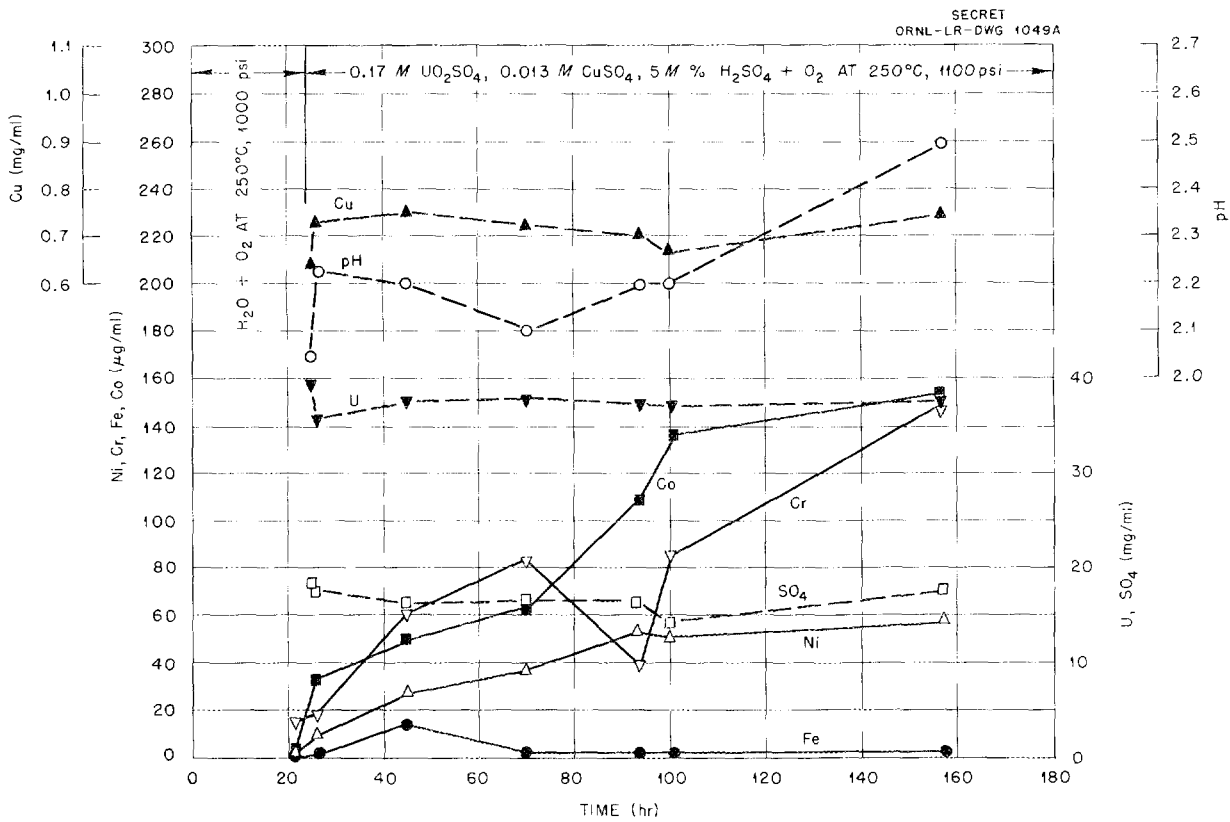


Fig. 42. Chemical Analyses of Run HT-6.

in hole HB-4 with no appreciable difficulty. However, when an attempt was made to remove the loop, the rubber gasket seal, previously mentioned, was torn and wedged in the annulus between the loop container and hole liner. Removal was finally accomplished with extreme difficulty. Fortunately, the loop assembly and hole liner were not damaged. As a result of this experience the cooling-water seal gasket was redesigned and was placed at the outer (LITR face) edge of the loop and plug assembly. The details of this change are discussed later in this report.

After the loop assembly was removed from the LITR, it was returned to Y-12, the mock-up HB-4 hole liner repaired, and test operation of the system started. Of primary concern was the effectiveness of the copper as an internal catalyst for the recombination of hydrogen and oxygen. From previous test runs on the initial mock-up loop, Serial No. BB, it appeared that the copper was not so effective as was calculated. Initial

tests in Loop CC confirmed these data. With the calculated concentration of copper of 0.013 *m*, the equilibrium partial pressure of hydrogen and oxygen in 0.17 *m* uranyl sulfate solution at 280°C was found to be 60 to 70 psi, whereas the expected value was approximately 12 psi. Additional runs were then made with increased concentrations of copper. A copper concentration of 0.031 *m* was found to be necessary in order to lower the equilibrium partial pressure of the hydrogen and oxygen to approximately 18 psi, which was considered a satisfactory value. These tests have established that the copper activity remains constant during the runs. The copper activity for recombining hydrogen and oxygen was calculated both from measurements of hydrogen and oxygen equilibrium pressures in the pressurizer and from analyses of the hydrogen concentration in the main circulating line. Fourteen such measurements were made over a combined operating period of about 420 hr with the use of copper concentrations of 0.013, 0.026,

TABLE 15. CORROSION OF IN-PILE LOOP, TYPE 347 STAINLESS STEEL COUPONS

Velocity Range (fps)	Weight Loss (mg/cm <sup>2</sup> )	Average Corrosion Rate (mpy)
Core Position, Run HT-7		
10.0-11.7	15.2-17.5 <sup>a</sup>	5.0
11.7-14.2	17.5-21.3	3.9
14.2-17.8	21.3-26.7	3.1
17.8-23.1	26.7-34.7	3.8
23.1-35.5	34.7-53.3	5.0
35.5-41.3	53.3-61.9	6.6
41.3-50.1	61.9-75.1	6.3
50.1-28.9	75.1-43.3	5.8
28.9-20.5	43.3-30.7	4.8
20.5-15.5	30.7-23.2	3.8
15.5-12.3	23.2-18.5	3.3
12.3-10.8	18.5-16.2	3.1
In-Line Position, Runs HT-3 to HT-7 <sup>b</sup>		
10.1-11.8	14.9-17.4 <sup>c</sup>	0.75
11.8-14.3	17.4-21.1	0.56
14.3-18.0	21.1-26.5	0.53
18.0-23.4	26.5-34.5	0.47
23.4-35.5	34.5-52.3	0.56
35.5-42.3	52.3-60.9	0.56
42.3-49.8	60.9-73.5	0.84
49.8-29.1	73.5-43.0	0.72
29.1-20.7	43.0-30.6	0.47
20.7-15.7	30.6-23.1	0.44
15.7-12.4	23.1-18.3	0.47
12.4-10.8	18.3-16.0	0.59

<sup>a</sup>Increased velocity ranges in this column are the result of the pump speed being increased during the last 50 hr of the run.

<sup>b</sup>Summary of exposure of above in-line coupons:

Run No.	Solution	Temperature (°C)	Time (hr)
HT-3	H <sub>2</sub> O + O <sub>2</sub>	250	100
HT-4	H <sub>2</sub> O + He	200	20
HT-5	UO <sub>2</sub> SO <sub>4</sub> (0.17 m) + 0.01 m CuSO <sub>4</sub> + 0.0425 m excess H <sub>2</sub> SO <sub>4</sub>	250	350
HT-6	H <sub>2</sub> O + O <sub>2</sub> UO <sub>2</sub> SO <sub>4</sub> (0.17 m) + 0.013 m CuSO <sub>4</sub> + 0.0085 m excess H <sub>2</sub> SO <sub>4</sub>	250	24
HT-7	Operating history presented in Table 14		

<sup>c</sup>Increased velocity ranges in this column are the result of the pump speed being increased during run HT-6 and the last 50 hr of run HT-7.

## HRP QUARTERLY PROGRESS REPORT

and 0.031 *m*. Very good agreement of rate constants was observed from the data obtained in the tests. A more complete report of these results is being prepared.

A complete operating history of Loop CC, operated for 554 hr, as tested in the in-pile mock-up is given in Table 16. No operational difficulty was encountered.

As was reported previously,<sup>9</sup> failure of the capillary tubing used for adding hydrogen and oxygen to Loop BB for recombination studies occurred after 200 hr of operation. Subsequent metallographic examination<sup>10</sup> showed that the failure in both lines resulted from transgranular cracking. The presence of uranyl sulfate solution in the oxygen line suggested that cracking in this case was the result of the combined effects of corrosion and stress. During the operation of Loop CC, extreme care was taken to keep all capillary tubing filled with water to prevent entry of the uranyl sulfate solution. Since no tubing failure occurred in Loop CC, it is presumed that the corrosion of the uranyl sulfate solution was a contributing

factor in the failure of the capillary tubes in Loop BB.

After completion of operation of Loop BB in the in-pile mock-up, the loop was disassembled and was cross-sectioned for visual and metallurgical examination of the component parts. The pressurizer was examined for evidence of corrosion attack at the liquid-gas interface and around the 0.060-in.-OD capillary pressure tube. Transgranular cracks were found in the base metal of the pressurizer adjacent to the end-cap weld in the portion of the pressurizer exposed to gas phase only. The pressurizer is made from a 1½-in. schedule-80, type 347 stainless steel pipe 19 in. long with end caps welded at each end. The longest crack observed was about 18 mils in length or about 10% of the wall thickness and appeared only within about ¼ in. of the weld. These transgranular cracks were probably due to stress corrosion from stresses set up in the metal in welding. The chloride concentration of the loop, which went as high as approximately 30 ppm, could presumably have contributed to the stress-corrosion cracks. The pressurizer had been in service for 190 hr at 280°C with a 0.17 *m* uranyl sulfate solution containing 0.013 *m* copper sulfate. Also, about 100

<sup>10</sup>E. C. Miller, W. O. Harms, and T. W. Fulton, *HRP Quar. Prog. Rep.* Apr. 30, 1954, ORNL-1753, p 117-122.

TABLE 16. COMPLETE HISTORY OF IN-PILE-LOOP MOCK-UP OPERATION, RUN CC-2

Solution	Time (hr)	Temperature (°C)		Pressure (psia)	Equilibrium Pressure p(2H <sub>2</sub> + O <sub>2</sub> ) (psi)	Gas
		Line	Pressurizer			
Water	1.8	250	280	1000		He
3% trisodium phosphate	3.4	100	110	~200		He
5% HNO <sub>3</sub>	16.8	90	100	~200		He
Water	117.0	100-250	100-280	200-1000		He + O <sub>2</sub>
0.17 <i>m</i> UO <sub>2</sub> SO <sub>4</sub> + 0.013 <i>m</i> CuSO <sub>4</sub>	148.0	250	280	1000	64-74	O <sub>2</sub> + H <sub>2</sub>
0.17 <i>m</i> UO <sub>2</sub> SO <sub>4</sub> + 0.013 <i>m</i> CuSO <sub>4</sub> + 0.0085 <i>m</i> H <sub>2</sub> SO <sub>4</sub>	98.7	250	280	1000-1100	55-60	O <sub>2</sub> + H <sub>2</sub>
0.17 <i>m</i> UO <sub>2</sub> SO <sub>4</sub> + 0.026 <i>m</i> CuSO <sub>4</sub> + 0.0085 <i>m</i> H <sub>2</sub> SO <sub>4</sub>	103.2	250	280	1000-1100	25-28	O <sub>2</sub> + H <sub>2</sub>
0.17 <i>m</i> UO <sub>2</sub> SO <sub>4</sub> + 0.031 <i>m</i> CuSO <sub>4</sub> + 0.0085 <i>m</i> H <sub>2</sub> SO <sub>4</sub>	50.8	250	280	1000-1100	8-20	O <sub>2</sub> + H <sub>2</sub>
Water	15.0	100-250	100-280	200-1000		O <sub>2</sub>
Total hours	554.7					

psi of oxygen was maintained above the solution in the pressurizer.

In view of the above, pressurizers in all subsequent in-pile loops have been stress-relieved at 950°F after welding. The design of the pressurizer end-cap welds was also improved by a redesign in the end caps to allow welding on metal sections of equal thickness.

Over-all corrosion rates based on the dissolved nickel in solution varied between 1.5 and 3 mpy for the four runs with uranyl sulfate solution in Loop CC (Table 16). These rates are based on the maximum dissolved nickel content of the solution. The values obtained from chemical analysis for dissolved nickel in solution were somewhat erratic; so they can be considered as only an over-all average based on the maximum nickel value and are included solely for reference. Cobalt in solution reached a high of approximately 140 ppm; chromium, approximately 100 ppm; and nickel, approximately 200 ppm. The amount of chloride in solution was somewhat uncertain, with analyses which varied in an unpredictable manner from 0 to as high as approximately 30 ppm and most of them ranged from 5 to 10 ppm chloride.

Loop CC has been removed from the mock-up and is now being disassembled in the remote handling facility at X-10. This operation is proceeding rather slowly as a result of the equipment having to be tested, since this is the first complete loop available for disassembly. The corrosion test specimens have not yet been removed and so corrosion data on them are not available but will be reported in the next quarterly report.

A fourth in-pile loop package, Serial No. DD, is now being assembled. This loop contains type 347 stainless steel corrosion specimens in Zircaloy-2 holders<sup>9</sup> in both the core and in-line position. In addition, specimens of Zircaloy-2 machined for impact testing are included in the core assembly. The loop contains an ORNL 5-gpm pump with Stellite 98M2 journal bushings and Graphitar No. 14 bearings. It is hoped that Loop DD may be installed in hole HB-4 in the LITR for a short operational test of all equipment after the initial test operation of the loop package is completed in the mock-up at Y-12.

#### In-Pile Pumps

**ORNL Pump for HB-4 Loop Package.** Additional tests of the circulating pumps<sup>9</sup> used in the in-

pile corrosion test loop have been made. It is concluded that the all-metal bearing combination (Stellite 98M2--Stellite 98M2) is not satisfactory, particularly for long-term operation. One pump equipped with metal bearings operated for about 500 hr but was found to have excessive thrust bearing wear when disassembled for inspection. Excessive radial bearing wear occurred in two additional pumps with all-metal bearings after less than 100 hr of operation. Therefore, present plans are to use the Stellite 98M2 journal bushings with Graphitar No. 14 bearings. It is believed that the cobalt in solution from the Stellite 98M2 journal bushings can be tolerated - at least for short-term operation. It has been found that the Graphitar No. 14 used in the bearings contains chloride in amounts approximating 200 ppm. If all the chloride in the bearings went into the circulating solution during operation, a chloride concentration of 20 to 40 ppm would result. An effort is being made to reduce the chloride content of the Graphitar No. 14 by exposure to a high gamma source, since preliminary tests indicated that gamma radiation might accelerate removal.

Work on improving the pump bearings is continuing. The pump as presently designed<sup>9</sup> has the bearings on the rotor shaft between the pump impeller and rotor body. It was believed that a bearing improvement could be accomplished by a bearing being placed on each side of the rotor body ("outboard" bearings), thus giving a better weight distribution. In addition, this will allow the use of thrust-bearing surfaces in both the forward and rear directions. At present only a forward thrust-bearing surface is provided. The proposed change should provide better weight distribution over the bearing surfaces and make dynamic balancing of the rotor easier. With two thrust bearings, the rotor and impeller assembly can be adjusted so that thrust loading of the bearings during operation is at a minimum. In the present case with one forward thrust bearing, the forward thrust load cannot be reduced to too low a value because of the danger of the rotor moving to the rear of the rotor housing and rubbing against the rear of the housing.

Two pumps incorporating the "outboard" bearings and double thrust surfaces are now being fabricated. Operational tests of these bearings should be made during the next quarter. Other bearing combinations such as hardened type 17-

## HRP QUARTERLY PROGRESS REPORT

4pH stainless steel against Graphitar No. 14 are now being investigated and eventually pure, sintered aluminum oxide against itself will be tried. Preliminary static-corrosion tests of sintered aluminum oxide in 0.17 *m* uranyl sulfate solution at 150°C indicate a low corrosion rate of approximately 2 mpy.

**Pump Development for Future In-Pile Loops.** As reported previously<sup>9</sup> a contract has been made with the Byron Jackson Co. for the development and construction of a pump for possible use in future loops. A similar contract has been made with the Allis-Chalmers Mfg. Co. The status of the development of these pumps is reported below.

*Byron Jackson Co.* – The design of this pump has been approved for construction. The first pump will be of flanged construction at the impeller end, and the diameter of the flanges will be greater than the specified 3.5 in. However, in later pumps of the same design which will be welded, this diameter will be reduced to 3.5 in.

The pump will be equipped with bearings of sintered aluminum oxide procured from the Kearfott Company, Inc., Clifton, New Jersey but it has not been decided which material will be used in the journals. The company has stated a preference for Star J alloy. On the basis of data from static-corrosion tests this material may prove to be suitable if the journal operating temperature is less than 100°C. However, the operating temperature cannot be predicted closely and may be as high as 150°C. At the higher temperature the material would not be satisfactory. Two other materials are being considered for possible use. These are rhodium-plated stainless steel and sintered aluminum oxide. Static-corrosion tests at 150°C indicate that either one may prove to be suitable and the Laboratory prefers the aluminum oxide. This pump can be delivered by late August if the bearing material is decided upon within a few days.

*Allis-Chalmers Mfg. Co.* – This pump is also under construction after final approval of drawings except for bearing materials. The bearing surfaces of the first pump will probably be of rhodium-plated type 347 stainless steel. In the few corrosion tests which have been made, rhodium plate has been found to be very resistant to  $UO_2SO_4$  solution at 250°C.<sup>11</sup> The company has sent test buttons

to ORNL for plating and the plated buttons will be used to determine the qualities as bearing material. This pump is 3.5 in. in diameter and 24 in. in length. The motor is cooled by the circulation of water through the tubular windings. It will operate on 9-v, 3-phase, 60-cycle current. Six tubular leads are used with the pump.

### LITR INSTALLATION

G. H. Jenks                      D. T. Jones  
R. A. Lorenz

#### Status

The instrument panels, both process and radiation, have been installed at the LITR. Connections have been made between the instruments and the valve boxes, but not between the instruments and the reactor-control circuits. The wiring for the latter is installed to the junction box but will not be connected until the instrument panel is completely checked out with a test loop.

All of the service headers to the valve boxes are installed. Installation of the various interconnecting lines and valves has been checked for correctness and all lines are now being leak tested. The testing is done by pressurizing the system with 500 psi of helium and probing for helium with a Consolidated helium leak detector at the outer surfaces.

The neutron shutter has been installed and checked to the satisfaction of the Operations Division. The movement of the shutter was checked by noting the water-surge pressures as the piston reached the end of its stroke.

#### Modification to Permit Cooling of Hole Liner

The in-pile loop installation as originally planned did not include provisions for cooling the beam-hole liner. However, it has since become clear that cooling is necessary. The concrete pile shielding which surrounds the beam hole is not forcibly cooled in any manner. Hence, without cooling the liner in this experiment, the temperature of the concrete immediately adjacent to the hole may approach that of the loop, that is, 250°C. At such elevated temperatures rapid deterioration of the concrete would be expected.

The method adopted for cooling the liner consists in passing water through the annular space between the loop jacket and the liner. Demineralized water for this purpose is obtained from the drain of the loop pump cooling-water circuit and

<sup>11</sup>E. L. Compere, personal communication.

is introduced into the space at the front of the jacket. The drain for the liner cooler, located near the face of the hole, is a tube which passes through the shell of the shielding plug and out the front of the plug. There is a water seal, formed by a chevron-type rubber gasket, between the plug and the liner near the outer end of the liner.

As originally planned, the various leads which passed between the loop and the plug were not separated from the space in the liner, and in order to use water as a coolant it was necessary to seal these connections. The design for this seal provides for ready removal of the seal and exposure of the leads after operation in the reactor. It is comprised of a brass foil, 5 mils thick, which completely encompasses all of the leads and is soldered to the adjacent ends of the plug and the loop jacket. Two 20-mil steel wires are passed completely around the inner surface of the foil, with one near each edge. One end of each wire passes through the foil and is exposed. By pulling the exposed wires against the foil, the metal can be torn and removed easily. The operational performance of neither the connector seal nor the chevron seal has been tested as yet.

It should be noted here that before the present cooling method was adopted, an attempt was made to provide a water seal between the loop liner and the rear of the loop jacket. The design of this seal would have required the use of stressed rubber, and some tests were made to determine the effect of irradiation on stressed rubbers. The adverse results of these tests led to the abandonment of the seal.

The rubbers tested were the following: Neoprene A, Neoprene B, Buna S, Buna N, and natural rubber. The test pieces of the first four rubbers were in the form of rods 0.5 in. in diameter and 3 in. in length. These rods were bent at a 90-degree angle and held in this position during irradiation. The test piece of natural rubber was, in essence, a hollow "O ring" tube, about 5 in. in diameter. The walls ranged in thickness from  $\frac{1}{32}$  to  $\frac{1}{16}$  in. The rubber was stretched about 25% in the thinnest portion by application of nitrogen-gas pressure to the annular space.

<sup>12</sup>C. D. Bopp and O. Sisman, *Radiation Stability of Plastics and Elastomers* (Supplement to ORNL-928), ORNL-1373 (July 23, 1953).

The exposures to radiation were made in a cobalt-gamma-ray source in a field of about  $2 \times 10^5$  r/hr. The duration of exposure in each case was 15 to 20 hr, and in all cases severe damage was noted. The Neoprene A specimen had broken in two at the bend and the other rod specimens had developed deep cracks in the region of the bends. The natural rubber specimen was also cracked severely, and the tube had opened in several places. Bopp and Sisman<sup>12</sup> have reported similar results with stressed natural rubber under irradiation and pointed out that the cracking attack is due to ozone formed by the irradiation of air.

#### RADIOACTIVE-SPECIMEN EVALUATION

J. J. Hairston            D. T. Jones  
A. R. Olsen

##### Loop-Dismantling Facility

The installation of all equipment in the dismantling cell was completed during this period and preliminary tests of individual components have been made. Except for the centrifugal dust-collection system, the components performed satisfactorily. The dust-collection system does not effect complete removal of particles, and it will probably be necessary to filter the exhaust air to ensure complete removal.

Preliminary tests with dummy loop-component subassemblies were made with the facilities of the Solid State Division. These tests proved that the required operations could be carried out, and the procedures are fairly well established.

A thorough test of the integrated procedure of loop dismantling and inspection is being made with Loop CC which was tested during this quarter in the Y-12 HB-4 mock-up.

##### Corrosion Examination Facility

Plans for this facility were mentioned previously.<sup>9</sup> The facility has AEC Approval Numbers CL-159 and CR-209 and construction is scheduled to begin July 26 and to be completed October 30. Design of this facility is about 95% complete and all drawings are scheduled to be completed by August 18. Details of this design follow the general description included in the last report.

##### HRE Inspection

During this quarter, work was begun on procuring specimens from various parts of the HRE which

## HRP QUARTERLY PROGRESS REPORT

are stored in the pool at the HRE site. It has become apparent that work on these parts will be at best a slow, tedious process and will require specialized procedures for each sample. To date access has been gained to the inside of the core by removing the inlet pipe together with a plug about 6 in. in diameter from the surrounding core wall. Removal of the plug necessitated the removal of the dump line and a portion of the inlet piping below the pressure-vessel flange. The portion of the core and the elbow from the inlet pipe adjacent to the core were transferred to one of the cells in the Solid State Division for inspection when it was found that close inspection of the surfaces was unsatisfactory under water. The surface was covered with a thin, loosely knit, rust-brown-colored scale. No localized attack was apparent under visual examination at magnifi-

cations up to 30X. A piece of the core and the portion of the inlet pipe elbow have been given to the Metallography Section of the Solid State Division for microscopic examination. Results of this examination should be available early in August.

The corrosion samples, which were located in the outlet line between the core and the heat exchanger, have also been examined. It should be noted that the location was in the heat-exchanger cell and thus outside of the prompt neutron flux. Preliminary evaluation of the data obtained from these coupons indicates that the results are not inconsistent with data obtained in out-of-pile dynamic-loop tests. A complete report will be issued when both the HRE and HRE mock-up inspections have been completed and a careful comparison with dynamic-loop data has been made.

## LABORATORY CORROSION STUDIES

E. L. Compere

CORROSION OF ZIRCALOY-2 WELDMENTS  
IN URANYL SULFATE SOLUTIONS AT  
250 AND 300°C

E. L. Compere      J. L. English

A considerable number of static tests were started during the past quarter to study the corrosion behavior of Zircaloy-2 weldments in oxygenated uranyl sulfate solutions at 250 and 300°C. The tests were concerned with weldments received from two different sources, the welding shop located in the Y-12 Area at ORNL and the Newport News Shipbuilding & Dry Dock Co., Newport News, Virginia.

The ORNL-welded specimens were prepared from 1/4-in.-thick Zircaloy-2 plate, supplied by Westinghouse in a hot-rolled, sand-blasted, and roller-leveled condition. The plate originated as Westinghouse Heat No. F-875 and was reported to have a typical Zircaloy-2 analysis. The weld rod was Zircaloy-2 which had been swaged by the ORNL Metallurgy Division to a 0.217-in.-dia bar. This Zircaloy-2 originated as Westinghouse Heat Nos. H-542 and/or F-879, remelted ingots from edge-trim pieces. After the bar was swaged, it was sand-blasted, pickled in HNO<sub>3</sub>-HF solution, annealed in vacuum for 2 hr at 750°C, and lathe-machined to produce a scale-free surface with a rod diameter of 0.196 in.

Appropriate lengths of the Zircaloy-2 plate were V-welded in a dry box by the Heliarc process. Specimens for corrosion testing were machined from the welded plate into 1.2-cm widths, normal to the direction of the weld. The weld was located at the mid-point of the 5.0-cm specimen length. The nominal surface area for each specimen was 23.0 cm<sup>2</sup>. Before the machined sides were tested, they were carefully abraded on Nos. 80, 120, and 320 grit papers.

Three different concentrations of uranyl sulfate solutions were used in the tests. The chemical compositions are listed in Table 17. Hydrogen peroxide was added to the solutions at room temperature to produce (by thermal decomposition) an oxygen partial pressure of approximately 150 psi at 250 and 300°C.

The tests were run in duplicate at each temperature with single specimens in 225-ml stainless

steel autoclaves. The specimens were supported in the solutions by stainless steel wire hangers which, in turn, were supported by quartz hangers located in the vapor phase above the solutions. This arrangement electrically insulated the Zircaloy-2 from the stainless steel autoclaves.

Test results for 506 hr of operation at 250 and 300°C are included in Table 18. The reported weight-loss-rate values are based upon as-removed and scrubbed weight losses.

The most corrosive environment for the Zircaloy-2 was the 2.5 *m* uranyl sulfate solution at 300°C. The 506-hr average corrosion rate was 1.5 mpy. The second most corrosive environment was the 1.56 *m* solution containing 0.00035 *m* cupric sulfate and run at a temperature of 250°C; the average corrosion rate after 506 hr was 0.6 mpy. Specimens exposed at 300°C in 0.08 *m* uranyl sulfate solution containing 0.0065 *m* cupric sulfate and sulfuric acid were corroded at an average rate of 0.3 mpy in 506 hr.

The appearance of all specimens was characterized by a thick layer of white corrosion products on the face of the weld and on a narrow area immediately adjacent to the weld. Scattered deposits of white corrosion products were also observed on the polished sides of the weldments. No accelerated attack was noted on or near the weld line of the specimens.

Top and side views of a specimen from each environment are shown in Fig. 43 after 506 hr of test. The roughness exhibited by the base metal is representative of the initial condition of the 0.67-cm Zircaloy-2 plate.

The four Newport News specimens were received as machined pins, 0.5 cm in diameter and 3.5 cm

TABLE 17. CHEMICAL COMPOSITION OF URANYL  
SULFATE SOLUTIONS USED FOR  
ZIRCALOY-2 CORROSION TESTS

UO <sub>2</sub> SO <sub>4</sub> ( <i>m</i> )	CuSO <sub>4</sub> ( <i>m</i> )	H <sub>2</sub> SO <sub>4</sub> ( <i>m</i> )	U Concentration (g per kg of H <sub>2</sub> O)	Initial pH
0.08	0.0065	0.008	19.4	1.90
1.56	0.00035		371.3	1.35
2.50			595.0	0.90

## HRP QUARTERLY PROGRESS REPORT

in length (nominal area per specimen, 6.2 cm<sup>2</sup>), with the welded portion near the center. Specimens ZW-6, ZW-7, and ZW-8 had originated in Newport News Plate No. 1, supplied by Westinghouse. Specimen ZW-22 originated in Newport News Plate No. 3, supplied by Westinghouse, and contained 2.91% titanium. The welds were made by four different techniques as follows: Specimen ZW-6, welded with five passes of  $\frac{1}{16}$ -in.-dia Zircaloy-2 rod with No. 1 Heliarc shield (helium on face side of weld); Specimen ZW-7, welded with three passes of  $\frac{1}{16}$ -in.-dia Zircaloy-2 rod with No. 1 Heliarc shield (helium on face side of

weld); Specimen ZW-8, welded with three passes of  $\frac{1}{16}$ -in.-dia iodide-zirconium rod with No. 1 Heliarc shield (helium on face side of weld); and Specimen ZW-22, welded with four passes of  $\frac{1}{10}$ -in.-dia Zircaloy-2 rod with No. 4 Heliarc shield (argon on face side of weld). All welds were presumably made with helium shielding on the back side. The grades of helium and argon, now known to be an important factor, were not stated. Newport News Shipbuilding & Dry Dock Co. carried out its original testing on whatever plate material was available and the plates prior to No. 7 contained material of uncertain history and quality.

The test environment was 1.56 *m* uranyl sulfate solution containing 0.00035 *m* cupric sulfate, and the test temperature was 250°C. Two specimens were exposed in each of two 225-ml stainless steel autoclaves. Insulation of the specimens from the autoclaves was accomplished by the use of quartz hangers as described previously. The solutions were pressurized with approximately 150 psi partial pressure of oxygen at 250°C by the technique of adding hydrogen peroxide.

Corrosion data for 506 hr are summarized in Table 19. Specimens ZW-6 and ZW-7 exhibited fair corrosion behavior, but the surfaces were spottily covered with a rather bulky and adherent, gray-black film. Otherwise, the surfaces were lustrous and black in color. No signs of unusual corrosion damage were found on or around the weld area. Specimen ZW-8 showed a weight loss rate of 0.3 mpy after 506 hr. Actual metal corrosion rates would doubtless be somewhat higher. With the exception of the weld zone, the surfaces of ZW-8 were lustrous and black in color. The weld area was coated with a thick layer of bulky, white corrosion products. This layer was quite adherent and was not removed to any great extent by brushing. The poorest specimen of the four tested was ZW-22; after 506 hr the weight-loss rate was nearly 12 mpy. The surfaces were heavily coated with white corrosion products, and spalling of the film was much in evidence. The weld surface was quite roughened, dull-gray in color, and showed a preferential attack at the edge of the weld zone. Furthermore, since no correction has been made for zirconium oxide and since the attack was concentrated in the weld zone, the true corrosion rate in this region must have been in excess of 100 mpy.

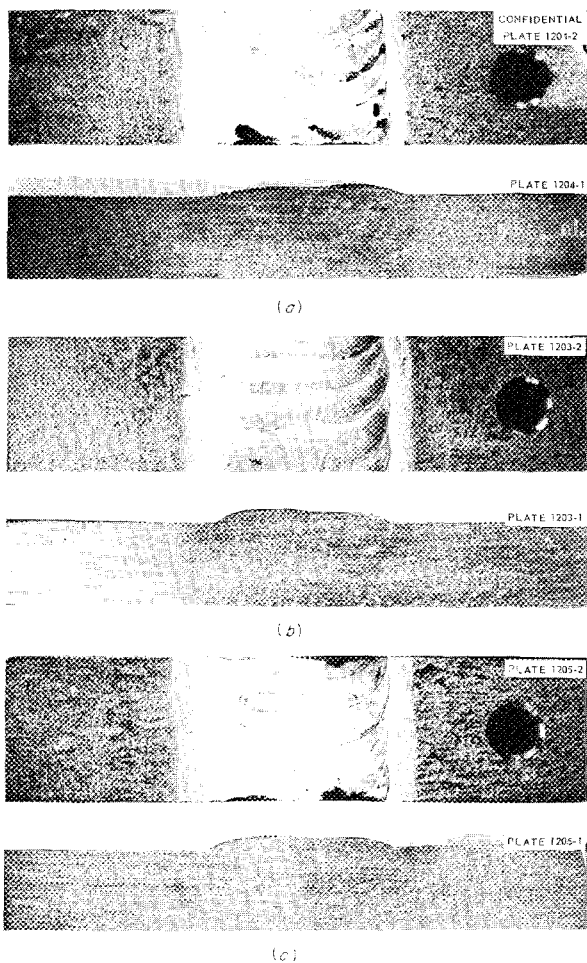


Fig. 43. Zircaloy-2 Weldments after 506 hr in Various Uranyl Sulfate Solutions. (a) Top and side view; 0.08 *m* UO<sub>2</sub>SO<sub>4</sub>, 0.0065 *m* CuSO<sub>4</sub>, 0.008 *m* H<sub>2</sub>SO<sub>4</sub> (300°C). (b) Top and side view; 1.56 *m* UO<sub>2</sub>SO<sub>4</sub>, 0.00035 *m* CuSO<sub>4</sub> (250°C). (c) Top and side view; 2.5 *m* UO<sub>2</sub>SO<sub>4</sub> (300°C). 3X. Reduced 46%.

TABLE 18. CORROSION OF ZIRCALOY-2 WELDMENTS IN OXYGENATED URANYL SULFATE SOLUTIONS AT 250 AND 300° C

Environment			Temperature (°C)	Total Time (hr)	Total Weight Loss (mg/cm <sup>2</sup> )*		Cumulative Weight Loss Rate (mpy)	
UO <sub>2</sub> SO <sub>4</sub> (m)	CuSO <sub>4</sub> (m)	H <sub>2</sub> SO <sub>4</sub> (m)			(1)	(2)	(1)	(2)
0.08	0.0065	0.008	300	25	0.10	0.10	2.0	2.0
				100	0.16	0.14	0.8	0.8
				200	0.16	0.10	0.4	0.3
				506	0.23	0.14	0.4	0.2
1.56	0.00035		250	25	0.07	0.09	1.5	1.9
				100	0.22	0.16	1.2	0.8
				200	0.29	0.19	0.7	0.5
				506	0.35	0.27	0.6	0.5
2.50			300	25	0.22	0.26	4.7	5.5
				100	0.37	0.38	2.0	2.0
				200	0.48	0.50	1.3	1.3
				506	0.85	0.90	1.5	1.5

\*As-removed and scrubbed weight losses.

TABLE 19. CORROSION OF ZIRCALOY-2 WELDMENTS IN OXYGENATED 1.56 m URANYL SULFATE CONTAINING 0.00035 m CUPRIC SULFATE SOLUTION AT 250° C

Specimen No.	Total Time (hr)	Weight Loss (mg/cm <sup>2</sup> )*		Weight Loss Rate (mpy)	
		Δ	Cumulative	Δ	Cumulative
ZW-6	25	+0.7	+0.7		
	100	0.2	+0.5	(1.1)**	
	200	0.2	+0.3	(1.0)	
	506	<0.1	+0.3	(0.1)	
ZW-7	25	+0.8	+0.8		
	100	0.1	+0.7	(1.0)	
	200	0.2	+0.5	(1.0)	
	506	0.1	+0.4	(0.1)	
ZW-8	25	+0.1	+0.1		
	100	<0.1	<+0.1	(0.3)	
	200	0.1	0.1	0.6	0.4
	506	0.1	0.2	0.1	0.3
ZW-22***	25	Nil	Nil		
	100	0.9	0.9	6.0	1.4
	200	2.1	3.0	10.8	7.6
	506	8.3	11.3	14.2	11.6

\*As-removed and scrubbed weight losses.

\*\*Values in parentheses are hypothetical corrosion-rate values.

\*\*\*This material contained 2.9% titanium.

## HRP QUARTERLY PROGRESS REPORT

The use of iodide-zirconium rod (purity and freedom from nitrogen not established) may have contributed to the poor showing of ZW-8, since the base metal appeared to be in good condition. The uncertain quality of the base plate used for ZW-22 and/or impurities in the argon used for shielding may have been responsible. The actual weld area in ZW-22 appeared to be considerably better than the base metal; hence it may be suspected that the quality of the plate was responsible.

Photographs of the specimens are shown in Fig. 44 for an exposure period of 506 hr. The tests will be continued for a minimum time of 1000 hr.

### STRESS-CORROSION CRACKING

E. L. Compere      J. L. English

The observation of two service failures by cracking of type 347 stainless steel pipe in dynamic-corrosion test Loop C was reported previously.<sup>13</sup> There is some possibility that stress-corrosion cracking was involved in these failures. Consequently, a program has been started to investigate the conditions under which this phenomenon can occur in uranyl sulfate solution-type 347 stainless steel systems. It should be noted

<sup>13</sup>H. C. Savage and F. J. Walter, *HRP Quar. Prog. Rep. Apr. 30, 1954*, ORNL-1753, p 59-61.

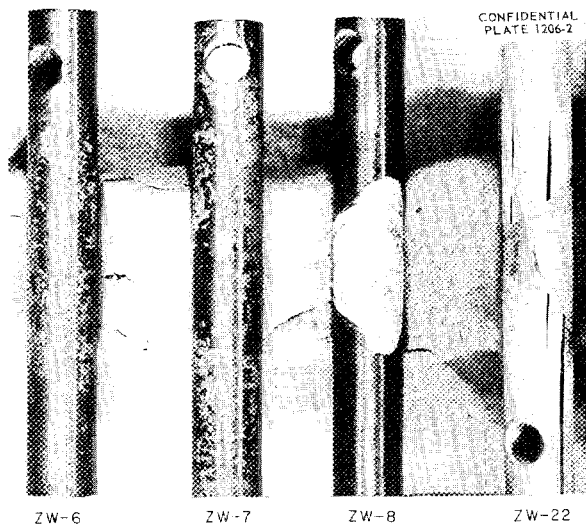


Fig. 44. Zircaloy-2 Weldments after 506 hr in 1.56 M Uranyl Sulfate Solution Containing 0.00035 M Copper Sulfate (250°C), 3X. Reduced 36%.

here, however, that considerable earlier laboratory testing, as well as extensive loop and HRE operating experience, indicates that stress-corrosion cracking is not normally experienced in uncontaminated uranyl sulfate solution-type 347 stainless steel systems.

As part of the testing program, two pieces of apparatus for particular service-type long-term tests have been constructed. These will be described below.

The pipe-bend-sprayer apparatus (Fig. 45) attempts to duplicate the tap-water spray, heated-pipe-bend condition which existed in Loop C before the failures occurred. Six pipe U-bends, three of  $\frac{3}{8}$ -in. schedule-40, welded, type 347 stainless steel pipe and three of  $\frac{1}{2}$ -in. schedule-40, welded, type 347 stainless steel pipe, are attached as shown to common steam and condensate headers. Steam pressure is maintained at 100 psig (168°C), and tap water is sprayed on the inside of each bend through bent, perforated copper tubing.

The apparatus was placed in operation on June 28, 1954, and has operated without failures occurring since that time. Considerable boiler scale has built up on certain areas of the hot pipe, but no other attack has been observed.

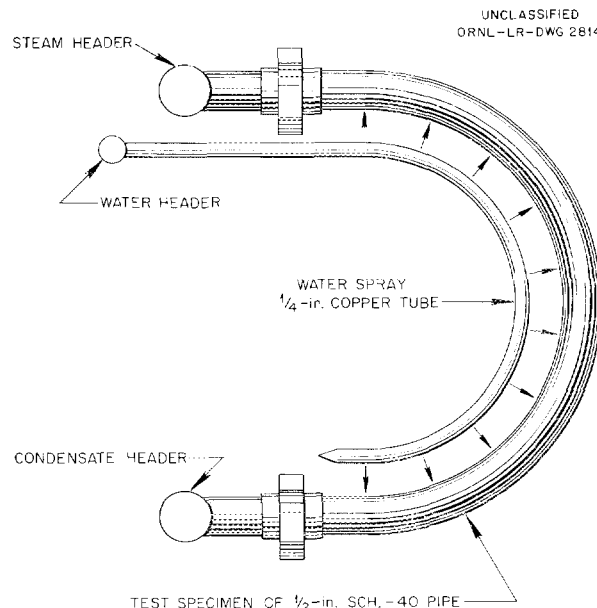


Fig. 45. Pipe-Bend Sprayer.

A small test evaporator has been constructed according to the sketch shown in Fig. 46. The purpose of operating this evaporator is to check the possibility of stress-corrosion cracking on the outside of heated tubes in contact with uranyl sulfate solution and also on stressed specimens which will be placed in the solution and vapor phases in the 5-in.-dia tank above the steam finger. This unit will be placed in operation very soon.

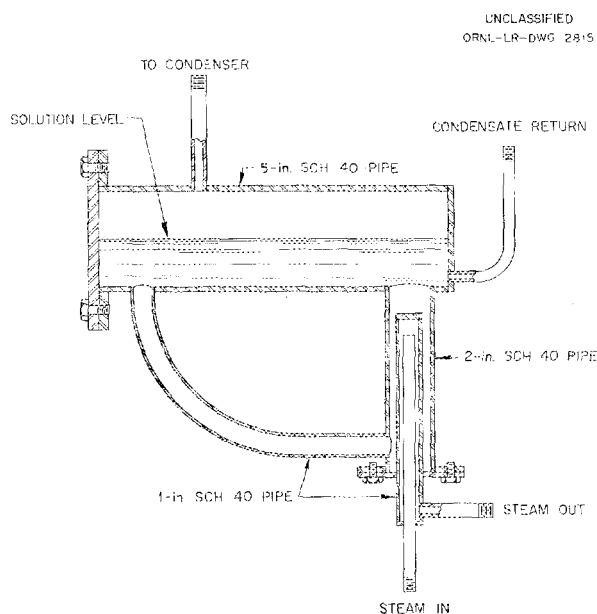


Fig. 46. Test Evaporator.

## HYDROGEN IN METALS

E. L. Compere      G. E. Moore

The program on the effect of atomic hydrogen on materials of reactor interest has continued only slowly during this quarter. A more versatile and more sensitive apparatus for determining the permeability of a metal to atomic hydrogen was constructed and tested by the use of carbon steel and electrolytic hydrogen. The results showed that there was little hydrogen permeability and do not agree with the results reported last quarter.<sup>14</sup>

The present apparatus consists of a diffusion cell as previously described.<sup>14</sup> A bar of the desired material was drilled lengthwise, but not

<sup>14</sup>E. L. Compere, W. O. Harms, and G. E. Moore, *HRP Quar. Prog. Rep.* 30, 1954, ORNL-1753, p 111-113.

throughout the complete length, to yield a  $\frac{1}{8}$ -in.-thick wall. Another piece of rod was machined to fit snugly into the drilled-out length, thus providing a practically volumeless crack between the two pieces of metal. The top of the cell was machined to accommodate a standard tube fitting and was connected to a Baldwin SR-4 pressure cell by means of capillary stainless steel tubing. As a result of a valve arrangement, the entire system can be pressure-checked with helium or other gas, and any pressure that might be built up later as a result of hydrogen diffusion can be released.

Atomic hydrogen can be produced on the cell in a number of ways, for example, by making it the cathode in an electrolytic bath. Much of the atomic hydrogen that is discharged on the cathode may be evolved as molecular gaseous hydrogen, but some may diffuse into the metal or form a metallic hydride. The purpose of this investigation is to explore these possibilities with type 347 stainless steel, titanium, and zirconium or Zircaloy-2.

The hydrogen that diffuses into the "hollow cathode" may be detected by an increase in pressure on the Baldwin pressure cell. Once the diffusing hydrogen (presumably atomic) reaches the inside crack of the cell, it combines to form molecular hydrogen, which has a diffusion rate quite small compared to that of the atomic hydrogen. Consequently, a build-up of pressure is observed.

If the metal used in the cell reacts with the hydrogen to form a hydride, a pressure increase is not apt to be observed, of course, and other methods for detecting this possibility must be found. Recent work by Hackerman<sup>15,16</sup> on the cathodic polarization of titanium and zirconium has shown the formation of a hydride phase by both these materials. Both X-ray diffraction and metallography have been used to determine the presence of the hydride phase.<sup>17,18</sup>

<sup>15</sup>N. Hackerman and C. D. Hall, Jr., *J. Electrochem. Soc.* 101, 321 (1954).

<sup>16</sup>N. Hackerman and O. L. Willbanks, Jr., *Technical Report to the Office of Naval Research on the Electrochemical Polarization of Zirconium in Distilled Water*, April 23, 1954.

<sup>17</sup>J. Belle, B. B. Cleland, and M. W. Mollett, *J. Electrochem. Soc.* 101, 211 (1954).

<sup>18</sup>G. A. Lenning, C. M. Craighead, and R. I. Jaffee, *J. Metals* 6, 367 (1954).

## HRP QUARTERLY PROGRESS REPORT

Carbon steel has been used in our experiments to date to test the apparatus because the permeability of carbon steel to atomic hydrogen is well known.<sup>19</sup> This permeability has been the subject of much attention primarily because of the "hydrogen blistering" encountered as a result of corrosion. The results of Marsh,<sup>20</sup> as well as our own efforts to duplicate these results, were described in the last quarterly report. In both of these experiments a cell as just described and a Bourdon-tube type of pressure gage were used. Atomic hydrogen was produced by immersing the cell in 2.4% hydrochloric acid. This particular arrangement has a number of disadvantages; particularly, the method of pressure measurement is not very sensitive and the wall thickness of the cell is constantly decreasing due to the attack by the acid. For these reasons the experimental apparatus previously described was used. The Baldwin pressure cell was capable of measuring pressures up to 500 psi, to a sensitivity of about  $\pm 0.5$  psi, while the use of electrolytically formed hydrogen reduced the attack on the cell walls.

In one experiment 0.01 N sulfuric acid was used as the electrolyte and a platinum wire served as the anode. A current density of about  $1.6 \times 10^{-4}$  amp/cm<sup>2</sup> (apparent cathode area was  $\sim 100$  cm<sup>2</sup>) at about 10 v was used. A pressure increase was observed after approximately 40 hr and continued to increase steadily for the following 80 hr, although the pressure rise was not so rapid as had been experienced in the earlier work in hydrochloric acid. After the 80 hr, with the pressure having risen to about 25 psia, no further increase in pressure was observed. No explanation of this behavior has been found. It is known that the initial pressure rise was real because the pressure could be released by venting the system. Abrading the cell so as to present a new, clean surface, varying the current density from  $7 \times 10^{-5}$  to  $4 \times 10^{-2}$  amp/cm<sup>2</sup>, and changing to sodium nitrate or sodium chloride as electrolyte were without effect. The cell was then cleaned by abrasion, immersed in 0.01 N sulfuric acid as the electrolyte (a saturated potassium chloride-agar salt bridge separated the platinum anode), and electrolyzed at a current density of  $1.5 \times 10^{-4}$  amp/cm<sup>2</sup>. A very steady but very small increase in pressure

was observed over a period of three weeks. The pressure at the end of this time was only 22.5 psia.

Hackerman<sup>15</sup> has rather clearly shown that both titanium and zirconium form hydrides on cathodic polarization. This is essentially the technique that was to be used in the current experiments. The practical question yet to be answered is whether hydrogen (or deuterium), formed by the decomposition of water (ordinary or heavy) by radiation, will have a deleterious effect on the components with which it comes in contact in a reactor under the operating conditions. Titanium and zirconium (or Zircaloy-2) are the materials of chief concern because of their known tendencies toward hydride formation, their brittleness under the operating conditions, and their anticipated use in the reactors where radiolytic gas will be present.

The reaction between hydrogen gas and pure zirconium, free of oxide film, has been reported recently by J. Belle and co-workers<sup>17</sup> of Battelle Memorial Institute. They found that the reaction follows the usual parabolic law, in the region 250 to 425°C, with the parabolic rate constant for hydrogen uptake being given by

$$k = 2.3 \times 10^5 e^{-17,200/RT} (\text{ml/cm}^2)^2/\text{sec} .$$

By an extrapolation with this law far beyond the 3 hr of actual observation, it is estimated that at 300°C and 1 atm of hydrogen a penetration of 1 cm would be experienced in about 1 year, or in about 3 months at 300 psi of hydrogen pressure. A penetration of 7 mils was observed in  $2\frac{1}{2}$  hr at 300°C and 1 atm. The penetration rate would double with approximately every 50°C increase in temperature and is proportional to the square root of hydrogen pressure.

Photomicrographs obtained by these workers indicate that a clear interface may be perceived between zirconium and zirconium hydride, at a magnification of 250X, without etching after metallographic polishing.

In recent discussions with M. W. Mallett, it was pointed out that the reaction with molecular hydrogen gas proceeds far more slowly in the presence of the oxide film ordinarily found on zirconium but that atomic hydrogen gas enters the metal rapidly even in the presence of the oxide film. The nature of attack by radiolytic hydrogen is, of course, not given by these experiments.

<sup>19</sup>L. S. Darken and R. P. Smith, *Corrosion* 5, 1 (1949).

<sup>20</sup>G. A. Marsh, *Corrosion* 10, 101 (1954).

## TESTS WITH HIGH-CONCENTRATION URANYL SULFATE SOLUTIONS

E. L. Compere      J. L. English

### Corrosion of Type 347 Stainless Steel, Titanium 75A, and Zircaloy-2 at 300°C in Oxygenated 5 m Uranyl Sulfate Solution

The corrosion of type 347 stainless steel, Titanium 75A, and Zircaloy-2 in oxygenated 5 m uranyl sulfate solution at 300°C was discussed in the previous quarterly report.<sup>21</sup> Data on the corrosion of the three alloys after 200 hr of test were summarized. The specimens were tested for a total of 1000 hr during the past quarter. The conclusions of the previous report are confirmed, namely, that under these conditions Titanium 75A and Zircaloy-2 are relatively unattacked, a hard solid uranyl sulfate hydrate is produced, and type 347 stainless steel is attacked most sharply in such static tests at the water line and in or near the region of the solid phase.

A uranyl sulfate concentration (5 m) and a temperature (300°C) were selected from the phase diagram for the  $\text{UO}_2\text{SO}_4\text{-H}_2\text{O}$  system so that the concentration-temperature combination would produce a system slightly below the region of two-liquid-phase separation. The resulting condition was somewhat representative of the type of corrosion environment that would exist in the heavy phase when the two-liquid-phase region was reached. This type of environment could be produced unintentionally by a not-too-extreme fluctuation in operating conditions of a homogeneous reactor.

The prepared uranyl sulfate solution was actually 4.9 m in concentration (1166 g of uranium per kilogram of water) with sulfate-to-uranium ratio of 1.008. New solution was used at the start of each test period due to the presence, at room temperature (after cooling from the 300°C test temperature), of an extremely hard and solid salt layer, which, by analysis, appeared to be a hydrated form of uranyl sulfate, possibly  $\text{UO}_2\text{SO}_4 \cdot 2\text{H}_2\text{O}$ .

The type 347 stainless steel test specimens were prepared from 0.05-cm-thick (0.019 in.), annealed and pickled sheet. The nominal surface area per specimen varied between 14.3 and 16.0  $\text{cm}^2$ . Specimens were exposed in the solution, in the vapor above the solution, and at the solution-

vapor interface. At periodic intervals during the 1000-hr test, specimens were removed for electrolytic defilming in inhibited 5% sulfuric acid and for measurement of actual metal-weight losses.

After the initial 24-hr run, duplicate specimens of Zircaloy-2 and Titanium 75A were placed in the solution phase of the 5 m uranyl sulfate. The Zircaloy-2 specimens were machined cylinders and were 0.5 cm in diameter and 2.5 cm in length; the apparent surface area was 4.8  $\text{cm}^2$ . The Titanium 75A specimens were machined from 0.6-cm-dia bar stock to a size 0.5 cm in diameter by 3.5 cm in length. The nominal area per specimen was 6.2  $\text{cm}^2$ .

Two 14.0-cm-long strip specimens of type 347 stainless steel were also placed in the test after the first 24 hr. These specimens were positioned in the autoclave so that the surfaces contacted the vapor phase, the solution-vapor interface, the solution phase, and the previously noted solid phase (whenever formed).

The 1000-hr stainless steel corrosion data are reported in Table 20, where the data for solution, vapor, and water-line-exposed specimens that were removed at periodic intervals for defilming are listed. The as-removed weight losses for the two long, type 347 stainless steel water-line specimens which were run for 976 hr are also presented in Table 20. Weight-loss rates, based upon as-removed weight losses, are included in the table for comparison with defilmed corrosion-rate values. However, only the defilmed corrosion rates can be regarded as valid. The difference between the two sets of values is attributed to the film weight on the as-removed specimens.

The defilmed weight losses on the solution-exposed specimens indicated that corrosion attack was pronounced during the initial 24 hr but thereafter showed little or no continued attack with increased exposure time. The final 1000-hr corrosion rate was 0.9 mpy. Likewise, no appreciable continued attack rate with increased time occurred on vapor-exposed specimens. Weight losses ranged predominantly between 0.4 and 0.7  $\text{mg}/\text{cm}^2$ . The final corrosion rate was 0.2 mpy or about 20% of the value measured on solution-exposed specimens.

Although corrosion attack on solution- and vapor-exposed specimens was of a generalized type, this was not the case on water-line-exposed specimens. Corrosion attack at and near the

<sup>21</sup>E. L. Compere and J. L. English, *HRP Quar. Prog. Rep. Apr. 30, 1954*, ORNL-1753, p 102-104.

HRP QUARTERLY PROGRESS REPORT

TABLE 20. CORROSION OF TYPE 347 STAINLESS STEEL IN OXYGENATED 5 m URANYL SULFATE SOLUTION AT 300°C

Specimen Position	Total Time (hr)	Total Weight Loss (mg/cm <sup>2</sup> )		Weight Loss Rate (mpy)		Specimen Condition
		As-Removed	Defilmed	As-Removed	Defilmed	
Solution	24	0.5	2.3	8.2	41.2	Uniform attack; no pitting
	48	0.3	2.5	2.7	22.9	Uniform attack; no pitting
	100	Nil	1.6	Nil	6.9	Uniform attack; no pitting
	200	+0.1	1.9		4.0	Uniform attack; no pitting
	500	0.1	2.1	0.1	1.8	Uniform attack; no pitting
	1000	+0.1	2.1		0.9	Uniform attack; no pitting
Vapor	24	Nil	0.7	Nil	12.0	Uniform attack; no pitting
	100	+0.1	0.4		1.9	Uniform attack; no pitting
	500	<0.1	0.1	<0.1	0.1	Uniform attack; no pitting
	1000	Nil	0.4	Nil	0.2	Uniform attack; no pitting
Water-line*	24	<0.1	0.7	0.4	13.5	Negligible water-line attack
	100	0.1	1.8	0.9	8.0	Mild water-line attack
	500	0.8	2.0	0.7	1.7	Mild water-line attack
	1000	5.3	7.5	2.3	3.3	Severe water-line attack
		As-Removed Weight Loss (mg/cm <sup>2</sup> )		As-Removed Corrosion Rate (mpy)		
		(1)	(2)	(1)	(2)	
Water-line**	24	0.3	0.9	5.3	16.0	Progressive increase in the intensity of water-line attack with time; severe pitting, 5 to 8 mils deep
	76	0.4	0.9	2.3	5.0	
	176	0.4	1.1	0.9	2.6	
	476	0.5	1.0	0.5	0.9	
	976	1.3	1.2	0.6	0.5	
				Defilmed Corrosion Rate (mpy)		
				1.2	1.4	

\*4-cm-long specimens.

\*\*14-cm-long specimens.

solution-vapor interface on stainless steel surfaces was highly localized and was markedly accelerated with increased exposure time. The attack was characterized by massive semilocalized areas of damage in which pit diameters greatly exceeded the depth of the penetration. Accompanying this type of attack was an extremely prolific pitting attack. Measured depths of the pits at the water line were as high as 7 mils after 200 hr. However, complete perforation of the 19-mil stainless steel strip was not obtained during the 1000-hr test.

Another area of pronounced corrosion attack was observed on the bottom portions of the 14-cm-long water-line specimens. This area was contacted by the solid phase found after cooling to room temperature. Evidence exists that this solid phase was formed at high temperature. The surfaces of the specimens exposed in this phase (either a solid or heavy liquid at 300°C) were heavily spotted with semilocalized and pitting attack. After repeated cathodic defilming treatments, the surfaces continued to show a strongly adherent and uniform, black film.

The Zircaloy-2 solution-exposed specimens exhibited negligible weight losses during the 976-hr test. Corrosion information for this alloy, as well as for Titanium 75A, was based upon as-removed weight changes since a reliable method for defilming the materials was not available. The surfaces of the Zircaloy-2 specimens were covered with a highly lustrous and adherent, gray-black film. Microscopic examination showed a shallow, stringer type of pitting attack which was parallel to the machining marks on the specimens. A fairly high frequency of single, shallow pits was also observed.

The as-removed weight changes on the two Titanium 75A solution-exposed specimens are shown in Table 21. The total exposure time was 976 hr.

TABLE 21. CORROSION OF TITANIUM 75A IN OXYGENATED 5 *m* URANYL SULFATE SOLUTION AT 300°C

Total Time (hr)	Cumulative As-Removed Weight Loss (mg/cm <sup>2</sup> )		Weight-Loss Rate (mpy)	
	(1)	(2)	(1)	(2)
	24	+0.1	+0.1	
76	+0.1	+0.1		
176	0.1	0.1	0.2	0.2
476	0.3	0.3	0.5	0.4
976	0.7	0.6	0.5	0.5

The data in Table 21 show that there is a somewhat accelerated weight-loss rate with time for the Titanium 75A after 176 hr. The final 976-hr weight-loss rate was 0.5 mpy. Unfortunately, the actual corrosion rate is obscure, since the specimen was not defilmed and no account was taken of the oxide film known to be present. No pitting attack was found on the titanium specimens. The surfaces, except for the bottom ends which were apparently contacted by the solid phase observed at room temperature, were covered with a thin, highly lustrous, bronze-colored film. These areas exhibited a thin, highly lustrous film of many colors, and no evidence of an accelerated corrosion attack was noted. It is concluded that Titanium 75A showed good corrosion resistance under the conditions of this experiment.

No suitable static quantitative data are currently available that would permit a comparison between the corrosivity of a 5 *m* uranyl sulfate solution and, for example, a 0.17 *m* uranyl sulfate solution at 300°C. However, indications are that the 5 *m* solution is considerably more corrosive than the 0.17 *m* solution. The intensity and rapidity of water-line attack on type 347 stainless steel in 5 *m* uranyl sulfate provide strong evidence of the extremely corrosive nature of this medium when compared with water-line effects on type 347 stainless steel in 0.17 *m* uranyl sulfate solution at 250°C as discussed elsewhere in this report.

#### Blowdown Experiments

Laboratory experiments with 5 *m* uranyl sulfate solutions at 300°C, described above, showed the presence of a hard, difficultly soluble solid in the bottom of the autoclaves. Further studies on the nature and the conditions of formation of this solid seemed of interest since some operating error could presumably carry an operating reactor into the two-phase region, particularly in the case of concentrated solutions. The presence or formation of such solids in a line such as a dump line is of particular concern because the plug would be very difficult to remove and the fission-product heat might seriously aggravate the situation.

In each experiment a quantity (500 or 800 ml) of uranyl sulfate solution was charged to a 1500-ml stainless steel autoclave equipped with a pressure gage, a gas inlet, and a  $\frac{3}{16}$ -in.-ID withdrawal line which extended into the bomb to within  $\frac{1}{4}$  in. of the bottom. Oxygen gas was added (to 150 psig) at room temperature, usually through the withdrawal line, and the system was heated to temperature. After the system remained at temperature for several hours, the withdrawal valve was opened and an effort was made to withdraw liquid from near the bottom of the bomb. The withdrawal was completely successful only when the system was operated at 275°C. In any event, the bomb was then allowed to cool overnight and was opened after noting that sufficient gas pressure remained to indicate that no leakage had occurred during the experiment. The residual liquid was poured off, and in some cases a solid layer,  $\frac{1}{2}$  to 2 in. deep, was noted. Samples of the various phases were obtained for analysis, and the withdrawal tube was examined. A summary of the results of the experiments is given in Table 22.

HRP QUARTERLY PROGRESS REPORT

TABLE 22. BLOWDOWN EXPERIMENTS ON CONCENTRATED URANYL SULFATE SOLUTIONS AT HIGH TEMPERATURES

Solutions placed in 1500-ml autoclave equipped with withdrawal tube  $\frac{1}{4}$  in. above bottom; oxygen gas pressurized to 150 psi at 25°C

Temperature, °C	300	300	300	300	275
Time, hr	4.5	2.2	1.2	2.7	2.0
Solids (oven dried)	Much hard residue	Much hard residue	Much hard residue	Extruded	None
Empirical formula					
UO <sub>2</sub>	1	1	1	1	
SO <sub>4</sub>	1.036	1.025	1.028	1.075	
H <sub>2</sub> O		2.32	2.24	0.3(?)	
Original charge					
U, molality	4.86	2.511	2.511	1.348	1.348
pH		0.9	0.9	1.36	1.36
Volume, ml	500	500	500	500	800
Withdrawn phase					
U, molality					1.847
SO <sub>4</sub> , molality					1.999
pH					1.10
Volume, ml	None	None	None	5-10	110
Residual liquid					
U, molality	2.103	0.729	0.929	0.816	1.351
SO <sub>4</sub> , molality	2.084	0.797	1.000	0.861	1.395
pH	0.95	1.13	1.25	1.30	1.38
Volume, ml	350	410	420	475	660
Remarks	Plugged at temperature before withdrawal	Plugged at temperature before withdrawal	Plugged at temperature before withdrawal	Plugged after extruding paste which solidified	Withdrawal OK; cooled; note analyses not consistent

A 4.86 *m* uranyl sulfate solution was tested at 300°C, inasmuch as this concentration represents roughly the high-concentration boundary of the two-liquid-phase region at this temperature. When the withdrawal valve was opened, no solution flowed out. After the system was cooled and the residual liquid was removed, a hard, yellow residue was found in the bottom of the bomb and also to a comparable level in the withdrawal dip tube. Accordingly, it is concluded that the solid did not form upon cooling but had existed at operating temperature. Analysis of the solid indicated that it was a simple uranyl sulfate and was presumably hydrated.

Similar results were obtained in two similar experiments in which 2.511 *m* uranyl sulfate was used, and again the solid appeared to have been

formed at operating temperature. The water of hydration of the solid was estimated by difference after drying to be 2.2 to 2.3 moles of H<sub>2</sub>O per mole of uranyl sulfate. However, this procedure for determining differences is not very accurate.

Also, two experiments in which 1.348 *m* uranyl sulfate solution was used, at 300 and at 275°C, were carried out. In the 275°C test, the withdrawal was straightforward, and 110 ml was removed, with cooling, from an original 800-ml charge. No plugging was experienced and no solids were found.

However, when withdrawal was attempted at 300°C from a similar 1.348 *m* uranyl sulfate solution, a small amount of heavy viscous paste was extruded. This occurred with a snapping, crackling sound like that which results when

heavy lubricating grease is forced from a grease gun. The paste became a semitransparent solid on cooling. After 5 to 10 ml of the material had been extruded through the  $\frac{3}{16}$ -in. line, the line became plugged. The solid was analyzed and found to be a uranyl sulfate hydrate.

The solid phase forming on the bottom of the autoclave from the 4.86 and 2.511 *m* solutions was extremely hard, dense, and slow to redissolve. It could be scratched by a screwdriver struck by a hammer, but to chip it out was impractical. It was dissolved after a day or so with boiling water. The lines provided by X-ray examination did not coincide with those of any ordinary known form of uranyl sulfate.

Similar experience with a high-temperature solid phase from concentrated uranyl sulfate solutions was described to Laboratory personnel by E. Stephan of Battelle Memorial Institute, who had obtained such solids during the course of measurements of gas solubilities in uranyl sulfate at high temperatures.

The solids herein reported appear at concentrations considerably lower than would be indicated at 300°C on the usual phase diagram for the two-component uranyl sulfate-water system, even with an allowance for reasonable error in temperature measurement.

The blowdown experiment for 300°C, in which 1.348 *m* uranyl sulfate was used and which resulted in the extrusion of some heavy-phase material and subsequent plugging, is indicative of dump-line difficulties which could be experienced in the high-concentration, uranyl sulfate blanket of a plutonium-producing reactor if the temperature became too high.

#### CORROSION OF MICROMETALLIC, SINTERED, TYPE 304 STAINLESS STEEL FILTER PLATE

E. L. Compere                  J. L. English

The corrosion behavior of a micrometallic, sintered, type 304 stainless steel filter plate was examined in acidified 0.06 *m* and in 1.34 *m* uranyl sulfate solutions at temperatures of 50 and 102 to 104°C (boiling). The use of micrometallic sintered stainless steel has received some consideration as a possible method for the removal of insoluble corrosion products etc. from a homogeneous reactor fuel solution. The operational temperature for the filtration process was estimated to be somewhere between 50°C and boiling.

Type 304 stainless steel filter plate was used for the study since it was readily available and since the corrosion of wrought type 304 stainless steel was known to be fairly characteristic of the behavior of the austenitic-stainless-steel alloys in uranyl sulfate solutions below 100°C. The test specimens were cut into strips and disks from a 15.2-cm-square by 0.25-cm-thick sheet. The average nominal area of the strip specimens was 18.1 cm<sup>2</sup>, whereas that of the disks was approximately 12.2 cm<sup>2</sup>.

The test solutions were (1) 0.06 *m* uranyl sulfate containing 0.006 *m* sulfuric acid and (2) 1.34 *m* uranyl sulfate. The solutions were not aerated during the tests.

In view of the high porosity of the specimens, the technique of drying to constant weight was employed after each exposure period. The operation consisted in soaking the specimens in hot distilled water for 30-min periods, drying at 110°C, and weighing. This cycle was repeated until a constant weight was obtained. The procedure proved to be entirely satisfactory except for those specimens exposed in the 0.06 *m* solution at boiling temperature. For unknown reasons, it was not possible to obtain constant weights on the specimens after each exposure period. Also, these specimens were the only ones which showed weight gains rather than losses, as will be shown later.

Since the true areas of the specimens are far greater than the apparent measured areas, the conversion of weight-loss data into rates would be almost meaningless. In order to present a more realistic evaluation of corrosion behavior, figures are included in Table 23 for the percentage weight losses of the specimens, based upon the initial dried-to-constant-weight values.

The behavior of the micrometallic filter plates at 50°C was much the same in the 0.06 *m* uranyl sulfate solution which contained excess sulfuric acid and in the 1.34 *m* uranyl sulfate solution. Weight losses for samples in these solutions after 504 hr averaged 0.23 and 0.19%, respectively. At boiling temperatures, the behavior of micrometallic type 304 stainless steel filter plate in 0.06 *m* uranyl sulfate with 0.006 *m* sulfuric acid after 504 hr was questionable. In boiling 1.34 *m* uranyl sulfate, the magnitude of as-removed weight losses (9.3% after 504 hr) was so great that the use of the material under these conditions was

## HRP QUARTERLY PROGRESS REPORT

TABLE 23. CORROSION OF MICROMETALLIC, SINTERED, TYPE 304 STAINLESS STEEL FILTER PLATE IN URANYL SULFATE SOLUTIONS

UO <sub>2</sub> SO <sub>4</sub> (m)	H <sub>2</sub> SO <sub>4</sub> (m)	Temperature (°C)	Total Time (hr)	Total Weight Loss (%)	
				(1)	(2)
0.06	0.006	50	50	0.08	0.14
			100	0.12	0.18
			200	0.13	0.24
			504	0.17	0.29
0.06	0.006	102	50	+2.39	+4.53
			100	+2.43	+3.31
			200	+0.41	+1.07
			504	+0.06	+0.05
1.34		50	50	0.09	<0.01
			100	0.12	0.06
			200	0.15	0.09
			504	0.20	0.18
1.34		104	50	3.16	4.65
			100	3.92	5.30
			200	5.24	6.38
			504	9.31	9.36

eliminated. However, no observable gross damage to any of the materials has as yet been noted. The tests are being continued.

### CORROSION OF PUMP-BEARING MATERIALS

E. L. Compere      J. L. English

Three different materials which were considered for possible use as bearings in a Byron Jackson canned-rotor pump which is being developed for in-pile use were examined in uranyl sulfate solutions at controlled temperatures of 100 and 150°C. The materials included Star J alloy, Alsimag 576, and sintered aluminum oxide. Tests were run for total periods of 100 to 414 hr in oxygen-pressurized 0.17 m uranyl sulfate solution.

The Star J alloy, manufactured by the Haynes Stellite Company, was received from the Byron Jackson Co. in the form of a 3.5-cm-OD ring. The measured hardness of the alloy was 78 Rockwell 30-N (60 Rockwell C). The nominal chemical composition of the alloy in weight per cent was cobalt, 40 (minimum); chromium, 35 (maximum); and tungsten, 20 (maximum). The apparent surface

area of the specimen was 22.5 cm<sup>2</sup>.

The Alsimag 576 was supplied also by the Byron Jackson Co. as a solid 1.3-cm-dia disk. The material was manufactured by the American Lava Corporation and is reported to consist of a mixture of ground talc (magnesium silicate) and sodium silicate. The specific gravity of the vitrified material was approximately 2.5. The measured surface area was 6.5 cm<sup>2</sup>.

The sintered aluminum oxide specimen was received from the Kearfott Company, Inc., Clifton, New Jersey. No other specific information was available on the material. The specimen was a solid disk, 3.1 cm in diameter, with an apparent surface area of 21.5 cm<sup>2</sup>.

The tests were run in an 850-ml-capacity stainless steel autoclave in which a solution volume of 500 ml was employed. The autoclave was pressurized with 150 psig of oxygen at the start of each run. The same specimens that were used for the 100°C tests were used for the 150°C tests.

The available results from the tests are summarized in Table 24.

Star J alloy showed promising corrosion resistance at 100°C, with a metal thickness loss of 0.01 mil in 236 hr. However, a metal-thickness loss of 0.10 mil in 100 hr (8 mpy) occurred when the temperature was increased to 150°C. The implication from these preliminary data was that the corrosion resistance of Star J alloy in 0.17 m uranyl sulfate was quite temperature sensitive and that the maximum safe operating temperature was limited to around 100°C. It is planned to continue tests at 100°C and also at 125°C.

The sintered aluminum oxide specimen was run for a total of 414 hr at 150°C. The rate of corrosion decreased from an initial rate of 2.4 mpy in 118 hr to 1.8 mpy after 414 hr. Incremental corrosion rates for three consecutive 100-hr exposure periods after the initial 118 hr showed an encouraging trend of 1.7, 1.7, and 1.1 mpy, respectively. At the end of the third run (total 314 hr), the surfaces of the specimen were slightly stained reddish-brown and exhibited randomly located, shallow pockmarks. Otherwise, no indications of corrosion damage were observed.

The corrosion data on Alsimag 576 definitely eliminated it from further consideration as a possible pump-bearing material. The material performed poorly at 100°C (72 mpy for 236 hr) and even more poorly at 150°C (248 mpy for 100 hr).

TABLE 24. CORROSION OF POSSIBLE BEARING MATERIALS IN OXYGENATED 0.17 M URANYL SULFATE AT 100 AND 150°C

Material	Temperature (°C)	Total Time (hr)	Weight Loss (mg/cm <sup>2</sup> )		Corrosion Rate (mpy)	
			Δ	Cumulative	Δ	Cumulative
Star J alloy	100	236	0.2	0.2	0.4	0.4
Star J alloy	150	100	2.0	2.0	8.0	8.0
Al <sub>2</sub> O <sub>3</sub>	150	118	0.3	0.3	2.4	2.4
		218	0.2	0.5	1.7	2.1
		314	0.2	0.7	1.7	2.0
		414	0.1	0.8	1.1	1.8
Alsimag 576	100	236	12.3	12.3	72.0	72.0
Alsimag 576	150	100	17.9	17.9	248.0	248.0

**CORROSION OF TYPE 347 STAINLESS STEEL AND TITANIUM 75A IN THORIUM NITRATE SOLUTION**

E. L. Compere      J. L. English

A 500-hr exploratory test was completed with type 347 stainless steel and Titanium 75A exposed at 250°C in a thorium nitrate solution which contained excess nitric acid to prevent hydrolysis of the thorium ion at the elevated temperature. By analysis, at room temperature the nitrate solution contained 305.5 g of thorium per liter (1.32 M) and 2.26 M nitric acid. The corrosion resistance of Titanium 75A was excellent under these conditions and that of type 347 stainless steel was fairly good (4.5 mpy), although pitting was observed.

The type 347 stainless steel specimen was prepared from 0.34-cm-thick annealed and pickled sheet. The surfaces were polished on Nos. 80 and 120 grit papers before exposure. The Titanium 75A specimen was cut from annealed 0.025-cm-thick sheet. Both specimens had a nominal surface area of 11.4 cm<sup>2</sup>.

The specimens and the thorium nitrate solution were contained in a 225-ml-capacity stainless steel autoclave; the solution-exposed specimens were insulated from contact with the autoclave by a quartz rod hanger. New solution was used at the start of each run because dense fumes of NO<sub>2</sub> gas, indicative of solution degradation, were observed when the 250°C autoclave was opened after each run.

The test was run for a total of 500 hr, during which time the specimens were examined four times. The as-removed weight losses are listed in Table 25.

The weight gain on the titanium specimen was due to the formation of a thick, uniform, black film on the surfaces. The cathodic defilming treatment in inhibited 5% sulfuric acid was quite successful in removing the bulk of the film at the completion of the test. The titanium surfaces beneath the film were lustrous and golden-yellow in color. No pitting attack was found. The black film is believed to be iron oxide deposited on the titanium.

The type 347 stainless steel specimen was also coated with a thick, black film after 500 hr. The film was removed almost completely by the defilming operation. The defilmed weight loss was equivalent to a metal-thickness loss of nearly 0.3 mil; the corrosion rate was 4.5 mpy. The film-free surfaces exhibited a pronounced acid-etched attack, and pitting attack was very prevalent, with pit depths between 6 and 8 mils not uncommon near the edges of the specimen.

It is planned to examine further the corrosion of type 347 stainless steel, Zircaloy-2, and Titanium 75A in thorium nitrate solutions of various concentrations and containing excess nitric acid. Temperatures of 100, 200, 250, and 300°C will be included in the tests, and specimens will be exposed in the solution, vapor, and water-line environments of the nitrate solutions.

## HRP QUARTERLY PROGRESS REPORT

TABLE 25. CORROSION OF TYPE 347 STAINLESS STEEL AND TITANIUM 75A AT 250°C IN 1.32 M THORIUM NITRATE SOLUTION CONTAINING 2.26 M NITRIC ACID

Material	Total Time (hr)	Total Weight Loss* (mg/cm <sup>2</sup> )	Weight-Loss Rate (mpy)
Type 347 stainless steel	24	0.5	9.5
	74	0.7	4.3
	197	0.4	0.8
	500	+2.5	
			Corrosion Rate (mpy)
Type 347 stainless steel (defilmed)	500	5.2	4.5
Titanium 75A	24	+1.7	
	74	+1.6	
	197	+2.0	
	500	+3.5	
Titanium 75A (defilmed)	500	+0.3	

\*As-removed weight losses.

### SMALL-SCALE DYNAMIC-CORROSION PROGRAM

E. L. Compere      G. E. Moore

#### McWherter-DeRieux Toroid Rotator I

Fabrication of the furnace for toroid rotator I has not yet been completed, and, consequently, no work with this rotator has been carried out.

#### Toroid Rotator II

Seven runs with the experimental toroid rotator II were carried out this quarter. These runs were designed to investigate the effect of the number of sample pins and of the solution velocity on the corrosion rate of type 347 stainless steel by 0.17 *m* uranyl sulfate at 250°C under 430 psi of oxygen pressure.

This rotator was patterned after the NACA toroid circulating apparatus<sup>22</sup> and was adapted to our requirements by R. A. Lorenz. Operation for 1900 hr during the quarter, in which 0.17 *m* uranyl sulfate was circulated simultaneously in four type 347 stainless steel toroids at velocities from 2.8

to 38.6 fps, confirmed the adequacy of the design. Four additional such rotators are being fabricated.

The toroids contained either one, two, or four type 347 stainless steel sample pins which were electrically insulated from the other parts of the system by small Teflon bushings. The pins were mounted perpendicularly to the direction of rotation of the liquid and entered from the outer side of the toroid. The toroids were wrapped with resistance wire and insulated so they could be heated; the temperature was controlled through an iron-constantan thermocouple welded to one of the toroids and connected to the appropriate electronic circuit. Excess oxygen pressure was provided by the addition of hydrogen peroxide calculated to yield 430 psi oxygen pressure at 250°C.

Corrosion rates were based on defilmed weight losses. Based on the available data (at a velocity of 19.6 fps), the weight loss appeared to be directly proportional to the time; there was no indication of an induction period at this velocity. The pins, however, were not always attacked uniformly; very often a definite flow pattern was apparent in which the upstream side of the pin showed no film at all, while the downstream side

<sup>22</sup>L. G. Desmon and D. R. Mosher, *Preliminary Study of Circulation in an Apparatus Suitable for Determining Corrosive Effects of Hot Flowing Liquids*, NACA RM E51D12 (June 1951).

was coated with a heavy black film. There appears to be no entirely satisfactory way to present corrosion rates as a single number in such a situation. For the purposes of this discussion, it was assumed that the area of the pin covered by the black film was relatively unattacked, as compared with the film-free part, and the corrosion rate was calculated on the basis of the film-free area alone.

The results obtained on this basis are shown in Fig. 47, in which the ranges in the corrosion rates (in  $\text{mg}/\text{dm}^2\cdot\text{day}$ ) for the various toroids have been plotted against the solution velocity. The simplest relationship between the corrosion rate and the solution velocity appears to be one of direct proportionality, as shown in the figure by the dashed lines. A more complicated dependence may exist, which perhaps may become apparent when more precise results are obtained. At the present time, however, a simple linear relationship seems to express the data adequately for the large

dispersion in results so far obtained.

The one- and two-pin toroid results are of interest because there appear to be at least three distinct kinds of attack on the pins as the velocity increased. At very low velocities (represented by the data at 2.8 fps) there was no flow pattern on the pins and they were uniformly covered with a black adherent film. At higher velocities (from at least 9.1 to 29.6 fps) the pins were relatively film-free and appeared to be identical to those obtained in the large-dynamic-loop tests, which started at somewhat higher velocities (above about 20 to 30 fps for 0.17 *m* uranyl sulfate at 250°C). The appearance of sample pins in this region appears to correspond to the "bare-metal" region described for the large dynamic loops. The maximum bare-metal corrosion rate obtained in the loops under these conditions is about 1400  $\text{mg}/\text{dm}^2\cdot\text{day}$  ( $\sim 250$  mpy). The third region occurred at the greatest velocity investigated (38.6 fps). Here the pins were not only film-free but their front surfaces were badly abraded and polished.

The results obtained in the four-pin toroid are somewhat different from those obtained in the one- and two-pin toroids, in that no abrasion was observed at the highest velocity. At very low velocities the sample pins were covered with an adherent black film. As the velocity was increased, only the typical bare-metal attack was observed, and there was no evidence of abrasion at 38.6 fps, as was observed in the other toroids.

The differences in the slopes of the curves in Fig. 47 for the one-, two-, and four-pin toroids (or at least the apparent general lowering of the corrosion rate with increasing number of pins) may possibly be due to a turbulence effect. High-speed photography of water in Lucite toroids at room temperature has shown that gas dispersion in the liquid phase is greater with four pins present than with either one or two pins. Hence the character of the circulating liquid "slug" does seem to change with the number of pins present; this difference may have an effect on the corrosion behavior.

A substantial quantity of a black precipitate was present at the end of almost every run. This material was shown by X-ray diffraction to be composed of more than 90%  $\text{Fe}_2\text{O}_3$ , and wet chemical analyses generally indicated that about 2 to 10% uranium was also present. From the

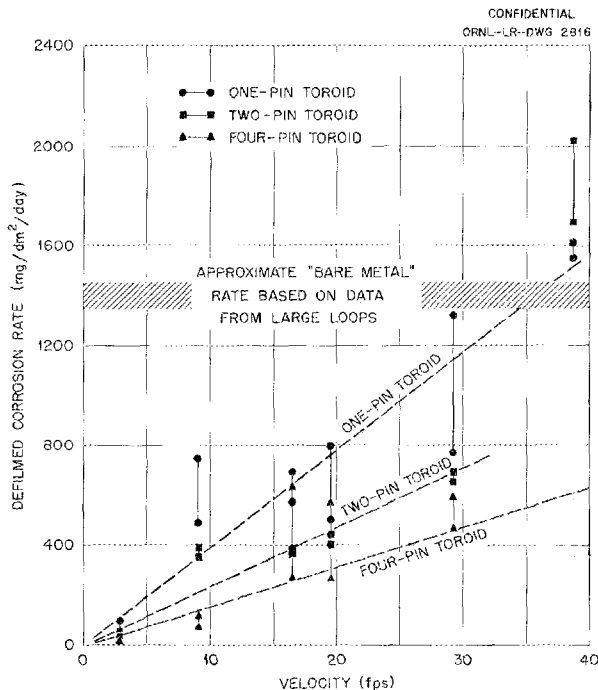


Fig. 47. Corrosion Rate from Toroid Data of Type 347 Stainless Steel as a Function of the Solution Velocity of 0.17 *m* Uranyl Sulfate at 250°C and 430 psi Oxygen Pressure (Run Duration, 100–500 hr).

weight loss of the sample pins, the amount of  $\text{Fe}_2\text{O}_3$  that was possibly present from this source can be estimated. As much as about 200 mg of  $\text{Fe}_2\text{O}_3$  could have been present from corrosion of the sample pins in the 21-ml volume of uranyl sulfate used in each of the toroids.

The appearance of the pins from the one- and two-pin toroid runs at 38.6 fps indicated a severe attack, as shown by the severe abrasion. There seemed to be an intensification of the attack on the pin at its root, where suspended solids would be expected to concentrate because of the centrifugal action of the rotation. Although the term

"abrasion" has been used, there was no indication of the mechanism of the attack; "erosion-corrosion" may describe the effect as well.

These velocity experiments with toroids suggest that the presence of suspended insoluble corrosion products of the stainless steel, as well as gas dispersion, may exert a very great effect on the corrosion of type 347 stainless steel in some circulating systems. The effect may not be apparent in the large-scale dynamic loops, since the arrangement of the sample holders serves as a filter for that system. This effect will be carefully considered in subsequent work.

Part IV

ENGINEERING DEVELOPMENT



## DEVELOPMENT OF FUEL-SYSTEM COMPONENTS

C. B. Graham

J. S. Culver	C. C. Hurtt
A. B. Daffron	R. J. Kedl
D. M. Eissenberg	W. B. Krick
K. E. Estes	R. G. Meza, Jr.
C. H. Gabbard	W. L. Ross
L. F. Goode, Jr.	I. Spiewak

### RECOMBINER DEVELOPMENT

I. Spewak      D. M. Eissenberg

The assembly of the high-pressure recombiner loop<sup>1</sup> was completed during this quarter. The electrical control circuits and the electrolytic cell-power circuit should be completed shortly.

Preliminary leak testing is under way; no serious leaks are present. Operation of the water jet at pressures up to 300 psi reveals that the maximum gas-flow rate is well above that required for loop operation.

Preoperational testing is being continued. It is expected that full operation can be started upon completion of the electrical circuits.

### SMALL REACTOR COMPONENTS

#### Allis-Chalmers 500-gpm Pump and 20-cfm Gas Circulator

W. L. Ross      R. J. Kedl

Allis-Chalmers Mfg. Co. has completed preliminary designs for a 500-gpm canned-rotor pump and a 20-cfm canned-rotor gas circulator.<sup>1</sup> The preliminary design and the Allis-Chalmers proposal have been evaluated. Negotiations have begun on a contract covering detail design and fabrication of one pump and its associated test loop and one gas circulator and its associated test loop. Also, Allis-Chalmers will perform a few hundred hours of operational testing on both the pump and the gas circulator.

#### ORNL Gas Circulator

W. L. Ross      R. J. Kedl

The ORNL 5-gpm pump has been converted, with minor modifications, to a high-suction-pressure, canned-rotor gas circulator. A reverse thrust bearing was installed so that the circulator will operate in a vertical position with the motor placed

end down, rather than in the normal horizontal position. This enables the bearings and rotor chamber to be run completely submerged in water at all times while the impeller circulates gas. Figure 48 is a characteristic curve of the circulator when operating with the ORNL pump impeller at the nominal synchronous speed of 3600 rpm. The conditions of the test were nitrogen gas at 73 psig and room temperature.

In the future it is planned to redesign the impeller in order to increase the capacity. Also, runs of higher frequencies are planned to determine whether higher developed heads and higher capacities can be attained satisfactorily.

#### ORNL 5-gpm Pump

W. L. Ross      C. C. Hurtt  
A. B. Daffron

The operating endurance test of the ORNL 5-gpm

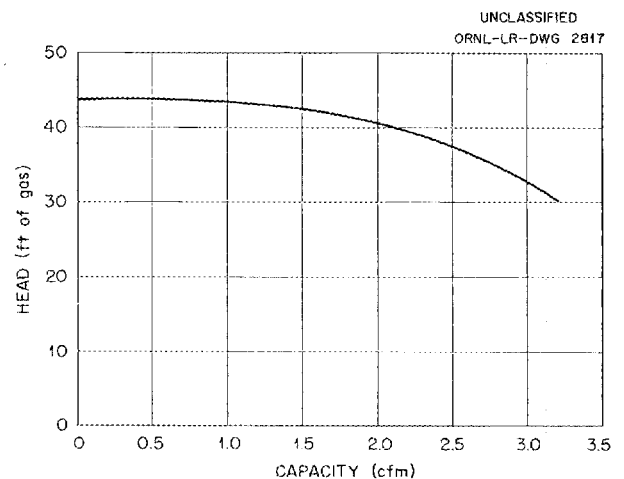


Fig. 48. Characteristic Curve for ORNL Blower. Speed, 3600 rpm (nominal); impeller, standard for ORNL pump; test conditions,  $N_2$  at 73 psig; electric current, 13.5 amp through entire test range.

<sup>1</sup>C. B. Graham *et al.*, *HRP Quar. Prog. Rep. Apr. 30, 1954*, ORNL-1753, p 53-58.

## HRP QUARTERLY PROGRESS REPORT

pump to determine the life expectancy of the various parts has continued. At this time, one pump has run for a total of about 2700 hr while circulating water at a temperature of 250°C. The pump has accumulated 2100 hr with the water exposed to a superpressure of helium and 600 hr with water exposed to oxygen pressure. One hundred start-and-stop operations were accumulated during one short test period, and additional ones occurred during the 2700 hr of run time.

The pump has been disassembled and examined after 100, 1100, 2100, and 2700 hr. None of the examinations revealed any unusual or severe wear on any of the pump parts. The radial- and thrust-bearing surfaces appear to be in very good condition, with only light burnish marks showing on the Graphitar No. 14 bearing and the chrome-plated journal.

The pump stator used in these tests has operated for a total of 4600 hr without failure. This stator has Class A insulation on the windings and is cooled with copper water coils embedded in the stator iron laminations.

The pump will continue on endurance-test operation, as described above, with water exposed to oxygen pressure.

### LARGE REACTOR COMPONENTS

#### 50-Mw Main Fuel Heat Exchanger

W. L. Ross      L. F. Goode  
K. E. Estes

Negotiation of a contract covering development, design, and fabrication of a fuel heat exchanger and a gas condenser is expected to be completed shortly. In the meantime, design and development are proceeding.

The Foster Wheeler-ORNL 50-Mw design study reported previously<sup>1</sup> is nearing completion. When cost estimates are complete, a comprehensive report will be issued.

In the tube-joint welding development program at Foster Wheeler Corp. a sound, high-ferrite root pass deposited by bare wire filler has been developed. Effect is being concentrated on depositing lower ferrite overlays to protect the root pass from the fuel solutions. A high ferrite content in the root pass is required to prevent cracking. Corrosion studies of the weldments is being conducted in order to determine permissible ferrite contents.

All tube-joint welds are now being made with the manually operated Heliarc torch mechanism, shown

in Fig. 49, which maintains a constant electrode position and arc length as well as a controlled arc distance from the tube wall. Filler wire is inserted in the form of preplaced rings. Typical single-pass welds are shown in Fig. 50.

The various tube-testing techniques involving the use of such instruments as the Reflectoscope, Probolog, magnetic analyzer flow detector, Bore-scope, X ray, and modified fluoroscope are being investigated. It is expected that tubing manufacturing, testing, and inspection specifications will be complete within the next three months.

#### Large Heat Exchanger

W. L. Ross      L. F. Goode  
K. E. Estes

Foster Wheeler Corp. is undertaking a study to determine the largest practicable heat exchanger which can be made with reasonable economy. Tentative designs have been worked out up to a capacity of 250 Mw. The study to date has been

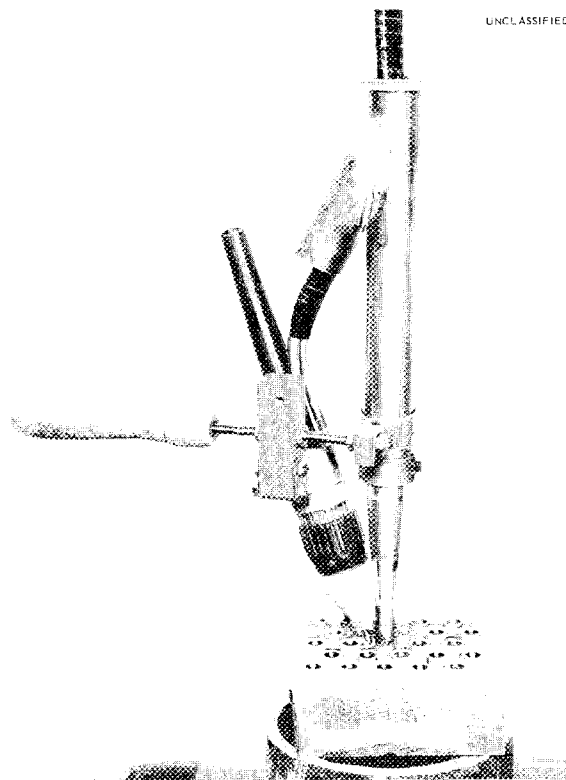


Fig. 49. Manually Rotated Heliarc Torch Mechanism.

UNCLASSIFIED

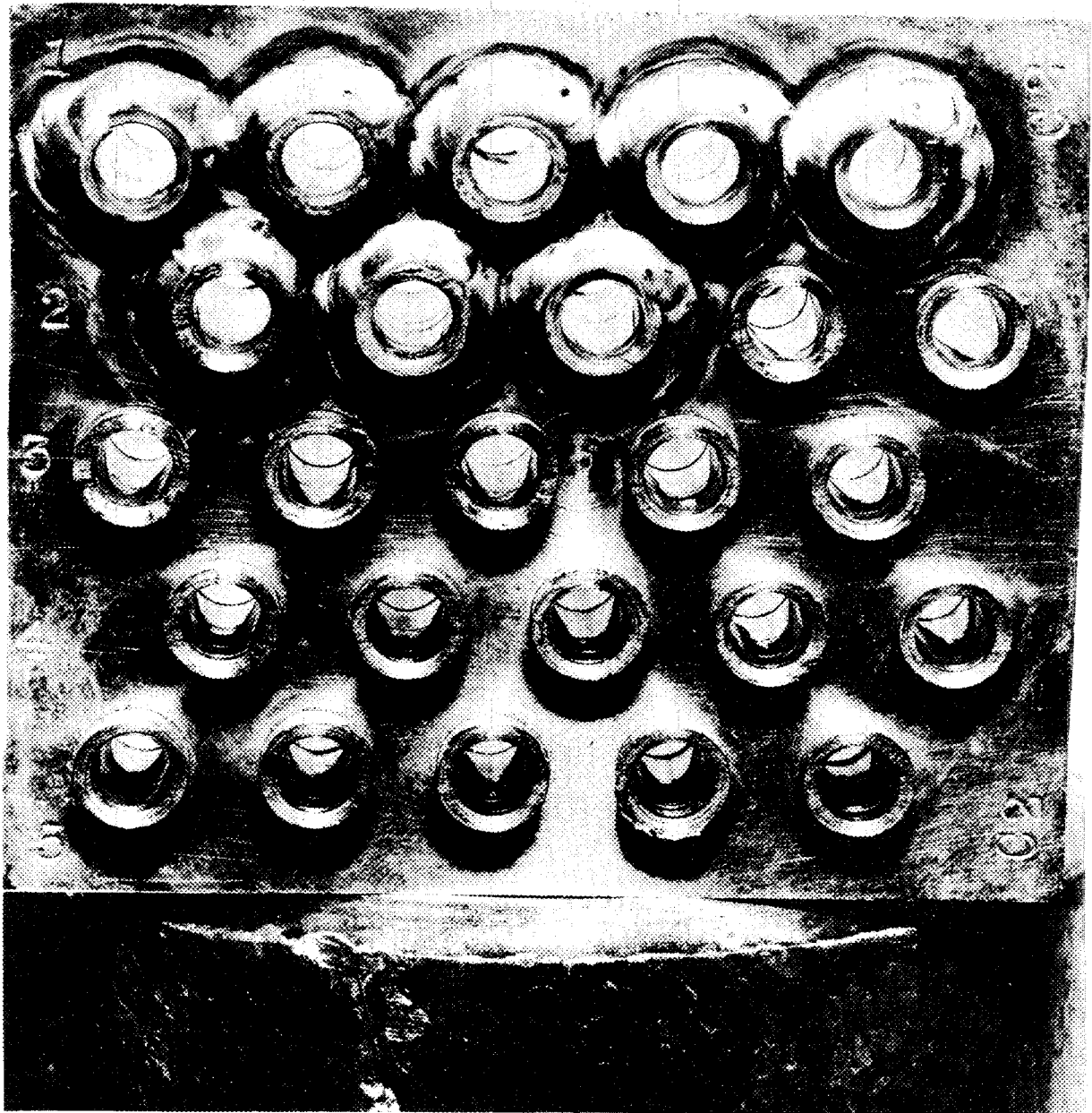


Fig. 50. Typical Single-Pass Welds Made with Manually Rotated Heliarc Torch.

## HRP QUARTERLY PROGRESS REPORT

limited to a single-pass, straight, fixed-tube-sheet heat exchanger.

### Main Gas Condenser

W. L. Ross      L. F. Goode

K. E. Estes

The basic design of the main gas condenser, as submitted by Foster Wheeler Corp., is shown in Fig. 51. No further work is being done on the unit at the present time.

### 4000-gpm Loop

J. S. Culver      R. Meza

C. H. Gabbard      W. B. Krick

By adding an 8-in. oil-diffusion pump to the vacuum system it was possible to reduce the pressure in the large pump loop to 4 to 6  $\mu$ . This materially increased the sensitivity of the helium leak detector and has revealed leaks not previously discovered.

Systematic leak hunting, followed by retightening

of the O-ring flanges where necessary, has produced a system of 6-, 8-, and 10-in. flanged pipe sections in which no leaks have been detected; one joint, however, has not yet been rechecked after it was tightened.

Calibration with a standard leak on the system showed a scale deflection of 4.0 on the leak detector for a 3.54  $\mu/\text{ft}^3/\text{hr}$  leak. Since the HRT leak specification is approximately 0.1  $\mu/\text{ft}^3/\text{hr}$ , leaks of this magnitude on the system would be detected.

Spare O-ring gaskets are being gold plated in an effort to make tight joints more easily. They will be tested either in the large loop or on other large equipment to be constructed.

Actual operation of the loop has been delayed in order that leak hunting techniques may be perfected and personnel may be trained in the use of the necessary equipment. As soon as some small accessory lines can be made tight, the loop will be hydrostatically tested and then prepared for operation.

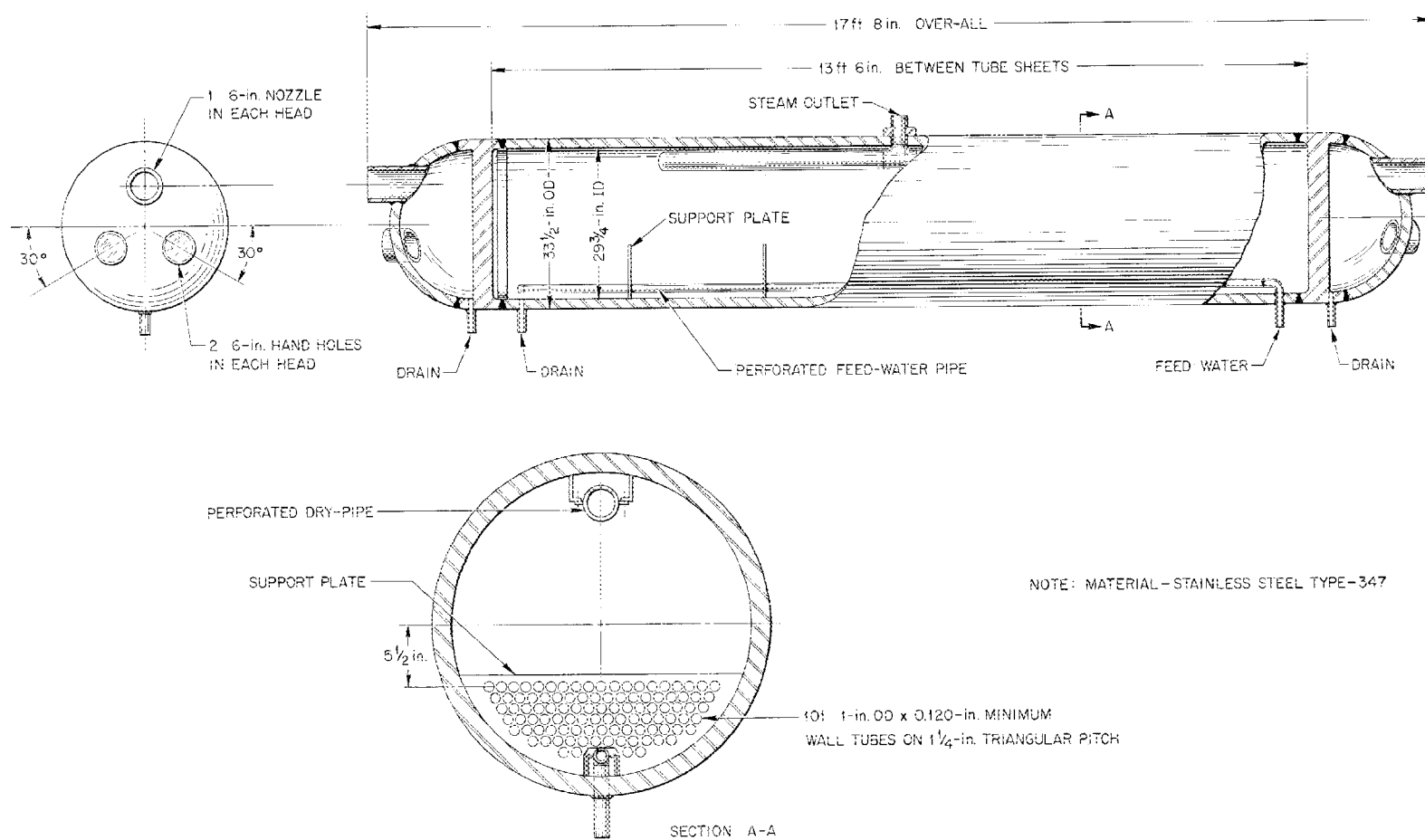


Fig. 51. Main Gas Condenser.

DEVELOPMENT OF BLANKET-SYSTEM COMPONENTS

R. N. Lyon, Section Chief  
 A. S. Kitzes, Group Leader  
 S. G. Bankoff<sup>2</sup>            W. Q. Hullings  
 P. R. Crowley            C. G. Lawson  
 R. B. Gallaher           S. A. Reed  
 C. B. Graham, Section Chief  
 I. Spiewak                R. Goodman  
 J. A. Hafford

CIRCULATING-LOOP TESTS

The two previously described<sup>3</sup> Loops, S and T, were in operation under various combinations of environmental conditions, additives, and types of thorium oxide. In all runs the Graphitar bearings of the pumps were continually lubricated with water (obtained as condensate from the pressurizer); both the front and back bearings showed slight wear after 2050 hr of continuous operation but are still in use. Careful dynamic balancing of the pump impeller and rotor and replacement of the stainless steel wear rings and thrust pads with titanium are considered to have assisted in prolonging the life of the bearings.

Effect of Oxygen on Erosion-Corrosion  
 Attack by ThO<sub>2</sub> Slurries

In run S-49, a slurry of thorium oxide containing approximately 400 g of thorium per kilogram of water was circulated in Loop S at 250°C for 1455 hr. During the first 1000 hr of the run a concentration of about 500 ppm of oxygen was maintained in the aqueous phase. The oxygen concentration was maintained by an oxygen partial pressure of 20 to 25 psi which was introduced into the cooled pressurizer at the beginning of the run and whenever the loop was shut down. Condensed steam from the pressurizer, which was injected at the motor end of the pump, contained enough dissolved oxygen, as shown by periodic analysis of slurry samples, to maintain the indicated concentration. It is believed that diffusion of oxygen down through the pressurizer contributed very little toward maintaining the oxygen concentration in the circulating system because of the net upward flow of water below the surface and of steam above the

surface. The thorium oxide was prepared by calcination of thorium formate at 650°C. The analytical and other data relating to loop operation during the run are presented in Table 26 and the changes in the Fe:Th and Cr:Th ratios are shown graphically in Fig. 52.

Just prior to run S-49 the system was pretreated by water containing 500 ppm oxygen being circulated at 250°C for 97 hr in the hope that a protective oxide film would be produced on the stainless steel components before they were exposed to attack by the circulating slurry.

After 567 hr of operation, run S-49 was interrupted for examination of the pump. All the pump parts, including the impeller, appeared to be unaffected except for the formation of a golden-brown film. The impeller had lost only 1 g in weight during this period of the test. The bearings showed no evidence of wear, and the dynamic balance of the pump had not changed.

After this examination the loop was reassembled and reloaded with the same slurry (plus an additional 1050 g of oxide to make up for mechanical and sampling losses). The operation was then resumed with an oxygen concentration of 500 ppm in the aqueous phase. At the end of 1000 hr of total operation, or 446 hr after the first shutdown, the loop was cooled to room temperature and the oxygen released from the pressurizer; then circulation was re-established at 250°C to determine whether the removal of the oxygen would lead to the rapid attack on stainless steel in high-velocity regions which had been characteristic of previous runs.

Run S-49 was arbitrarily ended after 441 hr of operation without oxygen, or a total of 1459 hr for the entire run. At this point analysis indicated that there was about 35 ppm O<sub>2</sub> in the slurry. Examination of the pump showed the presence of

<sup>2</sup>Research participant.

<sup>3</sup>R. N. Lyon *et al.*, *HRP Quar. Prog. Rep. Oct. 31, 1954*, ORNL-1658, Fig. 82, p 128.

TABLE 26. CIRCULATION OF ThO<sub>2</sub> SLURRIES CONTAINING O<sub>2</sub> AT 250°C WITH WESTINGHOUSE 100A PUMP, RUN S-49

Oxide prepared from thorium formate

Sample No.	Circulation Time (hr)	Solids (based on solvent)							pH (slurry)	Filtrate		
		Th (g/kg)	Fe (ppm)	Ni (ppm)	Cr (ppm)	Ti (ppm)	mg of Fe per g of Th	mg of Cr per g of Th		Fe (ppm)	Ni (ppm)	pH
0	1.5	476	30.9	7	24.6		0.065	0.052	8.2	1	1	6.05
1	18	395	65	11.5	167		0.165	0.423	6.8	1	1	6.08
2	42	374	107	25	270		0.286	0.775	6.0	1	2	5.8
3	66	361	133.5	23.4	290		0.370	0.805	5.3	1	3	5.6
4	90	341	160	25.0	247		0.470	0.82	5.0	1	4	5.08
5	162	335	220	29.2	128		0.657	0.38	4.4	1	5	4.8
6	234	370	285	38.5	102		0.770	0.392	4.18	1	6	4.43
7	330	376	338	30.5	75		0.90	0.199	3.97	1	7	4.29
8	427	355	320	31.3	72.5		0.90	0.24	3.78	1	4	3.93
9	429 <sup>a</sup>	450	264	32.6	204		0.585	0.453	5.10	1	4	4.9
10	518 <sup>b</sup>	276	232	28.3	58.5		0.840	0.212	3.99	1	4	4.23
11	523 <sup>b</sup>	290	253	29.4	55.3		0.874	0.190	4.03	1	4	4.45
12	567 <sup>c</sup>	475	368	47.2	107.2		0.775	0.226	4.20	1	6	4.86
13	568	429	312	44.0	205		0.730	0.480	4.63	1	6	4.39
14	575	560	331	40.3	219	44	0.590	0.390	7.25	1	1	5.40
15	589	600	368	48.0	322	34	0.613	0.538	7.05	1	1	4.9
16	609	438	305	41.0	138	34	0.695	0.315	6.30	1	2	5.1
17	632	381	293	43.0	132	36	0.740	0.346	5.80	1	3	5.2
18	750	384	370	44.0	24.4	59	0.965	0.064	5.16	1	6	5.3
19	822	385	392	21.6	33.2		1.02	0.086	4.75	1	6	4.9
20	918	380	426	22.2	41.0	39	1.02	0.108	4.0	1	7	4.3
21	1014 <sup>d</sup>	406	438	17.6	44.7	51	1.07	0.110	4.0	1	5	4.4
22	1016	565	538	9.85	166	39	0.95	0.294	4.45	1	6	4.4
23	1083	485	500	60.0	85.7	48	1.03	0.177	4.65	1	7	5.15
24	1155	465	519	58.4	73.0	51	1.11	0.157	4.53	1	7	5.13
25	1275	465	555	65.0	77.5	55	1.19	0.167	4.35	1	2	4.80
26	1415	465	550	68.3	113.7	31	1.18	0.244	4.55	1	9	6.2
27	1459	336	423	47.9	70.0	31	1.25	0.208	4.4	1	6	4.7

<sup>a</sup>Additional 1000 g of ThO<sub>2</sub> added to make up for depletion of solids due to sampling.

<sup>b</sup>Erratic operation of loop due to leaks in gas system; loop shut down repeatedly to repair leaks.

<sup>c</sup>Loop shut down for inspection of pump components; 1050 g of ThO<sub>2</sub> added upon start-up.

<sup>d</sup>Oxygen removed from system.

SECRET  
ORNL-LR-DWG 2819

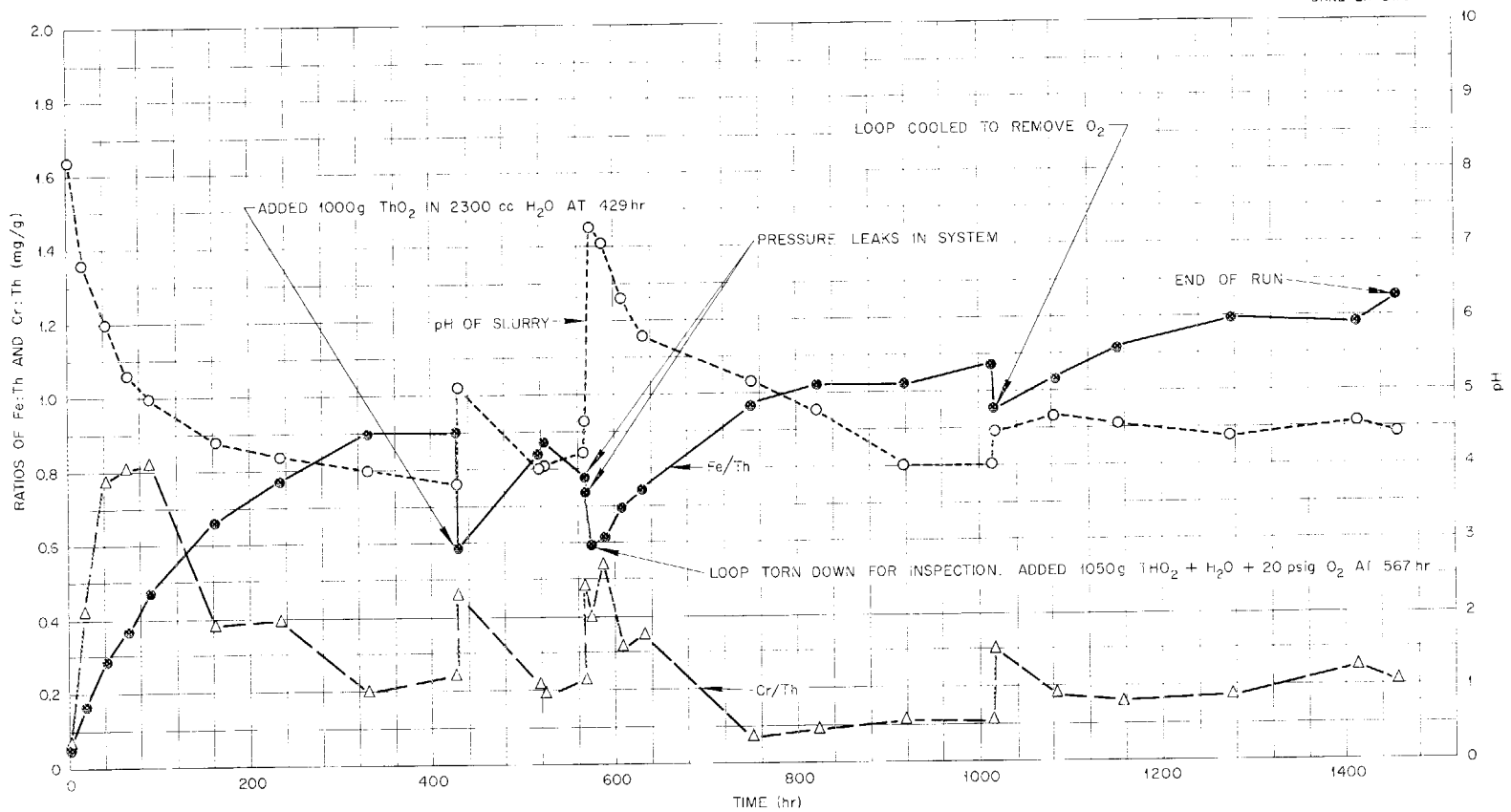


Fig. 52. Changes in Fe:Th and Cr:Th Ratios During Run S-49.

a dark-brown film on all parts except for the periphery of the impeller, where the film had apparently been removed. The impeller had lost only 2 g in weight during the last 887 hr of the run. The larger weight loss of the impeller can probably be accounted for by the complete removal of the brown film from the areas at radii greater than seven-eighths the distance from the axis to the edge. Since the maximum circumferential speed of the impeller at 3450 rpm is 120 fps, the critical velocity for film removal in the absence of oxygen during the final 441 hr of the run was approximately 100 fps. A stainless steel orifice plate, through which the slurry passed with a velocity of approximately 80 fps, was only slightly attacked in the throat and was covered with a brown film (Fig. 53) and had gained 59 mg in weight during the entire run. A chromium-plated stainless steel venturi tube had been included in the loop system downstream of the pump, with a  $\frac{3}{8}$ -in.-dia

type 347 stainless steel rod suspended axially in the tube by means of two spiders. This arrangement provided a velocity gradient along the rod. After the run the rod was covered with a brown film and had lost about 140 mg in weight, but showed no evidence of pitting. The film in the high-velocity ( $\sim 45$  fps) region of the rod appeared to be thinner (by visual observation) than that over the lower-velocity regions. The titanium impeller hubs showed no wear, although the inside diameter of the titanium wear rings increased 0.005 in. It is not established whether this increase was caused by the attack of slurry moving under a 250-ft head at the wear rings or by damage to the rings during disassembly of the pump.

Interpretation of the results of run S-49 suggests that a major improvement in resistance to slurry attack has been achieved through the pretreatment, choice of slurry, or oxygenation during the run, or through some combination of these three. Chemical

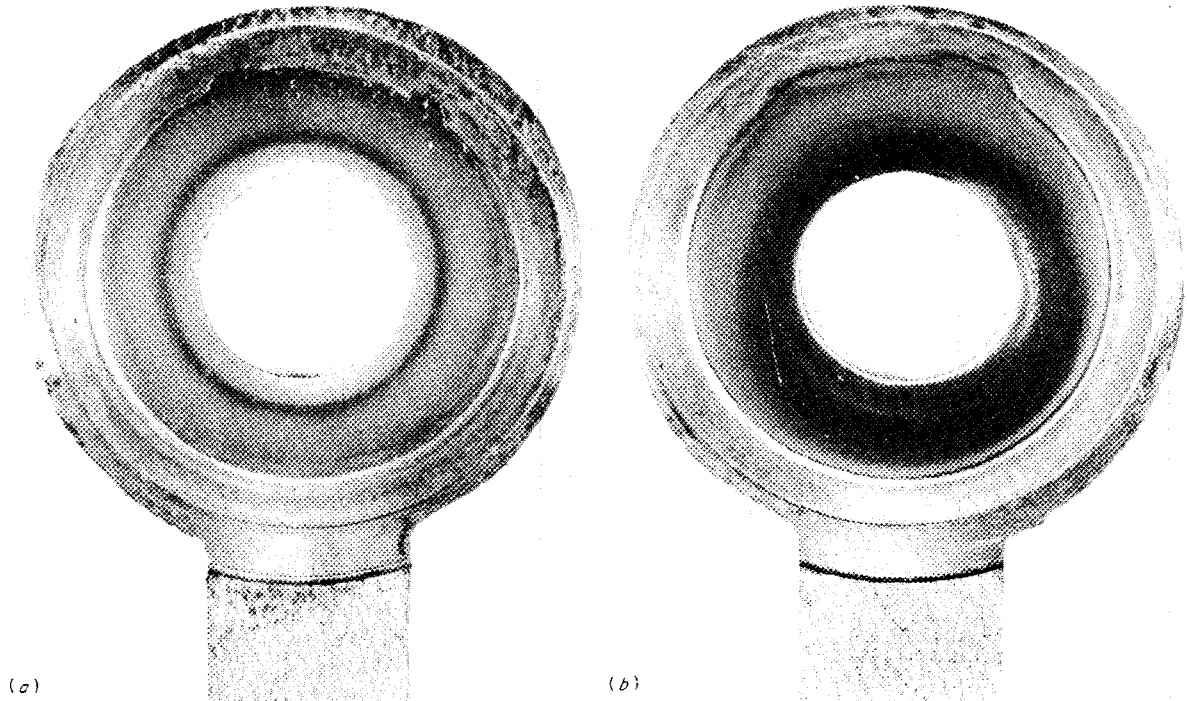
SECRET  
PLATE 1207-2SECRET  
PLATE 1207-1

Fig. 53. Oxygen Effect on Orifice Plate of Flow Restrictor after 1455 hr of Operation with  $\text{ThO}_2$  Slurries at  $250^\circ\text{C}$  (Run S-49). (a) Upstream face showing film formation. (b) Downstream face. 2.2X. Reduced 31.5%.

and metallographic examination of the brown film is now in progress. Reference to Table 26 reveals that the initiation and each interruption of the course of the run were followed by short periods of changing thorium concentration but that each of these periods was followed by a relatively long period of substantially constant concentration as determined by samples. Reference to Fig. 52 shows that the Fe:Th ratio in the solids (taken as an indication of attack on the stainless steel, since the aqueous phase showed no build-up of Fe; the brown film on the metal parts of the system represents additional corrosion products not shown by this ratio) leveled off after 300 hr of operation. The additions of fresh thorium oxide and the removal of oxygen caused well-defined changes in the pH of cooled slurry samples and in the Fe:Th ratio and the Cr:Th ratio of the solids. A very interesting correlation appears in these data. Except for the first few days, the Cr:Th ratio and the room temperature pH of the slurry behave in a very similar fashion, while the Fe:Th ratio varies in exactly the opposite manner. Thus when the pH is high (usually following the addition of fresh  $\text{ThO}_2$ ), the Cr:Th ratio is high and the Fe:Th ratio is lower than would be predicted by the addition of unadulterated  $\text{ThO}_2$ . Conversely, when the pH is low, the Cr:Th ratio is low and the Fe:Th ratio is high. In general, it appears that when about 500 ppm of  $\text{O}_2$  is in the slurry, the pH tends gradually toward a value of about 3.5 to 4, the Cr:Th ratio tends toward about 0.1 to 0.2 mg/g, and the Fe:Th ratio tends toward about 0.9 to 1 mg/g. The chromium content of the solids, identified by means of a test with diphenyl carbazide, was found to be, at least in part, adsorbed chromate ions. The results of a previous run, T-29, suggested that the attack on stainless steel was reduced by the presence of chromate ions, and that with the disappearance of the chromate ions there was an increased attack on the stainless steel. During that run, a slurry of Ames oxide (176 g of Th per kilogram of  $\text{H}_2\text{O}$ ) which contained 100 ppm of chromate was circulated in the absence of oxygen after the loop had been descaled with  $\text{HNO}_3$ -HF and pretreated with a solution of 100 ppm of chromate to form a protective film.

Runs T-35 and T-39 were carried out with a different preparation of thorium oxide in order to determine whether the effect of oxygen was reproducible. Oxide manufactured by the Lindsay

Light & Chemical Co. (Lindsay oxide) was used. This oxide had been prepared by calcination of thorium oxalate at  $950^\circ\text{C}$ . As a preliminary test in the absence of oxygen, run T-35 was started with a concentration of 418 g of thorium per kilogram of water at  $250^\circ\text{C}$ . After only 68 hr the run was stopped because of excessive build-up of corrosion products as measured by the Fe:Th ratio in the solids. The pH of the slurry was 8.0; addition of 0.015 M  $\text{H}_3\text{PO}_4$  to the slurry did not lower the measured pH. Although the impeller lost 21 g in weight during this period, it remained shiny and there was no evidence of severe pitting. The analytical data for run T-35 are given in Table 27.

A subsequent run, T-39, was conducted in a manner similar to that of run S-49. A pretreatment of the loop with oxygen and water at  $250^\circ\text{C}$  for 92 hr was followed by a 311-hr circulation of a slurry of Lindsay oxide at a concentration of 250 g of thorium per kilogram of water. The results of this run are shown in Table 28 and in Fig. 54. The initial pH of the slurry was about 9 instead of about 8 as in run S-49. The initial rate of increase of the Fe:Th ratio for runs T-35 and T-39 was quite rapid (about 3 mg/g in the first 100 hr compared with about 0.5 mg/g for run S-49). In run T-39 the pH of the slurry had reduced to about 5.5 in about 240 hr, and in about 200 hr the Fe:Th ratio appeared to have leveled off at about 5 mg/g; in run T-35 the Fe:Th ratio reached

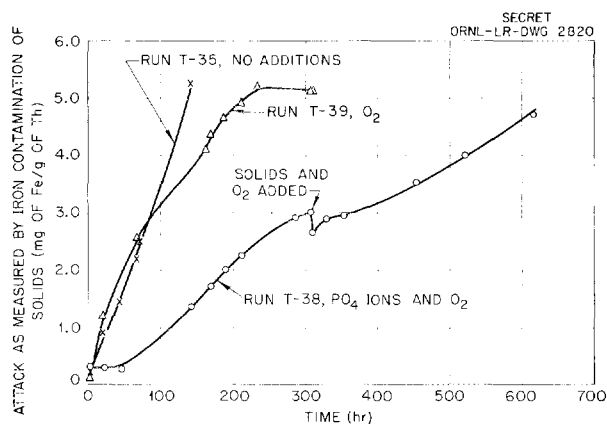


Fig. 54. Influence of Phosphate and Oxygen Additions upon Attack by  $\text{ThO}_2$  Slurries Circulated at  $250^\circ\text{C}$ . The oxide was prepared from thorium oxalate (Lindsay).

TABLE 27. CIRCULATION OF THORIA SLURRIES\* AT 250°C WITH WESTINGHOUSE 100A PUMP

Run No.	Circulation Time (hr)	Solids (based on solvent)							Filtrate				
		Th (g/kg)	Fe (ppm)	Ni (ppm)	Cr (ppm)	Po <sub>4</sub> <sup>3-</sup> (ppm)	pH	mg of Fe per g of Th	mg of Cr per g of Th	pH	Fe (ppm)	Ni (ppm)	Po <sub>4</sub> (ppm)
T-35-0	2	485	100	22	23		9.5	0.20	0.048	7.80	<1	<1	
1	21	523	470	29	120		8.60	0.90	0.230	7.63	<1	<1	
2	45	485	712	53	171		8.80	1.48	0.352	6.78	<1	<1	
3	69	389	850	90	158		8.75	2.20	0.410	6.90	<1	<1	
4	74	479	1200	140	294		8.73	2.50	0.614	7.54	<1	<1	
5	142	529	2930	480	740		7.62	5.50	1.400	6.75	<1	<1	
T-38-0	1	485	64	15	19	1780	3.55	0.13	0.040	3.61	<1	7	2
1	22	470	135	5	9	1650	4.68	0.29	0.024	4.72	<1	3	<1
2	46	513	132	11	22	1890	5.38	0.26	0.044	5.33	<1	1	<1
3	143	531	728	24	169	1950	6.20	1.36	0.332	6.22	<1	<1	<1
4	166	500	865	19	144	1870	6.39	1.73	0.482	6.31	<1	<1	<1
5	190	523	1040	21	192	1990	6.89	2.00	0.393	6.36	<1	<1	4
6	214	464	1055	20	291	2000	7.20	2.25	0.622	6.0	<1	<1	3
7	287	490	1435	22	330	1950	7.15	2.93	0.670	7.40	<1	<1	2
8	311	464	1460	20	322	1900	7.20	3.05	0.675	6.02	<1	<1	2
9	312**	532	1425	160	365	1930	6.50	2.67	0.690	6.28	<1	4	
10	330	532	1537	260	410	1962	5.52	2.90	0.770	5.73	<1	1	2
11	354	513	1515	270	373	1920	5.32	2.95	0.730	5.88	<1	<1	3
12	456	513	1825	300	182	2000	5.28	3.53	0.356	5.81	<1	<1	1
13	522	487	2020	350	220	1760	5.10	4.15	0.457	5.60	<1	<1	1
14	618	460	2180	377	215	1650	4.22	4.70	0.468	4.92	<1	<1	3

\*T-35: Lindsay oxide.

T-38: Lindsay oxide with H<sub>3</sub>PO<sub>4</sub> for 311 hr, then oxygen added.

\*\*Loop cooled to room temperature, 500 g of ThO<sub>2</sub> in 840 cc of H<sub>2</sub>O and 39.3 liters of O<sub>2</sub> added.

HRP QUARTERLY PROGRESS REPORT

TABLE 28. CIRCULATION OF LINDSAY ThO<sub>2</sub> SLURRIES WITH O<sub>2</sub> AT 250°C WITH WESTINGHOUSE 100A PUMP, RUN T-39

Sample No.	Circulation Time (hr)	Solids* (based on total solvent)							Filtrate		
		Th (g/kg)	Fe (ppm)	Ni (ppm)	Cr (ppm)	pH	mg of Fe per g of Th	mg of Cr per g of Th	pH	Fe (ppm)	Ni (ppm)
0	1	215	38	10	64	9.0	0.18	0.30	5.4	1	1
1	21	244	295	46	82	7.8	1.22	0.34	6.4	1	1
2	44	244	475	82	138	7.0	1.45	0.57	6.3	1	1
3	68	275	712	102	197	6.7	2.58	0.72	6.2	1	1
4	164	260	1070	164	227	5.7	4.1	0.87	6.6	1	2
5	170	223	974	163	196	5.7	4.35	0.88	6.0	1	1
6	188	227	1050	169	220	5.8	4.63	0.97	5.7	1	1
7	212	218	1070	165	225	5.8	4.90	1.03	5.7	1	1
8	236	209	1070	171	174	5.5	5.18	0.83	5.8	1	1
9	308	210	1070	178	202	5.0	5.10	0.96	5.8	1	1
10	311	210	1070	177	210	5.1	5.10	1.00	6.1	1	1

\*Apparent drop in solids concentration due to removal of solids during sampling.

5 mg/g in about 150 hr, when it was shut down because there was no indication of reduction in the rate of Fe:Th increase. In T-39 the pump impeller lost 10 g in weight and the orifice lost 300 mg, but neither was severely pitted.

Comparison of the chemical data with those obtained when UO<sub>3</sub> slurries containing dissolved oxygen and Na<sub>2</sub>HPO<sub>4</sub> were circulated at 250°C shows the same results.<sup>4</sup> In both cases the pH of the slurry was alkaline, 8 to 9, and the attack on the stainless steel was rather rapid. A solution of Na<sub>2</sub>HPO<sub>4</sub> with oxygen at 250°C produced the same effect as both the alkaline uranium and thorium slurries. A run (T-43) is now in progress in which the oxygen effect is being studied as a function of the pH of the slurry. The pH of a slurry prepared from Lindsay oxide has been lowered from 9 to 6 by the addition of sulfuric acid prior to loading in the loop.

The differences between the results from run T-39 and those from S-49 may also be due, in part, to greater hardness and greater resistance to comminution of the aggregates in the Lindsay oxide, which characteristics are inferred from the high firing temperature used in its preparation.

<sup>4</sup>R. N. Lyon et al., *HRP Quar. Prog. Rep. Mar. 31, 1953, ORNL-1554, p 120-125.*

A slurry containing approximately 500 g of thorium per kilogram of water as Lindsay oxide was circulated at 250°C for 618 hr (run T-38). Prior to being loaded in the loop, the oxide was washed with 0.01 M H<sub>3</sub>PO<sub>4</sub> at 70°C for 1 hr and then with distilled water to a pH of 4 for the slurry. Toward the end of run T-38, oxygen was added to determine its effectiveness in slowing down the attack. The data are presented in Table 27, and a comparison of the data is shown in Fig. 54. Photographs of the flow restrictors are shown in Fig. 55. The attack as measured by the Fe:Th ratio in each case shows the effect of phosphate and oxygen additions. In the data in Fig. 54, the oxygen effect was not apparent in the presence of phosphate ions.

**Slurry Attack on Carboloy and Stellite 98M2**

In the previous quarterly report<sup>5</sup> it was stated that stainless steel in straight pipes and elbows had shown little, if any, attack by Ames oxide slurries at flow rates below 20 fps. In regions of higher velocity, titanium, zirconium, gold, platinum, and Zircaloy-2 were relatively free from attack. In addition, two extremely hard and wear-

<sup>5</sup>R. N. Lyon et al., *HRP Quar. Prog. Rep. Apr. 30, 1954, ORNL-1753, p 157-172.*

SECRET

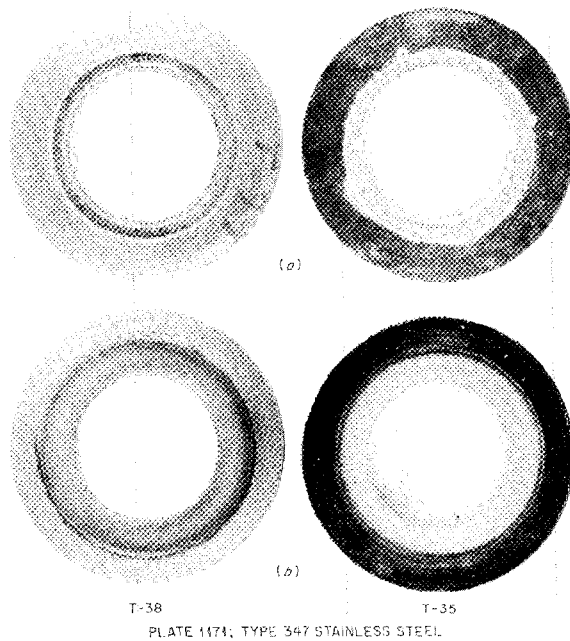


Fig. 55. Effect of Phosphate Ions on the Attack of Type 347 Stainless Steel by  $\text{ThO}_2$  Slurries at  $250^\circ\text{C}$ ; Run T-38 Operated for 618 hr with Phosphate, and Run T-35 Operated for 140 hr without Phosphate. (a) Upstream faces. (b) Downstream faces. 2X. Reduced 47%.

resistant alloys that have been tested are Carboloy (tungsten-carbide-base alloy) and Stellite 98M2 (cobalt-base alloy). Quartered sections of these and other metals, separated from each other with Teflon, were placed in a holder to form an orifice plate. The Carboloy, because of its brittleness and method of fabrication, was sintered into the desired quartered shape. The velocity through the orifice was approximately 80 to 90 fps. For each test run, Lindsay thorium oxide slurries, at about 400 g/liter without oxygen were circulated at  $250^\circ\text{C}$  for approximately 160 hr. The results of these tests are presented in Table 29. In run T-33 the Stellite 98M2 was most severely attacked (Fig. 56). In both runs T-33 and T-36 the chemical analytical data suggested that cobalt was being leached from the Stellite and the Carboloy. In the case of the Carboloy this permitted minute pieces of tungsten carbide to be circulated with the slurry. The Carboloy specimen was shattered in removal from the holder, and weight changes were not determined for it. Metallographic examination of the cobalt-base specimens may confirm the chemical analysis data as to the method of attack.

#### 5-gpm-Loop Construction

In order to be able to test the effects of a wide variety of oxides (laboratory-prepared samples)

TABLE 29. RESISTANCE OF CONSTRUCTION MATERIALS TO ATTACK BY  $\text{ThO}_2$  SLURRIES CIRCULATED AT  $250^\circ\text{C}$  WITH WESTINGHOUSE 100A PUMP

Run No.	Circulation Time (hr)	Th (g/kg)	Materials	Superficial Hardness (Rockwell)	Weight Change (mg)	Remarks
T-33	162	300	Crystal-bar zirconium	B-71	-17	Slightly pitted around opening
			Stellite 98M2	C-58	-247	Severely attacked on upstream face
			Titanium	B-83	-18	Slightly pitted on upstream face
			Type 347 stainless steel	B-80	-144	Severely attacked on upstream face
T-36	162	480	Carboloy	C-92		Evidence of attack; leading edge of opening became well rounded

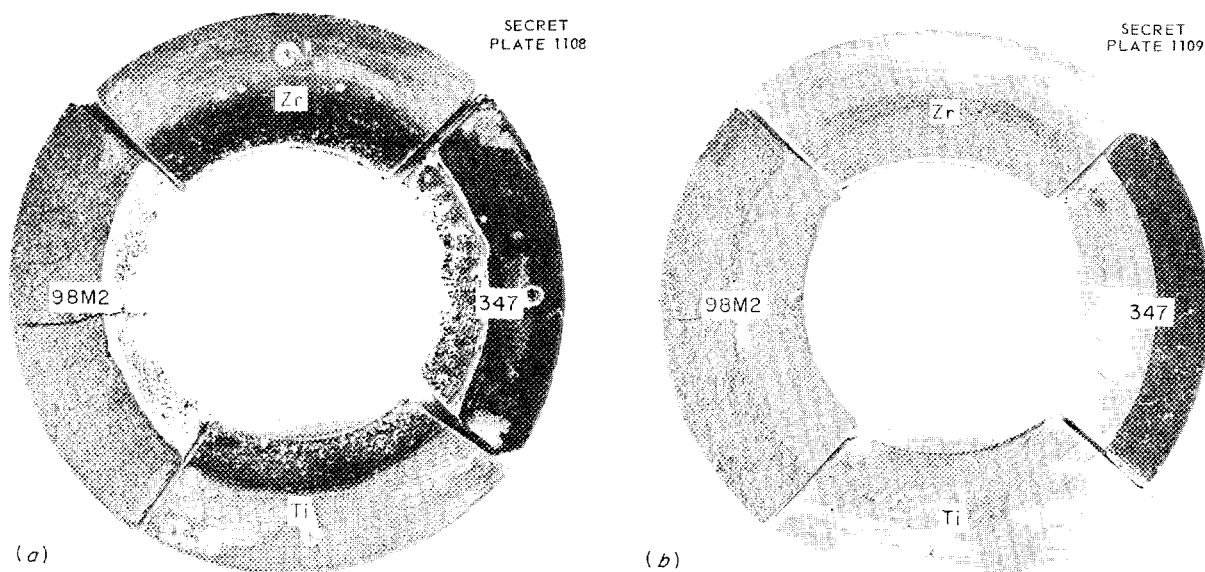


Fig. 56. Composite Flow Restrictor Showing Attack on Different Metals by  $\text{ThO}_2$  Slurries at  $250^\circ\text{C}$  for 160 hr (Run T-33). (a) Upstream face. (b) Downstream face. 2.5X. Reduced 19%.

under different environmental conditions, small loops have been designed which will require only 1 kg of solids for a concentration of 1000 g of thorium per kilogram of water. A 5-gpm ORNL pump<sup>6</sup> will be used to circulate the slurries. One loop is now in the stage of preliminary testing, and a second loop is about 90% complete. A loop to test the 5-gpm Allis-Chalmers hydrostatic-bearing pump is about 75% complete. Five other loops are in various stages of construction. Thus a total of eight small loops should be in operation during the next quarter.

#### 200-gpm-Loop Construction

A loop is now being constructed to test the Westinghouse 200A slurry pump which is a standard Westinghouse 150C pump redesigned at the wet end for use with slurries as shown by Fig. 57. The 150C and 200A pumps differ from the 100A model in that they have a Kingsbury thrust bearing to absorb all the thrust load of the rotor and impeller. The rotor and all bearings are isolated from the impeller by a labyrinth seal. In the 100A pump the balance of thrust forces is dependent upon the relative flow between the front and back weld pads.

<sup>6</sup>R. J. Kedl *et al.*, *HRP Quar. Prog. Rep. Jan. 1, 1953*, ORNL-1478, p 58.

The 200A pump is vertically mounted, suitable for top maintenance, and delivers 200 gpm of a fluid with density of 2 against a 100-ft head. The casing has been designed with inserts which can be removed and replaced with materials other than stainless steel.

A graphic representation of the loop is shown in Fig. 58. The velocity of the slurry through the straight runs of pipe will be 10 fps; velocities through the orifices (flow restrictors) will be less than 20 to 30 fps. The loop will be constructed of type 347 stainless steel.

#### HRT GAS-SEPARATOR SLURRY TEST

Successful tests of the plastic model HRT gas separator are described in the previous quarterly report<sup>7</sup> and in greater detail in a central files memorandum.<sup>8</sup>

After completion of the water runs, room-temperature thoria slurry has been circulated through the gas separator in concentrations up to about 150 g of  $\text{ThO}_2$  per kilogram of  $\text{H}_2\text{O}$ . Preliminary results indicate that although there is a definite concentration gradient in the rotational field of the

<sup>7</sup>C. B. Graham *et al.*, *HRP Quar. Prog. Rep. Apr. 30, 1954*, ORNL-1753, p 44-48.

<sup>8</sup>J. A. Hafford, *HRT Gas Separator*, ORNL CF-54-6-112 (June 14, 1954).

UNCLASSIFIED  
ORNL-LR-DWG 2821

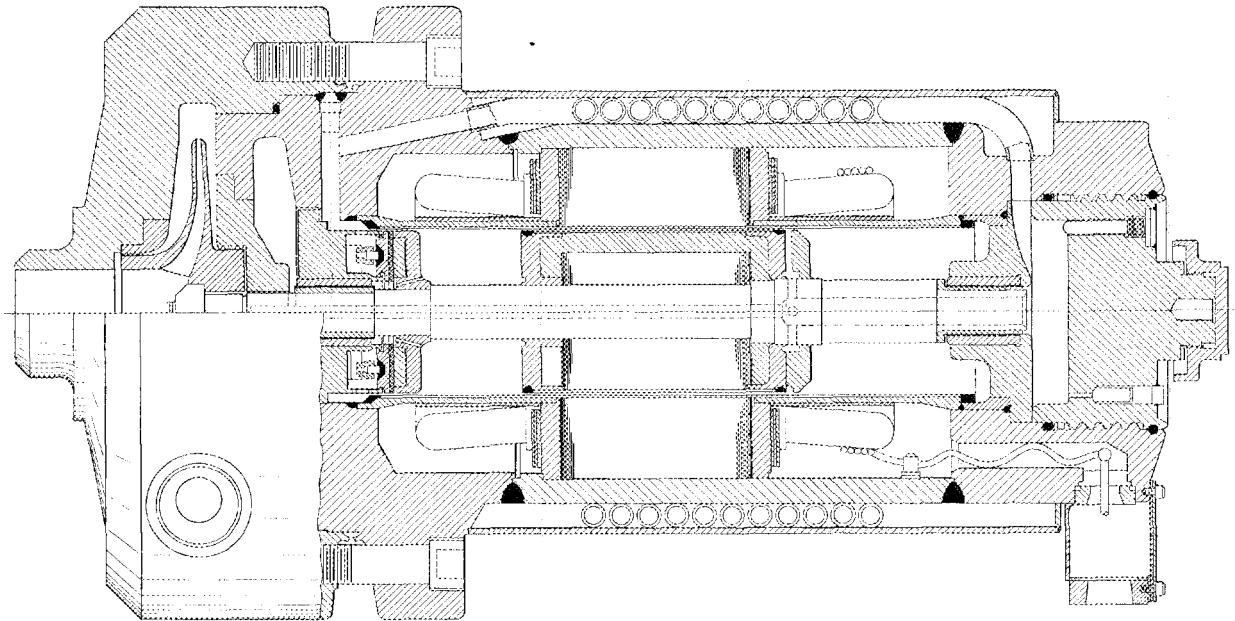
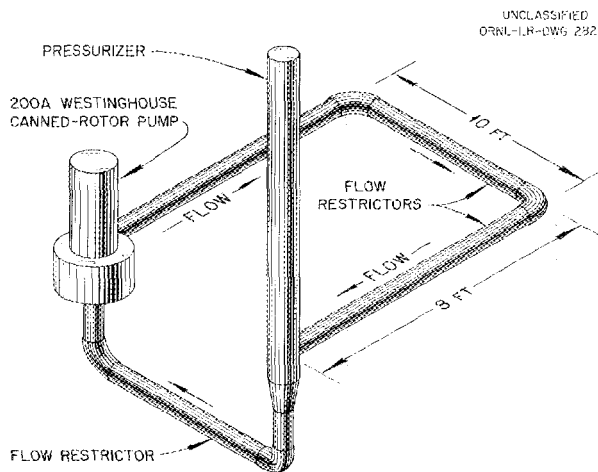


Fig. 57. 200A Vertical Slurry Pump.



UNCLASSIFIED  
ORNL-LR-DWG 2922

Fig. 58. 200-gpm Pump.

separator no thorium actually settles out. The concentration at the center of the separator is about 20% below that of the stream average.

Further runs will be made to determine the gas separating efficiency. Preliminary indications are that gas removal and the quantity of entrainment are about the same as those for water.

#### HIGH-PRESSURE ABRASION TESTER

The abrasion tester described previously<sup>5</sup> has been operated at 250°C for approximately 160 hr with a slurry containing 1000 g of thorium per kilogram of water. Upon completion of the test, the stainless steel disk, 1.496 in. in diameter, through which three 0.040-in. holes had been drilled on a 1-in. bolt circle, was found to be coated with a film on both faces. The holes were enlarged 0.002 in. on the diameter and the disk lost 53 mg in weight. The maximum velocity of the slurry through the opening was estimated at 50 fps. As soon as a few modifications are incorporated in the actuating system, a run will be made in which oxygen will be added to the slurry.

The stainless steel bellows have now been cycled 500,000 times at 250°C and are still in use.

#### SMALL-SCALE SLURRY BLANKET MOCK-UP

A system simulating the HRT pressure vessel is now being constructed for the study of the flow characteristics of slurries through such a system. Preliminary investigations in a plastic model indicate that although the slurry is homogeneous

**HRP QUARTERLY PROGRESS REPORT**

in flowing through the blanket mock-up, resuspension of solids after a shutdown and possible settling out of solids at the anticipated flow rate through the reactor of 0.05 fps may cause serious problems.

The system described in Fig. 59 consists of an 18-in. iron sphere in which a 9-in. iron core is suspended. The core will be steam heated to 150°C to simulate heat generation in the core of a reactor. Gas removal, effect of thermal convection on the slurry flow, and possibly some heat-transfer data can be obtained, in addition to flow characteristics being studied. It has been estimated that slurry velocities of 1 fps are obtainable with

a 40°F temperature drop from the core vessel to the colder slurry. If possible, utilization of these thermal-convection currents will be made to keep the solids suspended and scoured off the bottom of the vessel.

**FULL-SCALE HRT SLURRY BLANKET MOCK-UP**

Design of a mock-up of the slurry blanket for the HRT has been started by a group at K-25 for testing the operation of several of the major loop components with slurry. As currently conceived, the mock-up will consist of a 230-gpm canned-rotor pump, pressurizer-gas separator, three-tube heat exchanger with bypass choke, and gas let-

UNCLASSIFIED  
ORNL-LR-DWG 2823

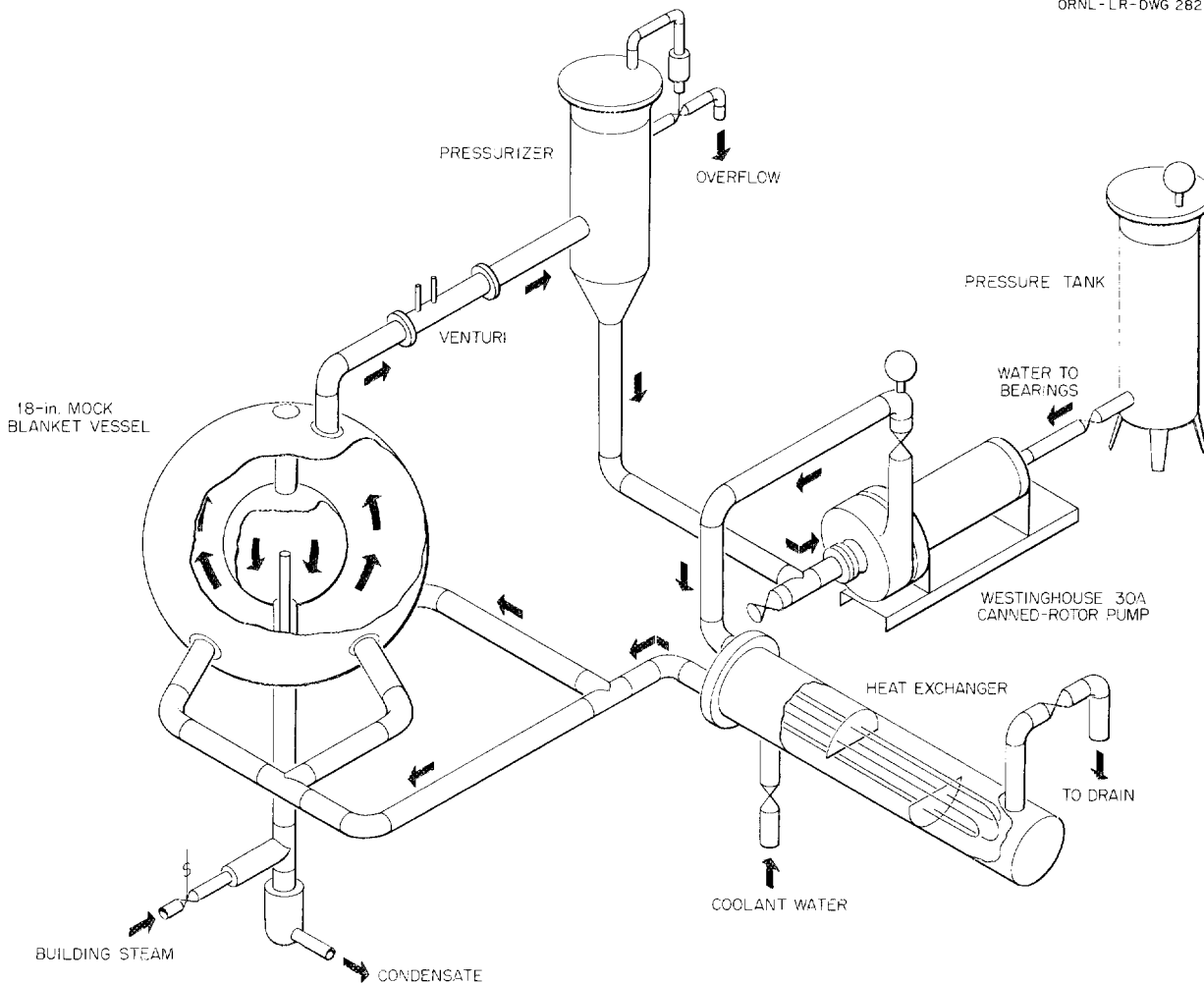


**Fig. 59. Model of HRT Blanket-Flow Test.**

down system, but it will not include a pressure vessel. The pressurizer-gas separator appears to present the major design problem in the slurry loop. Several designs have been conceived, but none can be considered as acceptable until completion of some currently planned experiments for obtaining a clear-cut picture of the ease or difficulty of separating gas from the slurry, entrainment problems, caking, etc.

One major decision still to be made is whether to use steam pressurization with a low-pressure recombiner or inert-gas pressurization with a high-pressure catalytic recombiner. If it is assumed that no suitable catalyst can be found to effect recombination in the slurry loop itself and that the off-gas must be diluted to less than explosive limits before being let down to low pressure, use of the high-pressure recombiner will result in a substantial gain in net power yield.

#### CAKING, PLUGGING, AND SEDIMENTATION PROPERTIES OF SLURRIES

##### Plugging of Pipes by Sedimentation

Preliminary tests with plugs deposited by centrifugal sedimentation were conducted in order to obtain a severe test. Slurries containing 1000 g of unpumped Lindsay thorium oxide per liter were placed in  $\frac{1}{8}$ - and  $\frac{1}{2}$ -in. IPS stainless steel nipples and centrifuged at about 1100 g for 30 min. The resulting cakes were blown out by air pressure, and the wall shear stresses at failure were computed to be 0.05 to 0.5 psi, with an average stress of about 0.1 psi. If a 1-ft plug deposited in a 0.2-in.-ID tube exhibited this average stress, a differential pressure of 24 psi would be required to cause it to flow.

The results were quite different with gravity sedimentation. After seven days of sedimentation the plug dropped out from the nipple under its own weight. This corresponds to a calculated shear stress of less than 0.01 psi. However, after evaporation of the supernatant liquid and drying of the plug over a period of 16 days, an average shear stress of 0.6 psi was recorded for three plugs. On the other hand, gravity-sedimented plugs heated in a muffle furnace to 500 to 800°C could be tapped out as a free flowing powder, indicating that the residual film of water is probably responsible for most of the cohesive strength of dried cakes of new thorium oxide.

##### Plugging of Pipes by Pumped Solids

A sample of slurry from run S-49 containing 0.7 g of thorium oxide per cubic centimeter was held at 20°C for 1 hr in a horizontal 7-ft length of  $\frac{1}{4}$ -in. stainless steel pipe. An air pressure of 5.1 in. Hg, corresponding to a wall shear stress of 0.03 psi, was required to initiate flow. A differential pressure of approximately 30 psi would be required with this material in a 0.2-in.-ID tube 40 ft long. This oxide had been produced by the formate process and was calcined at 650°C. Further testing under operating conditions would seem to be indicated.

##### Caking Phenomena in Loops

In the great majority of loop tests to date, caking has been negligible. Such small deposits as have been found when the circulating system was shut down have been easily removed by washing with water. Some solids have accumulated in the pressurizer, especially at the slurry interface; but they also have been easily removed with water. However, the potential importance of the caking problem focuses attention on the few earlier runs in which severe caking difficulties were encountered. In run T-14, the first thorium oxide run, the loop had been charged with solids containing 0.2 mg of nitrate and 4.9 mg of carbonate ion per gram of thorium oxide. This relatively impure material caked very badly, but the next run in Loop T, in which Ames oxide of much higher purity was used, was essentially free from caking. No caking difficulties were experienced for several runs thereafter. Before run T-21 was made, a titanium pump impeller was substituted for the stainless steel impeller, and the thorium content of the circulating slurry remained fairly constant for both run T-21 (20 hr) and run T-22 (108 hr). However, run T-23 in which titanium seal rings, orifice plate, and impeller were used had to be stopped after 68 hr because a strongly adherent cake formed on the pipe walls. Run T-24 showed similar results after 18 hr. The pump sounded noisier than usual, indicating cavitation or gas binding; and it was postulated that vortex formation due to improper positioning of an insert on the suction side of the pump had resulted in gas entrainment in the pump. Mechanical difficulties were experienced in runs T-25 and T-26; in runs T-27 and T-28, however, in which a titanium impeller and wear rings and a quartered

## HRP QUARTERLY PROGRESS REPORT

orifice plate were used, the thorium content of the circulating slurry again dropped rapidly, and an easily removed cake was found on the pipe walls after 21 and 88 hr, respectively. Run T-29 in which were used a stainless steel impeller with Stellite hubs, a quartered orifice plate consisting of Inconel X, Armco type 17-4pH stainless steel, titanium, and type 347 stainless steel sections, and titanium wear rings and labyrinth rings showed no caking, although there was some decrease in thorium content of the slurry after 159 hr. Since then, no adherent cakes have been found.

As a preliminary test of the postulate that centrifugal settling and gas entrainment can produce caking, an existing loop was modified by the insertion of a 4-ft length of 1½-in. glass pipe on the suction side of the pump. A slurry containing about 0.5 g of new Lindsay oxide per cubic centimeter was circulated at atmospheric pressure and 60°C at velocities of 2 to 30 fps. An insert of the same shape and size as those of the tee insert used in the loops was rotated during operation. The insert was designed to convert the flow path of the tee into that of a 90-deg elbow. When the plane of symmetry was rotated fewer than 10 deg from the normal vertical position, very little swirl could be observed, but at greater angles a barber-pole appearance was observed. At 90 deg the helical pitch was about 11 in. With clear water a central gaseous vortex core could be observed to be extending the length of the glass section. This corresponds to an approximate centrifugal field of 30 g at a linear velocity of 20 fps. The continuing visibility of entrained bubbles indicated that there was no caking on the walls of the glass section under these conditions. Hence it is concluded that caking is not purely a centrifugal settling phenomenon.

In run T-40 the tee insert was rotated 45 deg from its normal position in another attempt to produce caking by centrifugal sedimentation and/or gas entrainment. The loop was loaded with solids from run T-39, which was Lindsay material containing a considerable proportion of corrosion products. After running overnight the pump amperage showed no change, and upon opening the loop there was no appreciable caking. The stainless impeller and orifice plate were next replaced with titanium, and the tee insert was rotated 90 deg from normal to give maximum swirl. On running over the week end no caking was observed,

substantiating the conclusion that caking is not due solely to centrifugal settling. As yet there is no satisfactory explanation for the caking in the runs T-23 to T-27.

### Sedimentation Properties

The sedimentation properties of several slurries were studied in the hope of casting light upon the degree of peptization as a function of time of pumping in the loops. Analysis of sedimentation data on a pumped Lindsay thorium oxide showed that the slurry density at which the settling rate began to decrease was relatively independent of the initial slurry density. This critical slurry density marks the transition from hindered settling to consolidation settling and is interpreted to be the bulk density at which the lyspheres of the flocs begin to intersect. Lindsay slurry has a critical sedimentation density of 2.0 g of ThO<sub>2</sub> per cubic centimeter of slurry before being pumped and 0.86 to 0.90 g/cc after being pumped for several days at 70°F. Similar results were obtained in tests upon samples from loop run S-49. The thorium oxide in this run was made by the formate process and was calcined at 650°C. The results are given in Table 30. Several interesting conclusions emerge:

1. Most of the dispersion by pumping occurred in the first 1.5 hr. There may be some tendency to reaggregate upon prolonged pumping.

2. The mean floc size calculated by the method given by Brown<sup>9</sup> ranges from 8 to 16 μ. Apparently almost all the primary particles are bound up in these flocs, since the supernatant liquid is quite clear. This is not true of the unpumped material, the bulk of whose particles sediment very rapidly but whose supernatant liquid remains cloudy for a long period.

3. The proposed slurry densities in the blanket are well above critical. Sedimentation would occur relatively slowly by consolidation and by squeezing of water from the void spaces. This represents, apparently, a much lesser problem with thorium oxide from run S-49 than the formation of a viscous gel in low-shear regions.

### Centrifugal Sedimentation

Slurries containing 0.2 g of ThO<sub>2</sub> per centimeter from runs S-39 and T-40 were centrifuged at 25 g

<sup>9</sup>G. G. Brown, *Unit Operations*, Wiley, New York.

TABLE 30. SEDIMENTATION PROPERTIES AS FUNCTIONS OF TIME OF PUMPING, LOOP RUN S-49

Time of Pumping (hr)	Initial Density (g of ThO <sub>2</sub> per cm <sup>3</sup> )	Critical Density (g of ThO <sub>2</sub> per cm <sup>3</sup> )	Hindered Settling Velocity (cm/min)
0	0.20	1.82	*
1.5	0.076	0.21	1.9
1.5	0.050	0.17	3.6
427	0.032	0.11	2.1
427	0.050	0.12	1.4
1014	0.025	0.14	4.1
1014	0.050	0.14	2.1

\*Most particles greater than 10.5  $\mu$ m.

for 1 to 5 min. The sedimentation densities followed the same pattern as the critical densities noted above. This procedure may prove to be useful as a rapid analytical method.

#### Adhesion to Polished Surfaces

A completely wetted, polished type 347 stainless steel surface was immersed in a sample of pumped slurry from run S-45 and washed with a stream of running water for 1 min. When viewed under dark-field illumination at 250X, a fairly heavy and uniform coating of particles was observed. This method has been used with success<sup>10</sup> in determining the coating tendency of fine particles.

#### Temperature Rise of Quiescent Slurry Layer

The relatively high-yield shear stress of 0.03

<sup>10</sup>S. G. Bankoff, *Trans. Am. Inst. Mining Met. Engrs.* 144 (November 1941).

psi with slurry from run S-49 noted above makes probable the existence of stagnant layers in areas of low shear rate. If the temperature rises 35°C above that of the surrounding slurry, evaporation accompanied by the formation of a hard cake may take place. A rough calculation of the thickness of a stationary layer required to give a steady-state temperature rise of 35°C at the blanket wall was performed essentially according to the method of W. E. Winsche.<sup>11</sup> Assuming the heat generation to be 6000 w/ft<sup>3</sup> and the thermal conductivity to be 0.1 Btu/hr·ft<sup>2</sup>·(°F/ft), the required thickness at steady state is found to be about 0.6 in. If, in addition, a heat flux of 150 w/ft<sup>2</sup> must be dissipated from the wall, the allowable thickness is decreased to 0.2 in.

<sup>11</sup>W. E. Winsche, *EPPD - Partial Analysis of Heat Transfer in Soils Containing Radioactive Material*, correspondence to M. C. Leverett, Aug. 1, 1946.

## BOILING REACTOR STUDIES

R. N. Lyon, Section Chief  
C. G. Lawson                      M. Richardson  
H. A. MacColl                    D. G. Thomas  
P. C. Zmola

### VAPOR TRANSPORT IN THE LIQUID

Work directed toward determining the influence of diameter, height, pressure, and the fluid physical properties on the relation of power density to mean fluid density of boiling systems has been continued.

Construction of the 6 × 6 in. natural-circulation apparatus has been completed and some data have been obtained. The test section of the apparatus is 6 in. square in cross section and 4 ft high. A downcomer of 4-in.-dia glass pipe enters the side of the test section very near the bottom. The boiling mixture leaving the test section enters a 5-ft<sup>3</sup> steam chest in which vapor separation is afforded and from which the downcomer is fed. Condensate is refluxed from the condenser mounted above the steam chest. Electrical-resistance heating is used to boil the water.

Power densities to 5.8 kw/liter and vapor fractions to 0.65 have been attained. At the highest power, liquid and vapor velocities at the outlet of the test section were 9.1 and 17.3 fps, respectively. These data are currently being compared with results from the 1.25 × 4 in. circulating system to determine the influence of the test-section diameter and the height-to-diameter ratio. Direct comparisons cannot be made because the two systems are not geometrically similar.

The density-measuring technique has been improved by substitution of a scintillation detector for the G-M tube used in the past. Error in density measurement due to statistical error in counting has been reduced to approximately 3%. Instrumentation for measuring the density of a boiling ThO<sub>2</sub> slurry is being developed. The slurry will be run in the 6 × 6 in. system.

The contract for the construction and operation of the high-pressure boiling apparatus is still under negotiation with the Babcock & Wilcox Co. The purpose of these experiments is to determine the influence of pressure on the vapor transport capability of a volume boiling system.

The influence of the physical properties, height and diameter, on the gas transport in two-phase systems is being studied under subcontract at

Tulane University by R. V. Bailey and associates. Two experimental systems are being operated. The first is a natural-vapor-rise apparatus 6 in. in diameter in which mixture heights up to 10 ft can be investigated. Air or steam is bubbled through liquids of various densities and viscosities. The second is a forced-circulation loop through which an air-water mixture is pumped and the mean density is measured by gamma-ray attenuation. Diameters of 2, 6, and 12 in. and heights of 5, 10, and 20 ft are being investigated.

### VAPOR SEPARATION

The separation of vapor from the entraining liquid in a boiling reactor system must be effected with a minimum fuel holdup. To design vapor separation for this application it is necessary to know the available pressure drop for the separator and associated manifolding as a function of the inlet fuel-mixture density and the fuel-mixture flow rate for the range of operating variables which are of interest. Such calculations based on an earlier report (Case II of ORNL CF-53-11-145) have been performed and the results are shown in Fig. 60. The curves which have the height of the reactor,  $Z$ , as a parameter represent the head available for circulation. The curves for which the parameter is designated by letters represent the flow resistance of the unit exclusive of separators and associated manifolding. The parameter for the resistance curves is a product of the power density,  $P$ , and the height,  $Z$ . The appropriate resistance curve for given values of these variables can be obtained from the small chart in Fig. 60. For a given unit operating at a specified power density, the pressure drop available for steam separation is the difference between the appropriate available head curve and the resistance curve. Possible operating conditions are found only in those regions in which this difference is positive. The separator-inlet density ratio is obtained from Fig. 61 as a function of the mean density decrease in the unit. All calculations are based on an operating pressure of 1000 psi.

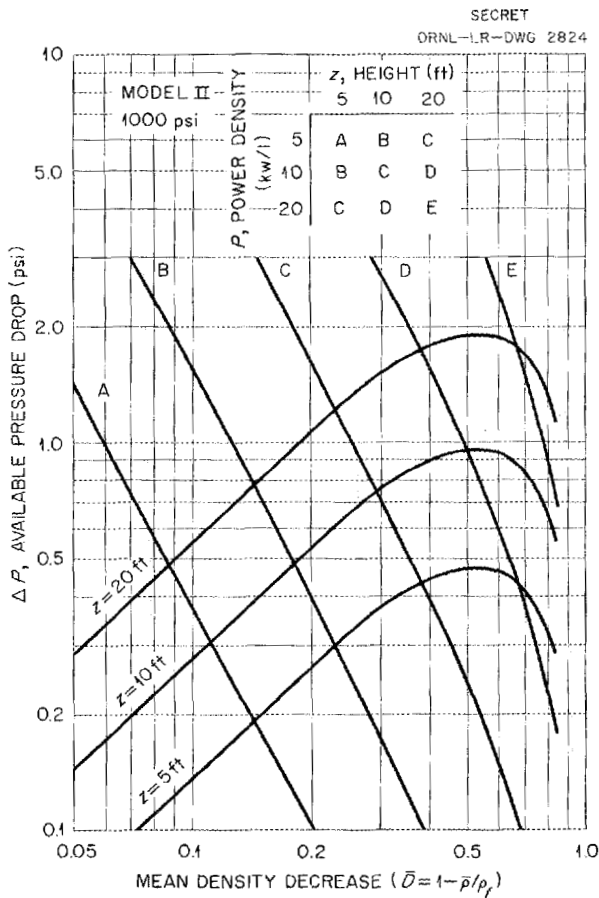


Fig. 60. Performance Chart for Determination of Allowable Pressure Drop in Separators.

**FORCED CIRCULATION**

Information has been presented previously by which estimates may be made of the circulation-rate and pump-head requirements for forced-circulation boiling reactors.<sup>12,13</sup> It is of interest to estimate the limit of the developed head obtainable by the pump in a boiling system before cavitation occurs in the pump.

The maximum developed head in a pumping system is determined by the specific speed of the pump and the net positive suction head (NPSH). The NPSH is defined as

$$NPSH = H_a + H_s - H_e - H_f - H_v;$$

<sup>12</sup>C. G. Lawson, HRP Quar. Prog. Rep. Apr. 30, 1954, ORNL-1753, p 128-132.

<sup>13</sup>R. J. Goldstein et al., HRP Quar. Prog. Rep. Jan. 31, 1954, ORNL-1678, p 15-18.

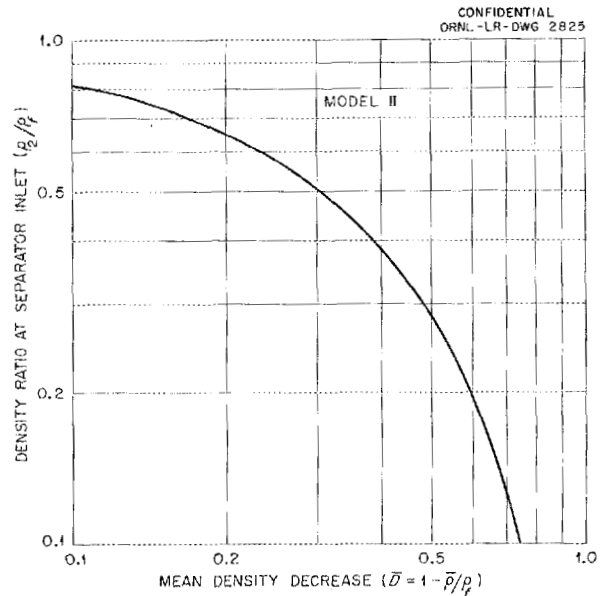


Fig. 61. Relationship Between Density Ratio at Separator Inlet and Mean Density Decrease.

- $H_a$  = absolute pressure at the surface of the pump-suction supply,
- $H_s$  = static pressure from the surface of the pump-suction supply to the center line of the pump,
- $H_e$  = vapor pressure of the liquid in the pump impeller,
- $H_f$  = pressure loss in the suction pipe and impeller approach,
- $H_v$  = pressure equivalent of the average velocity head of the fluid at the eye of the impeller.

The relationship<sup>14</sup> between the NPSH and the developed pressure is normally expressed as

$$\frac{NPSH}{\Delta P} = f(N_s) = \sigma,$$

where

$\Delta P$  is the operating head of the pump expressed as psi rather than feet of head.

NPSH, as defined above, is the cavitation constant and determines the minimum NPSH required to operate without cavitation at the design point.

<sup>14</sup>A. J. Stepanoff, *Centrifugal and Axial Flow Pumps; Theory, Design, and Application*, Wiley, New York.

## HRP QUARTERLY PROGRESS REPORT

$$f(N_s) = f(\text{specific speed}) = f \frac{\text{RPM GPM}}{\Delta H^{0.75}},$$

where

*GPM* is the capacity of the pump in gallons per minute,

*RPM* is the revolutions per minute of the pump,

$\Delta H$  is the pump head, expressed as ft lb force/lb mass.

A plot of  $\sigma$  vs specific speed is shown in Fig. 62.

For a given specific-speed pump the permissible developed head may be increased by increasing the *NPSH*. One way to increase the *NPSH* is to subcool the liquid entering the pump impeller. If the condensate from the boiling system is subcooled to 80°C and if no additional heat is added to the circulating liquid before the condensate is mixed with it, then reasonably high values of *NPSH* may be obtained. Figure 63 is a plot of the *NPSH* obtainable with the above assumptions. From Figs. 62 and 63 the permissible operating pressure drops for a specific pump may be estimated.

It is apparent from Fig. 62 that lower specific-speed pumps operate at higher developed heads, other factors remaining equal. However, the pump impeller may become ridiculously large in diameter.

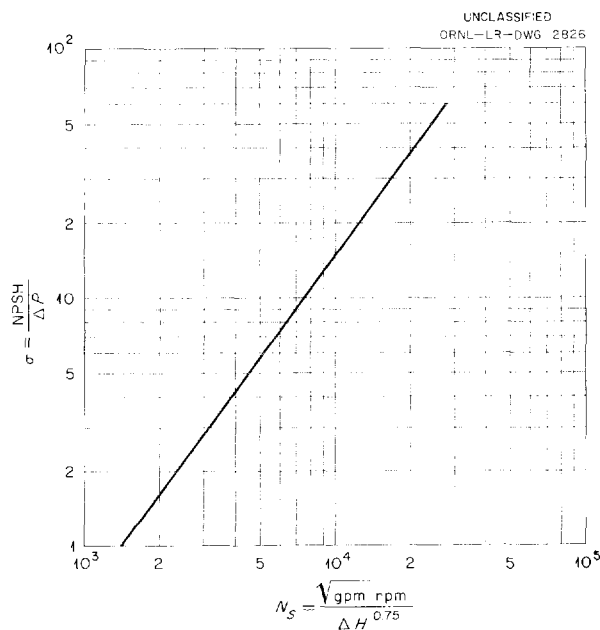


Fig. 62. Relationship Between Cavitation Constant and Specific Speed of the Pump.

The relationship between impeller diameter and the design capacity and head for various specific-speed pumps is shown in Fig. 64. The information shown in Fig. 64 was obtained by using Stepanoff's data<sup>14</sup> for the ratio between the square of the peripheral velocity of the pump impeller and the pump head as a function of the specific speed. It is apparent that some compromise is necessary between the specific speed and the pump diameter.

### SEPARATOR PUMPS

Several models of separator pumps were tested during the past quarter. All the models discussed here have had the gas-liquid mixture, in this case air and water, entering a vortex through a tangential inlet. The liquid and gas were separated in the vortex.

Model 1 contained a spinner which was located along the axis of the vortex. It was believed that rotation of the spinner by the tangential component of the liquid and air would help to form a more stable vortex region for the gas outlet. A divider plate perpendicular to the vortex axis was located half way between the inlet and the entrance to the outlet. The divider plate had a concentric hole through which the spinner fitted. It was thought

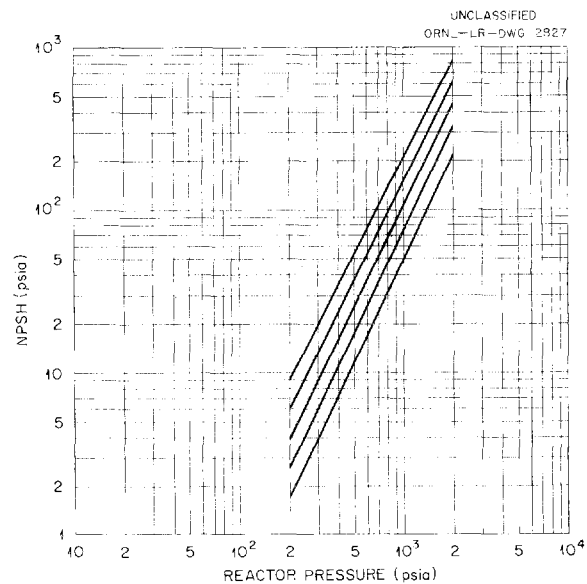


Fig. 63. Net Positive Suction Head Obtainable by Subcooling Condensate to 80°C Before Returning It to Circulating System.

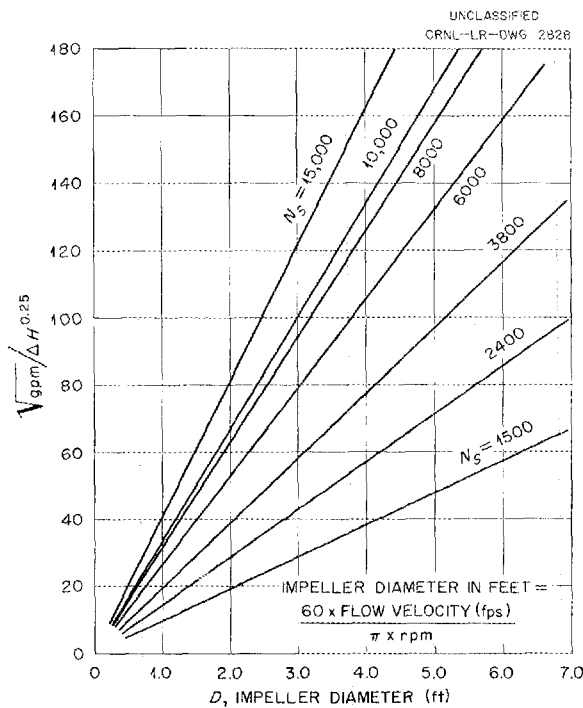


Fig. 64. Relationship Between Impeller Diameter and the Ratio  $\sqrt{\text{gpm}}/\Delta H^{0.25}$

that the divider plate would help to form two vortices, one of low-density mixture moving inward and a second of high liquid density moving outward. The liquid takeoff was located at the outer edge of the higher density vortex. The pressure drop was measured from downstream of the separator inlet to the exit of the liquid outlet to determine whether there was any pressure recovery from the kinetic energy of the inlet stream. The measured pressure drop was positive for all flow conditions tested. For any given liquid rate the pressure drop increased as the air-to-liquid ratio was increased.

Model 2 was the same as Model 1 except for omission of the divider plate. The same measurements were made, and a slight pressure recovery

was obtained for vapor-to-liquid volume ratios of approximately 2 and higher. The indications for this separator were that the divider plate was increasing the pressure drop rather than recovering kinetic energy.

Model 3 was identical to Model 2 except for removal of the spinner. The measurements indicated that the pressure recovery was slightly greater than that observed for Model 2 under the same flow conditions.

Model 4 was of somewhat different design. A nozzle was mounted tangentially on a 7-deg diffuser with the liquid outlet at the wider diameter and the gas outlet at the narrow diameter. The liquid was passed through a volute entering the eye and leaving tangentially at the periphery. Measurements were made of the pressure drop across the nozzle entrance and of the pressure drop from downstream of the nozzle entrance to the liquid exit. The apparatus showed a recovery across the separator and the volute which amounted to about 30% of the nozzle pressure drop for all flow conditions tested. Of all the models tested, Model 4 appeared to be the most efficient separator. The pressure drop across the entire unit was computed to be about 0.7 inlet velocity head for water. Improved nozzle design should minimize the pressure drop further. The vortex was observed to have a tendency to tail out to the liquid outlet, but this tendency was corrected by removal of a small amount of liquid at the eye of the volute.

#### GENERAL STUDIES

Preliminary design studies of two homogeneous boiling reactor systems are being made by groups of Reactor School students. Feasibility of employing boiling as a means of power removal from the slurry blanket of a two-region homogeneous reactor has been reported previously.<sup>15</sup>

<sup>15</sup>P. C. Zmola, *Power Removal from a Boiling Slurry Blanket*, ORNL CF-53-9-111 (Sept. 21, 1953).

METALLURGY

E. C. Miller

W. J. Fretague

W. J. Leonard

W. O. Harms

T. W. Fulton

J. J. Woodhouse

PROPERTIES OF TITANIUM AND ZIRCONIUM ALLOYS

Iodide-Titanium

Four iodide-titanium impact-test specimens were exposed to a solution of 0.06 *m* uranyl sulfate-0.006 *m* sulfuric acid at 310 to 320°C for 977 hr in dynamic test loop run A-67. The results of subsequent impact tests are presented in Table 31. When the results were compared with previously reported<sup>16</sup> data for impact tests on unexposed iodide-titanium, no significant effects of the exposure to the corrosive environment were noted.

Tensile Properties of Welded Zircaloy-2

Tensile tests made at room temperature and at 600°F on specimens cut from 5/16-in.-thick welded Zircaloy-2 plate are listed in Table 32. The welded plate was prepared by Newport News Shipbuilding & Dry Dock Co. from an experimental plate rolled for them by Crucible Steel Co. of America and was identified as Plate 7 by Newport News.

CORROSION OF WELDS

Welds were made in 1/4-in. plate of type 347 stainless steel, Titanium 75A, and Zircaloy-2; in each case the welding wire was of the same material as the plate. These welds were made, insofar as applicable, by the Heliarc process according to HRP-2 Welding Specification procedure. Two types of type 347 stainless steel wire were used, low ferrite (2 to 4%) and high ferrite (7 to 9%). The titanium and Zircaloy-2 welds were made in a dry box in a helium atmosphere.

The welded plates were sectioned and machined into dynamic-corrosion-test-loop coupons, and the weld reinforcements were left on the coupons in the majority of cases. The coupons were machined in such a way that the flow over the coupons would approximate actual service conditions in butt-welded pipes. Due to the differences in the height of face and root reinforcements of the welded coupons, flow rates over different individual samples in the

holders varied, and more severe velocity effects were thought to be present than would normally be experienced at a butt-welded pipe joint.

Visual inspection of the stainless steel samples after the run indicated that the film on the high-ferrite samples was less tenacious than that on the low-ferrite samples. The visual inspection, plus

TABLE 31. IMPACT ENERGY vs TESTING TEMPERATURE DATA FOR IODIDE-TITANIUM SPECIMENS EXPOSED TO UO<sub>2</sub>SO<sub>4</sub>

Specimen	Temperature (°C)	Impact Energy (in.-lb)
14-1	26.5	84*
	26.5	66
	-196.8	38
	-100	55
15-1	26.5	83*
	26.5	138**
	-196.8	56
	29.0	160
	29.0	129
17-2	-100.0	97
	26.5	86*
	26.5	64
	-196.8	48
18-2	-100	67
	-100	51
	26.5	100*
	26.5	84**
	-196.8	48
	-100	74

\*The specimen rod contained four notches and was threaded on each end so that it could be held firmly in the fixture for exposure in the dynamic test loop. In the first impact test on each rod the pendulum struck the threaded end and expended some of its energy in deforming the threads. Thus these values are possibly higher than they would have been in the absence of threads.

\*\*The specimen bent and did not break on the first impact of the pendulum, but broke on the rebound. These results are therefore not accurate as absolute values, but they do indicate minimum toughness values for the test materials and conditions.

<sup>16</sup>W. J. Fretague, HRP Quar. Prog. Rep. Jan. 1, 1953, ORNL-1478, p 89.

TABLE 32. TENSILE PROPERTIES OF WELDED ZIRCALOY-2\*

Specimen	Testing Temperature (°F)	Yield Strength (psi) (0.2% offset)	Tensile Strength (psi)	Ultimate Strength (psi)	Elongation (%)	Reduction in Area (%)	Reduction in Width (%)	Reduction in Thickness (%)
ZW-33-1**	Room temperature	55,000	65,000	54,700	0	0	0.0	0.0
ZW-33-2***	600	28,000	37,000	67,500	20	63.4	56.0	17.5

\*The original dimensions of the test sections were approximately 0.500 × 0.312 in.

\*\*Broke in the weld, with little evidence of any plastic deformation before rupture.

\*\*\*The parent base metal became constricted on either side of the weld and finally broke in one of these two sections outside the weld.

the corrosion data listed in Table 33, suggests that under these conditions the low-ferrite weld metal had somewhat superior corrosion resistance in the as-welded condition.

After the specimens were exposed to a higher velocity corrosion environment, no corrosion was observed, either visually or by measured weight changes, on the Titanium 75A and Zircaloy-2 specimens. Both types of specimens were covered by a tenacious bulk scale of iron and chromium oxides. A thin, light-green film was observed beneath the bulk scale on the Zircaloy-2 and there was a light-gold film on the Titanium 75A. It is obvious from the data in Table 34 that only the Titanium 75A-welded samples were exposed to velocities above 52 fps and that none of the samples showed any significant weight loss.

MISCELLANEOUS SERVICE ASSISTANCE

Tubing Failures from Loop H Pressurizer Mixing Line

Metallographic examinations of three tubing failures from the pressurizer mixing line of dynamic-corrosion Loop H were completed during this period. These failures, which were in 1/4-in. austenitic-stainless-steel tubing of 0.035-in. wall thickness, occurred after at least 190 hr of exposure to 1.34 m uranyl sulfate at 225°C and at an estimated solution velocity of 25 fps. Results of the examinations are summarized below.

**Seamless Type 347 Stainless Steel Tube.** The seamless type 347 stainless steel tube had been exposed to 1.34 m uranyl sulfate for 492 hr at 225°C and had failed in run H-30. Previously, it had been used in low-concentration runs (0.02 to

TABLE 33. CORROSION TEST RESULTS OF TYPE 347 STAINLESS-STEEL-WELDED COUPONS IN 1.34 m URANYL SULFATE SOLUTIONS AT 250°C

O<sub>2</sub> pressure: 200 psi  
 Time: 100 hr  
 Average velocity: 10 fps  
 Maximum velocity: 16 fps

Weld Rod	Position	Scrubbed Weight Loss (mg)
Type 347 stainless steel (7 to 9% ferrite)	A	1400*
	B	676
	C	917
	D	779
	E	711
Type 347 stainless steel (2 to 4% ferrite)	F	664
	G	451
	H	446
	I	700
	J	714

\*Position A usually associated with high weight losses regardless of sample.

0.11 m uranyl sulfate) at 225°C. The penetration occurred about 1/2 in. from the inlet fitting (Fig. 65), and examination of the interior (Fig. 66) indicated that it had been subjected to severe velocity effects in this area. The photomicrograph in Fig. 67 reveals some intergranular type of attack and a grain size between ASTM Nos. 7 and 8.

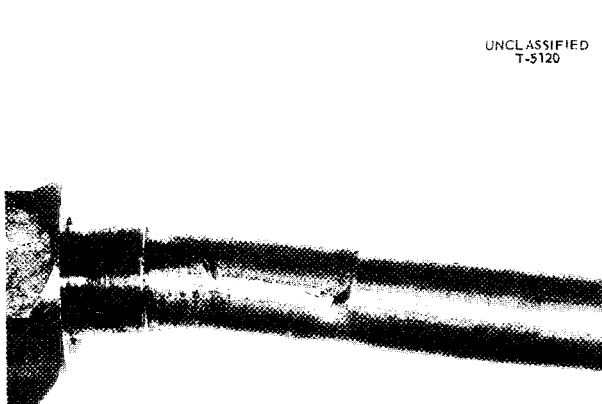
**Welded Type 316 Stainless Steel Tube.** The welded type 316 stainless steel tube was in service for 22 hr before failure occurred in the seam weld, approximately 5 in. from the inlet end, during run

**HRP QUARTERLY PROGRESS REPORT**

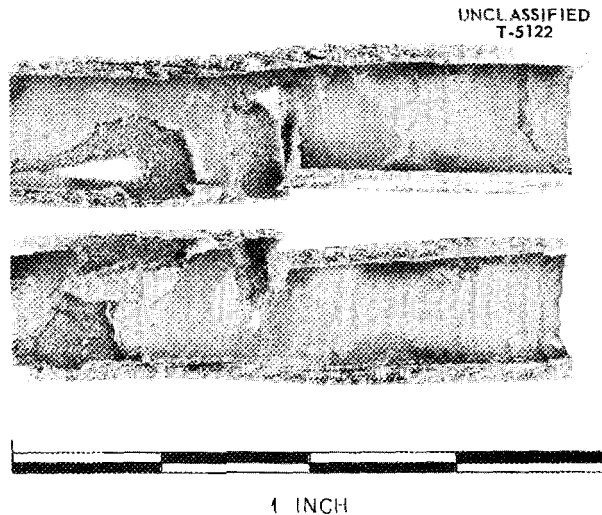
H-32. The photomicrograph, Fig. 68, shows that this failure was caused by an intergranular type of penetration. Grain size ranged between ASTM Nos. 5 and 7, being somewhat smaller in the seam

metal than in the base material.

**Welded Type 347 Stainless Steel Tube.** After 188 hr of run H-33, the welded type 347 stainless



UNCLASSIFIED  
T-5120



UNCLASSIFIED  
T-5122

1 INCH

**Fig. 65. Failure of Seamless, Type 347 Stainless Steel Tubing from Pressurizer Mixing Line of Loop H. 3X. Reduced 30.5%.**

**Fig. 66. Inside of Seamless, Type 347 Stainless Steel Tubing from Pressurizer Mixing Line of Loop H Showing Severe Effects of Velocity in Vicinity of Failure. 3.5X. Reduced 12%.**

**TABLE 34. CORROSION TEST RESULTS OF TITANIUM 75A AND ZIRCALOY-2 COUPONS IN 1.34 m UO<sub>2</sub>SO<sub>4</sub> URANYL SULFATE SOLUTION AT 250°C**

O<sub>2</sub> pressure: 200 psi  
Time: 200 hr  
Velocity range: 50 to 92 fps

Position	Specimen	Velocity (fps)	Weight Change (mg)		Corrosion Rate (mpy)
			Scrubbed	Defilmed	
A	Zircaloy-2 weld	52	+93		
B	Titanium 75A base metal	52	+122		
C	Zircaloy-2 weld	52	+115	+46*	
D	Titanium 75A weld	74	+121	-1.3	0.37
E	Titanium 75A weld	92	+120		
F	Titanium 75A weld	91	+128		
G	Titanium 75A weld	87	+128		
H	Zircaloy-2 weld	52	+122		
I	Zircaloy-2 base metal	50	+117		
J	Zircaloy-2 weld	52	+119		

\*Removal of film not complete.

steel tube failed in the seam weld. It appeared almost as though a keyway type of groove had been machined along the entire length of the inside of



Fig. 67. Microstructure at Penetration in Seamless, Type 347 Stainless Steel Tubing from Pressurizer Mixing Line of Loop H. Etch, aqua regia. 250X. Reduced 30%.

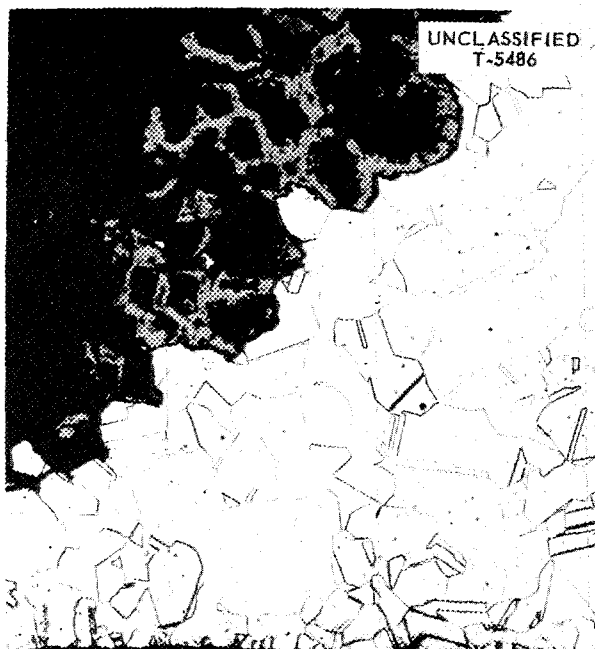


Fig. 68. Microstructure at Penetration in Welded, Type 316 Stainless Steel Tubing from Pressurizer Mixing Line of Loop H. Etch, aqua regia. 250X.

this tube, indicating an extremely selective attack on the weld metal. Metallographic examination (Fig. 69) revealed an intergranular attack and showed that the base material had a grain size between ASTM Nos. 6 and 8, while the weld-seam-metal grain size was ASTM No. 8 or smaller. A microhardness traverse showed the hardness of the weld seam metal (VHN 168 to 181) to be greater than that of the base alloy (VHN 121 to 162).

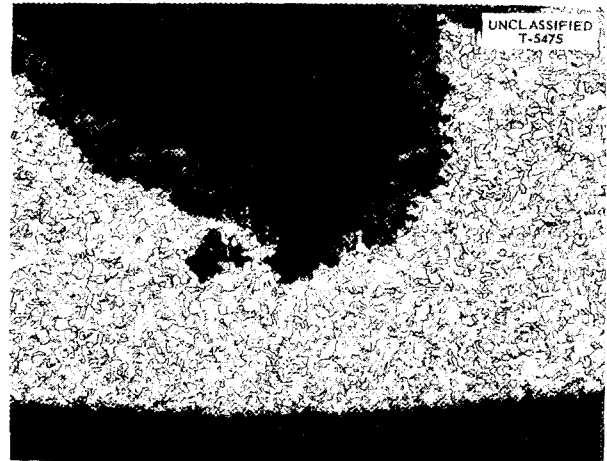


Fig. 69. Microstructure near Penetration in Welded, Type 347 Stainless Steel Tubing from Pressurizer Mixing Line of Loop H. Etch, aqua regia. 250X. Reduced 30%.

#### Metallographic Examination of Dynamic-Corrosion Specimens

At the request of the Dynamic Corrosion Group, several stainless steel corrosion specimens which were exposed to 1.34 M uranyl sulfate solutions at 225°C in runs H-28, H-32, and H-33 were examined metallographically for evidence of intergranular attack. It had been observed that at solution velocities of 17 to 18 fps all type 347 stainless steel pins in these runs were covered with an oxide scale, while all other 300-series stainless steels had only partial scales and the upstream side was generally scale-free. At a flow rate of 65 fps, all 300-series stainless steels were scale-free and corroded at about the same rate. Types 316L, 316, 304L, 309SCb, 347, and 304 (sensitized) stainless steel were represented in these runs.

The results of the investigation were as follows:  
 1. All except the type 304L stainless steel

specimen were attacked intergranularly at the high flow rate, and types 316L, 316, and 309SCb showed the poorest resistance to this type of attack.

2. At low flow, types 316L, 304 (sensitized), and 316 stainless steel were intergranularly attacked; a typical microstructure of the sensitized type 304 is shown in Fig. 70. Only a welded specimen (type 304 stainless steel joined by type 347 by use of the Heliarc process) did not show definite indication of intergranular penetration; however, severe general attack at the fusion zone was observed on this specimen.

### Titanium Pressurizer Failure

Failure of the titanium pressurizer from dynamic-corrosion Loop G, described in a previous quarterly report,<sup>17</sup> was analyzed metallographically. The rupture occurred adjacent to the bottom heater below which the solution level had fallen. Figure 71 is a photograph through the rupture showing normal grain structure at *b*, the grain growth in the heat-affected area at *a*, and the grain elongation in the heat- and stress-affected area immediately adjacent to the failure. There was no evidence of

<sup>17</sup>H. C. Savage and F. J. Walter, *HRP Quar. Prog. Rep. Apr. 30, 1954*, ORNL-1753, p 59-61.

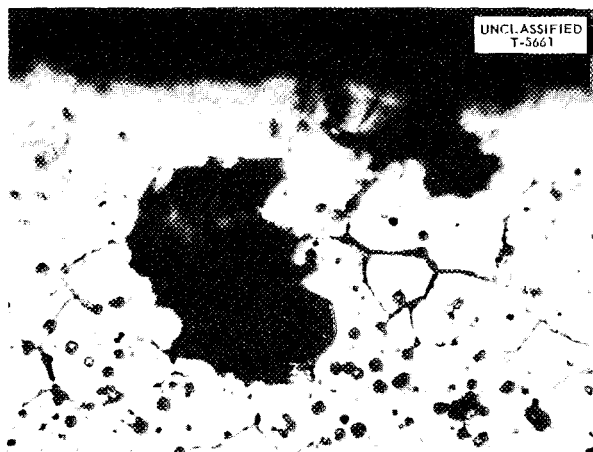


Fig. 70. Microstructure of Sensitized, Type 304 Stainless Steel after Corrosion Testing in 1.34 *m* Uranyl Sulfate at 225°C. Etch, aqua regia. 1000X. Reduced 31.5%.

any seam or inclusion which could have initiated the fracture.

A photomicrograph of area *b* of Fig. 71 showed the typical structure resulting from cold-working titanium followed by annealing at a temperature sufficiently high to produce a recrystallized alpha structure without exceeding the transformation temperature. Metallographic examination of the coarse-grained region *a* of Fig. 71, in the immediate vicinity of the actual failure, showed the structure characteristic of titanium heated into the beta range followed by transformation to alpha structure upon cooling. These changes indicated that the material at the point of failure had been heated well above the contemplated operating temperature.

### Stress-Corrosion Cracking

Tubes of type 347 stainless steel in the as-received condition and tubes expanded 0.006 in. in a 1-in. tube sheet as fabricated by the Foster Wheeler Corp. were tested in boiling 42% MgCl<sub>2</sub>. Results of this test indicated a crack in the expanded end at the interface of the expanded region, after 5 hr of exposure. No cracks were detected in the as-received tubes. Further tests will involve a tube-to-header section expanded 0.0015 in.

The type 347 stainless steel pressurizer for use in the in-pile test was partially stress-relieved at 950°F for 6 hr in a hydrogen atmosphere.

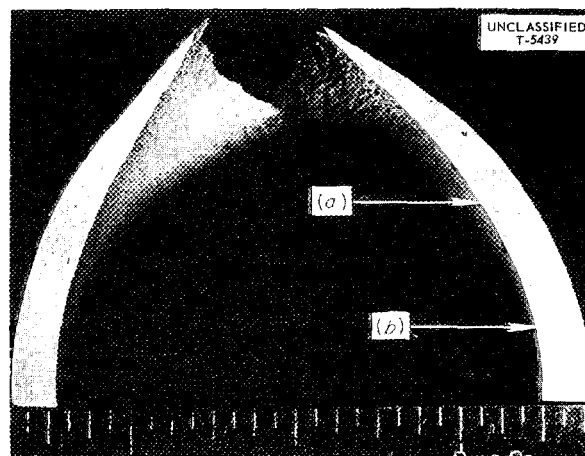


Fig. 71. Section through Titanium Pressurizer Fracture Showing (a) Region of Grain Growth and (b) Normal Grain Structure.

Part V

CHEMICAL ENGINEERING DEVELOPMENTS



## SLURRY FUEL AND BLANKET STUDIES

D. E. Ferguson	W. K. Eister	
J. P. McBride	J. T. Roberts	E. O. Nurmi
L. E. Morse	J. L. Patton	C. C. Williams
W. L. Pattison	V. L. Fowler	

In the thorium oxide slurry program, emphasis is now being placed on the effect of neutron irradiation on slurry properties and on a study of gas production and recombination in the slurry system. Both pure thorium oxide slurries and slurries of uranium oxide and thorium oxide are being investigated.

### THORIUM OXIDE SLURRY IRRADIATION STUDIES

#### In-Pile Studies

Preliminary observations of the effects of reactor irradiation on a pure thorium oxide slurry and on a thorium oxide slurry containing 4 mole % of 93.14% enriched uranium have been made. During 30 days of irradiation at 250°C, gas production in the pure thorium oxide slurry was negligible. With the mixed oxide slurry, at the end of five days of irradiation, gas pressure less than 100 psi in excess of steam pressure was observed when the temperature was above 270°C, although a nonequilibrium rising gas pressure of 2500 psi had been observed at 205°C. Since previous experience with  $\text{UO}_3$  had indicated that with slurries containing this much  $\text{U}^{235}$  a steady-state pressure of 1500 to 3000 psi would be expected, the results indicate that catalytic gas recombination was occurring at 270°C.

The irradiations are being carried out in hole 11 of the ORNL Graphite Reactor at 200 to 300°C at maximum flux, about  $7 \times 10^{11}$  neutrons/cm<sup>2</sup>-sec. During the irradiation the slurry is contained in a stainless steel bomb equipped with a remotely activated dash-pot type of magnetic stirrer. Improper performance of the stirrer can be readily detected since its position relative to the activating solenoid determines the voltage induced in an induction coil on the solenoid. Heating is accomplished by an in-pile furnace. The temperature is controlled by air cooling. A 35-mil stainless steel capillary connects the bomb to a pressure cell, and a continuous record of pressure is thus obtained. Ten milliliters of slurry was placed in the bomb at room temperature. At the

temperature of the experiment the ratio of slurry volume to gas volume was approximately 1 to 1.

The pure thorium oxide slurry was prepared from oxide obtained by a 650°C calcination of nitrate-free thorium oxalate; it contained 806 g of thorium per kilogram of  $\text{H}_2\text{O}$ . At intervals during the irradiation the stirring was stopped and the slurry was allowed to settle for as long as two or three days; it was readily redispersed when stirring was resumed. This slurry has not yet been examined for radiation effects other than gas production.

The slurry containing the enriched uranium was prepared by reacting, at 250°C in water, 93.14% enriched  $\text{UO}_3 \cdot \text{H}_2\text{O}$  platelets with thorium oxide prepared from thorium oxalate by pyrohydrolysis at 250°C and subsequent calcination at 350°C (see p 140). The  $\text{UO}_3$  is a solid solution in the  $\text{ThO}_2$ . Thorium and uranium concentrations in the slurry were 532 and 21.3 g per kilogram of  $\text{H}_2\text{O}$ , respectively. In-pile irradiation of this slurry is continuing.

#### Out-of-Pile Studies

Prior to the enriched uranium-thorium oxide slurry being irradiated, out-of-pile gas combination runs were made in a simulated in-pile setup using a similar slurry preparation made up from natural uranium. Substantial gas combination was observed at temperatures above 250°C.

The experiments were performed by adding oxygen and hydrogen in stoichiometric ratios to the slurry bomb at room temperature, heating the bomb to the temperature of the experiment, and following the decrease in pressure on a Brown strip-chart recorder. As in the in-pile experiments, 10 ml of slurry was used and the ratio of slurry volume to gas volume at the temperature of the experiment was approximately 1 to 1.

The combination data gave the familiar linear plot obtained in solution recombination work<sup>1</sup> when the pressure drop per time increment was plotted against the pressure; this indicates a first-

<sup>1</sup>C. H. Secoy, *HRP Quar. Prog. Rep. Mar. 15, 1952*, ORNL-1280, p 163.

## HRP QUARTERLY PROGRESS REPORT

order dependence on pressure. The combination rate showed a marked temperature dependence, which indicates a high activation energy for the substance catalyzing the reaction. At 1000 psi of oxygen and hydrogen in excess of the steam pressure, the hydrogen combination rate was approximately  $1.8 \times 10^{-3}$  mole/hr (0.15 mole/hr/liter of slurry) at 290°C,  $0.67 \times 10^{-3}$  mole/hr (0.05 mole/hr/liter of slurry) at 270°C, and an estimated  $0.15 \times 10^{-3}$  mole/hr (0.01 mole/hr/liter of slurry) at 244°C.

Since the experiments were run in a setup which simulated the in-pile experiments, it is likely that the above rates were not independent of diffusion effects. Apparatus for the study of gas recombination in thorium oxide slurries is being prepared in which diffusion effects will be negligible. Under these conditions it may be expected that faster recombination rates will be observed at the above temperatures for the same slurry. In any case, the substantial out-of-pile combination rates obtained and the obvious fact that in-pile recombination is taking place are very encouraging from the point of view of the gas recombination problem in a thorium oxide slurry blanket.

### CHEMISTRY OF THORIUM OXIDE SLURRIES

#### Reactions with Uranium Oxide

An investigation of the reaction between thorium oxide and uranium oxide in water at 250 to 300°C has been started. The study was prompted by the interest in thorium-uranium slurry systems, the effect of small concentrations of uranium on thorium oxide slurry properties, and the necessity of preparing mixed oxides of thorium and enriched uranium for use in the in-pile irradiation-damage studies.

Mixtures of  $UO_3 \cdot H_2O$  platelets and various thorium oxide preparations in weight ratios of uranium to thorium of 1 to 50 were autoclaved overnight at 250°C in water. In all cases the uranium oxide was more or less completely absorbed by the thorium oxide to give orange-colored solids, presumably a solid solution of the  $UO_3$  in the  $ThO_2$ .

The thorium oxide preparations used were made up of oxide from (1) a 300°C calcination of thorium oxalate, (2) a 700°C calcination of thorium oxalate, (3) pyrohydrolysis of thorium oxalate in water at 250°C and subsequent calcination at 350°C, (4) pyrohydrolyzed material calcined at 900°C, and (5) a 500°C calcination of thorium hydroxide pre-

cipitated from thorium formate solution. A more intense orange color was obtained from the calcined oxalates than from either the pyrohydrolyzed or hydroxide preparation, presumably an effect of the smaller particle sizes of the latter preparations.

Samples of the mixed-oxide preparation were shaken overnight in 8 M  $HNO_3$  to remove unreacted uranium oxide. The recovered solids were then washed and subjected to a second nitric acid treatment (Table 35). The percentage of uranium removed by the first nitric acid treatment increased with increasing temperature of calcination in thorium oxide preparation, which indicates that the reaction of the uranium with the high-burned thoria was less complete than with the low-burned. In the second wash, no significant amounts of uranium were removed from any of the preparations except the mixed oxide prepared from the 900°C thorium oxide.

A sample of the mixed oxide from the calcined hydroxide- $UO_3 \cdot H_2O$  reaction was reautoclaved overnight under a hydrogen pressure of 50 psi. During the heating, gross crystal growth occurred, and the uranium was reduced to yield a slurry with two solid phases, one gray-white and readily dispersed and the other gray-black and sandlike. Subsequent treatment of the solid overnight with 8 M nitric acid reoxidized the uranium, restoring the orange color; it did not leach the uranium from the solid and did not completely redisperse the sandlike crystals although it changed their color.

#### Effect of Electrolytes

In studies on the stabilization and deflocculation of thorium oxide slurries, 0.005 m  $Na_4P_2O_7$  was found to be a good deflocculent at room temperature for Lindsay oxide, prepared by calcination of thorium oxalate at 900°C, and for an oxide prepared by the pyrohydrolysis of thorium oxalate at 285°C in the presence of 0.005 m  $Na_4P_2O_7$  and subsequent drying at the temperature of the autoclave. The addition of 0.005 m  $Na_4P_2O_7$  did not markedly affect the room-temperature properties of oxide prepared (1) from thorium hydroxide by calcination at 500°C and subsequent autoclaving in water at 250°C, (2) by the pyrohydrolysis of oxalate at 250°C followed by calcination at 900°C, or (3) by pyrohydrolysis of oxalate at 285 to 290°C.

Three slurry preparations of Lindsay oxide, containing 1000 g of thorium per liter, were used for

TABLE 35. ACID LEACH OF THORIUM OXIDE-URANIUM OXIDE

Conditions of preparation: 5.7 g of  $\text{ThO}_2$ , 0.128 g of  $\text{UO}_3 \cdot \text{H}_2\text{O}$ , and 10 ml of  $\text{H}_2\text{O}$ , heated 16 hr at  $250^\circ\text{C}$ 

ThO <sub>2</sub> Preparation	Final Calcination Temperature (°C)	Uranium Dissolved with 8 M Nitric Acid (%)	
		First Treatment	Second Treatment
Oxalate calcination	300	7.2	0.04
Oxalate pyrohydrolysis (250°C)	350	9.6	0.06
Hydroxide calcination	500	12.4	0.06
Oxalate calcination	700	14.4	0.04
Pyrohydrolysis (250°C)	900	72	7.5

the study: one of the material as received, one of less than  $4\text{-}\mu$  particles, and one of 4- to  $5\text{-}\mu$  particles. The last two were prepared with a Roller air elutriator. The effects of the addition of  $0.005\text{ }m\text{ Na}_4\text{P}_2\text{O}_7$  on the apparent density of settled oxides and on the settling rates were observed.

The apparent density of settled solids of the Lindsay oxide as received was about 2300 g of thorium per liter. The addition of the pyrophosphate did not greatly affect either the density of the settled solids or the settling rate.

The addition of pyrophosphate to the slurries of the sized oxides increased the apparent density of the settled solids from 2100 to 4100 g of thorium per liter in the case of the less than  $4\text{-}\mu$  material and from 2600 to 3800 g of thorium per liter in the case of the 4- to  $5\text{-}\mu$  material. The increase in the density of the settled solids is indicative of considerable deflocculation by the pyrophosphate. The slurries containing the pyrophosphate settled much more slowly but were very much harder to redisperse after infinite settling than those not containing the phosphate.

The oxide prepared by pyrohydrolysis of thorium oxalate at  $285^\circ\text{C}$  in the presence of  $0.005\text{ }m\text{ Na}_4\text{P}_2\text{O}_7$  and subsequent drying was found to be readily dispersed by the addition of more pyrophosphate to give slurries of 674 and 1133 g of thorium per kilogram of  $\text{H}_2\text{O}$  which were very fluid and showed extremely slow settling rates of about 1 mm/hr. Samples of the preparations were readily flocculated by placing them in dialysis bags and

suspending them in distilled water. Replacing the water surrounding the bags with  $0.005\text{ }m\text{ Na}_4\text{P}_2\text{O}_7$  solution readily restored the dispersion in a short time, which indicates that the optimum concentration of  $\text{Na}_4\text{P}_2\text{O}_7$  for deflocculation is  $0.005\text{ }m$  or less.

#### ABRASIVE PROPERTIES OF THORIUM OXIDE Effect of Method of Preparation of Thorium Oxalate

The abrasiveness of a series of thorium oxide preparations of approximately the same average size prepared by calcination of thorium oxalate increased markedly with the temperature of calcination.<sup>2</sup> It was demonstrated that for a constant calcination temperature ( $650^\circ\text{C}$ ) the abrasiveness of the resultant oxide depends also on the method of precipitation of the oxalate and presumably on the particle size of the oxide, since the particle size of the oxide from the calcination of thorium oxalate is determined primarily by the particle size of the original oxalate, whose particle size, in turn, is determined by the method of preparation.<sup>3</sup>

The oxides from five oxalate precipitation methods were investigated:  
 $0.8\text{ }M\text{ Th}(\text{NO}_3)_4$ - $3.2\text{ }M\text{ HNO}_3$  and 10% excess solid  $\text{H}_2\text{C}_2\text{O}_4$  at room temperature

<sup>2</sup>D. E. Ferguson *et al.*, *HRP Quar. Prog. Rep. Oct. 31, 1953*, ORNL-1658, p 117.

<sup>3</sup>R. N. Lyon *et al.*, *HRP Quar. Prog. Rep. Apr. 30, 1954*, ORNL-1753, p 167.

## HRP QUARTERLY PROGRESS REPORT

1.0 M  $\text{Th}(\text{NO}_3)_4$  and 10% excess solid  $\text{H}_2\text{C}_2\text{O}_4$  at  $40^\circ\text{C}$

0.5 M  $\text{Th}(\text{NO}_3)_4$  and 10% excess solid  $\text{H}_2\text{C}_2\text{O}_4$  at  $70^\circ\text{C}$

0.5 M  $\text{Th}(\text{NO}_3)_4$ -1.0 M  $\text{HNO}_3$  at  $70^\circ\text{C}$  and 1.2 M  $\text{H}_2\text{C}_2\text{O}_4$  at  $70^\circ\text{C}$

0.5 M  $\text{Th}(\text{NO}_3)_4$ -1.0 M  $\text{HNO}_3$  and 10% excess solid  $\text{H}_2\text{C}_2\text{O}_4$  at  $70^\circ\text{C}$

The average particle size of the oxalate preparations increased in the order given and ranged from about  $1\ \mu$  for the cold-precipitated material to above  $7\ \mu$  for the hot preparations. The oxalate preparations were converted to the oxides by first calcining at  $380^\circ\text{C}$  for 16 hr and then at  $650^\circ\text{C}$  for 16 hr.

Abrasion tests were conducted in the laboratory jet-impingement abrasion test apparatus.<sup>4</sup> All the oxide preparations were markedly less abrasive than Ames oxide, inasmuch as they failed to penetrate a 1-mil carbon-steel test plate after a 1-hr test. Relative abrasiveness of the oxides increased with increasing particle size of the original oxalate from which the oxide had been prepared.

X-ray diffraction tracings indicated that the mean dimensions of the microcrystallites composing the oxides were the same for all preparations, approximately  $100\ \text{\AA}$ . Hence the differences in relative abrasiveness were probably the result of differences in particle size and size distribution.

### Mixed-Oxide Studies

Another approach to the problem of minimizing the abrasive character of thorium oxide was suggested by the work of Weiser, Milligan, and Mills,<sup>5</sup> who found that in many cases the addition of an oxide to a second oxide by the coprecipitation of the hydroxides would markedly inhibit the crystallization of the oxide mixture when the mixed hydroxides were converted to the oxides by calcination.

In the present study the effects of the addition to  $\text{ThO}_2$  of 10 to 40 mole %  $\text{ZrO}_2$ , 10 to 40 mole %  $\text{Bi}_2\text{O}_3$ , 10 to 30 mole %  $\text{Al}_2\text{O}_3$ , 10 to 40 mole %  $\text{SnO}_2$ , and 10 to 50 mole %  $\text{MgO}$  were investigated. Only the  $\text{Al}_2\text{O}_3$  and  $\text{SnO}_2$  showed a marked inhi-

tion of the thorium oxide crystallization, as indicated by a broadening of the X-ray diffraction bands when compared with a thorium oxide standard. However, the most promising preparation, that containing 10 mole %  $\text{Al}_2\text{O}_3$ , showed no decrease in abrasive character over the pure thorium oxide preparation.

## THORIUM HYDROXIDE STUDIES

### Crystalline Character

X-ray diffraction studies on thorium hydroxide prepared from thorium formate solution by addition of ammonium hydroxide showed that the hydroxide as precipitated is amorphous to X rays. Drying the solid for four days at  $105^\circ\text{C}$  apparently does not change the amorphous character of the solid. Heating at  $500^\circ\text{C}$  for 24 hr converted the hydroxide to a crystalline  $\text{ThO}_2$  which exhibited a broad-band diffraction pattern very similar to that of an oxide prepared by a  $500^\circ\text{C}$  calcination of thorium oxalate.

Autoclaving the undried hydroxide in water at  $250^\circ\text{C}$  for 912 hr converted it to a crystalline material, as indicated by the X-ray diffraction pattern, but did not increase the density of the settled solids (300 to 400 g of thorium per liter) or increase the abrasiveness of the hydroxide. Autoclaving in water at  $250^\circ\text{C}$  for 324 hr the oxide that had been prepared by heating the hydroxide at  $500^\circ\text{C}$  did not markedly increase the bulk density or the abrasiveness of the preparation, which is the least abrasive of any of the calcined preparations. The density of the settled solids of the  $500^\circ\text{C}$  material, after being autoclaved, dispersed in a Waring Blendor, and allowed to settle, was about 600 g of thorium per liter.

## THORIUM OXIDE SLURRY PREPARATION EQUIPMENT

Equipment for preparing thorium oxide slurries in 5-kg batches by various processes is being designed and constructed. The method that will probably be used is calcination of thorium oxalate or formate. Preliminary sketches are being made of equipment for 100-kg batches. The material produced will be used for loop and component tests by the Reactor Experimental Engineering Division. The preparation of this material will provide experience and data needed for designing a continuous thorium oxide slurry production unit to supply large breeder reactors.

<sup>4</sup>J. P. McBride and W. L. Pattison, *HRP Quar. Prog. Rep. July 31, 1953*, ORNL-1605, p 139.

<sup>5</sup>H. B. Weiser, W. O. Milligan, and G. A. Mills, *J. Phys. Chem.* 52, 942 (1948).

## PLUTONIUM-PRODUCER BLANKET PROCESSING

	D. E. Ferguson	
	R. E. Leuze	
R. H. Rainey	D. C. Overholt	O. K. Tallent
W. E. Tomlin	J. M. Delozier	D. R. Hendrix

The objective of processing the uranium sulfate solution blanket of the plutonium producer is to remove plutonium and possibly neptunium as rapidly as possible in order to minimize  $\text{Pu}^{240}$  build-up. During this quarter the chemistry of both plutonium and neptunium under reactor-blanket conditions has been studied; the adsorption of plutonium on stainless steel and titanium has been determined, and a preliminary neutron cross section of less than 100 barns for  $\text{Np}^{239}$  was obtained (see p 168).

#### SOLUBILITY OF Pu(IV) IN URANYL SULFATE SOLUTIONS

The solubility of Pu(IV) in uranyl sulfate solutions at 300°C did not vary with uranium concentration over the range 1.0 to 1.6 *m*  $\text{UO}_2\text{SO}_4$  and increased slightly when the  $\text{UO}_3/\text{SO}_3$  mole ratio decreased from 1.03 to 0.95. At four different uranium concentrations the Pu(IV) solubility observed was  $3.0 \pm 0.6$  mg per kilogram of  $\text{H}_2\text{O}$  at  $\text{UO}_3/\text{SO}_3$  mole ratios of 1.03 and 1.00 and between 3.8 and 5.1 mg per kilogram of  $\text{H}_2\text{O}$  at a  $\text{UO}_3/\text{SO}_3$  mole ratio of 0.95. It should be noted that in all these tests two liquid phases were obtained at 300°C, and the solubility results were calculated from the average composition of both phases. The solubility of plutonium in the light phase was less than 0.2 mg per kilogram of  $\text{H}_2\text{O}$ .

#### ADSORPTION OF PLUTONIUM ON STAINLESS STEEL AND TITANIUM

After 11 cycles of adding 1.4 *m*  $\text{UO}_2\text{SO}_4$  solution containing plutonium, heating to 250°C, removing the solution and precipitate, and rinsing with water, two type 347 stainless steel containers had each adsorbed plutonium to the extent of 0.11  $\text{mg}/\text{cm}^2$  and two titanium containers had adsorbed plutonium to the extent of 0.05 and 0.06  $\text{mg}/\text{cm}^2$ , with no indication that equilibrium had been reached. These values were determined by analyzing all solutions placed in and removed from the vessels. The plutonium unaccounted for was assumed to be adsorbed on the metal walls. When the metal surfaces were descaled and the scale

solution was analyzed for plutonium, the amount of plutonium adsorbed on the stainless steel was shown to be 0.11 and 0.10  $\text{mg}/\text{cm}^2$ , the same amount as was calculated from the material-balance calculation. However, 0.12 and 0.11  $\text{mg}/\text{cm}^2$  was found on the titanium by actual analysis. It is important to note that the plutonium was actually contained in the film, since it was necessary to destroy the film to remove the plutonium. Of the total amount of plutonium used, 40% was adsorbed on the stainless steel and 35% on the titanium.

The stainless steel vessels used were made from 8-in. lengths of  $\frac{1}{4}$ -in.-dia pipe and the titanium vessels from 8-in. lengths of 0.625-in.-ID tube. With the stainless steel containers 5 ml of 1.4 *m*  $\text{UO}_2\text{SO}_4$  solution containing plutonium was used; 10 ml was used with the titanium vessels. Loose caps were placed on all vessels so that they would be exposed to the atmosphere in the autoclave. After being heated for 12 hr or more at 250°C under 80 psi  $\text{O}_2$  and 160 psi  $\text{H}_2$ , the solutions were cooled and removed along with any precipitate. This was followed by a water rinse, but no attempt was made to remove the adherent scale. This procedure was repeated 10 times for each container.

The plutonium build-up on the metal walls during these 11 cycles is shown in Fig. 72. The results are quite consistent considering the variations in the conditions, which were, primarily, as follows: (1) in runs 1-3, only oxygen pressure was used, which caused high plutonium solubility; (2) excessive evaporation caused extremely high uranyl sulfate concentrations and high plutonium solubility in runs 4, 6, and 10; (3) the plutonium concentration in the feed was 300 mg per kilogram of  $\text{H}_2\text{O}$  in runs 6-8 and only 30 mg per kilogram of  $\text{H}_2\text{O}$  in the others; (4) the uranium was reduced and hydrolyzed, which caused high acidity and high plutonium solubilities in one container in run 6 and in both stainless steel containers in runs 7-11. As a result of these variations, it was decided to discontinue this series even though

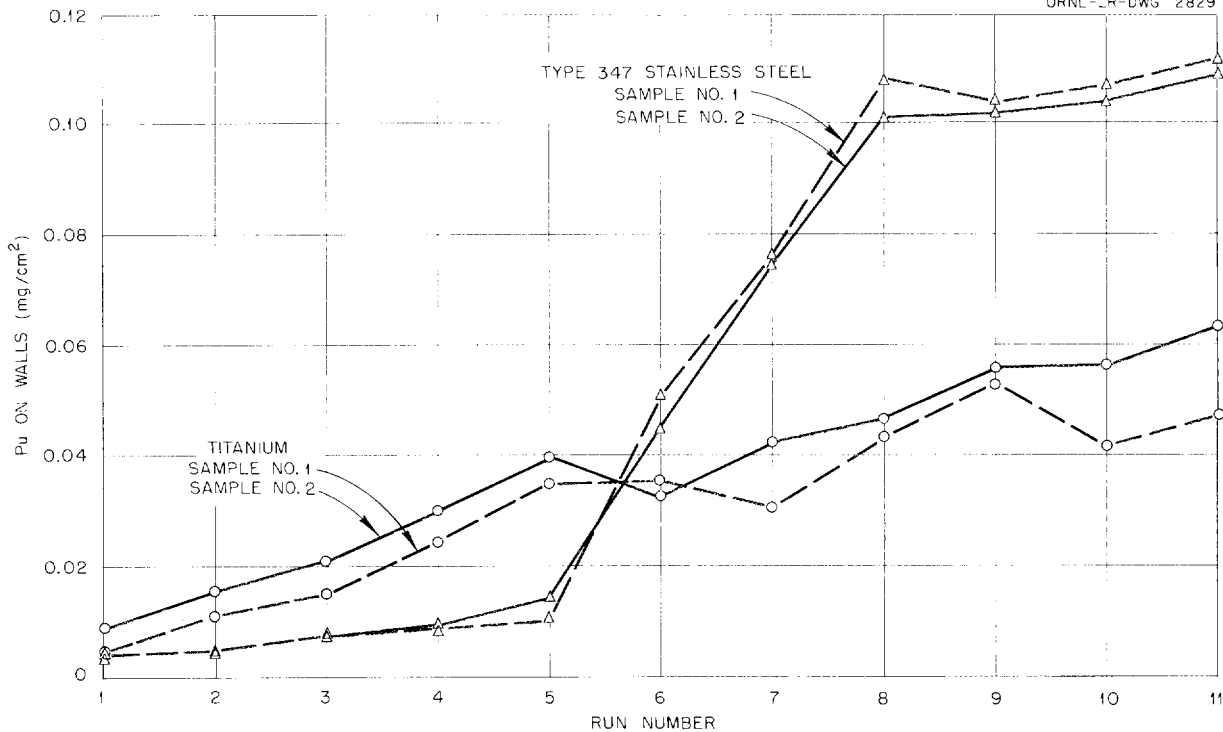


Fig. 72. Adsorption of Plutonium on Titanium and Type 347 Stainless Steel Vessel Walls. Conditions: 1.4 *m* UO<sub>2</sub>SO<sub>4</sub>; plutonium, 30 mg per kg of H<sub>2</sub>O in Runs 1 to 5 and Runs 9 to 11, and 300 mg per kg of H<sub>2</sub>O in Runs 6 to 8; solution heated at 250°C for more than 12 hr.

equilibrium had not been reached. The experience gained in these experiments should make it possible to complete a new series in which the conditions are not varied.

The data presented in Fig. 72 indicate that the rate of plutonium adsorption on type 347 stainless steel is directly proportional to the initial plutonium concentration, since about 10 times as much was adsorbed in runs 6-8, in which the initial plutonium concentration was 300 mg per kilogram of H<sub>2</sub>O, as in the other experiments, in which the initial plutonium concentration was 30 mg per kilogram of H<sub>2</sub>O. The rate of plutonium adsorption on titanium was apparently not dependent on the plutonium concentration for the two conditions studied. Another outstanding difference noted between the stainless steel and the titanium reactors was the amount of corrosion. In all cases the solutions removed from the stainless steel contained considerable quantities of precipitated corrosion products, while solutions from the

titanium vessels were clear, with only PuO<sub>2</sub> precipitated. The corrosion products from the stainless steel reactors apparently acted as good carriers for Pu(IV) and reduced the amount in solution below the solubility limit by as much as a factor of 10.

PARTICLE SIZE OF PuO<sub>2</sub>

Thermal cycling of PuO<sub>2</sub> suspensions in uranyl sulfate solution resulted in the formation of fine particles, 0.5 to 2.0 μ (see Table 36). Vigorous agitation of the solution during the heating appeared to favor smaller-particle-size formation. The observations were made on 1.35 *m* UO<sub>2</sub>SO<sub>4</sub> solutions with a plutonium content of 0.1 g per kilogram of H<sub>2</sub>O in a quartz tube.

RATE OF PuO<sub>2</sub> PRECIPITATION FROM Pu(IV) SOLUTION

When 1.35 *m* UO<sub>2</sub>SO<sub>4</sub> solutions with a Pu(IV) concentration of 0.1 or 0.2 g per kilogram of H<sub>2</sub>O

TABLE 36. EFFECT OF TEMPERATURE AND AGITATION ON PARTICLE SIZE OF  $\text{PuO}_2$  PRECIPITATED FROM 1.35 *m*  $\text{UO}_2\text{SO}_4$  SOLUTION

Treatment	Estimated Particle Size*
Heated approximated 17 hr at temperature fluctuating between 270 and 245°C; vigorous shaking twice each minute	Very fine particles, less than 0.5 $\mu$ ; chains or filaments of small particles; few aggregates of about 4.0 $\mu$
Heated approximately 16 hr at temperature fluctuating between 270 and 245°C; no shaking	1.0 to 2.0 $\mu$ ; very uniform
Heated four days at temperature fluctuating between 270 and 245°C; no shaking	Bulk of material 1.0 to 2.0 $\mu$ ; range from less than 1.0 $\mu$ to aggregates of 6 to 10 $\mu$
Heated to 270°C and immediately cooled and examined; no shaking	From approximately 1.0 $\mu$ to what appeared to be well-formed crystals of 5.0 to 10.0 $\mu$ ; aggregates up to 60 $\mu$
Heated to 270°C and immediately cooled; allowed to stand at room temperature for three days; no shaking	0.5 to 1.0 $\mu$ ; aggregates up to 30 $\mu$
Heated 64 hr at 270°C and immediately cooled; allowed to stand at room temperature for three days; no shaking	0.5 to 1.0 $\mu$ ; aggregates up to 15.0 $\mu$

\*Particle-size determinations were made by T. E. Willmarth of the Analytical Chemistry Division.

were sealed in quartz tubing and heated, the formation of solid  $\text{PuO}_2$  could be observed. The heating time necessary to produce a visible amount of  $\text{PuO}_2$  was shortened by either raising the temperature or increasing the initial plutonium concentration of the solution (Table 37). The valence state of the plutonium also affected the precipitation time [see the following section, "Rate of Precipitation of  $\text{PuO}_2$  from  $\text{Pu(VI)}$  Solutions"].

From two sets of data taken at 200°C (codes 3 and 4, Table 37) it is possible to estimate the rate of the precipitation reaction and the amount of precipitate formed, if the reaction is assumed to be first order with respect to plutonium concentration and if the time of precipitation is taken as the time at which a constant concentration of solid is present. The expression used was

$$k = \frac{1}{t} \ln \frac{a}{a-x},$$

where  $k$  is the reaction constant,  $t$  is the time (in seconds) for precipitation to be observed,  $a$  is the initial concentration of plutonium (in grams per kilogram of  $\text{H}_2\text{O}$ ), and  $x$  is the concentration of solid  $\text{PuO}_2$  present (in grams of plutonium per

kilogram of  $\text{H}_2\text{O}$ ) when precipitation was observed. When times of 6 and 2 min for plutonium contents of 0.1 and 0.2 g per kilogram of  $\text{H}_2\text{O}$ , respectively, at 200°C were used, simultaneous solution of the two equations gave a rate constant of the order of 300  $\text{days}^{-1}$  and a solid-phase plutonium concentration in the system of 0.08 g per kilogram of  $\text{H}_2\text{O}$ . It is interesting to note that no precipitate was observed when 1.35 *m*  $\text{UO}_2\text{SO}_4$  solutions with a plutonium content of 0.05 g per kilogram of  $\text{H}_2\text{O}$  were heated to 250°C.

#### RATE OF PRECIPITATION OF $\text{PuO}_2$ FROM $\text{Pu(VI)}$ SOLUTIONS

When 1.35 *m*  $\text{UO}_2\text{SO}_4$  solutions which contained  $\text{PuO}_2\text{SO}_4$  in solution were heated to 250°C under an atmosphere of air, a precipitate of  $\text{PuO}_2$  was observed. Several samples gave close agreement on a precipitation time of 160 sec at 250°C when the initial plutonium concentration was 0.1 g per kilogram of  $\text{H}_2\text{O}$  and 82% of the plutonium was in the hexavalent state. If it is again assumed that a first-order rate expression is applicable and that a solid-phase  $\text{PuO}_2$  content in the system equivalent to a plutonium concentration of 0.08 g per

TABLE 37. EFFECT OF TIME, TEMPERATURE, VALENCE STATE, AND CONCENTRATION ON THE RATE OF PuO<sub>2</sub> PRECIPITATION FROM 1.35 *m* UO<sub>2</sub>SO<sub>4</sub> SOLUTION

Temperature (°C)	Initial Plutonium Concentration of Solution (g per kg of H <sub>2</sub> O)		Precipitation Time	Code
	Pu(IV)	Pu(VI)		
100	0.1	0	>6 hr	1
150	0.1	0	>1 hr	2
200	0.1	0	6 min	3
200	0.2	0	2 min	4
250	0.1	0	<60 sec	5
250	0.018	0.082	160 sec	6
200	0.1	0	110 sec	7
250	0.1	0	55 sec	8
250	0.004	0.096	240 sec	9

kilogram of H<sub>2</sub>O was the minimum amount observable, a rate constant of the order of 500 days<sup>-1</sup> is obtained from the data for code 6 of Table 37. The rate constant for code 9 (Table 37) was calculated as about 500 days<sup>-1</sup>. For the rate of PuO<sub>2</sub> precipitation from Pu(IV) solutions at 250°C, the data of code 8 gave a rate constant of about 2000 days<sup>-1</sup>. These rate constants are indicative of rapid reactions, compared with the processing period of 0.5 day, and lead to the conclusion that the amount of plutonium in solution in the blanket under dynamic conditions will be less than 1 mg per kilogram of H<sub>2</sub>O in excess of the equilibrium solubility value.

NEPTUNIUM CHEMISTRY

The solubility of neptunium in 1.2 *m* UO<sub>2</sub>SO<sub>4</sub> at 275°C under pressures of 120 psi O<sub>2</sub> and 240 psi H<sub>2</sub> is more than 100 mg per kilogram of H<sub>2</sub>O. Attempts to hold the neptunium in the tetravalent state with 0.02 *M* FeSO<sub>4</sub> and to precipitate neptunium oxide have been unsuccessful. Apparently the ferrous ion and Np(IV) are both oxidized during the heating period.

Analytical methods for plutonium valence determination were unsatisfactory for neptunium. F. L. Moore of the Analytical Chemistry Division reports that three reliable methods are available for total neptunium analysis, and a TTA extraction method for Np(IV) gave good precision but has not been checked for absolute accuracy. When neptunium

was spiked into 1.35 *m* UO<sub>2</sub>SO<sub>4</sub> to the extent of 100 mg per kilogram of H<sub>2</sub>O, 84% was recovered after the solution had stood about one day and 10% after it had stood approximately two weeks. This indicates that in uranyl sulfate solution in contact with atmospheric oxygen Np(IV) is oxidized at room temperature.

DETERMINATION OF REACTOR NEUTRON-CAPTURE CROSS SECTION OF Np<sup>239</sup>

A preliminary value of <100 barns (see p 168) for the cross section of Np<sup>239</sup> was calculated from results obtained by spontaneous-fission counting of samples of plutonium isolated from irradiated uranium. Uranium was irradiated in the LITR for 0.5, 1, 2, and 4 days, and the plutonium was recovered and purified before being transferred to the Chemistry Division. The quantities of plutonium recovered from the four batches of uranium were 3.2, 7.4, 11.0, and 8.9 mg, respectively. Uranium was also irradiated for 8 and 16 days, but these specimens will have to cool two to three months before being processed.

BLANKET-PROCESSING FLOW SHEET

A preliminary process and equipment flow sheet for separating plutonium oxide from the U<sup>238</sup> blanket solution is given in Fig. 73. Work on this phase of the problem is being coordinated with the development of the process for removal of fission products from the reactor fuel.

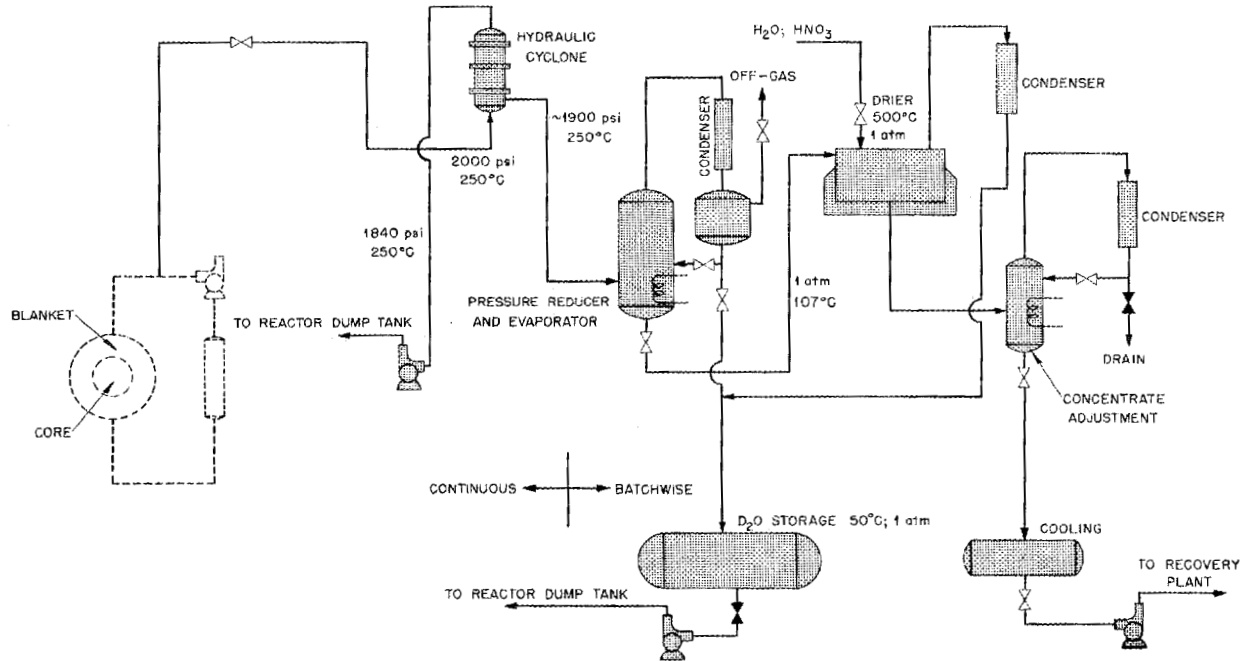


Fig. 73. Preliminary Flow Sheet for HRT Blanket Process.

THERMAL-BREEDER FUEL AND BLANKET PROCESSING

D. E. Ferguson	W. K. Eister	H. E. Goeller	W. E. Unger
R. A. McNees	E. O. Nurmi	W. L. Carter	
R. G. Mansfield	M. E. Whatley	A. M. Rom	
S. Peterson	R. W. Horton	H. O. Weeren	
H. C. Trippe	J. L. Patton	R. B. Lindauer	
W. B. Howerton	C. C. Williams	F. C. McCullough	
	V. L. Fowler		

Long-Range Planning Group

R. J. Klotzbach	A. T. Gresky	E. D. Arnold
-----------------	--------------	--------------

The chemical processing of the fuel solution of a thermal breeder, as presently conceived, consists in concentrating the insoluble fission and corrosion products produced in the fuel into about a 100-liter volume of fuel solution with a hydroclone liquid-solid separator. This solids removal will be on a one-day cycle. The 100 liters of fuel containing the insoluble fission products will be sent through the blanket processing plant (Thorex plant) each day for recovery of D<sub>2</sub>O and U<sup>233</sup>. This scheme of processing will adequately control the build-up of neutron poisons and long-lived fission products in the reactor fuel.

During this period, a cost study was made of the chemical processing of the thermal breeder which indicated that the actual cost of chemical processing, for both fuel and blanket, will be about 0.8 mill/kwhr of electricity produced. The chemistry of iodine, iron, and three rare-earth fission products in the reactor fuel was studied. A preliminary evaluation of the Dorr TM-3 hydroclone liquid-solid separator was completed.

CHEMICAL FLOW SHEET

As initially conceived, the slurry concentration method for removing insoluble fission products from the core solution of a homogeneous reactor would operate on a 23-day cycle based on poison removal alone. There are several advantages to shortening this process time cycle to about one day.

First, the knowledge gained from the HRE shut-down and decontamination indicates that only about one day's production of fission products from the K-23 reactor would remain in solution, with the exception of comparatively soluble elements like the rare earths and cesium. Processing the entire

core every day would then hold the insoluble fission-product build-up in the reactor to about two days' production instead of 24. Such a tenfold reduction in fission-product concentration will improve the neutron economy of the system significantly. In addition, it seems desirable to minimize the amount of solids in the fuel solution to avoid erosion.

Secondly, processing on a one- instead of a 23-day cycle would decrease by an order of magnitude the long-lived fission products present in the high-pressure system and the resultant biological hazards associated with a fuel leak.

Finally, efficient operation of hydroclone liquid-solid separators requires a large liquid throughput. This must be provided either by a feed to the hydroclone directly from the reactor or by recycling liquid through the hydroclone system. The recycling of solution through the hydroclone system presents no obvious advantage, and it appears that the one-day cycle would not significantly increase the cost of this operation.

In view of these advantages it seems reasonable at this time to plan for the hydroclone processing scheme to operate on a one-day cycle instead of the 23-day cycle previously suggested (Fig. 74). This scheme of processing will control the fission-product poisons at 5.6% or less and minimize the build-up of long-lived fission-product radioactivity.

FUEL COST FOR THERMAL BREEDER REACTOR

An estimate of costs for fuel and chemical processing for a three-reactor power station using the

SECRET  
ORNL-LR-DWG 2831

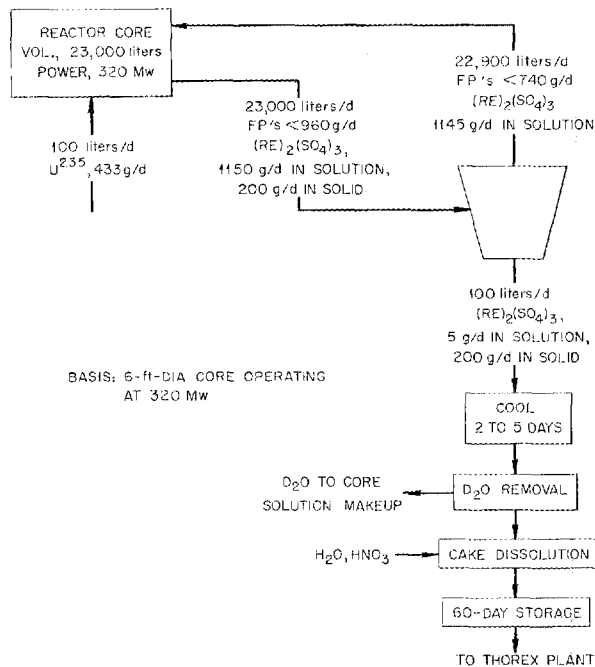


Fig. 74. Schematic Flow Sheet for Thermal Breeder (K-23) Fuel Processing. Basis: 6-ft-dia core operating at 320 Mw.

proposed K-23 system<sup>6</sup> was made. The process considered included removal of the insoluble high-cross-section fission products from the uranyl sulfate core solution by liquid-solid centrifugal separators and solvent-extraction processing of the combined core solution and blanket slurry by the Thorex process. Results indicated unit costs, including inventory charges, to be \$10.90 per megawatt-day of heat or 1.96 mills per kilowatt-hour of electricity produced (Table 38). Of this 1.96 mills/kwhr, the chemical processing cost 0.8 mill; the remainder is contributed almost completely by inventory charges on D<sub>2</sub>O and U<sup>233</sup> in both the reactor and chemical plant. An interesting fact learned from this study is that the net cost of the electricity produced is increased only 0.13 mill/kwhr and that the total processing cost is only \$1000 per day more if the use of hydroclones

<sup>6</sup>E. D. Arnold, A. T. Gresky, A. R. Irvine, and R. J. Klotzbach, *Chemical Processing or Fuel Costs Associated with a Power Station of Three K-23 Reactors*, ORNL-1761 (in preparation).

is eliminated (Table 39). However, the use of hydroclones would result in a saving over the reactor lifetime for a three-reactor station of more than \$2,000,000, and their development would be justified in any case for control of biologically hazardous levels of radioactivity. Thorex processing alone does not significantly reduce the biological hazard of the core activities, but hydroclones would reduce the long-lived gamma emitters by a factor of at least 30; the amount of fission products removed by the hydroclones was estimated conservatively in the study. The reactor poison value of 5.6% used in the calculations is near the optimum for processing both with and without hydroclones.

The total fixed investment in the 200-kg/day Thorex plant was estimated at \$7,000,000 on the basis of present-day experience and philosophy of processing and construction. Use of the Hope philosophy in this case would conceivably reduce the above cost by a significant fraction. The annual operating cost, with contingency, was \$1,470,000. Daily costs for Thorex chemical processing were approximately \$3000 for amortization and \$4000 for operation. These costs amounted to less than 40% of the total fuel cost, as indicated in the unit electrical cost above.

#### CALCULATION OF RADIATION HAZARD OF REACTOR FUEL

Calculations of radiological hazards of activities produced during operation of homogeneous reactors indicate that I<sup>131</sup>, Ba<sup>140</sup>-La<sup>140</sup>, and total rare earths are biologically the most dangerous activities, especially where short-term exposures involving a leak are considered.<sup>7</sup> The lungs, thyroid, and gastrointestinal tract are the organs most affected. The I<sup>131</sup> is especially important since it may be expected to concentrate in the gas phase and be readily air-dispersible in case of stream leaks and it would receive further rapid concentration in the human thyroid. The relatively lesser importance of Sr<sup>89</sup> and Sr<sup>90</sup>-Y<sup>90</sup> as shown by this study, in contrast to their importance as indicated by other studies, probably reflects a lack of attention in this case to the selectivity of geochemical cycles and the effects of stream pollution or life

<sup>7</sup>E. D. Arnold and A. T. Gresky, *Relative Biological Hazards Associated with Radiation Expected with Homogeneous Reactors K-23 and K-49*, ORNL-1765 (in preparation).

## HRP QUARTERLY PROGRESS REPORT

TABLE 38. FUEL COSTS FOR TWO-REGION BREEDER REACTOR OPERATED AT 250°C WITH THORIUM OXIDE SLURRY BLANKETS CONTAINING 1000 g OF THORIUM PER LITER

Three-Reactor Station (320 Mw of Electricity)	
Concentration of U <sup>233</sup> in core, g/liter	1.24
Fission-product poison level in core, $\frac{\text{neutrons absorbed in poison}}{\text{U}^{233} \text{ atoms consumed in core}}$	0.056
Breeding gain, $\frac{\text{U}^{233} \text{ atoms produced}}{\text{U}^{233} \text{ atoms consumed in core}} - 1$	0.144
Total power	
Mw of heat	1,392
Net Mw of electricity	324
Total U <sup>233</sup> + Pa <sup>233</sup> requirements, kg	463.5
Total thorium requirements, metric tons	63
Total D <sub>2</sub> O requirements, metric tons	145.5
Cost, dollars/day	
Thorium consumption	39
Hydroclone processing	210
Thorex processing of core and blanket and D <sub>2</sub> O recovery	
Operation	4,033
Amortization	3,057
Uranium and thorium losses	39
Uranium inventory at 12%	4,284
Thorium inventory at 12%	669
D <sub>2</sub> O inventory and losses at 17%	5,970
Total cost at 12% inventory charges	15,220
Value of excess U <sup>233</sup> produced	3,300
Net Cost (dollars/Mwd of heat) at 12% inventory charges	10.90
Net Cost (mills/kwhr of electricity) at 12% inventory charges	1.96

cycles of plants and animals in the long-term considerations of fission-product dispersal. This study points out a need for control during chemical processing of I<sup>131</sup> as well as of the rare earths, strontium, and other fission products already contemplated.

### FISSION-PRODUCT AND CORROSION-PRODUCT CHEMISTRY

During the past quarter, studies on fuel processing for the aqueous homogeneous thermal breeder have been directed toward determining the behavior of rare-earth fission products under simulated re-

actor conditions. In addition, attention has been given to the chemistry of iron, a corrosion product, and to iodine, which adds to the radiological hazards associated with this reactor.

### Rare Earths

In order to duplicate more nearly the dynamic conditions that will exist in the core system of a homogeneous reactor, equipment was constructed which made it possible to add rare-earth-bearing fuel solution to a hot, pressurized vessel while filtered samples of the solution in the vessel were being taken. This equipment was used in determin-

TABLE 39. COMPARISON OF FUEL COST WITH AND WITHOUT HYDROCLONES

Basis: 5.6% neutron poisons in core  
Three-reactor station, 450 Mw each

Item	Cost (dollars/day)	
	Hydroclones + Thorex	Thorex Only
Thorium consumption	39	39
Hydroclone processing	210	
Thorex processing and D <sub>2</sub> O recovery		
Operation	4,033	4,353
Amortization	3,057	3,057
Uranium and thorium losses	39	39
Uranium inventory at 12% per year	4,284	4,962
Thorium inventory at 12% per year	669	669
D <sub>2</sub> O inventory and losses at 17% per year	5,970	6,170
Value of excess U <sup>233</sup> produced	3,080	3,080
Net cost	15,220	16,210
Net cost of electricity, mills/kwhr	1.96	2.09

ing the equilibrium solubilities of individual rare-earth sulfates while a mixture of rare earths approximating that obtained in fission was being precipitated. Data were obtained for cerium, neodymium, and europium.

**Cerium Sulfate.** The equilibrium solubility of cerium sulfate was found to be less than 0.01 g per kilogram of H<sub>2</sub>O when 500 ml of a simulated fuel solution, 0.02 *m* UO<sub>2</sub>SO<sub>4</sub>-0.005 *m* H<sub>2</sub>SO<sub>4</sub>, containing 1 g of mixed rare-earth sulfates (48% Ce, 24% La, 19% Nd, 6% Pr, 2% Sm, 1% others) per kilogram of water and traced with Ce<sup>144</sup>, was heated to 270°C. During five days of operation, 400 ml of feed identical with the initial charge was added in small lots to the vessel, and 600 ml of filtered solution was withdrawn as samples. The cerium activity in solution remained essentially constant during this period. Assignment of an exact value to the cerium sulfate equilibrium solubility is difficult since the filtration rate definitely affected the activity level in the filtered sample. Rapid filtration rates gave high solubility values, while at slow rates low solubility was indicated. At sufficiently slow sampling rates (0.3 ml/min or less per square centimeter of filter area), the solubility values obtained were between 0.003 and 0.004 g per kilogram of H<sub>2</sub>O.

**Europium Sulfate.** The experiment just described was repeated at 280°C but with Eu<sup>155</sup> as the tracer instead of Ce<sup>144</sup>. From the composition of the mixed rare-earth sulfates (which contained less than 0.5% europium sulfate) in the feed and the activity of the heated and filtered solution (40% of the initial Eu<sup>155</sup> remained in solution), the equilibrium solubility of Eu<sub>2</sub>(SO<sub>4</sub>)<sub>3</sub> was calculated to be not more than 0.002 g per kilogram of H<sub>2</sub>O under these conditions.

**Neodymium Sulfate.** When a simulated fuel solution containing mixed rare-earth sulfates [33% Nd<sub>2</sub>(SO<sub>4</sub>)<sub>3</sub>] in the amount 0.1 g per kilogram of H<sub>2</sub>O and traced with Nd<sup>147</sup> was heated to 275°C in the equipment previously described, 95% of the tracer activity remained in solution. When more fuel solution containing larger amounts of neodymium sulfate was added to the reaction vessel, no large activity removal was observed until the neodymium sulfate concentration had reached 0.07 g per kilogram of H<sub>2</sub>O. Further addition of neodymium sulfate did not change the concentration of that salt in solution above 0.09 g per kilogram of H<sub>2</sub>O, and the most frequently observed value was 0.07 g per kilogram of H<sub>2</sub>O.

It should be noted that, under the conditions just described, 10 times as much neodymium as other

## HRP QUARTERLY PROGRESS REPORT

rare earths combined was being added to the system and precipitated. This is one possible reason for the apparently much greater solubility of neodymium sulfate as compared with cerium and europium sulfates. Even so, the solubility is less than half that previously reported<sup>8</sup> for neodymium sulfate alone. Repetition of the experiment with the proper ratio of neodymium to other rare earths should result in a more reliable equilibrium neodymium sulfate solubility value.

### Iron

When simulated fuel solutions containing various amounts of iron in solution and traced with  $\text{Fe}^{55}$ - $\text{Fe}^{59}$  were heated under an atmosphere of oxygen to 250°C and filtered, only 0.0004 g of iron per kilogram of  $\text{H}_2\text{O}$  remained in solution. This amount of iron in solution would contribute much less than 0.001% poison to the K-23 reactor.

### Iodine

Frequent processing for removal of iodine from the core solution of a homogeneous reactor is desirable for several reasons. Chief among these are the biological hazards associated with radioactive iodine, the poison contribution of  $\text{I}^{131}$  to the core system, and the possible deleterious effect of iodine on corrosion in the core system. Preliminary experiments have shown that when simulated core solutions containing either  $\text{I}_2$ ,  $\text{KI}$ , or  $\text{HIO}_3$  at a concentration of  $10^{-4}$  M were sealed in quartz tubes under an atmospheric pressure of oxygen and heated to 250°C, free iodine was found to be present after cooling in all samples. When untreated metal samples such as type 347 stainless steel, titanium, or zirconium were present, attack on the metal surfaces was evident. In those cases where zirconium was present, uranium and iodine were completely removed from solution and a heavy, black, loose corrosion scale was evident.

## ENGINEERING STUDIES

### Hydroclone Separation Equipment

Hydroclone liquid-solid separators are being investigated for continuous removal of insoluble fission-product poisons from reactor-fuel solutions and for continuous removal of  $\text{PuO}_2$  from uranium blanket solutions.

Tests are being made on the Dorr TM-3 hydroclone unit, which is reported to separate 2- $\mu$ -dia particles of clay from water. If allowances are made for the decreased viscosity of solutions at high temperatures, at the proposed operating temperature of the homogeneous reactors such a unit should remove particles smaller than 1  $\mu$ . The TM-3 unit contains three stages or banks of hydroclones arranged in series to give maximum clarification. Each stage consists of 32 hydroclones in parallel, each with an inside diameter of 0.4 in. In the commercial unit the hydroclones are of molded Bakelite, the gaskets for the individual hydroclones and between the stages are of soft rubber, and the body of the unit, which provides the manifolding arrangement to give the desired flow pattern, is of stainless steel. A similar unit for use in a reactor would probably be constructed of titanium.

In studies on a single stage of a disassembled TM-3 unit, the pressure drop across the stage varied approximately as the square of the flow rate. Variation in the amount of liquid reporting to the underflow, up to 20% of the feed rate, had little effect on the pressure drop. At 25 gpm, a good operating flow rate, the pressure drop was 35 psi. There appeared to be a minimum flow rate, 15 to 20 gpm, below which the performance of the unit dropped off and above which there was very little increase in effectiveness (Table 40).

Thorium oxide was the solid chosen for these studies because its specific gravity is of the same order of magnitude as that of  $\text{PuO}_2$  and because it can be chemically analyzed by methods standard in our analytical laboratories. A very dilute slurry of thorium oxide was pumped through the single stage, the overflow and underflow being returned to a feed tank, which usually contained about 30 gal of liquid.

Slurries prepared from thorium oxide classified by two different methods were used. One slurry was prepared from nominal 8.5- $\mu$  material that had been classified by settling and decanting. With this material, 75% of the solids reported to the underflow from the hydroclones over a feed range from 15 to 38 gpm at 20% liquid to underflow (Table 40). However, under microscopic examination this slurry was seen to contain considerable fines, probably 20% of the material having a particle size of 1  $\mu$  or smaller. With a slurry of nominal 4.5- $\mu$  particles, 50 to 60% of the solids reported to the underflow under the

<sup>8</sup>W. K. Eister *et al.*, *HRP Quar. Prog. Rep.* Apr. 30, 1954, ORNL-1753, Fig. 128, p 178.

TABLE 40. PERFORMANCE OF A SINGLE STAGE OF THE TM-3\* HYDROCLONE IN REMOVING ThO<sub>2</sub> FROM A WATER SLURRY

Feed Rate (gpm)	Per Cent Liquid to Underflow	Per Cent Solids to Underflow	Concentration Ratio**	Material Balance (% error)
Nominal*** Particle Size, 8.5 $\mu$				
38	18.0	86	4.8	5
	14.0	71	5.1	19
30	20.0	89	4.4	17
	16.0	86	5.4	7
	12.0	86	7.1	3
	8.3	84	10.0	0
20	20.0	85	4.2	22
	16.0	83	5.2	4
	12.5	70	5.6	15
	10.0	67	6.7	21
15	20.0	79	3.9	2
	13.3	69	5.2	1
	10.0	55	5.5	13
7.5	20	47	2.3	0
Nominal*** Particle Size, 4.5 $\mu$				
38	18	59	3.2	4
	14	46	3.3	11
35	20.0	61	3.1	5
	16.0	59	3.7	13
	12.0	51	4.3	7
	8.0	33	4.1	3
	6.0	25	4.1	13
	2.0	8	4.1	5
20	20.0	42	2.7	3
	16.0	50	3.2	2
	12.0	47	3.9	7
	8.0	43	5.3	13
	4.0	13	3.3	9
	2.0	8	4.0	14
10	22.0	27	1.2	1
	21.6	22	1.0	2
	12.0	17	1.4	7

\*32 unit hydroclones in parallel, each 0.4 in. in inside diameter.

\*\*Concentration of thorium oxide in underflow divided by that in feed.

\*\*\*The nominal 8.5- $\mu$  material was prepared by settling and decanting and showed, under microscopic observation, considerable fines, probably 10 to 20% being 1  $\mu$  or smaller. The nominal 4.5- $\mu$  material was prepared by air elutriation, but 75% was less than 2  $\mu$ , 45% less than 1.2  $\mu$ , and 35% less than 1  $\mu$ , as analyzed by an activation method.

best conditions of flow rates. However, 75% of the thorium oxide was found to be less than  $2 \mu$  in size, 45% less than  $1.2 \mu$ , and 35% less than  $1 \mu$ . Since hydroclone liquid-solid separators act as classifiers, it is safe to assume that the hydroclones were removing a high percentage of the material greater than  $1.2 \mu$  in diameter. Because of the importance of particle size in determining performance of equipment, methods of sizing materials are being investigated further (see the following section, "Methods for Sizing Samples").

Considerable difficulty was experienced in obtaining good material balances with this system. The errors (Table 40) are due to sampling errors in addition to normal analytical inaccuracies.

To allow for the possibility that the TM-3 design will not provide adequate separation in reactor processing, studies are under way to design a hydroclone of higher efficiency. The work is in its early stages and has been primarily on hydroclones of cylindrical design. So far, no design as good as the TM-3 has been assembled.

### Methods for Sizing Samples

Of the various methods available for sizing particles in the region of 1 to  $15 \mu$  diameter, the most successful one tried is a liquid-elutriation technique. The method consisted in metering a 0.005 M solution of sodium pyrophosphate through an open standpipe into the bottom of a 4-in.-dia glass column. Particles small enough to be lifted by the velocity of the rising liquid were carried out with the overflow, while the large particles remained in the column. The desired particle size was obtained by setting the liquid flow rate at values determined from Stokes' law. A tendency for the heavy particles to settle and pack at the bottom of the column was overcome by an air lift which took liquid from about 6 in. above the bottom of the column and circulated it through the standpipe to the bottom of the column. Approximately 1.5 kg of thorium oxide has been treated by this method for removal of particles less than 1 and over  $15 \mu$  in diameter, and an 11- to  $15\text{-}\mu$  cut has been isolated.

Results with an air-elutriation technique, using commercial equipment, indicated that a particle separation would be effected with this. However,

it was difficult to prevent degradation of samples. Sedimentation methods are slow and laborious.

Microscopic inspection of the sized samples shows that the large particles are composed of smaller crystals which have either grown together or have been fused. These large particles have been found to degrade under shear stress. The extent of the degradation that occurs in a hydroclone has not yet been determined. To allow for the possibility that this degradation might be intolerable, other materials, such as the mineral galena, are being considered as a substitute for  $\text{ThO}_2$  for testing hydroclones.

### High-Pressure Test Loop

A loop to operate at  $250^\circ\text{C}$  and 1000 psig has been designed and is under construction. It will be used to test devices for sampling the loop contents under operating conditions so that physical properties of the rare-earth sulfates and other solids expected to be formed in the homogeneous reactor core may be determined. Since the solubilities of these salts vary inversely with the temperature, sampling at reactor conditions is necessary. Once the sample of solids has been taken and separated from the solution, the pressure on and temperature of the solids may be allowed to fall before the particles are examined.

### Process-Design Studies

A tentative flow sheet for the HRT core process is given in Fig. 75. It is desirable to simulate in the HRT core processing equipment conditions anticipated in the ultimate K-23 reactor processing system. However, the relative volume flow rates of the HRT are so small that equipment for continuous operation becomes impracticably small. It is now planned to employ standard equipment about one-half the K-23 scale, operated intermittently. In this scheme a 1-hr solids separation will remove the fission products accumulated during the preceding 30-hr period of reactor operation.

Shielded cells for chemical processing facilities for the HRT core and blanket, tunnels for the associated auxiliary equipment, samplers, instruments, and operating areas will be provided by expanding the present HRE building (Fig. 76).

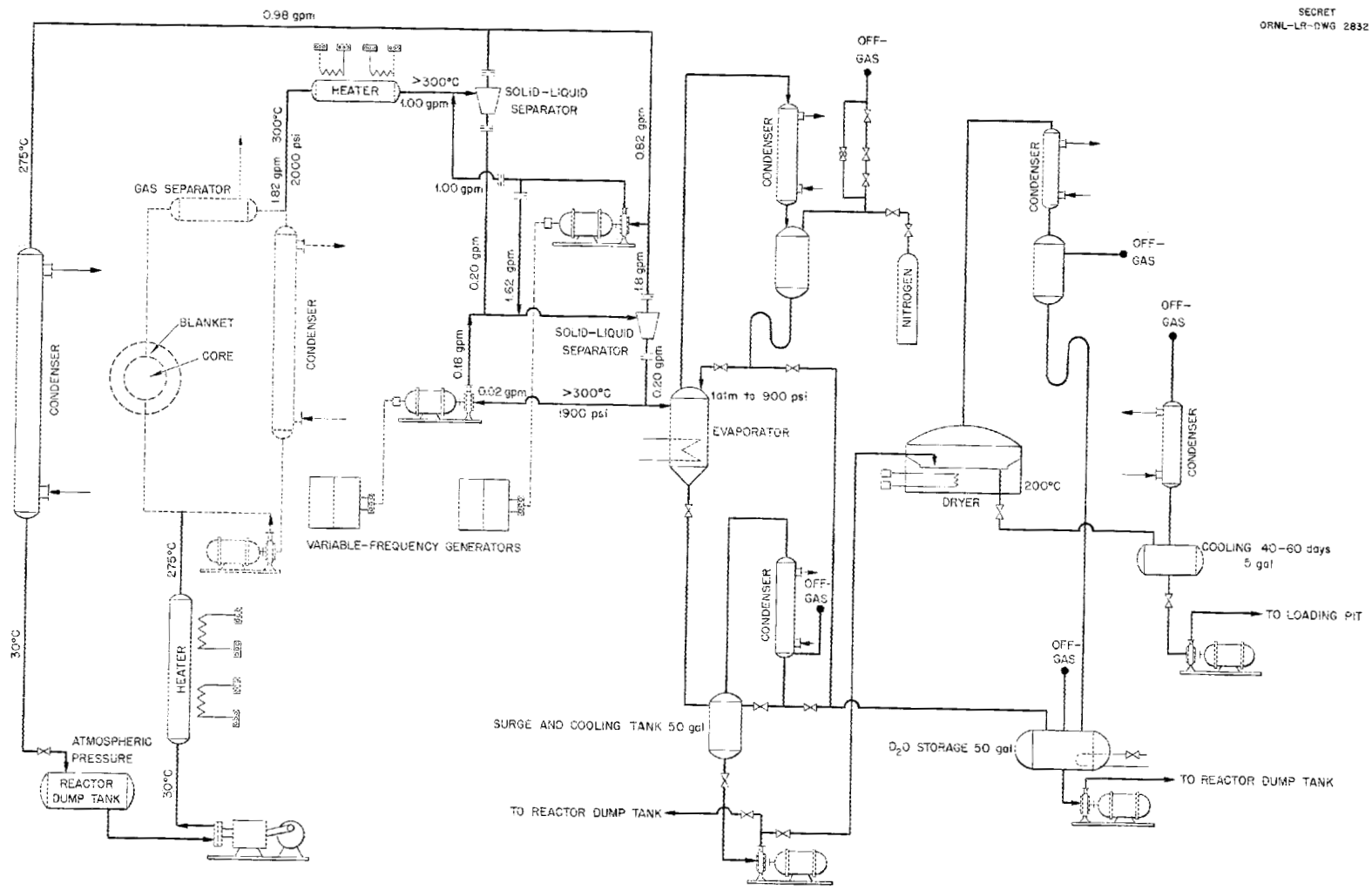


Fig. 75. Tentative Flow Sheet for HRT Core Process.

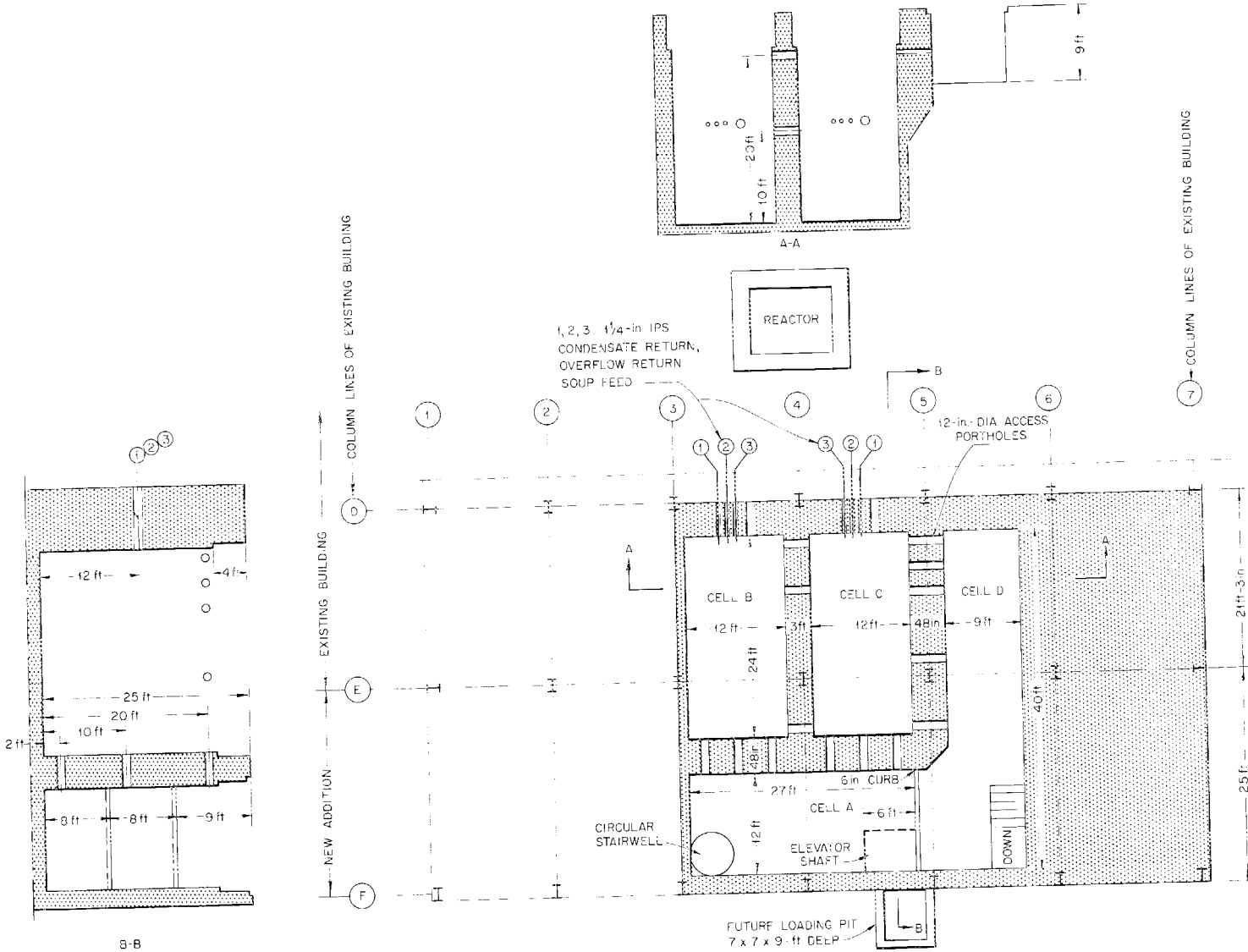


Fig. 76. Chemical Processing Facilities for HRT Core and Blanket.

SUMMARY OF WORK BY VITRO LABORATORY<sup>9</sup>CaF<sub>2</sub> PROCESS

Removal of fluoride from a CaF<sub>2</sub>-column effluent by addition of Th(SO<sub>4</sub>)<sub>2</sub> to precipitate ThF<sub>4</sub> and filtration at 100°C gave a product with a fluoride content of 0.076 g per kilogram of H<sub>2</sub>O and a thorium content of 0.19 g per kilogram of H<sub>2</sub>O. The filtrate would be subsequently heated to 275 to 300°C and filtered to remove the calcium as calcium sulfate. Filtration at a higher temperature to remove fluoride and calcium simultaneously would not be satisfactory. When solid ThF<sub>4</sub> was contacted with a simulated fuel solution and filtered at 275°C, the filtrate had a fluoride content of 0.53 g per kilogram of H<sub>2</sub>O and a thorium content of 0.02 g per kilogram of H<sub>2</sub>O. Incorporation of the separate ThF<sub>4</sub> filtration step increases the cost of the process 3.2%, or from 19 cents to 19.6 cents per gram of uranium processed.

## RARE-EARTH SULFATE SOLUBILITY

A comparison of rare-earth sulfate solubility data obtained in quartz and in stainless steel containers showed that the container material did not affect the results.

The effect of precipitating a mixture of rare-

earth sulfates on the solubility of an individual rare earth was shown to be different for various rare earths (Table 41). The solubility of Ce<sub>2</sub>(SO<sub>4</sub>)<sub>3</sub> at 280°C when a commercial mixture of rare-earth sulfates containing 50% Ce<sub>2</sub>(SO<sub>4</sub>)<sub>3</sub> was being precipitated from a simulated fuel solution was 0.02 g per kilogram of H<sub>2</sub>O, less than one-third the solubility of pure Ce<sub>2</sub>(SO<sub>4</sub>)<sub>3</sub> (0.07 g per kilogram of H<sub>2</sub>O). When a mixture of rare-earth sulfates containing 57% Nd<sub>2</sub>(SO<sub>4</sub>)<sub>3</sub> was heated to 280°C in a simulated fuel solution, the solubility of Nd<sub>2</sub>(SO<sub>4</sub>)<sub>3</sub> was the same as for pure Nd<sub>2</sub>(SO<sub>4</sub>)<sub>3</sub>, or 0.14 g per kilogram of H<sub>2</sub>O. However, when the rare-earth mixture contained only 15% Nd<sub>2</sub>(SO<sub>4</sub>)<sub>3</sub>, the solubility of this material was only 0.06 g per kilogram of H<sub>2</sub>O at 280°C. When a mixture of rare-earth sulfates containing 20% Eu<sub>2</sub>(SO<sub>4</sub>)<sub>3</sub> was heated in simulated fuel solution, the solubility of Eu<sub>2</sub>(SO<sub>4</sub>)<sub>3</sub> was 0.06 g per kilogram of H<sub>2</sub>O at 280°C and 0.04 g per kilogram of H<sub>2</sub>O at 310°C.

A simulated fuel solution containing 40 g of mixed rare-earth sulfates per kilogram of solution was heated to 300°C for 1 hr and filtered. A significant portion of the precipitated sulfates was attached to the wall of the container. Thus this behavior must be considered in any process involving the addition of rare-earth sulfates to a processing stream and subsequent followed by heating.

<sup>9</sup>Vitro Laboratory Quar. Prog. Rep. Apr. 1 to June 30, 1954, KLX-1722 (July 30, 1954).

TABLE 41. SOLUBILITY OF RARE-EARTH SULFATES IN SIMULATED FUEL SOLUTION AT 280°C

Batch precipitation of rare earths as indicated

Rare-Earth Sulfate	Solubility (g per kg of H <sub>2</sub> O)	Source of Rare Earths
Ce <sub>2</sub> (SO <sub>4</sub> ) <sub>3</sub>	0.02	Commercial rare-earth mixture*
Ce <sub>2</sub> (SO <sub>4</sub> ) <sub>3</sub>	0.07	Pure Ce <sub>2</sub> (SO <sub>4</sub> ) <sub>3</sub>
Nd <sub>2</sub> (SO <sub>4</sub> ) <sub>3</sub>	0.14	Pure Nd <sub>2</sub> (SO <sub>4</sub> ) <sub>3</sub>
Nd <sub>2</sub> (SO <sub>4</sub> ) <sub>3</sub>	0.14	Commercial rare-earth mixture spiked with Nd <sub>2</sub> (SO <sub>4</sub> ) <sub>3</sub> to give final Nd <sub>2</sub> (SO <sub>4</sub> ) <sub>3</sub> concentration of 57%
Nd <sub>2</sub> (SO <sub>4</sub> ) <sub>3</sub>	0.06	Commercial mixture adjusted to give 15% Nd <sub>2</sub> (SO <sub>4</sub> ) <sub>3</sub>
Eu <sub>2</sub> (SO <sub>4</sub> ) <sub>3</sub>	0.06	Commercial mixture plus Eu <sub>2</sub> (SO <sub>4</sub> ) <sub>3</sub> to give 20% Eu <sub>2</sub> (SO <sub>4</sub> ) <sub>3</sub>

\*Commercial rare-earth mixture: 48% Ce<sub>2</sub>(SO<sub>4</sub>)<sub>3</sub>, 24% La<sub>2</sub>(SO<sub>4</sub>)<sub>3</sub>, 19% Nd<sub>2</sub>(SO<sub>4</sub>)<sub>3</sub>, 6% Pr<sub>2</sub>(SO<sub>4</sub>)<sub>3</sub>, 2% Sm<sub>2</sub>(SO<sub>4</sub>)<sub>3</sub>, 1% others.

#### IODINE REMOVAL

When one volume of silver-impregnated Alundum pellets was contacted for 3 min with 20 volumes of simulated fuel solution with an  $I_2$  content of

0.075 g per kilogram of  $H_2O$  at 90 to 100°C, the iodine was completely removed. Precipitated silver iodide was found partly adhering to the pellets and partly as a fine sediment in the solution.

Part VI

SUPPORTING CHEMICAL RESEARCH



## RADIATION CORROSION STUDIES

S. F. Clark  
H. O. Day  
H. A. Fisch  
B. O. Heston  
C. H. Secoy  
M. D. Silverman  
H. H. Stone  
L. F. Woo  
W. C. Yee

### IN-PILE EXPERIMENTS

Since the introduction of the technique for rocking in-pile bombs, six experimental runs have been completed, three of them during the quarter now ending. All runs were made in type 347 stainless steel bombs, used the same solution and the same percentage fill, and gave practically the same volume-to-surface ratio. (The solution was 0.17 M  $\text{UO}_2\text{SO}_4$ , 0.01 M  $\text{CuSO}_4$ , the percentage fill (cold) was 67%, and the test temperature was 250°C. During in-pile exposures the power density in the solution was 6.4 kw/liter.) Four of the six runs were carried out in the same manner, but the last two were varied by heating the bomb and contents outside the reactor until the initial rapid rate of oxygen absorption was complete, when it was assumed that a film had been formed and that further corrosion would have to take place by transfer through the film or as the result of spalling and subsequent attack on the fresh surface.

A plot of oxygen consumption as a function of time is shown in Fig. 77, where log corrosion is plotted against log time. This graph shows that the following features are common to all runs: (1) an initial rapid rate, (2) a plateau of much lower rate, and (3) a sharply rising curve having practically the same slope as the initial portion. It will be seen that step 2 has longer duration in the last two runs than in the first four. A typical out-of-pile run is also plotted in Fig. 77, and it, too, shows features 1 and 2; feature 3, however, is not so pronounced as for the in-pile tests.

### OUT-OF-PILE EXPERIMENTS

Thirteen out-of-pile experiments have been completed during this quarter, and others have been initiated. Additional experiments of a qualitative nature, intended to indicate the possibility of obtaining information from a more carefully controlled experiment, were also carried out. For example, some pin specimens were heated for about 15 hr in a previously used bomb containing a solution to which potassium dichromate had been

added. The film on the pin was examined and appeared to be somewhat different from that being obtained in loadings which did not contain chromate. It seemed advisable, therefore, to make some runs in which the chromate had been added in known amounts and to study the oxygen consumption with time. The more carefully controlled experiments may be grouped as follows: (1) approximate duplication of in-pile experiments, (2) tests of the effect of added chromate or of dichromate, (3) test of the effect of added iodine, (4) an exact duplicate of an in-pile run in which the rocking rate was the same and temperature cycling could be duplicated, (5) the use of a platinum-lined noncorrosive bomb, and (6) the use of all-titanium systems. These runs are discussed below.

1. *Approximate duplication of in-pile experiments (runs H-36 to H-40).* These runs differ somewhat from those performed under in-pile conditions. The rate of rocking for runs H-36 to H-40 was 40 times per minute, while for the in-pile runs it was 9 or 10 times per minute. In-pile measurements of pressure were made at 100°C, and the temperature was lowered rapidly from 250°C, whereas the out-of-pile runs were maintained at 250°C at all times. The results obtained are fairly reproducible in this group. In general, the estimates of corrosion as determined by oxygen consumption, by the nickel content of the solution after the run, and by the loss in weight of the pin specimens contained in the bomb are in good agreement.

2. *Effect of added chromate (runs H-41, -44, and -45).* It was pointed out in the last quarterly report that, at the end of the runs, the solutions used in out-of-pile experiments contained an appreciable amount of hexavalent chromium, while those used in in-pile experiments contained no detectable amount. This difference could result from radiation instability of chromate or from its reduction by chemical reaction during the "cooling period" of the bomb. It was suggested that, if the

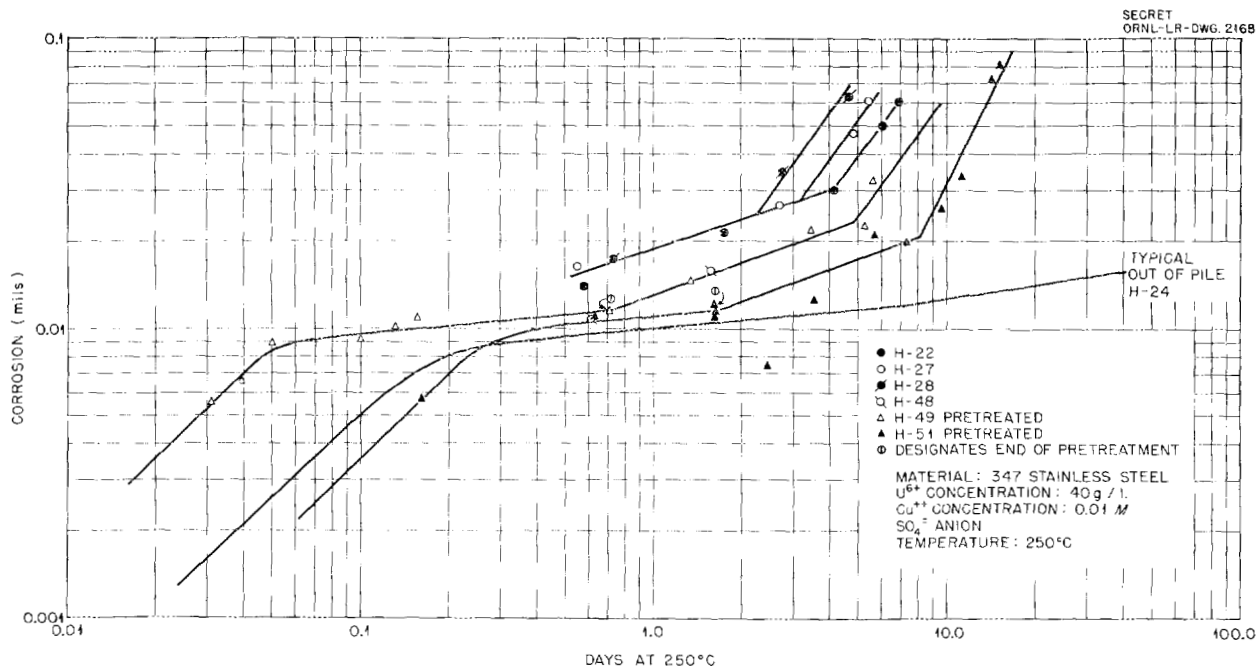


Fig. 77. Oxygen Consumption as Indicated by Corrosion vs Time.

chromate acted as a protective agent, its presence could explain the failure of out-of-pile tests to show a second rapid corrosion rate such as was observed in in-pile tests. Based on this hypothesis, if the solutions used in out-of-pile tests contained chromate at the beginning, less corrosion would be expected during the initial stages. Two qualitative tests and three controlled experiments were made to test this hypothesis. The films formed in every case were golden instead of black, did not rub off with handling, and were more difficult to strip by the electrolytic process. The nickel content of the solutions and the consumption of oxygen in the one run for which it was available were in agreement with the pin-weight-change data.

3. *Effect of added iodine (run H-43).* Fission-product iodine has been suggested as a possible cause of accelerated corrosion of in-pile bombs. Some qualitative runs and one long-time study were made with solutions containing 9 ppm of iodide. In each case the films on the pins appeared to be harder, but none of the data obtained indicated that there was any difference in the amount of corrosion. However, at the high temperature and low pH of the solution, the iodine is possibly all oxidized to iodate. In the reactor the presence of

hydrogen, peroxide, and various free radicals would probably prevent this oxidation.

4. *Exact duplicate of in-pile run (run H-50).* The accelerated in-pile corrosion had been considered as a possible result of spalling of the film due to temperature changes. An apparatus was assembled that exactly duplicated the in-pile agitation and that allowed the same kind of rapid temperature changes to be carried out. A type 347 stainless steel bomb and a solution duplicating the then-current in-pile run (H-51) were used. The corrosion behavior was essentially the same as in the other out-of-pile runs, which indicates that rapid temperature changes, such as those observed in in-pile runs, do not cause spalling and accelerated corrosion.

There had also been a question as to the amount of gamma heating of thermocouples during temperature measurements in-pile, with the reactor down. The temperature-pressure relationships observed in this duplicate run were so nearly the same as those observed in-pile that it is almost certain that gamma heating does not amount to more than 0.5°C.

5. *Corrosion in platinum-lined bomb (run Pt-1).* One out-of-pile experiment was performed with a

platinum-lined bomb. The objective was to study the rate of corrosion of pin specimens in a bomb which could not corrode. The fittings and pins were of type 347 stainless steel. No attempt was made to insulate the pins from the bomb wall. This experiment showed rapid pin corrosion. The data for oxygen consumption and the nickel content of the solution indicate that fittings as well as pins were attacked. No chromate was produced in this run. It is believed that electrochemical effects augmented the chemical reaction in this case.

6. *All-titanium systems.* Two titanium systems are now being investigated. The bomb, fittings, and capillary pressure tubing are all of this metal. One of the systems shows no signs of attack, as measured by oxygen consumption after a week, while the other has lost pressure, either because of chemical attack or because of imperfections in the system. Further investigation will be necessary to determine which of the systems is the more reliable.

The problem of determining the initial oxygen pressure is still unsolved. Oxygen is generated by the decomposition of hydrogen peroxide at about 150°C. The initial rate of consumption is so fast at higher temperatures and possibly even at the temperature of peroxide decomposition that extrapolation to zero time has appeared to be unreliable. There is no certainty that peroxide decomposition does not begin even before the bomb is sealed; in fact, this has been observed in a few cases, especially so in the platinum-lined bomb. A higher initial pressure was found in a titanium bomb than in a type 347 stainless steel bomb when an identical loading was used. There is a little evidence from run H-50 (paragraph 4 above) that an appreciable amount of corrosion occurs at temperatures considerably below 250°C. In this run the measured oxygen consumption was very low, while corrosion measured on pin specimens was fairly high.

A summary of experimental data is presented in Table 42.

**HRP QUARTERLY PROGRESS REPORT**

**TABLE 42. RESULTS OF RADIATION CORROSION EXPERIMENTS**

Bomb No.	Duration (days)	Solution Analysis (mg/ml)		Corrosion (mils)		Oxygen Data	Remarks
		Ni <sup>++</sup>	Cr <sup>6+</sup>	Nickel Data	Pin Data		
In-Pile Experiments							
H-48	1.58	0.225	0.00	0.012	0.0163	0.0159	
H-49	5.64	0.376	0.00	0.0198	0.0186	0.0313	
H-51	15.5	*	*	*	*	0.082	
Out-of-Pile Experiments							
H-36	9.12	0.13	0.10	0.0080	*	0.0129	
H-37	12.8	*	*	*	*	0.014	
H-38	2.2 0.2	0.095	0.062	0.0066	0.0067	0.0269 0.013	Capillary plugged
H-39	7.0	0.1	0.1	0.0075	0.0094	*	
H-40	12.04	0.11	0.11	0.0081	0.0141	0.0106	
H-41	12.04	0.05	0.15	0.0037	0.0092	0.0079	185 ppm of CrO <sub>4</sub> <sup>---</sup> added
H-44	11.84	0.10	0.54	0.0072	0.0086	*	1729 ppm of CrO <sub>4</sub> <sup>---</sup> added
H-45	11.84	0.082	0.11	0.0061	0.0061	*	185 ppm of CrO <sub>4</sub> <sup>---</sup> added
H-43	21.77	0.13	0.1	0.0096	0.0123	*	9.5 ppm of I <sub>2</sub> added
H-50	8.0	*	*	*	0.019	0.007	Exact duplicate of in-pile run
Pt-1	6.99	0.11	<3 ppm	0.0220	0.0157	0.020	

\*Data are not available. Analyses were not obtained in every case, and where oxygen data are missing the pressure capillary was plugged and no reliable measurements could be made.

## THORIUM NITRATE RADIATION STUDIES

J. W. Boyle

H. A. Mahlman

Thorium nitrate solutions irradiated in a reactor or reactor blanket for extended periods of time will build up significant concentrations of  $U^{233}$  from  $Th^{232}$ . The energy absorbed in the thorium nitrate solutions and, therefore, the rate of radiation decomposition will increase with time as the  $U^{233}$  concentration increases. The quantity of decomposition gas is increased not only because more energy is absorbed by the solution but also because a higher yield of gas results from the absorption of fission-recoil energy than from the absorption of an equal amount of gamma-ray energy.

A study of the effect of the fission recoils on the gas yield has been started, and a hydrogen and nitrogen yield is reported for 5.80 *m*  $Th(NO_3)_4$  solutions containing a Th/U ratio of about 500. The thorium nitrate solutions were spiked with  $U^{235}$  to simulate  $U^{233}$  build-up. For these solutions about 81% of the total energy absorbed came from  $U^{235}$  fission in the solution itself. These results then can be compared with the results for pure thorium nitrate containing no added uranium.<sup>1</sup>

$G$ , the yield of gas per unit energy input, is obtained by measuring the amount of gas produced by an irradiation of known energy input. Errors in  $G$  can arise from inaccuracies either in the collection and analysis of the gases produced or from calculations of the energy absorbed during the irradiation.

Considerable effort has been spent on minimizing errors in the gas analysis. It was found that the method for  $NO_2$  analysis outlined previously was unsatisfactory for small quantities of gas. The best method at present seems to be reduction to  $N_2$  by hydrogen on hot copper turnings. Copper is one of the better metals to use as a catalyst, since it neither dissolves  $N_2$  nor forms stable nitrides.<sup>2</sup>

The analyses of gas samples from four ampoules of 5.80 *m*  $Th(NO_3)_4$  containing one atom of  $U^{235}$  for each 500 atoms of  $Th^{232}$  gave  $43 \pm 1\%$   $H_2$ ,  $48 \pm 1\%$   $O_2$ , and  $9 \pm 1\%$   $N_2$  for the permanent gases and small but measurable amounts of  $N_2O$  and  $CO_2$  and a trace of  $NO_2$ . It is seen that the material

balance is quite good. The oxygen is approximately equal to three times the nitrogen plus one-half the hydrogen. This is what would be expected if the water present was decomposed to hydrogen and oxygen and the nitrate ion was decomposed to nitrogen and oxygen.

The energy absorbed by the 5.80 *m* thorium nitrate solutions containing uranium irradiated in hole 12 of the ORNL Graphite Reactor comes from the following processes:

	Per Cent
$U^{235}$ fission	80.8
$H_2O - \gamma + \text{fast neutron}$	11.1
$Th^{233} \beta$	3.2
$NO_3^- - \gamma + \text{fast neutron}$	2.7
$Th - \gamma$	2.2

The energy from the fission process  $E_F$  is determined by the equation

$$E_F = nvt \sigma_f N \Delta E,$$

where  $nv$  is the slow-neutron flux in neutrons/cm<sup>2</sup>/sec;  $t$  is the time in seconds;  $\sigma_f$  is the fission cross section for  $U^{235}$ , equal to 549 barns;  $N$  is the number of  $U^{235}$  atoms present; and  $\Delta E$  is the energy per fission absorbed in the solution, which is equal to  $173 \pm 7 \times 10^6$  ev/fission.<sup>3</sup> The slow-neutron flux is determined from the induced radioactivity of a manganese monitor,

$$nv = \frac{A}{S\sigma N},$$

where  $A$  is the disintegrations/sec at time of removal from the pile,  $S$  is the saturation factor, which is equal to  $1 - e^{-\lambda t}$ , where  $t$  is the radiation time in seconds and  $\lambda$  is the decay constant;  $\sigma$  is 13 barns for  $Mn^{55}$ ; and  $N$  is the number of atoms of  $Mn^{55}$  present in the monitor.

The gamma and fast-neutron contribution for  $H_2O$  was calculated by using the calorimetrically determined value<sup>4</sup> of 0.0202 cal/ml/Mw·min.

<sup>1</sup>J. W. Boyle, *HRP Quar. Prog. Rep.* Apr. 30, 1954, ORNL-1753, p 147-150.

<sup>2</sup>S. Dushman, *Scientific Foundations of Vacuum Technique*, p 596, Wiley, New York.

<sup>3</sup>C. G. Hanna, *The Total Energy Released in the Slow Neutron Fission of  $U^{235}$* , CRR-489 (May 18, 1951).

<sup>4</sup>J. A. Ghormley, T. J. Sworski, and C. J. Hochandel, *Chem. Quar. Prog. Rep.* Sept. 30, 1951, ORNL-1153, p 75.

## HRP QUARTERLY PROGRESS REPORT

The gamma and fast-neutron contribution in  $\text{Th}(\text{NO}_3)_4$  was calculated by using the neutron and gamma heating measured in hole 12 calorimetrically.<sup>5</sup>

The  $\text{Th}^{233}$  beta heating was calculated in a manner similar to the fission heating mentioned above. It was assumed that only 80% of the beta energy was absorbed in the ampoules, because of the smallness of the sample. The over-all energy determination is probably no better than  $\pm 5$  to  $\pm 10\%$  on an absolute basis.

The hydrogen and nitrogen yields are given in Table 43, together with values for other solutions for comparison.

When the results for thorium nitrate are compared, it is seen that the gas yields are much higher for the solutions containing uranium (heavy-particle

radiation) than for solutions without uranium (light-particle radiation). This same relationship is seen for pure water. If the uranium concentration were increased even more in the thorium solutions, no large increase in gas yields over those quoted here would be expected, since 81% of the energy already comes from heavy-particle radiation.

The lower hydrogen yield for 5.8 m  $\text{Th}(\text{NO}_3)_4$ , as compared with 2.0 m  $\text{UO}_2(\text{NO}_3)_2$ , is undoubtedly due to a concentration effect. This lower yield seems to fit an extrapolation of the  $\text{UO}_2(\text{NO}_3)_2$  curve presented in the article in *Reactor Science and Technology*.

<sup>5</sup>D. M. Richardson, *Calorimetric Measurement of Radiation Energy Dissipated by Various Materials Placed in the Oak Ridge Pile*, ORNL-129 (October 1, 1948).

TABLE 43. HYDROGEN AND NITROGEN YIELDS FOR  $\text{Th}(\text{NO}_3)_4$  SOLUTIONS TOGETHER WITH VALUES FOR OTHER SOLUTIONS FOR COMPARISON

$(G_{\text{H}_2} \text{ molecules of } \text{H}_2)/(100 \text{ ev}^{-1})$	$(G_{\text{N}_2} \text{ molecules of } \text{N}_2)/(100 \text{ ev}^{-1})$	Composition Solution	Radiation	Reference
$0.25 \pm 0.05$	$0.05 \pm 0.01$	5.8 m $\text{Th}(\text{NO}_3)_4$ Th/U = 500	81% fission energy	
0.04	0.002-0.005	5.8 m $\text{Th}(\text{NO}_3)_4$	Gamma + fast neutron	ORNL-1753
0.55	0.44	2.0 m $\text{UO}_2(\text{NO}_3)_2$ 8.8% U235	Fission recoil	W. F. Kieffer and J. W. Boyle, 1952
0.46		$\text{H}_2\text{O}$	Gamma	<i>Reactor Sci. Technol.</i> 3, 32
1.80		$\text{H}_2\text{O}$	Fission recoil	<i>Reactor Sci. Technol.</i> 3, 32

## ANALYTICAL CHEMISTRY RESEARCH

P. F. Thomason  
C. L. Burros

A. D. Horton  
U. Koskela

## OBJECTIVES

The need for improvement in the accuracy and precision of homogeneous reactor analytical procedures has been firmly established on the basis of phase-study and radiation-stability research, corrosion studies, and operating experience with the HRE. In order to meet this need and the anticipated HRT requirements, the Analytical Chemistry Division has initiated a program of research directed toward evaluation and improvement of these procedures. Precision studies of analyses for nickel, copper, and uranium are reported below. These studies will be continued and extended to remote-control conditions in the presence of high-level radioactivity when the facilities are available.

STATISTICAL EVALUATION OF THE  
POLAROGRAPHIC DETERMINATION  
OF NICKEL IN HOMOGENEOUS  
REACTOR FUEL

Several synthetic homogeneous reactor fuels that contained 40 mg of uranium per milliliter as  $\text{UO}_2\text{SO}_4$ , 10  $\mu\text{g}$  of iron per milliliter as  $\text{Fe}_2(\text{SO}_4)_3$ , and varying concentrations of nickel as  $\text{NiSO}_4$  were prepared and analyzed polarographically for nickel.

The synthetic samples were adjusted to 6 M in HCl and passed through a Dowex A-1 ion-exchange-resin column. The uranium remained in the column, and nickel was quantitatively collected in the effluent. The effluent was evaporated almost to dryness, and sufficient pyridine was added to provide a supporting electrolyte of approximately 0.1 M pyridine, 0.1 M pyridinium chloride. The solution was adjusted to a known volume, and nickel was determined polarographically by the method of standard addition at  $E_{1/2}$  equals  $-0.78$  v vs the S.C.E.

The relative standard deviation of the method for a series of unknowns that contained 10 to 25  $\mu\text{g}$  of nickel per milliliter was found to be 0.55%.

STATISTICAL EVALUATION OF THE  
POLAROGRAPHIC DETERMINATION  
OF COPPER IN HOMOGENEOUS  
REACTOR FUEL

Several synthetic homogeneous reactor fuel solutions that contained 40 mg of uranium as  $\text{UO}_2\text{SO}_4$ , 10  $\mu\text{g}$  of iron per milliliter as  $\text{Fe}_2(\text{SO}_4)_3$ , 1 mg of nickel per milliliter as  $\text{NiSO}_4$ , and varying concentrations of copper as  $\text{CuSO}_4$  were prepared and analyzed polarographically for copper.

A supporting electrolyte of 0.5 M disodium dihydrogen ethylenediaminetetraacetate (Versenate) solution was prepared in copper-free redistilled water and adjusted to pH 7.0 with  $\text{Na}_2\text{CO}_3$  and then to pH 8.5 with NaOH. Equal volumes of the Versenate solution and the synthetic homogeneous reactor fuel solution were mixed thoroughly and analyzed polarographically for copper. The concentration of copper in the polarographic cell was 1 to 10  $\mu\text{g}$  per milliliter. The  $E_{1/2}$  for copper in this supporting electrolyte is approximately  $-0.55$  v vs S.C.E.

The relative standard deviation for 18 examples was found to be 0.95%.

TITRATION OF URANIUM IN HOMOGENEOUS  
REACTOR FUEL SOLUTIONS

Considerable effort is being made to improve the precision of the semimicro automatic titration of uranium in HR fuel solutions. About 50 titrations of 5-mg quantities of uranium show the relative standard deviation to be of the order of 0.6%. It is thought that this deviation can be improved by modification of the mechanical details of stirring and blanketing the titration vessel with  $\text{CO}_2$ .

## $\text{Np}^{239}$ CAPTURE CROSS SECTION

J. Halperin  
D. E. Ferguson  
D. R. Hendrix

D. C. Overholt  
C. M. Stevens<sup>6</sup>  
R. W. Stoughton

Depleted uranium slugs have been irradiated in the LITR for  $\frac{1}{4}$ ,  $\frac{1}{2}$ , 1, 2, 4, 8, and 16 days. The slugs irradiated for  $\frac{1}{2}$ , 1, 2, and 4 days have been processed for plutonium, and the resulting plutonium samples are now being analyzed for  $\text{Pu}^{240}$  content both by spontaneous-fission count and by

mass-spectrographic means. By using effective values of 3.5, 22, and 430 barns for capture by  $\text{U}^{238}$ ,  $\text{U}^{239}$ , and  $\text{Pu}^{239}$ , respectively, an estimate has been made of the  $\text{Np}^{239}$  cross section. Based on very preliminary plutonium isotopic-analysis data, the capture cross section of  $\text{Np}^{239}$  for LITR neutrons appears to be fairly definitely less than 100 barns. A more accurate and precise value will be reported as soon as additional data become available.

---

<sup>6</sup>Argonne National Laboratory.